Exploring molecular patterns and determinants of melanoma cell susceptibility to natural killer cell cytotoxicity

Dissertation
for the award of the degree
"Doctor rerum naturalium"
of the Georg-August-Universität Göttingen

within the doctoral program *Molecular Medicine*
of the Georg-August University School of Science (GAUSS)

submitted by
Sabrina Cappello

Born in Neunkirchen (Saar)

Göttingen 2020

Thesis Committee

Prof. Dr. Ivan Bogeski

Institute of Cardiovascular Physiology

University Medical Centre, Georg-August University Göttingen

Prof. Dr. Alexander Flügel

Institute for Neuroimmunology and Multiple Sclerosis Research

University Medical Centre, Georg-August University Göttingen

Prof. Dr. Michael P. Schön

Department of Dermatology, Venereology and Allergology

University Medical Center Göttingen

Further members of the Examination Board

Prof. Dr. Ralf Dressel

Department of Cellular and Molecular Immunology

University Medical Centre, Georg-August University Göttingen

Prof. Dr. Lutz Walter

Department of Primate Genetics

German Primate Center, Göttingen

Prof. Dr. Thomas Meyer

Department of Psychosomatic Medicine and Psychotherapy

University Medical Center Göttingen

Date of oral examination: 16th June 2020

Affidavit

I hereby declare that my doctoral thesis entitled

"Exploring molecular patterns and determinants of melanoma cell susceptibility to natural killer cell cytotoxicity" has been written independently with no other sources and aids than quoted.

Göttingen, April 2020

Sabrina Cappello

List of publications

Zhang, X., Gibhardt, C.S., Will, T., Stanisz, H., Korbel, C., Mitkovski, M., Stejerean, I., Cappello, S., Pacheu-Grau, D., Dudek, J.*, et al.* (2019). Redox signals at the ER-mitochondria interface control melanoma progression. EMBO J *38*, e100871

Zhou, X., Friedmann, K.S., Lyrmann, H., Zhou, Y., Schoppmeyer, R., Knorck, A., Mang, S., Hoxha, C., Angenendt, A., Backes, Cappello, S.*, et al.* (2018). A calcium optimum for cytotoxic T lymphocyte and natural killer cell cytotoxicity. J Physiol *596*, 2681-2698

Frischauf, I., Litvinukova, M., Schober, R., Zayats, V., Svobodova, B., Bonhenry, D., Lunz, V., Cappello, S., Tociu, L., Reha, D.*, et al.* (2017). Transmembrane helix connectivity in Orai1 controls two gates for calcium-dependent transcription. Sci Signal *10* (507): eaao0358

List of content

List of abbreviations

4E-BP1	Eukaryotic translation initiation factor 4E binding protein 1
7-AAD	7-Aminoactinomycin D
A	
ACT	Adoptive cell transfer
ADCC	Antibody dependent cellular cytotoxicity
AIM2	Absent in melanoma 2
AM	Acetoxymethyl ester
AML	Acute myeloid leukemia
ANXA7	Annexin A7
APC	Antigen presenting cell
APS	Ammonium persulfate
APAF-1	Apoptotic protease activating factor 1
ATP	Adenosine triphosphate
B	
B2M	Beta-2-microglobulin
BAG-6	Bcl-2-associated athanogene 6
BAD	Bcl-2-associated agonist of cell death
BAK	Bcl-2 homologous antagonist killer
BAX	Bcl-2-associated X protein
BCL-2	B-cell lymphoma 2
BID	BH3-interacting domain death agonist
BiKEs	Bi-specific killer engagers
BRAF	V-raf murine sarcoma viral oncogene homolog B
BSA	Bovine Serum Albumin
C	
C1S	Complement Component 1, Subcomponent
$CaCl_2$	Calcium chloride

CARs	Engineered chimeric antigen receptors
CASP3	Caspase 3
CD	Cluster of Differentiation
CDKN1B	Cyclin-dependent kinase inhibitor 1B
CFP	Complement factor P
COPS5	COP9 Signalosome Subunit 5
CTL	Cytotoxic T cell
CTLA-4	Cytotoxic T-lymphocyte–associated antigen 4

D

DAP10	DNAX-activation protein 10
DAP12	DNAX-activation protein 12
DEPC	Diethyl pyrocarbonate
DEPTOR	DEP domain-containing mTOR interacting protein
DGE	Differential gene expression
DIABLO	Direct IAP-binding protein with low PI
DISC	Death inducing signalling complex
DMSO	Dimethyl sulfoxide
DNA	Deoxyribonucleic acid
DNAM-1	DNAX Accessory Molecule-1
DPBS	Dulbecco's Phosphate-Buffered Saline
dsRNA	double stranded RNA molecule
DVL3	Dishevelled segment polarity protein 3

E

E. coli	Escherichia coli
EDTA	Ethylenediaminetetraacetic acid
EGTA	Ethylene glycol-bis(2-aminoethylether)-N,N,N',N'-tetraacetic acid
EGFR	Epidermal growth factor receptor
EMT	Epithelial-to-mesenchymal transition

ERK	Extracellular signal-regulated kinase
E:T	Effector-to-target
F	
FACS	Fluorescence activated cell sorting
FADD	Fas associated death domain protein
FCS	Fetal calf serum
FDA	Food and Drug Administration
FDR	False discovery rate
G	
GAPDH	Glyceraldehyde-3-phosphate dehydrogenase
GFP	Green fluorescent protein
GM-CSF	Granulocyte-macrophage colony-stimulating factor
GRB2	Growth factor receptor-bound protein 2
H	
HCP5	HLA complex 5
HER2	Human epidermal growth factor receptor 2
HGF	Hepatocyte growth factor
HK2	Hexokinase 2
HLA	Human Leukocyte Antigen
hPSCs	Human pluripotent stem cells
HS	Heparan sulphate
HSBP1	Heat Shock Factor Binding Protein 1
I	
IDO	Indoleamine 2,3 dioxygenase
IgG	Immunoglobulin G
IL-2	Interleukin 2
IFN-γ	Interferon gamma
iPSCs	Induced pluripotent stem cells

ITAM	Immunoreceptor tyrosine-based activation motif
ITIM	Immunoreceptor tyrosine-based inhibition motif
ITSM	Immunoreceptor tyrosine-based switch motifs

K

$KHCO_3$	Potassium bicarbonate
KIR	Killer cell immunoglobulin-like recepotors
KLR	Killer cell lectin-like receptors
KLRG1	Killer cell lectin-like receptor subfamily G member 1

L

L1AM	L1 cell adhesion molecule
LB	Lysogeny broth
LCK	Lymphocyte cell-specific protein-tyrosine kinase
LIR	Killer lectin-like receptors

M

MEK	Mitogen-activated protein kinase
MFI	Median fluorescence intensity
MHC	Major histocompatibility complex
MICA/B	MHC class I chain-related genes A/ B
MLST8	Mammalian lethal with SEC13 protein 8
MLL5	Mixed lineage leukemia-5
MOMP	Mitochondrial outer membrane permeabilisation
mSIN1	Target of rapamycin complex 2 subunit MAPKAP1
mTOR	Mammalian target of rapamycin

N

NaCl	Sodium chloride
NaF	Sodium fluoride
NaN_3	Sodium azide
NAPSA	Napsin A aspartic peptidase

NCR	Natural cytotoxicity receptors
NH_4Cl	Ammoniumchlorid
NK cells	Natural killer cells
NKiToxMel	NK cell-induced cytotoxicity against melanoma cells
NRAS	Neuroblastoma RAS viral oncogene homolog
O	
OXPHOS	Oxidative phosphorylation
P	
PBLs	Peripheral blood lymphocytes
PBMCS	Peripheral blood mononuclear cells
PCA	Principal component analysis
PDGFRB	Platelet derived growth factor receptor beta
PEA15	Proliferation and apoptosis adaptor protein 15
PEG2	Prostaglandin E2
PD-1	Programmed death 1
PDGF	Platelet-derived growth factor
PDK1	Pyruvate dehydrogenase kinase 1
PFA	Paraformaldehyde
PGR	Progesterone receptor
PI3K	Phosphatidylinositol-3-kinase
PI-3,4,5-P3	Phosphatidylinositol-3,4,5-triphosphate
PI-4,5-P2	Phosphatidylinositol-4,4-bisphosphate
PIK3R1	Phosphatidylinositol 3-kinase regulatory subunit alpha
PKC	Protein kinase C
PMSF	Phenylmethanesulfonyl fluoride
PRAS40	Proline-rich Akt substrate of 40 kDa
Protor 1 / 2	Protein observed with Rictor-1/-2
PTEN	Phosphatase and tensin homolog deleted on chromosome 10

PTK2	Protein Tyrosine Kinase 2

Q

qPCR	Quantitative polymerase chain reaction

R

RAS	Rat sarcoma
RAF	Rapidly accelerated fibrosarcoma
RAPTOR	Regulatory-associated protein of TOR 1
RICTOR	Rapamycin-independent companion of mTOR complex 2
RNA	Ribonucleic acid
RPPA	Reverse phase protein array
RPS6	Ribosomal protein S6
RPS6K	Ribosomal protein S6 kinase
RPS6KB1	Ribosomal protein S6 kinase B1
RT	Room temperature

S

SDS	Sodium dodecyl sulfate
SDS-PAGE	Sodium dodecyl sulfate polyacrylamide gel electrophoresis
SEM	Standard error of the mean
SGK1	Serum/glucocorticoid regulated kinase 1
siRNA	small interfering RNA
SMAC	Second mitochondria-derived activator of caspase
SNPs	Single nucleotide polymorphisms

T

TCR	T cell receptor
TEL2	Tel-related Ets factor
TEMED	Tetramethylethylenediamine
TFs	Transcription factors
TFRC	Transferrin receptor

TGF-β	Transforming growth factor β
TGM2	Transglutaminase-2
TIGIT	T-cell immunoreceptor with Ig and ITIM domains
TMEM158	Transmembrane protein 158
TNF-β	Tumour necrosis factor beta
TRAIL	TNF-related apoptosis inducing ligand
T_{regs}	regulatory T cells
TriKEs	Tri-specific killer engagers
TTI1	TELO2-interacting protein 1 homolog
TWIST1	Twist-related protein 1
U	
ULBPs	UL16-binding proteins
UV	Ultraviolet
V	
VDAC	Voltage-dependent anion channel
VGP	Vertical growth phase
W	
WT	Wild type
WWTR1	WW Domain Containing Transcription Regulator 1
X	
XIAP	X chromosome-linked inhibitor of apoptosis
XBP1	X-Box binding protein 1
XRCC1	X-Ray Repair Cross Complementing 1
Y	
YBX1	Y-box-binding protein 1
Z	
ZEB1	Zinc finger E-box-binding homeobox 1

Units

°C	Centigrade
Rpm	Rounds per minute
g	Gram
h	Hour
l	Litre
m	Meter
mg	Milligram
min	Minute
U	Units
V	Volt

Prefix

c	Centi (10^{-2})
k	Kilo (10^{3})
µ	Micro (10^{-6})
m	Milli (10^{-3})
n	Nano (10^{-9})
p	Pico (10^{-12})

List of figures

List of tables

List of supplemental tables

Abstract

Malignant melanoma is the deadliest form of skin cancer. Due to its genetic heterogeneity and high potential to metastasize, the treatment of melanoma is challenging. Despite the promising result of T-cell based therapeutic strategies in combination with targeted therapies, therapeutic resistance or relapse occur. Hence, the advancement and improvement of melanoma immunotherapies need to be considered.

Natural killer (NK) cells, which show an innate ability to recognize and kill cancer cells without prior sensitization, could be a useful additional therapeutic tool in melanoma immunotherapy. To investigate the therapeutic potential of NK cells, we assessed the cytotoxicity of primary NK cells as well as the NK-92 cell line to genetically diverse human melanoma cell lines. A broad range of susceptibility of different melanomas to activated NK cells was observed. Proteome analyses (RPPA) of melanoma cells indicated a correlation between melanoma protein expression and susceptibility to NK cells and allowed the establishment of a 'melanoma killing signature'. Using this novel tool the NK cell-mediated killing of additional and untested melanoma cell lines was successfully predicted. Furthermore, manipulation of single identified proteins such as SNAI1 and signalling pathways such as the PI3K-AKT-mTOR pathway affected the NK cell-mediated killing of melanoma cells.

The success of immune therapy is not only dependent on the initial positive treatment effect but also the prevention of therapy resistance. Therefore, melanoma-NK cell co-cultures in order to identify new molecular targets, which might control NK cell escape mechanisms in melanoma, were established. NK cell resistance in melanoma cells seems to be strongly associated with the downregulation of MHC class I but also MHC class II molecules.

In summary, this study identifies novel prognostic immunotherapy-response biomarkers and possible resistance mechanism and thus reveals new insights into the potential use of NK cells in melanoma therapy.

1 Introduction

1.1 Malignant melanoma: definition, origin, risk factors

Skin cancers are the most common type of cancer (American cancer society, 2019). There are two major types of skin cancer: non-melanoma skin cancers, including basal-cell skin cancer (BCC) and squamous-cell skin cancer (SCC), and melanoma. Melanoma arises from genetically altered melanocytes, which in normal tissue are known to produce the pigment melanin (Shain and Bastian, 2016). Though malignant melanoma is less frequent than the other skin cancers, it is much more aggressive and lethal than other skin cancers (Siegel et al., 2019). Globally, 132.000 new melanoma skin cancers are diagnosed every year (World Health organization, 2020). Of those, around 20.000 new cases alone are reported for Germany (Robert-Koch-Institut and e.V., 2017). The incidence of melanoma has been increasing worldwide over the last two decades, especially in Australia, North America and Europe (American cancer society, 2019; Robert-Koch-Institut and e.V., 2017; World Health organization, 2020). The risk factors of this disease are diverse as the development of melanoma is a complex multifactorial process. One of the major environmental risk factors is the exposure to UV radiation (Gandini et al., 2005b; Kulichova et al., 2014) and a history of sunburns (Whiteman et al., 2001). Especially the exposure to UVB can cause genetic damage and can initiate the malignant transformation of melanocytes (Jhappan et al., 2003). In the course of a lifetime, UV induced DNA damage accumulates and thereby also the risk to develop a malignant melanoma (Siegel et al., 2019). In addition to the UV irradiation, other endogenous factors also contribute to the melanoma risk. Fair skin (Howlader et al., 2018; Scherer and Kumar, 2010), the number (Bauer and Garbe, 2003; Holly et al., 1987) and type of melanocytic nevi (moles) (Gandini et al., 2005a; Grob and Bonerandi, 1998), as well as a family history (Debniak, 2004) which can be often associated with a certain genetic predisposition (Potrony et al., 2015), correlate with melanoma incidence.

1.2 Melanoma progression: Important signalling pathways

The survival rate associated with malignant melanoma strongly depends on disease stage and the mutation status of the patient's tumour. After the development of distant metastasis, the survival rate decreases to 6-9 months (Balch et al., 2009). Therefore, not only an early disease diagnosis but also the administration of an effective patient personalized treatment to prevent disease progression is required. During melanoma development and progression, different signalling pathways contribute to cell proliferation and survival. These include:

1.2.1 The RAS-RAF signalling pathway

One of the most frequently mutated pathways in melanoma is the RAS-RAF signalling cascade (Davies et al., 2002). The starting point of this signalling pathway is the binding of an external ligand such as growth factors or cytokines to the extracellular side of a receptor tyrosine kinase. A subsequent phosphorylation cascade, involving rat sarcoma (RAS), rapidly accelerated fibrosarcoma (RAF), mitogen-activated protein kinase (MAP2K or MEK) transfer the signal via extracellular signal-regulated kinase (ERK) to the cell nucleus. The translocated ERK can activate several transcription factors and influence the expression of genes controlling cell growth and cell death (see Figure 1). Hence, mutations in these kinases often cause a constantly activated signalling pathway that contributes to dysregulated proliferation (Lopez-Bergami et al., 2008). Mutations in BRAF (v-raf murine sarcoma viral oncogene homolog B), mostly V600E substitutions, are found in 35 %–50 % of melanoma whereas neuroblastoma RAS viral oncogene homolog (NRAS) is mutated in 10-25 % of melanoma lesions (Cancer Genome Atlas, 2015; Davies et al., 2002). The RAF-MEK-ERK pathway is upregulated in most melanocytic lesions, although additional genetic alterations, through mutations or other factors is not sufficient for the initiation of melanoma (Poynter et al., 2006). Nevertheless, mutations in BRAF and NRAS are associated with a poor prognosis and favour tumour progression (Houben et al., 2004; Kumar et al., 2003). Therefore, inhibitors targeting mutated BRAF or MEK are one of the frontline treatment strategies to halt or slow disease progression (Deutsche Krebsgesellschaft et al., 2019).

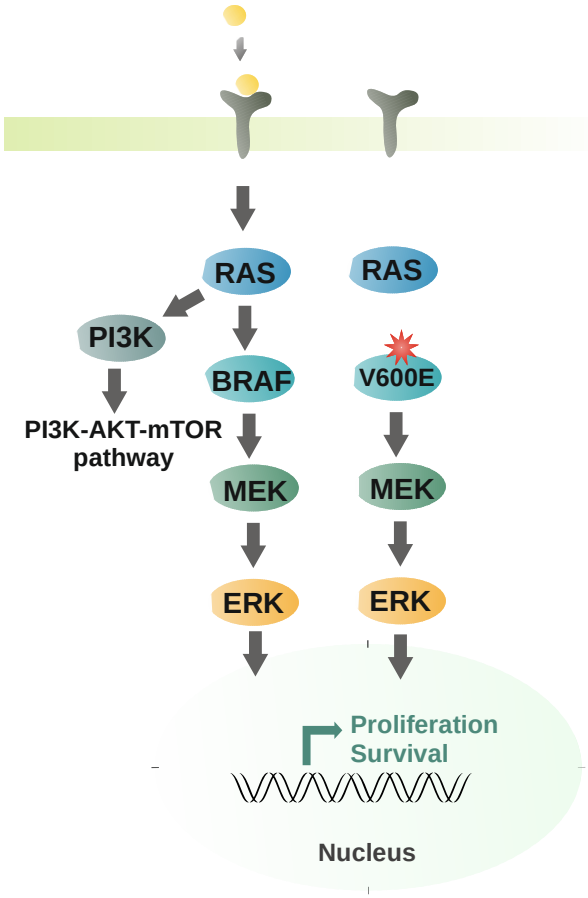

Figure 1. The RAS-RAF signalling pathway. Binding of growth factors to the extracellular side of a receptor tyrosine kinase triggers an intracellular phosphorylation cascade through RAS, BRAF and MEK that in turn activates ERK. This final kinase is translocated to the nucleus where it activates several transcription factors that mediate expression of genes promoting cell proliferation and survival. As a result of mutations in BRAF (e.g. BRAF V600E) or other downstream kinases, this signalling pathway cascade is often constitutively active in melanoma. Figure was adopted from (Cappello, 2015).

1.2.2 The PI3K/AKT/mTOR pathway

Another key player in multiple malignant processes is the pI3K/AKT/mTOR network shown in Figure 2 (Chalhoub and Baker, 2009; Saxton and Sabatini, 2017). Activation of receptor tyrosine kinase receptors or G protein-coupled receptors recruits phosphatidylinositol-3-kinase (PI3K) to the membrane. There, PI3K phosphorylates phosphatidylinositol-4,4-bisphosphate (PI-4,5-P2) to phosphatidylinositol-3,4,5-trisphosphate (PI-3,4,5-P3), which recruits protein kinase B, also called AKT to the plasma membrane (Porta et al., 2014). The phosphorylation of AKT by pyruvate dehydrogenase kinase 1 (PDK1) (at threonine 308) and mammalian target of rapamycin complex 2 (at serine 473) modulates AKT activity (Sarbassov et al., 2005).

In melanoma, the AKT activation (phosphorylated AKT) is strongly increased and correlates with disease progression (Dai et al., 2005). A common reason for the AKT activation in melanoma is the reduction of PTEN (phosphatase and tensin homolog deleted on chromosome 10) expression or activity (Steelman et al., 2004). PTEN antagonizes PI3K/AKT signalling by the

dephosphorylation of phosphatidylinositol 3,4,5-trisphosphate and phosphatidylinositol 3,4-bisphosphate (Simpson and Parsons, 2001). Thereby the activation of AKT is promoted and cell survival is supported (Miller and Mihm, 2006). The gene PTEN is mutated in 30-50 % of melanoma cell lines and in ~ 10 % of primary melanomas (Guldberg et al., 1997; Wu et al., 2003) but also alterations at the protein level can occur without any gene mutation (Zhou et al., 2000). Also mutations in AKT itself have been found and show increased phosphorylated AKT levels in melanoma as well as other cancers (Davies et al., 2008). AKT has many different downstream targets, which regulate cell metabolism. One of them is the mammalian target of rapamycin (mTOR) complex 1, referred to as mTORC1. This complex consists of mTOR and six other proteins (see Figure 2) that regulate the functionality of the whole complex (assembly, substrate specificity as well as the stability) (Laplante and Sabatini, 2012). The central part of this complex is the catalytic serine/threonine kinase mTOR that has substrates involved in various cellular processes. Best characterised is the involvement of the mTOR pathway in regulating protein synthesis by the activation of p70S6 kinase as well as the phosphorylation of eukaryotic translation initiation factor 4E binding protein 1 (4E-BP1) (Ma and Blenis, 2009). Besides mTORC1, a second mTOR-containing complex exists. The mTORC2 consist of seven proteins that show overlap with mTORC1 (Figure 2). Upon mTORC1 stimulation, mTOR activates p70S6 kinase and inactivates 4E-BP1 to promote cell proliferation and survival (Proud, 2011). Beside the AKT activation, the mTOR complex 2 regulates cytoskeletal organisation and cell survival. In contrast to mTORC1, mTORC2 shows low sensitivity to rapamycin, a potent mTOR inhibitor (Saxton and Sabatini, 2017).

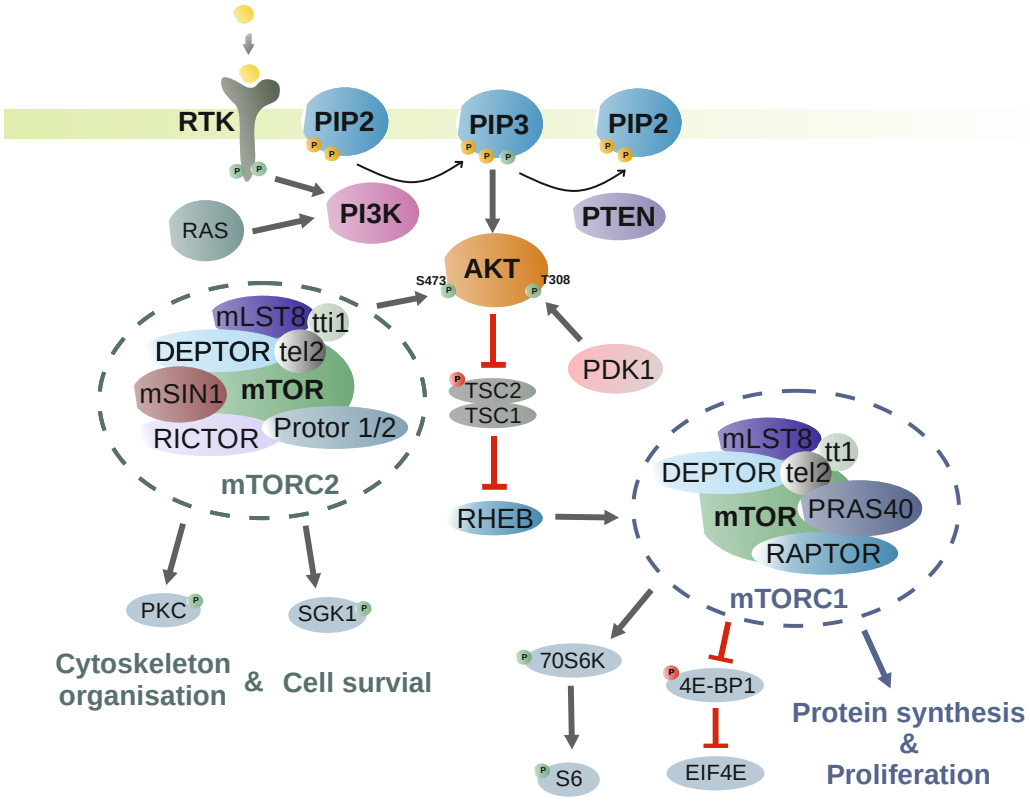

Figure 2. The PI3K/AKT/mTOR pathway. The activation of a receptor tyrosine kinase by a growth factor leads to the phosphorylation of the intracellular tyrosine residues. This recruits PI3K to the membrane where it phosphorylates PIP2 to PIP3. This process can be reversed by PTEN. PIP3 recruits AKT that is phosphorylated at S473 by the mTORC2, and at T308 by PDK1. Activated AKT leads to the indirect activation of the mTORC1 by repressing the tuberous sclerosis proteins 1 and 2 (TSC1/2) complex. The mTORC1 stimulates protein synthesis and proliferation via the activation of p70S6 kinase and inhibition of the 4E-BP1. Beside the indirect activation of mTORC1, also the mTORC2 can stimulate cell survival via serum and glucocorticoid-regulated kinase 1 (SGK1). Furthermore, it regulates the cytoskeleton organisation by phosphorylation of protein kinase C (PKC). Figure was adopted from (Yu and Cui, 2016).

1.2.3 Epithelial-to-mesenchymal transition (EMT)-like phenotype switching

During malignant transformation and the metastatic process, melanocytes as well as melanoma cells experience an epithelial-to-mesenchymal transition (EMT)-like phenotype switch (Li et al., 2015a). Although melanocytes originate from the neural crest and are not of epithelial lineage, they also undergo a phenotype switch with similar characteristics as EMT. In the course of this phenotype switch, melanoma cells undergo morphological as well as functional changes by losing epithelial characteristics such as cell polarity and cell-cell adhesion. At the same time they gain mesenchymal properties including high potential for migration and invasion (Derynck and Weinberg, 2019). These properties are caused among others by the loss of E-cadherin and an increase in N-cadherin expression (Kuphal and Bosserhoff, 2006; Yan et al., 2016). This switch of cadherin class is regulated by different transcription factors (TFs) such as Zinc finger E-box-binding homeobox 1 or 2 (ZEB1/2) or Twist-related protein 1 (TWIST1). Another essential TF

regulating EMT is the zinc finger protein snail family transcriptional repressor 1 (SNAI1) which represses E-cadherin expression (Kaufhold and Bonavida, 2014; Poser et al., 2001). It has been shown that the aberrant expression of EMT transcription factors and the corresponding alteration of cadherin class expression correlate with melanoma metastasis and poor prognosis (Caramel et al., 2013; Yan et al., 2016).

1.3 Anti-melanoma therapies

The treatment of melanoma is strongly dependent on cancer stage and genetics i.e. the mutational profile of the disease (Deutsche Krebsgesellschaft et al., 2019). At early stages, when melanoma cells are still non-invasive (Stage 0, melanoma in-situ) or only invaded in the upper parts of the dermis (Stage I, Breslow depth < 1mm), the affected section of the skin can be removed by excisional surgery. After melanoma cells have reached deeper regions of the dermis (Stage II, Breslow depth > 1mm) not only the primary tumour has to be removed, but also the spreading of melanoma cells to lymph nodes (Stage III) has to be excluded by sentinel lymph node biopsy. Adjuvant radiotherapy can reduce the risk of melanoma recurrence (Strojan, 2010). The last stage (IV) of melanoma is characterised by distant metastasis. With melanoma progression (Stage II-Stage IV) the administration of additional drugs or immune-treatments to dampen tumour growth and prevent metastasis are recommended (American cancer society, 2020; The Skin Cancer Foundation, 2020). Conventional chemotherapy with, for example dacarbazine or cisplatin, is no longer used as a frontline therapy since other treatment strategies have shown better clinical results and less side effects (Wilson and Schuchter, 2016). A common therapeutic approach involves the use of targeted therapies that interfere with tumour cell proliferation as well as survival. The RAS-RAF signalling pathway (see chapter 1.2.1) plays an important role in tumour proliferation and patient survival and it is a frequent therapeutic target (Houben et al., 2004; Kumar et al., 2003). Selective drugs such as vemurafenib, dabrafenib and encorafenib supress the activity of RAF and prevent the initiation of the signalling cascade (Chapman et al., 2011; Koelblinger et al., 2018; Menzies and Long, 2014). Unfortunately, these drugs are only effective in melanoma patients with mutated constitutively active BRAF (most commonly V600E). When used in BRAF wildtype patients, adverse effects can be detected since these drugs can cause higher RAF signalling by inducing dimerization, membrane localization and interaction with RAS-GTP (Hatzivassiliou et al., 2010). Beside the suppression of BRAF, targeting its signalling downstream partner MEK has also been effective in the clinics with drugs such as trametinib, cobimetinib and binimetinib (Menzies and Long, 2014; Samatar and Poulikakos, 2014). Another target for the inhibition of melanoma proliferation is the PI3K/AKT/mTOR

pathway (see chapter 1.2.2), that can be blocked with multiple drugs at different levels of the signalling chain. BKM-120 (Buparlisib) and other PI3K inhibitors are currently being tested in several clinical trials (Yang et al., 2019). In addition, the mTOR inhibitor rapamycin (Sirolimus/Everolimus) and the AKT inhibitor MK2206 (Dronca et al., 2014) in combination with other drugs showed promising clinical activity (Domingues et al., 2018). However, these are not considered as frontline therapeutic options yet (Deutsche Krebsgesellschaft et al., 2019).

In the recent years, especially immune checkpoint blockade therapies have been successful in melanoma treatment (Seidel et al., 2018). These therapies are based on the decreased activation threshold of cytotoxic T-cells (CTLs). CTLs are part of the adaptive immune system and detect specific antigens in association with MHC class I molecules by the T-cell receptor (TCR) (Smith-Garvin et al., 2009). However, this signal alone is not sufficient to activate CTLs. The additional engagement of B7-molecules with CD28, which is expressed on CTLs, allows positive co-stimulation and activation (Smith-Garvin et al., 2009). To prevent autoimmunity, this process is regulated by cytotoxic T-lymphocyte–associated antigen 4 (CTLA-4). CTLA-4 competes with CD28 for binding to B7 molecules and extenuate the CTL response (Rowshanravan et al., 2018). Currently, these processes can be regulated by immunotherapies, for example, the anti-CTLA-4 antibodies ipilimumab and tremelimumab inhibit the interaction of CTLA-4 with B7 molecule expressing antigen presenting cells (APC) thus enhancing T-cell activation (Domingues et al., 2018; Seliger et al., 2013). Beside CTLA-4, another target for immunotherapy is the inhibitory receptor PD-1 (programmed death 1); PD-1 dampens T-cell function by binding to its ligands PD-L1 and PD-L2. In melanoma, the ligands for PD-1 are also commonly expressed (Kitano et al., 2018). Antibodies targeting the PD-1/PD-L1 axis such as nivolumab and pembrolizumab (anti-PD-1) (Postow et al., 2015; Wei et al., 2018) are in the clinical use. Both antibodies, alone and combined, show encouraging effects in melanoma treatment (Larkin et al., 2015). In addition, PD-L1 antibodies such as atezolozumab and avelumab entered first clinical trials (Keilholz et al., 2019; Sullivan et al., 2019).

Former immunotherapeutic approaches include the use of immune-stimulating interleukin-2 (IL-2) that was abandoned despite initial promising results due to the toxic side-effects in higher dosages (Hoffman et al., 1989; Rosenberg et al., 1985). In addition, the administration of INF-γ was shown to stimulate immune response and decrease tumour growth by promoting tumour cell apoptosis and inhibiting of tumour proliferation (Castro et al., 2018; Ni and Lu, 2018). However, clinical success of INF-γ treatment in melanoma as well as other cancers was limited due to its role in immune evasion and an observed INF-γ insensitivity in melanoma patients (Alavi et al., 2018; Castro et al., 2018).

Current subject of clinical trials is the adoptive cell transfer (ACT) of autologous tumour-infiltrating lymphocytes to attack melanoma cells. The *ex vivo* expansion and transfer of autologous, activated tumour-specific lymphocytes to melanoma patients showed promising clinical results (Mehta et al., 2018; Phan and Rosenberg, 2013; Rohaan et al., 2018; Saint-Jean et al., 2018).

Nevertheless, the clinical response to targeted therapies as well as immune checkpoint blockade is limited as not all patients respond or can relapse (Almeida et al., 2019; Petrova et al., 2020; Seidel et al., 2018). Hence, the development of alternative therapeutic strategies that complement or improve current therapies is highly needed.

1.4 Natural killer cells

The success of current immunotherapies is usually attributed to the improvement of T-cell cytotoxicity against cancer cells. However, natural killer cells (NK cells) are also able to detect and eliminate tumour cells. Natural killer cells develop in the bone marrow and represent up to 15 % of all lymphocytes (Abel et al., 2018). They are characterised as CD3 negative and CD56 positive cells and can be divided into two major NK cell subsets differing in their CD16 and CD56 expression as well as their resting immunological potential (Freud et al., 2017). For example, $CD16^{++}$ $CD56^{dim}$ NK cells show increased cytotoxicity in comparison to $CD16^{\pm}$ $CD56^{bright}$ NK cells (Arnon et al., 2006). However, these $CD56^{bright}$ NK cells have important immune regulatory functions by increased cytokine production of e.g. Interferon gamma (IFN-γ), tumour necrosis factor beta (TNF-β) as well as granulocyte-macrophage colony-stimulating factor (GM-CSF), among others (Cooper et al., 2001). After stimulation with interleukin (IL)-2, both NK cell subsets increase their cytotoxic potential dramatically (Poli et al., 2009). In contrast to CTLs, NK cells are part of the innate immune system and are cytotoxic without previous antigen-specific stimulation (Farag and Caligiuri, 2006). Furthermore, NK cells complement the immunosurveillance of T-cells, which are dependent on the engagement of TCR and MHC-I antigens (Freud et al., 2017). MHC-I molecules are often downregulated in tumour cells, so these cells can evade T-cell recognition. However, tumour cells with particularly low MHC-I expression can be detected and eliminated by NK cells (Karre, 2002).

1.4.1 NK cell receptors

NK cells recognise tumour cells by their large repertoire of germ-line encoded receptors, which have different structural and functional properties. Therefore, NK cell receptors can be divided into killer cell immunoglobulin-like receptors (KIR) and killer cell lectin-like receptors (KLR) (Murphy, 2012). Besides their structural properties, they can be further classified into activating and inhibitory receptors.

Inhibitory receptors

Inhibitory receptors have an immunoreceptor tyrosine-based inhibition motif (ITIM), a long cytoplasmic domain with a conserved terminal amino acid sequence (V/I/LxYxxL/V). This ITIM contains tyrosine residues that can be phosphorylated by proto-oncogene tyrosine-protein kinase Src thus initiating a signalling cascade. After receptor-ligand engagement, the signal transduction results in the inhibition of NK cell activity, thereby preventing the elimination of the target cell (Cerwenka and Lanier, 2001; Farag and Caligiuri, 2006; Yokoyama, 2005). One of the best investigated inhibitory ligands are the major histocompatibility complex class I (MHC class I) molecules. As depicted in Figure 3, classical MHC-I molecules (HLA-A, B, C) are detected by KIR2DL (recognizes HLA-C alleles) and KIR3DL (recognizes HLA A, B alleles). Beside these KIR receptors, the lectin like NKG2A/CD94 heterodimer recognises HLA-E, a non-classical MHC-I molecule (Sivori et al., 2019). Although MHC-I molecules are the strongest inhibitory ligands, there are reports that stimulation of non-MHC-I dependent receptor can also dampen NK cell activation (Li et al., 2009; McNerney et al., 2005)

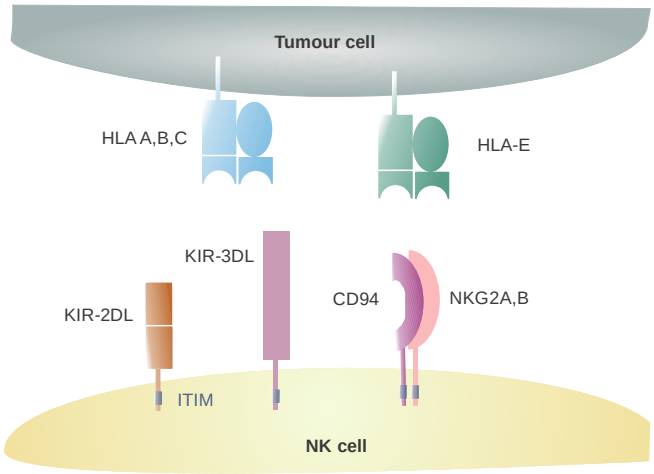

Figure 3. Inhibitory NK cell receptors and their corresponding tumour ligands. 2DL/3DL indicate the number and type of immunoglobulin domains and, L= long cytoplasmic domain; NKG2A, B, are splice variants. ITIM = immunoreceptor tyrosine-based inhibition motif. Figure was adopted from (Cappello, 2015)

Activating receptors

In contrast to the inhibitory receptors, activating receptors need an adapter molecule that carries the conserved terminal sequence YXX[L/I]6-9YXX[L/I]. This sequence is named immunoreceptor tyrosine-based activating motif (ITAM) and it initiates a phosphorylation cascade resulting in the activation of NK cells (Murphy, 2012). With the help of the adapter molecule DAP12, the KIR receptors KIR2DS and KIR3DS recognize HLA-C and other unknown ligands (Cerwenka and Lanier, 2001). The same adapter molecule DAP12 is used by the heterodimer CD94/NKG2C,E that detects HLA-E. These activating receptors compete with their inhibitory counterparts, but with a lower ligand affinity (Bryceson et al., 2006).

The most important example of the activating KLR receptor is NKG2D. This receptor, unlike the other lectin like receptors, is a homodimer that is associated with the adaptor molecule DAP 10. This adaptor molecule carries a phosphatidylinositol-3 kinase (PI3K) binding motif YxxM instead of an ITAM (Bryceson et al., 2006; Kumar, 2018). MIC (MHC class I chain-related genes) A and B as well as UL16-binding proteins 1-6 (ULBPs) are ligands for NKG2D (Casado et al., 2009; Vivier et al., 2012). Essential members of the activating KIR receptors are the three natural cytotoxicity receptors (NCRs): NKp46, NKp30 and NKp44. The latter is *de novo* expressed after IL-2 stimulation, whereas NKp46 and NKp30 are constitutively expressed on NK cells (Arnon et al., 2006). NCRs also require an adapter molecule for signal transduction. In contrast to NKp44, which associates with the adaptor molecule DAP12, NKp46 and NKp44 use homodimers of CD3 ζ or heterodimers of CD3 ζ -FcεRγ heterodimers to initiate the phosphorylation cascade (Arnon et al., 2006). Although the ligands for NCRs are still not fully understood, the identified ligands are often only expressed on tumour cells or virus-infected cells. All natural cytotoxicity receptors recognize different viral proteins; e.g. hemagglutinins or hemagglutinin neuraminidases (Kruse et al., 2014) as well as heparan sulphate (HS) sequences, which are also shown to be upregulated on tumour cells (Barrow et al., 2019).

Beside heparan sulphates (HS), the complement factor P (CFP) is a known ligand for the NCR NKp46 (Narni-Mancinelli et al., 2017). NKp30a, b is known to bind BCL2-associated athanogene 6 (BAG-6) (Binici et al., 2013) as well as B7-H6, which is only expressed on tumour cells (Bjornsen et al., 2019). Identified activating ligands for NKp44 (NKp44L) are an unusual isoform of MLL5 (mixed lineage leukemia-5), often referred as NKp44L (Rajagopalan and Long, 2013) and PDGF-DD, one of the four polypeptides of the platelet-derived growth factor (PDGF) (Barrow et al., 2018).

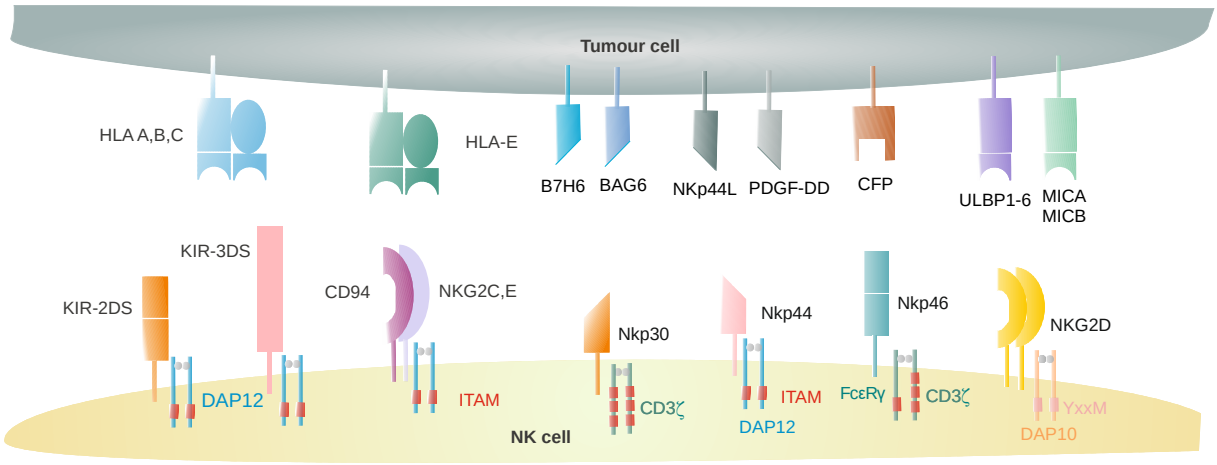

Figure 4. Activating NK cell receptors and their corresponding tumour ligands. 2DS/3DS indicate the number and type of immunoglobulin domain; S= short cytoplasmic domain. Adaptor proteins and binding motifs are also shown in colour. Figure was adopted from (Cappello, 2015).

Several other activating receptors were also shown to play an important role in tumour recognition. The DNAX Accessory Molecule-1 (DNAM-1), recognizes poliovirus receptor (CD155) and nectin adhesion molecule (CD112) (Chester et al., 2015; Long et al., 2013). The DNAM-1-mediated signalling cascade requires the phosphorylation of conserved tyrosine as well as asparagine residues (Kumar, 2018). The receptor CD244, also known as 2B4, leads to NK cell activation by the engagement to CD48 and the subsequent phosphorylation of Tyr-based motif S/TxYXXL/I, referred to as immunoreceptor Tyr-based switch motifs (ITSM), in their cytosolic tails (Chester et al., 2015; Kumar, 2018).

In addition, CD16 plays a special role among the activating receptors, as it can to induce antibody-dependent cellular cytotoxicity (ADCC). CD16 is an Fεcγ receptor, which can bind antibodies, such as IgG. Therefore, NK cells are able to recognize antibody-coated target cells and act as mediators between innate and adaptive immunity.

1.4.2 NK cell recognition of tumour cells

The 'missing self' hypothesis of Klas Kärre was the first attempt to describe the recognition of tumour cells by NK cells. This hypothesis is based on the observation that tumour cells expressing low or no MHC class I molecules are more susceptible to NK cells than healthy (MHC-I positive) cells (Kärre, 1985). Nevertheless, the lack of inhibitory signals alone was shown to be insufficient to trigger NK cell activation and initiate tumour cell lysis (Arnon et al., 2006; Lanier, 2005). In fact, the balance of signals derived from all activating and inhibitory receptors determines the final NK cell activation status (summarised in Figure 5) (Dustin and Long, 2010). Although, the weighting of single receptors is not known, the overall signals derived from the

inhibitor receptors tend to be stronger and overrule the signals from the activating receptors (Long et al., 2013). However, the integration of several activating stimuli can overcome the inhibitory signals, thus allowing the initiation of a cytotoxic signal cascade in the target cell (Cerwenka and Lanier, 2001).

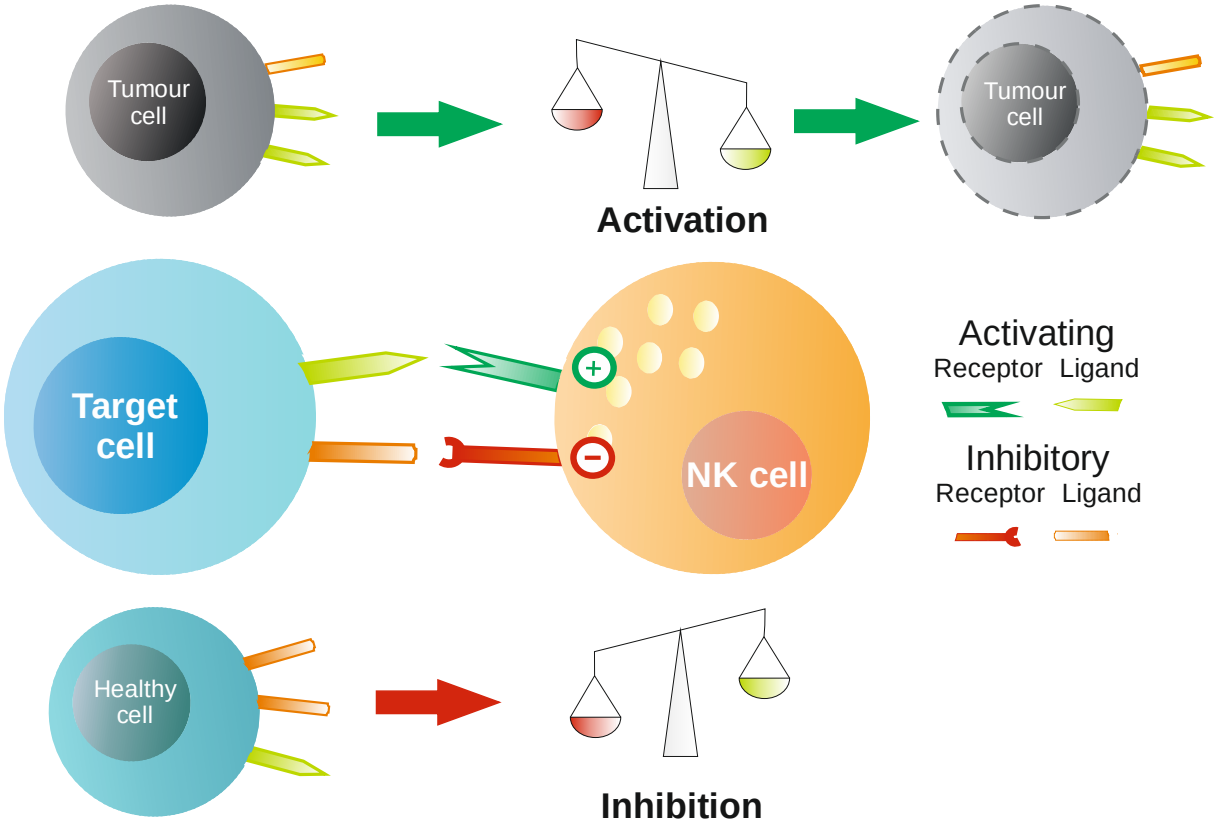

Figure 5. Principles of NK cell-mediated tumour recognition. NK cells have a large repertoire of activating and inhibitory receptors, which allow the recognition of tumour cells. The integration of all arriving stimuli determine the activation status of the NK cell. The engagement of many inhibitory ligands prevents an activation, whereas increasing activating stimuli can overcome NK cell inhibition, leading to the elimination of the target cell. Figure was adopted from (Cappello, 2015).

1.5 The cytotoxic effector mechanism

After the formation of an immunological synapse, NK cells are able to initiate a cytotoxic signalling cascade in target cells (summarised in Figure 6). The initiation point of this cascade has either an extrinsic or an intrinsic origin. Extrinsically, NK cells express ligands such as FasL or TRAIL (TNF-related apoptosis inducing ligand) that bind to death receptors such as Fas or TRAIL-R1/2 expressed on the target cell. This external receptor-ligand binding recruits FADD (Fas-Associated protein with Death Domain) that binds procaspase-8 and forms the death inducing signalling complex (DISC). Subsequent activation of caspase-8 initiates the caspase cascade (Russell and Ley, 2002). Although NK cells express death receptors, the intrinsic cytotoxic pathway mediated by lytic granules is more dominant (Cullen and Martin, 2008).

During the granule exocytosis pathway, granules containing perforin and granzymes, are secreted in the immunological synapse (Cullen and Martin, 2008). The calcium-dependent polymerisation of perforin monomers allows the formation of pores in the target cell membrane and endosomes uptaken by the target cell. These pores allow either the direct lysis of the target cell or the entry of granzymes into the target cell cytosol. Granzymes are serine proteases, which trigger the caspase cascade either through BH3-interacting domain death agonist (BID)-dependent mitochondrial permeabilisation or through a direct activation of caspase-3 (CASP3) (Cullen and Martin, 2008; Russell and Ley, 2002). Granzyme B mediates the partial proteolysis of the BH3-only protein BID, so that the truncated BID (tBID) can be targeted to the mitochondria. There, it initiates the oligomerisation of BAK (Bcl-2 homologous antagonist killer) and/or BAX (Bcl-2-associated X protein) in the outer mitochondrial membrane; thereby promoting cytochrome c release. Together with the apoptotic protease activating factor 1 (APAF-1) and procaspase-9, cytochrome c allows the assembly of a large complex. This so-called apoptosome leads to caspase-9 activation and the initiation of the caspase cascade. Extrinsic and intrinsic initiation of the cytotoxic effector mechanism lead to the activation of a final caspase (CASP3) that cause apoptosis (Cullen and Martin, 2008).

Furthermore, the activation of this cascade is supported by the parallel mitochondrial release of DIABLO (Direct IAP-binding protein with low PI). This second mitochondria-derived activator of caspases (Smac) inhibits the X chromosome-linked inhibitor of apoptosis (XIAP), thereby allowing the initiation of apoptosis (Martinez-Lostao et al., 2015). The mitochondrial outer membrane permeabilisation (MOMP) is further controlled by the anti-apoptotic Bcl-2 family, e.g. B-cell lymphoma 2 (BCL-2) that antagonizes the apoptosis mediators Bcl-2 homologous antagonist/killer (BAK) and Bcl-2-associated X protein (BAX). The members of the Bcl-2 family will be negatively regulated by BH3-only proteins such as Bcl2-associated agonist of cell death (BAD) (Martinez-Lostao et al., 2015).

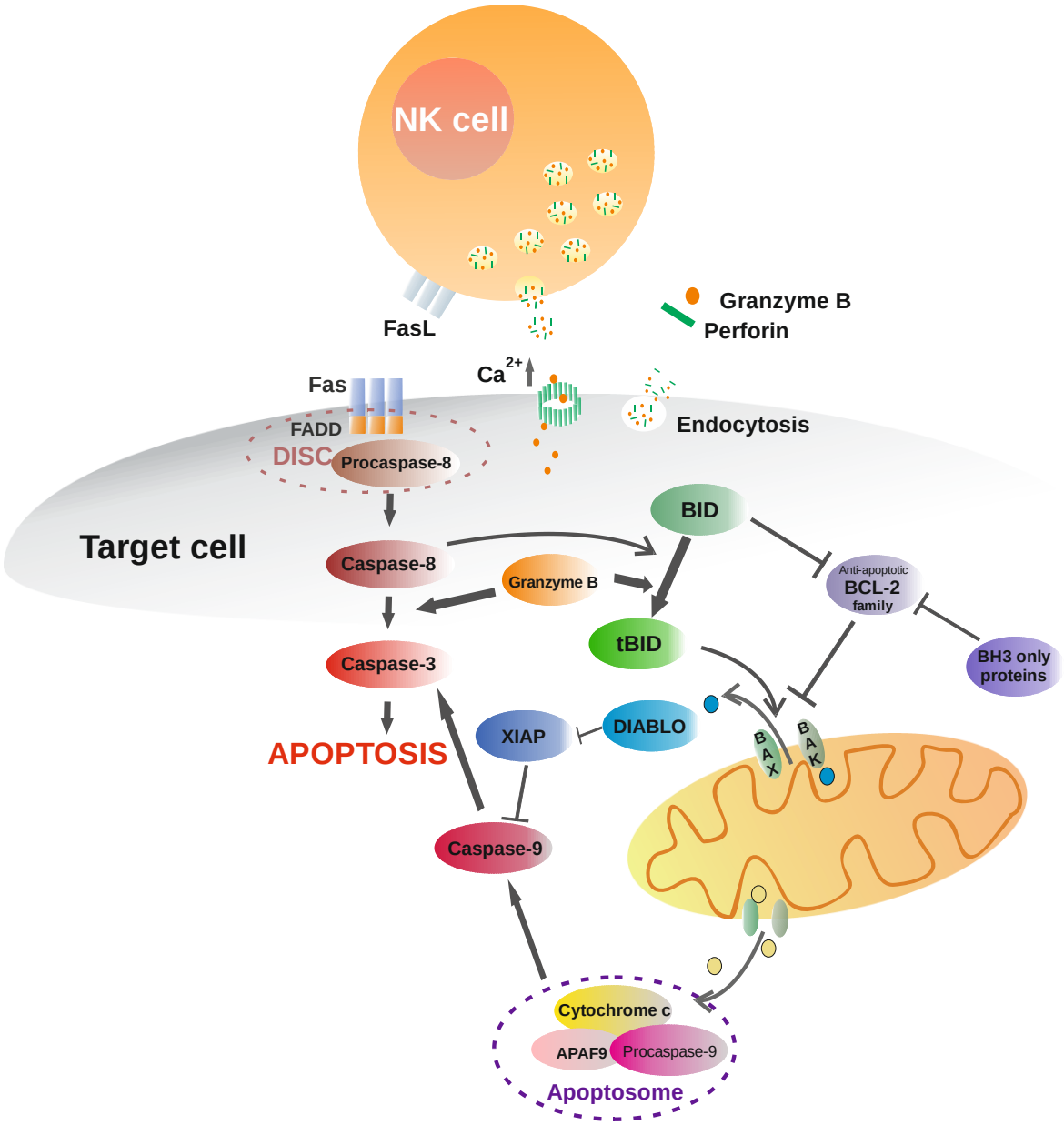

Figure 6. The cytotoxic signalling cascade. The cytotoxic signal cascade can be activated by the binding of the death receptor Fas to its ligand FasL (left). After the recruitment of FADD, that activates caspase-8, the final caspase-3 is activated and leads to the initiation of apoptosis. The release of lytic granules, containing granzymes and perforin represents the second mechanism starting the cytotoxic signal cascade (right). Calcium- dependent polymerisation of perforin forms pores in the target cell or endosomes so that the granzymes can enter the cell. Especially granzyme B leads to the release of cytochrome c from the mitochondria that activates caspase-3.

1.6 NK cells in cancer immunotherapy

NK cells play a crucial role in immune surveillance as their cytotoxic activity was shown to correlate with a generally lower cancer risk (Imai et al., 2000). Moreover, the number or type of tumour-infiltrating NK cells have been shown benefits in therapy response and overall patient survival in cutaneous melanoma (Cursons et al., 2019; Ladanyi, 2015) as well as in other cancers (Barry et al., 2018; Chiossone et al., 2018; Cursons et al., 2019). Nevertheless, the success of NK cells as a tool for immunotherapy against solid tumours belies expectations. One of the possible reasons for the past failure of these therapies may lie in the tumour microenvironment that could dampen NK cell activity (Paul et al., 2016; Terren et al., 2019). Accordingly, to maintain or even boost the NK cell activity in cancer patients, different therapeutic strategies have been developed. Cytokine-based therapies have been used to increase NK cell cytotoxicity. To this end, IL-2 was the first cytokine with the desired properties that showed initial promising results *in cellulo* and in animal-model based studies (Grimm et al., 1982; Hoffman et al., 1989; Miller and Lanier, 2019; Rosenberg et al., 1985). However, the systemic administration of IL-2 alone achieved only limited clinical response and had even toxic and life-threatening effects when applied at higher doses (Hoffman et al., 1989; Miller and Lanier, 2019). These unsatisfactory results by IL-2 supplementation can be, at least partially, explained by the unintended expansion and activation of immunosuppressive regulatory T cells (T_{regs}) (Miller and Lanier, 2019). Furthermore, the long-lasting administration of IL-2 induces the downregulation of the NK cell IL-2 receptors (Pillet et al., 2011). These difficulties can be circumvented by *ex vivo* activation as well as the use of other interleukins such as IL-15, IL-12, IL-18 or IL-21 (Nayyar et al., 2019; Zhang et al., 2020). IL-15 was shown to be the most promising therapeutic cytokine. IL-15 not only increased NK cell cytotoxicity more specifically (no cross activation of T_{regs}) but also enhanced NK cell expansion (Miller and Lanier, 2019). The administration of IL-15 achieved clinical success in haematopoietic cancers (Cooley et al., 2012; Nayyar et al., 2019) and showed also promising results in solid tumours including metastatic melanoma (Conlon et al., 2015). However, the short half-life of IL-15 and the observed toxicities at higher dosages are still limiting the clinical usage (Robinson and Schluns, 2017). The development of super-agonist complexes such as ALT-803 (IL-15N72D/IL-15Rα-FC) further improved the *in vivo* half-life time and the clinical efficacy (Felices et al., 2017).
Another approach to enhance NK cell cytotoxicity is to reduce the threshold of NK cell activation by lowering inhibitory stimulation. This can be achieved by blocking the engagement of KIR receptors with MHC class I molecules on the target cells. The use of allogeneic NK cells prevents the inhibition by self-MHC molecules and facilitates NK cell activation (Souza-Fonseca-Guimaraes et al., 2019). Unfortunately, this can also induce graft-versus-host effects, so that NK

cell donors with haploidentical HLA phenotypes are preferably used in adoptive cell transfer (ACT) (Souza-Fonseca-Guimaraes et al., 2019). Although, ACT has been successful in the treatment of haemopoietic cancers such as acute myeloid leukemia (AML) (Tanaka and Miller, 2020), so far it fails in the treatment of solid tumours (Paul and Lal, 2017). Also, the direct inhibition of KIR receptors with antibodies such as lirilumab was only effective in haematopoietic malignancies (Konjević et al., 2017; Miller and Lanier, 2019). Another important inhibitory NK cell receptor is CD94-NKG2A, that recognizes HLA-E, and can be blocked by the antibody monalizumab (Li and Sun, 2018). The administration of checkpoint inhibitors has been successful for T-cell activation. Moreover, tumour-infiltrating NK cells were also shown to express PD-1 (Liu et al., 2017b) and can thus benefit from checkpoint inhibitors (Sanseviero et al., 2019). Accordingly, the clinical successes of anti-PD-1 therapy might also be contributed by increased anti-tumour NK cell activity (Hsu et al., 2018; Pesce et al., 2019). Additional checkpoint inhibitors targeting different inhibitory NK cell receptors (TIGIT, IL1R8) require further investigation (Khan et al., 2020; Nayyar et al., 2019).

Another approach to boost anti-tumour NK cell activity is to strengthen the activating stimuli in order to overcome the inhibitory signals. Bi-specific antibodies, known as bi- specific killer engagers (BiKEs) promote the formation of an antigen-specific immunological synapse between NK cells and tumour cells and thereby enhance the NK cell-mediated killing of the antigen expressing target cell (Miller and Lanier, 2019; Shimasaki et al., 2020). One fragment of the BiKE binds to an activating NK cell receptor such as the CD16 receptor that induces ADCC (Felices et al., 2016). The part of the killer engager is directed against tumour associated antigens such as CD30 in Hodgkin lymphoma, CD33 in myelodysplastic syndromes, CD133 in colorectal cancer or human epidermal growth factor receptor 2 (HER2) in breast cancer (Li and Sun, 2018). To increase the NK cell cytotoxicity, tri-specific killer engagers (TriKEs) with additional linkage to IL-15 such as GTB-2550 (anti-CD16 x IL-15 x anti-CD33 TriKE) have recently entered their first clinical trials in haematopoietic malignancies (Miller and Lanier, 2019).

The use of NK cell lines (NKL, NK-92, KYHG-1, YT and NKG) derived from malignant NK cell leukemia or lymphoma has several advantages and opens new possibilities to modify effector cell cytotoxicity (Miller and Lanier, 2019). The most promising NK cell line for clinical application is NK-92. The IL-2 dependent NK-92 cell line is known to express several activating surface proteins and receptors such as CD56, NKG2D, NKp30 and NKp46 (Klingemann et al., 2016). Furthermore, it lacks most KIR receptors (with the exception of KIR2DL4) (Suck et al., 2016). However, the activating receptors NKp44 and CD16 are absent and other inhibitory receptors such as CD94/NKG2A and LIR-1 are expressed, hence lowering its cytotoxic potential (Suck et al., 2016). Nevertheless, NK-92 was approved by the U.S. Food and Drug

Administration (FDA) and was already applied in clinical trials including patients with renal carcinoma and malignant melanoma with modest success but good tolerance (Arai et al., 2008).
NK cell lines can be genetically modified to display different receptor profiles. For example, parental NK-92 cells lack CD16 expression and are therefore not able to mediate ADCC. The artificial expression of high-affinity CD16 (haNK) increases their cytotoxicity (Klingemann et al., 2016), a modification that was shown to be very effective in combination with tumour epitope specific monoclonal antibodies in preclinical studies (Williams et al., 2018). Even more advanced are NK cell lines, which have been armed with engineered chimeric antigen receptors (CARs). CARs targeted to specific tumour epitopes such as CD19, CD7 and CD33 in leukemia and lymphoma have successfully entered their first clinical trials (Kloess et al., 2019; Liu et al., 2020). Also preclinical studies in solid tumours directed against HER2 or epidermal growth factor receptor (EGFR) showed promising results (Paul and Lal, 2017).
In addition to NK cell lines, NK cells differentiated from human pluripotent stem cells (hPSCs) could be used as 'off-the-shelf' immunotherapy (Wang et al., 2019). HPSCs include human embryonic stem cells, hematopoietic stem/progenitor cells from umbilical cord blood and induced pluripotent stem cells (iPSCs) (Hu et al., 2019). These stem cell derived NK cells can be produced on a large scale and genetically modified (Nianias and Themeli, 2019; Shimasaki et al., 2020; Zhu et al., 2018).
One important aspect that might explain the modest clinical success of NK cell therapy in solid tumours so far, in comparison to hematopoietic malignancies are the immunosuppressive effects of the tumour microenvironment (see following chapter). Therefore, increasing number of clinical investigations try to improve the conditions for effector cells in the tumour. For example, several drugs can prevent the shedding of MICA/MICB and promote NK cell cytotoxicity against tumours (Ferrari de Andrade et al., 2018). Alternatively, soluble MICA/MICB can be neutralized by antibodies such as IPH4301 (Li and Sun, 2018; Nayyar et al., 2019). Also the secretion of other soluble factors such as transforming growth factor β (TGF-β) or adenosine in the tumour microenvironment was shown to suppress NK cell proliferation and function (Leone and Emens, 2018; Viel et al., 2016). The TGF-β neutralizing antibody Fresolimumab (GC1008) has been used in a Phase I study for the treatment of advanced malignant melanoma and renal cell carcinoma (Morris et al., 2014). Furthermore, Galunisertib (LY2157299 monohydrate), an inhibitor of TGF-β receptor 1 (TGFbR1) has also been evaluated in clinical trials in solid tumours (Fujiwara et al., 2015; Yingling et al., 2018).

1.7 Immunoediting of melanoma by NK cells

Immunosurveillance describes the process by which immune cells detect and kill tumour cells due to their tumour ligand profile. (Schreiber et al., 2011). Malignant melanoma cells are immunogenic as they express ligands on their cell surface that can be recognized by NK cells and other immune cells (Kleffel et al., 2015; Morgado et al., 2011; O'Donnell et al., 2019). Most melanoma cell lines (85 %) express at least one NKGD receptor ligand that is also present on all cytotoxic immune cells including NK cells and CTLs. The most frequently expressed ligands are MICA/MICB (80 %), whereas ULBPs (ULBP1, 15 %; ULBP2, 25 %; ULBP3, 20 %) are less common (Casado et al., 2009). Besides NKG2D, also natural cytotoxicity receptors, especially NKp30, and DNAM-1, are crucial for melanoma detection by NK cells (Besser et al., 2013; Carrega et al., 2009; Chan et al., 2010; Morgado et al., 2011). However, it is well known that cancer cells are very adaptable and can evade immune surveillance (Chouaib et al., 2014). This dynamic process of tumour cells altered immunogenicity during cancer progression is known as cancer immunoediting (see Figure 7). After an initial elimination phase, some tumour cells with lower susceptibility to immune cells arise. During an equilibrium phase, the tumour mass under permanent immune-selection pressure begins to show increasingly higher numbers of poorly immunogenic tumour cell subpopulations. When these variant immune-edited cells are allowed to proliferate unrestrained and they become the dominant tumour cell population, the tumour becomes largely resistant to immune detection and is no longer restrained, i.e. tumour cells proliferate and survive without elimination (Dunn et al., 2004; Zitvogel et al., 2006).

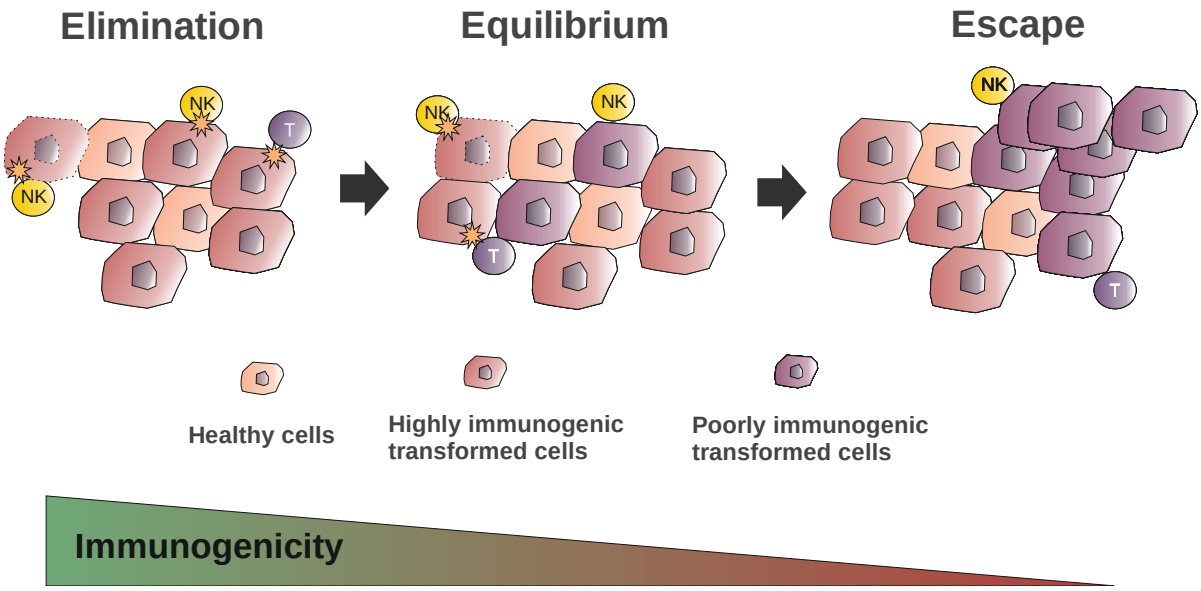

Figure 7. The immunoediting process. During the elimination phase, immune cells, here reflected by NK and T-cells, are able to kill most transformed cells. In the following equilibrium phase, immune cells can still control tumour growth, but tumour cells with lower immunogenicity arise and proliferate. With a continuing selection process, the immunogenicity of the tumour cells decreases and more cells elude immune cell recognition. These variant cells escape immune surveillance, proliferate and form a tumour. Figure was adopted from (Cappello, 2015).

In addition, melanoma cells transform their ligand profile to diminish their immunogenicity (Balsamo et al., 2012; Carretero et al., 2008). An often-observed mechanism of immune escape in tumours including melanoma is the shedding of the NKG2D ligands such as MICA/MICB and ULBP-2 (Paschen et al., 2009; Salih et al., 2002). This will not only occupy the NKG2D receptor, but also contribute to its downregulation (Konjevic et al., 2007). An enhancing factor in this process is TGF-β that lowers the expression of NKG2D and in addition decreases MICA, ULBP2 and ULBP4 expression on the melanoma surface (Casado et al., 2009; Morgado et al., 2011). In addition, the increase of MHC class I molecules on melanoma cell surfaces induced by IFN-γ has been reported (Balsamo et al., 2012; Stojanovic et al., 2013). Moreover, the general decrease of NCR ligands during melanoma progression and metastasis support the theory of immunoediting in melanoma (Morgado et al., 2011). Also soluble factors such as IDO (indoleamine 2,3 dioxygenase) and PEG2 (prostaglandin E2), released by the tumour cells, inhibit the expression of activating NK cell receptors and hence NK cell cytotoxicity (Pietra et al., 2012b).

Taken together, NK cells are a very promising tool for cancer immunotherapy. However, their full potential is currently not being exploited in the clinical practice. The reasons are multiple and complex and a better understanding of the factors influencing NK cell cytotoxicity is highly warranted.

1.8 Aims

Melanoma is the deadliest form of skin cancer with increasing incidence. It is characterised by a high metastatic potential and the development of resistance to currently available therapies. Although targeted therapies and immune checkpoint therapies have shown clinical success, the treatment response is variable and many patients still relapse after an initial effective treatment. Therefore, advancement and improvement of melanoma immunotherapies are of major interest and necessity. Natural killer cells are a promising tool for immune therapy, as they possess an innate cytotoxicity against tumour cells without prior sensitization.

In this doctoral thesis, I aimed to investigate the therapeutic potential of human natural killer (NK) cells against melanoma and to reveal new biomarkers that might predict which patients could best benefit from NK cell-based melanoma therapy. I addressed this purpose through the following aims:

1.) Determination of NK cell susceptibility of heterogeneous melanoma cell lines reflecting different disease stages and mutation status

2.) Identification and validation of melanoma biomarkers, which are related to the NK cell-mediated killing

3.) Unravelling of a protein signature, which helps to predict the susceptibility of unknown melanoma cell lines to NK cells

4.) Regulation of NK cell killing potential by manipulating killing related proteins

5.) Establishment and further characterisation of (long term) melanoma-NK cell-co-culture

2 Material

2.1 Antibodies

2.1.1 Primary antibodies

Table 1. Primary antibodies used, under specification of host organism, dilution, supplier and catalogue number

Antibody	Host organism	Dilution	Supplier	Catalogue number
Calnexin	rabbit	1:1,000	ENZO	ADI-SPA-860-F
Snail (L70G2)	mouse	1:500	CST	3895S
Smac/Diablo	mouse	1:500	CST	2954S

2.1.2 Secondary antibodies

Table 2. Secondary antibodies used, under specification of host organism, dilution, supplier and catalogue number

Antibody	Host organism	Dilution	Supplier	Catalogue number
IRDye 680LT Donkey	mouse	1:10,000	Licor	926-68022
IRDye 800CW Donkey	rabbit	1:10,000	Licor	926-32213

2.1.3 Fluorochrome labelled antibodies

Table 3. Fluorochrome labelled antibodies used, under specification of host organism, dilution, supplier and catalogue number

Antibody	Fluorochrome	Isotype	Supplier	Catalogue number
B7-H6	PE	IgG1, κ	R&D	FAB7144P
Mouse IgG1, κ Isotype Control	PE	IgG1, κ	R&D	IC002P
CD16	APC/Cy7	IgG1, κ	BioLegend	302017
Mouse IgG1, κ Isotype Control	APC7Cy7	IgG1, κ	BioLegend	400127
CD56 (NCAM)	PE/Cy7	IgG1, κ	BioLegend	318317
Mouse IgG1, κ Isotype Control	PE/Cy7	IgG1, κ	BioLegend	400125
CD314 (NKG2D)	PerCP/Cy5.5	IgG1, κ	BioLegend	320817
Mouse IgG1, κ Isotype	PerCP/Cy5.5	IgG1, κ	BioLegend	400149
CD337 (NKp30)	PE	IgG1, κ	BioLegend	325207

Antibody	Fluorochrome	Isotype	Supplier	Catalogue number
Mouse IgG1, κ Isotype Control	PE	IgG1, κ	BioLegend	400113
Granzyme B	Alexa Fluor® 647	IgG1, κ	BioLegend	515405
Mouse IgG1, κ Isotype Control (ICFC)	Alexa Fluor® 647	IgG1, κ	BioLegend	400135
HLA-A,B,C	Alexa Fluor® 647	IgG1, κ	BioLegend	311416
Mouse IgG1, κ Isotype Control	Alexa Fluor® 647	IgG1, κ	BioLegend	400234
MICA/MICB	Alexa Fluor® 488	IgG2a,κ	BioLegend	320912
Mouse IgG2a,κ Isotype Control	Alexa Fluor® 488	IgG2a,κ	BioLegend	400233
Perforin	FITC	IgG2b, κ	BioLegend	308103
Mouse IgG2b, κ Isotype Control	FITC	IgG2b, κ	BioLegend	400309
ULBP-2/5/6	PerCP	IgG2a	R&D	FAB1298C
Mouse IgG2a Isotype Control	PerCP	IgG2a	R&D	IC003C

2.2 Buffer solutions and other reagents

2.2.1 Purchased buffer solutions

Table 4. Purchased buffers used, under specification of supplier and catalogue number

Buffer solution	Supplier	Catalogue number
4x LaemmLi Sample buffer	Bio-Rad	1610747
Coulter Isoton ii Diluenz	Beckmann coulter	8448011
DPBS (1x) Dulbecco's Phosphate-Buffered Saline	Life Technologies	14190-094
Trans-Blot®Turbo™ 5x Transfer buffer	Bio-Rad	10026938

2.2.2 Prepared buffer solutions and other reagents

Table 5. Prepared buffer solutions used, under specification of composition and purpose

Buffer solution	Composition	Purpose
Bradford reagents	70mg Serva Blue G 50mL 96 % Ethanol 100mL of 85 % phosphoric acid Add $H_2O_{dest.}$ to 250mL	Determination of protein concentration
Erythrocyte lysis buffer	155 mM NH_4Cl 9,99 mM $KHCO_3$ 130 µM EDTA pH 7.3	PBMC isolation
Permeabilisation buffer	5 % FCS 0.5 % BSA 0.07 % NaN_3 0.1 % Saponin in 1x DPBS Sterile filtrated	Intracellular FACS staining
TGH buffer stock solution	1 % Triton X-100 10 % glycerol 50 mM NaCl 50 mM HEPES 1 mM EGTA 1 % sodium deoxycholate 53.5 mL $H_2O_{dest.}$ Sterile filtrated	Protein extraction
TGH lysis buffer always prepared fresh	88 % TGH buffer 1 mM Na_3VO_4 1 mM PMSF 1mM NaF 1x Complete (protease inhibitor)	Protein extraction
Trans-Blot®Turbo™ 1x Transfer buffer	20 % 5x Transfer buffer 20 % Ethanol 60 % $H_2O_{dest.}$	Western Blot
Stacking gel buffer	0.5 M Tris base 0.4 % SDS pH 6.8	SDS-PAGE
Separation gel buffer	1.5 M Tris base (Trizma) 0.4 % SDS pH 8.8	SDS-PAGE
10x Running Buffer	250 mM Tris base 1.92 M glycine 1 % SDS pH 8.3	SDS-PAGE

Buffer solution	Composition	Purpose
10x TBS: 1L	500 mM Tris-base 1.5 M NaCl pH 7.6	Western Blot
1x TBS-T	0.1 % Tween20 10 % 10x TBS 89.9 % $H_2O_{dest.}$	Western Blot

2.3 Chemicals

Table 6. Chemicals used, under specification of supplier and catalogue number

Chemicals	Supplier	Catalogue number
2-Mercaptoethanol	AppliChem	A1108
2-Propanol	Sigma	19516
7-Aminoactinomycin (7-AAD)	Sigma	A9400-1MG
Acrylamid Rotiphorese Gel 40	Roth	A515.1
Ammoniumchlorid (NH_4Cl)	Sigma-Aldrich	A0171
Accutase® solution	Sigma Aldrich	A6964
Agar	AppliChem	A-3858
Ammoniumpersulfat (APS)	Sigma Aldrich	A3678
Bovine Serum Albumin (BSA)	Sigma-Aldrich	A9418
Bromophenol Blue	Sigma-Aldrich	B0126
Calcium chloride ($CaCl_2$)	Sigma-Aldrich	21115
Calcein- AM	Life Technologies	C1430
Chloroform	Fisher Scientific	15677730
Complete (Proteinase Inhibitor)	Roche	04 693 132 001
Dimethyl sulfoxide (DMSO)	Sigma-Aldrich	D8418
Diethylpyrocarbonat (DEPC)	Sigma	C5758
EDTA	Sigma-Aldrich	ED2SS
Ethanol ROTIPURAN®	Roth	9065
Ethylene glycol-bis (2-aminoethylether) -N,N,N',N'-tetraacetic acid (EGTA)	Sigma-Aldrich	E3889
Fetal calf serum (FCS)	Sigma	F7524
Glycerol	Sigma-Aldrich	G2025
Glycogen	Fisher Scientific	10814010

Chemicals	Supplier	Catalogue number
HEPES	Sigma-Aldrich	H-7523
Horse serum	Thermo fisher	16050122
Interleukin 2, human (IL-2)	Life Technologies	15596-026
Insulin, human	Sigma-Aldrich	I9278
Isopropanol	AppliChem	A3928
Kanamycine	Sigma	60615
L-Glutamine solution	Life Technologies	67513
Methanol	Sigma-Aldrich	34860
Paraformaldehyde (PFA)	Polysciences Inc.	380
Potassium bicarbonate ($KHCO_3$)	Aldrich	237205
Phenylmethanesulfonyl fluoride (PMSF)	Sigma-Aldrich	P7626
Phosphoric acid 85 %	Roth	9079
Saponin	Sigma	S7900
Serva Blue G	SERVA	35050
Sodium azide (NaN_3)	Sigma-Aldrich	S2002
Sodium chloride (NaCl)	Roth	9265.1
Sodium fluoride (NaF)	Sigma-Aldrich	S7920
Sodium deoxycholate ($C_{24}H_{40}O_4$)	Sigma-Aldrich	30970
Sodium dodecyl sulfate (SDS)	BioChemica	A2572
Sodium hydrogen carbonate ($NaHCO_3$)	MERK	6329
Sodium orthovanadate (Na_3VO_4)	Sigma-Aldrich	S6508
Tetramethylethylenediamine (TEMED)	Sigma	T7024
TRIS PUFFERAN®	Roth	5429
Triton X-100	Eurobio	18774
Trizol	Life Technologies	15596018
Trypan Blue Stain (0.4 %)	Life Technologies	15250-061
Tryptone	AppliChem	A1553
Tween 20	AppliChem	A4974
Yeast extract	AppliChem	A1552

2.4 Inhibitors

Table 7. Inhibitors under specification of the targeted protein, supplier and catalogue number

Inhibitor	Target	Supplier	Catalogue number
NVP-BKM120	PI3K	Selleckchem	S2247
Rapamycin	mTOR	Selleckchem	S1039
RiboLock	RNase A,B,C	Life Technlogies	E00382
MK2206 2HCL	AKT1/2	Selleckchem	S1078

2.5 Kits

Table 8. Kits under specification of supplier and catalogue number

Kit	Supplier	Catalogue number
Cell Titer Blue Cell Viability Assay	Promega	G8081
Dynabeads® Untouched™ Human NK Cells Kit	Life Technologies	11349D
GoTaq®qPCR Master Mix	Promega	A6002
HiSpeed Plasmid Maxi Kit	Qiagen	12662
INTERFERin® siRNA transfection reagent	Polyplus	409-10
Nucleospin® RNA Plus Kit	Macherey-Nagel	740984.250
Superscript®IV Reverse Transcriptase Kit	Invitrogen	18090050
Trans-Blot® Turbo™ RTA Mini Nitrocellulose Transfer Kit	Bio-Rad	1704270

2.6 Laboratory consumables

All general laboratory consumables, e.g. pipettes, reaction tubes, cell culture flasks, were purchased through Sarstedt (Nürnbrecht, Germany) or VWR (Randor, Pennsylvania, USA). Other special consumables are referred to in the respective method section.

2.7 Laboratory devices

Table 9. Laboratory devices under specification of manufacturers and purpose

Device	Designation	Manufacturers	Purpose
96 well plate reader	Infinite M200 Pro	Tecan	Real-time Killing Assay
	CLARIOStar®	Bmglabtech	Proliferation
	Mithras LB940	Berthold technologies	Bradford CytoTox 96® Non-Radioactive Cytotoxicity Assay
Cell counter	Z2 coulter particle count and size analysis	Beckman Coulter	Determination of cell numbers
	Countess II FL	Life technologies	
Centrifuges	5415 C	Eppendorf	Obtaining cell pellet
	5415R		
	54150		
	Minispin		
	Universal 30 F	Hettich	
	Universal 32 R		
	Labofuge 400R	Heraeus	
	Biofuge fresco		
	Megafuge 40R		
	Fresco17	Thermoscientific	
Electrophoresis system	Mini-PROTEAN® Tetra System	Bio-Rad	SDS-PAGE
Flow cytometer	FACS Canto II FACS Verse	BD BD	Receptor/Ligand profile
Heating block	ThermoMixer F2.0	eppendorf	Protein/DNA denaturation
Imaging system	Odyssey® CLx	LI-COR Bioscinces	Membrane imaging
Incubator	CB53	Binder	Cell cultivation
	HERASAFE	Heraeus	
	Biowizard Silverline	KOJAIR	
Magnets	DynaMag- 50 DynaMag-15	Invitrogen	NK cell isolation
Mikroscope	CK30	Olympus	Validation of cell viability and transfection efficiency
	Primovert Telaval 31	Zeiss	

Device	Designation	Manufacturers	Purpose
pH meter	pH/Ion level 2	ionoLab	Adjustment of pH
Power supply	PowerPac™ Basic	Bio-Rad	SDS PAGE
Quantitative PCR instrument	Stratagene-Mx3000P	Agilent	qPCR
Rocker shaker	PMR-30	Grant-bio	Homogeneous Solution mixing
	MS1	IKA Labortechnik	
	Hula Mixer	Invitrogen	
Spectrophotometer	Nanodrop 2000C	Thermoscientific	Determination of RNA concentration and quality
Thermal Cycler	C1000™	Bio-Rad	DNA amplification
Transfer sytsem	Trans-Blot®Turbo™	Bio-Rad	Western Blot
Vortex mixer	Vortex Genie 2	Scientific Industries	Preparation of solutions

2.8 Media

2.8.1 Purchased media

Table 10. Purchased media under specification of supplier and catalogue number

Medium	Supplier	Catalogue number
AIMV	Life Technologies	12055-091
HBSS - Hank's Balanced Salt Solution	PAA	H15-009
Leibovitz's L-15 Medium	Biochrom AG	F1314
Lymphocyte Separation Medium 1077	PromoCell	C-44010
M2 Melanocyte Medium	PromoCell	C-24300
MCDB153- Basalmedium	Biochrom AG	F 8105
MEM Alpha Medium	Life Technologies	11900-016
Opti-MEM®	Thermo Fisher	31985088
RPMI-1640	Life Technologies	21875-034

2.8.2 Prepared media

TU-Medium, 2 % FCS (500 mL):

400 mL MCDB153- Basalmedium

100 mL Leibovitz's L-15 Medium

10 mL FCS

840 µL $CaCl_2$ (stock solution: 1M)

250 µL Insulin (stock solution: 10 µg/mL)

Sterile filtrated

NK-92 cell medium (MEMα*):

MEM Alpha Medium powder was dissolved in 950 mL $H_2O_{dest.}$ and 29.3 mL 7.5 % soln. $NaHCO_3$. Afterwards, the pH was adjusted to 7.0-7.4 and the solution was filled up to 1000 mL.

400 mL MEM Alpha medium was supplemented with:

12.5 % FCS

12.5 % Horse serum

2 mM L-Glutamine

And always supplemented freshly with 10 ng/mL Interleukin-2

Lysogeny broth (LB)-medium (1 l):

10 g Tryptone

10 g NaCl

5 g yeast extract

2.9 Oligonucleotides

2.9.1 qRT-PCR Primer

Table 11. qRT Primer used, under specification of target mRNA, forward as well as reverse primer sequence

Target mRNA	Forward primer 5´-3´	Reverse primer 5´-3´
SNAI1	ACCCCAATCGGAAGCCTAACT	GGTCGTAGGGCTGCTGGAA
TATA-binding protein (TBP)	CGGAGAGTTCTGGGATTGT	GGTTCGTGGCTCTCTTATC

2.9.2 Silencing RNA (siRNA)

Table 12. Silencing RNA used, under specification of target gen and sequence, concentration as well as supplier

Target mRNA	Target gen	Concentration	Target sequence 5‘-3‘	Supplier
DIABLO_1	DIABLO	40 µM	GGAAACCACUUGGAUGACU	Microsynth
DIABLO_2	DIABLO	40 µM	GCAGAUCAGGCCUCUAUA	Microsynth
Non-silencing	None (control)	40 µM	unknown	Microsnyth

2.9.3 Other mono-/oligonucleotides

Table 13. Nucleotides used, under specification of supplier and catalogue number

Nucleotides	Supplier	Catalogue number
Oligo(dT)$_{12-18}$ Primer	Invitrogen	18418012
dNTP mix	Invitrogen	18109017

2.10 Cell lines

Human melanoma cell lines were previously described (Garman et al., 2017; Satyamoorthy et al., 2003) and were a gift from Meenhard Herlyn (The Wistar Institute, Philadelphia, USA). Human melanocytes were used for comparisons to the melanoma cells in RNA sequencing and were provided by Dr. Hedwig Stanisz-Bogeski (Dermatology, Universitätsmedizin Göttingen, Göttingen). The melanocytes were isolated from neonatal foreskins obtained after donor circumcision. The cell lines K562 and NK-92 were provided by ATCC and DSMZ, respectively.

Table 14. Cell lines used, under specification of disease and mutation status according to Rockland Immunochemicals, Inc.; web site, https://rockland-inc.com/melanoma-cell-lines.aspx. The mutation data of the cell line K562 was obtained from the Sanger Institute Catalogue of Somatic Mutations in cancer; web site, http://www.sanger.ac.uk/cosmic. ND= not detected; N/A = not available

Melanoma cell line	Disease Stage	Mutation status of		
		BRAF	PTEN	N-RAS
1205Lu	Lung metastasis Xenograft	V600E	Mu/Hem Del	WT
451Lu	Lung metastasis Xenograft	V600E	WT	WT
WM1366	Primary (VGP)	WT	WT	WT
WM164	Metastasis	V600E	WT	WT
WM3268	Primary (VGP)	WT	ND	Q61K
WM3482	Metastasis	V600E	WT	WT
WM3682	Lymph node metastasis	WT	WT	Q61L
WM3734	Brain metastasis	V600E	ND	WT
WM3918	Metastasis	WT	ND	WT
WM47	Metastasis	V600E	ND	WT
WM793	Primary (VGP)	V600E	Mu/Hem Del	WT
WM88	Lymph node metastasis	V600E	WT	WT
WM858	Lymph node metastasis	V600E	WT	WT
WM9	Lymph node metastasis	V600E	Hem Del	WT
WM902B	Primary (VGP)	V600E	Hem Del	WT
WM983B	Lymph node metastasis	V600E	WT	WT
Other cell lines	**Disease**	**Mutation status of**		
		BRAF	PTEN	NRAS
K562	Chronic myelogenous leukemia	WT	WT	WT
NK-92	Non-Hodgkin's lymphoma	N/A	N/A	N/A

2.11 Plasmids

Table 15. Mammalian expression plasmids used, under specification of backbone, supplier, catalogue number and publication

Plasmid	Backbone	Supplier	Catalogue number	Publication
pSMAC-GFP	peGFP-N1	Addgene	40881	(Tait et al., 2010)
GFP Snail WT	peGFP-C1	Addgene	16225	(Zhou et al., 2004)
peGFP-C1	-	BD Bioscience Clontec	6084-1	
pmaxGFP™	pmax	LONZA	V4XC-2032	Included in Lonza nucleofection kits

3 Methods

3.1 Subculturing of cell lines

The suspension cell lines K562 and NK-92 were subcultured three times a week and incubated in hydrophobic cell culture flasks (83.3910.502, Sarstedt). Depending on the splitting ratio (1:10 over the week and 1:12 over the weekend) a part of the K562 cell suspension was transferred to a cell culture flask with fresh RPMI, 10 % FCS.

NK-92 cells are sensitive to density and were always adjusted to a cell number of 3 x 10^5/mL during the week and to 2 x 10^5/mL over weekends. The complete cell solution was transferred to a 50 mL tube and centrifuged (200 x g, 5 min) to remove dead cells and debris. The cell pellet was resuspended in 1 mL MEMα* and the cell number was determined. The required cell number was transferred to a new cell culture flask and filled up to 25 mL medium with 10 ng/mL IL-2. This cell line was cultured in standing cell culture flasks to reduce the attachment surface and optimise cell density.

Melanoma cells are adherent and they were regularly subcultured twice a week. Used medium and debris were discarded by removing the used medium supernatant and washing the cells with 1x DPBS. To detach the melanoma cells from the cell culture flask and loose cell-cell contacts, 1 mL accutase® solution, an enzyme mixture, was added. After 3 min, the detached cells were resuspended in fresh cell culture medium and a part of this cell suspension was transferred to a new cell culture flask for adherent cells (83.3911.002, Sarstedt) and additional medium was added to a final volume of 12 mL. The usual splitting ratios and used cell culture media of each cell line is summarised in Table 16 . The cells were further cultured in humidified incubators at 37 °C and with a 5 % CO_2 atmosphere.

Table 16. Splitting ratio of cells under specification of culture properties, medium and splitting ratio

Melanoma cell line	Medium	Splitting ratio
1205Lu	TU, 2 % FCS	1:5
451Lu	TU, 2 % FCS	1:3
WM1366	TU, 2 % FCS	1:6
WM164	TU, 2 % FCS	1:5
WM3268	TU, 2 % FCS	1:3
WM3482	TU, 2 % FCS	1:3
WM3682	TU, 2 % FCS	1:4
WM3734	TU, 2 % FCS	1:3

Melanoma cell line	Medium	Splitting ratio
WM3918	TU, 2 % FCS	1:4
WM47	TU, 2 % FCS	1:4
WM793	TU, 2 % FCS	1:4
WM88	TU, 2 % FCS	1:4
WM858	TU, 2 % FCS	1:6
WM9	TU, 2 % FCS	1:4
WM902B	TU, 2 % FCS	1:5
WM983B	TU, 2 % FCS	1:5
Suspension cell line	**Medium**	**Splitting ratio**
K562	RPMI, 10 % FCS	1:10
NK-92	MEMα*	2-3 x 10^5 cells/mL

3.2 Determination of cell number

The determination of cell number is a crucial step in many experiments. Cells were either counted using the Z2 coulter particle and size analysis from Beckmann Coulter or by the Countess II FL Automated counter from Fisher Scientific. The first apparatus is a Coulter counter that counts and measures cell size in suspension by detecting the changes in electrical resistance of the liquid. The cell suspension was diluted with Coulter Isoton ii Diluenz (1:200). A volume of 500 µL from this prepared solution was drawn trough the micro channels and cells that have a defined size range were counted. The displayed cell number in 1 mL has to be multiplied by the dilution factor 200 to get the original cell density. The second cell counting method is based on using a haemocytometer. The cell suspension was diluted 1:1 with trypan blue that will stain only dead cells. Then, 10 µL of this solution was loaded to a reusable glass slide (cell lines) or disposable slides (blood samples). The instrument from Fisher Scientific automatically counts cells with set size, shape and brightness.

3.3 Plasmid preparation

1 µg/µL plasmid was added to chemical competent *E.coli* XL1 blue cells and incubated for 30 min on ice. Subsequently, the cells were heated to 42 °C for 45 sec. After a second incubation of 2 min on ice, the cells were added to 250 µL lysogeny broth (LB) medium and incubated for 1 h at 37 °C and 300 rpm. Then bacteria suspension was plated to agar plates with kanamycin for

bacterial selection. After over-night incubation, one bacteria clone was picked and added to 5 mL LB medium supplemented with kanamycin. After few hours of incubation at 37 °C and 300 rpm, 1 mL of this pre bacteria culture solution was transferred into 150 mL kanamycin supplemented LB medium and was incubated for another night at 37 °C and 300 rpm. Subsequent plasmid purification was performed using HiSpeed Plasmid Maxi Kit of QIAGEN according to the manufacturer's instructions.

The LB culture was centrifuged at 2500 x g for 15 min at 4°C. The bacteria pellet was resuspended in 10 mL Buffer P1 (supplemented with RNAse and LyseBlue reagent). Subsequently, 10 mL Buffer P2 was added and the reaction tube was inverted 4–6 times until the solution was turned blue. After an incubation (5 min, RT), 10 mL prechilled buffer P3 was added and the solution was mixed by inverting until it was completely colorless. Then the lysate was poured into the barrel of the QIAfilter Cartridge and was incubated for 10 min at RT. In the meantime, the HiSpeed Tip was equilibrated with 10 mL Buffer QBT. Then the cell lysate was filtered into the equilibrated HiSpeed Tip by inserting the plunger into the QIAfilter Cartridge. Afterwards, the HiSpeed Tip was washed with 60 mL Buffer QC. The DNA was eluted with 15 mL Buffer QF and was precipitated by adding 10.5 mL isopropanol. After a short mixing, the eluate–isopropanol mixture was incubated for 5 min. During this incubation, the QIAprecipitator was placed over a waste bottle. Afterwards, the mixture was transferred into the syringe and the plunger was inserted under constant pressure in order to filter the eluate–isopropanol mixture through the QIAprecipitator. To wash the DNA, this process was repeated with 2 mL 70 % ethanol. Then the membrane was dried by pressing air through the QIAprecipitator forcefully several times. Finally, the DNA was eluated into a collection tube by filtering 1 mL Buffer TE to a new 5 mL syringe This eluate was transferred to the 5 mL syringe and elute for a second time into the same 1.5 mL tube.

3.4 Transient transfection

Genes of interest can be overexpressed or downregulated by introducing artificial genetic material such as DNA or RNA into melanoma cells.

3.4.1 Plasmid DNA transfection

The FuGene® HD transfection reagent was used to add plasmids (circular DNA molecules) into melanoma cells. This transfection reagent belongs to the chemical non-liposomal transfection methods and is characterised by a high transfection efficiency and reduced toxicity to the cells.

Melanoma cells (7 x 10^5) were seeded into 60 mm cell culture dishes one day before transfection. Opti-MEM® and FuGene® reagent were pre-warmed to room temperature. After the equilibration, 2.3 µg of the plasmid was diluted in 230 µL Opti-MEM®. Then 9.2 µL of FuGene® transfection reagent was added and the components were mixed. During 15 min of incubation at RT, the FuGene® transfection reagent forms vesicles containing the construct. Afterwards 240 µL of the transfection mixture was added dropwise to the dish. The prepared dishes were further incubated at 37 °C and 5 % CO_2. To remove the remaining transfection reagent, the medium was changed 6 h after transfection. The dishes were further cultivated in the incubator until used for experiments.

3.4.2 siRNA transfection

Genes were silenced by RNA interference (RNAi) using the transfection reagent INTERFERin®. The cells are transfected with siRNA that can bind to its target mRNA and form a double stranded RNA molecule (dsRNA). This dsRNA is cleaved with the help of the RNA-induced silencing complex (RISC) and thereby hinder the subsequent protein translation. Melanoma cells (7 x 10^5) were seeded into 60 mm dishes one day before transfection. Then, 1 nM siRNA was diluted in 100 µL Opti-MEM®, with mixing. After adding 2 µL INTERFERin® the solution was homogenized immediately. In the subsequent incubation of 20 min, the siRNA and INTERFERin® formed transfection complexes. In the meantime, half of the growth medium was replaced by fresh culture medium. After complex formation, 100 µL of the transfection mixture was added and homogenized by gently swirling the dish. For further cultivation, the dishes were incubated at 37 °C and in 5 % CO_2.

3.5 Cell proliferation and viability assay

Important hallmarks of cancer development include uncontrolled proliferation and survival (Hanahan and Weinberg, 2011). The determination of cell proliferation/survival potential can give information about melanoma cells' aggressive nature/status/phenotype/cell cycle. Furthermore, the efficacy of drugs can be estimated and the ideal drug concentration can be determined by monitoring tumour cell proliferation and viability. In this study, the CellTiter-Blue® Cell Viability assay was used to monitor cell behavior. This assay is based on the indicator dye resazurin. Metabolites of viable cells reduce resazurin into resorufin that differs in its spectral properties (Ex: 579 nm, Em: 584 nm). This change in fluorescence can be detected and can be used to determine the number of viable cells.

If not stated differently, 50,000 melanoma cells were resuspended in 200 µL medium/well and were seeded to a black, clear bottom 96-well plate. When melanoma cells were treated with drugs, the cells were resuspended in 50 µL medium and seeded in the wells. Then, the remaining 50 µL medium containing different drug concentrations was added. Furthermore, additional medium controls were prepared to subtract background signal. The plates were incubated for 2 h, 24 h, 48 h, 72 h at 37 °C and 5 % CO_2. After the indicated time, 20 µL of CellTiter-Blue® reagent were added to each well and mixed. After 3 h, the fluorescence signal of resorufin was measured with the plate reader Mithras LB940 of Berthold Technologies. The absolute fluorescence signal was normalised to the starting (t = 2 h) values.

Taken that cancer cells have often an uncontrolled cell cycle, the obtained fluorescence signal not necessarily correlate with cell number. The production of metabolites between different melanoma cell lines might differ a lot, so that the proliferation potential of different cell lines was determined by counting the melanoma cell numbers (see chapter 3.2.).

3.6 Isolation of peripheral blood mononuclear cells

Peripheral blood mononuclear cells (PBMCs) are isolated from leucocyte reduction chambers (LRS chambers). These are a waste product from the thrombocyte donation of the local blood banks of the Institute of Transfusion Medicine at the UMG and the Institute of Clinical Hemostaseology and Transfusion Medicine at UKS.

For the isolation, 17 mL of the lymphocyte separation medium 1077 was filled in a leucosep tube. During the following centrifugation (1000 x g, 30 s, RT), the medium was pressed through the filter to allow subsequent blood cell separation by a density gradient. The LRS chambers were adjusted above the leucosep tube so that after cutting, the lower and upper pipe of the LRS chamber allowed a steady blood flow (Knorck et al., 2018). After the separation medium was overlayed with blood, the LRS chamber was flushed with 20 mL HBSS to remove the remaining blood. Subsequently, the leucosep tubes were filled with HBSS to dilute the blood and facilitate the cell separation. In the next centrifugation (450 x g, acceleration: 1, deceleration: 0, 30 min, RT) the blood cells migrated depending on their density and formed different visible layers. The white leucocyte ring was localized between the yellow blood plasma and the transparent separation medium above the leucosep filter. This leucocyte ring was transferred to a fresh 50 mL tube, filled up with HBSS and centrifuged (250 x g, 15 min, RT). Remaining erythrocytes in the cell pellet were lysed by the use of erythrocyte lysis buffer (2-3 mL, 2 min). To stop the activity of this buffer, the 50 mL tube was filled up with HBSS and was centrifuged (200 x g, 10 min, RT).

After that, the cell pellet was resuspended in 20 mL cold isolation buffer (1x DPBS + 5 % FCS). The PBMCs were stored at 4 °C until further use.

3.7 Isolation of natural killer cells

Natural killer cells (NK cells) were isolated with the Dynabeads® Untouched™ Human NK cells Kit from Life Technologies. The following protocol is based on 100 x 10^6 PBMCs:

The PBMC cell suspension was transferred to a 15 mL tube and centrifuged (220 x g, 8 min, 4 °C). Thereafter, the cell pellet was resuspended in cold isolation buffer (1x DPBS + 5 % FCS) and 200 µL FCS as well as 200 µL antibody mix was added. This mix contains antibodies for CD3, CD14, CD36, CDw123, HLA class II DR/DP and CD235a (Glycophorin A) that target erythrocytes and all lymphocytes, excluding NK cells. Additional FCS reduced unspecific binding of the antibodies. During this incubation (20 min), 1 mL Dynabeads® solution was washed with equal volume of isolation buffer by using the Dyna-Mag 15 magnet and placed on ice until next use. After antibody incubation, 20 mL isolation buffer was added and gently mixed to remove unspecific-bound antibodies. Then the cell suspension was centrifuged (350 x g, 8 min, 4 °C) and the cell pellet was resuspended in 1 mL isolation buffer. The resuspended cells were added to the washed Dynabeads® that bind the antibodies, which cover the non-required PBMCs. A subsequent incubation of 15 min at RT was stopped by adding 10 mL cold isolation buffer. The tube containing the cell-Dynabeads® solution was placed in the Dyna-Mag 15 magnet for approx. 6 min. All lymphocytes that were loaded with Dynabeads® were pulled to the walls of the tube by magnetic attraction. The NK cells were found in the clear, magnet bead free, supernatant that was transferred to a new tube. The remaining Dynabeads® were resuspended with 10 mL isolation buffer and the magnet isolation process was repeated. In the last step, the magnet isolation procedure was repeated with the united supernatants to remove remaining Dynabeads® from the NK cell solution. Finally, the purified NK cell suspension was centrifuged (200 x g, 8 min, RT) and NK cells were resuspended in AIMV + 10 % FCS and seeded into 24 well plate (2 x 10^6/ mL).

3.8 Modulation of NK cell activity

3.8.1 Stimulation with Interleukin-2

After isolation, NK cells were stimulated with 0.05 μg/mL IL-2. This procedure extends the cultivation period and augments NK cell cytotoxicity to tumour cells in general (Henney et al., 1981), but also to melanoma cells by increasing the numbers of activating receptors on the NK cell surface (Morgado et al., 2011).

3.8.2 Irradiation

Unwanted proliferation of NK cells in the co-culture experiments was blocked by irradiation (30 Gy, Cs 137 γ-emitter) that will induce apoptosis after 6 hours in NK cells (Seki et al., 1994) and will limit their survival.

3.9 Real-time Killing Assay

The key experimental technique used in this study is the real-time killing assay, which was applied to evaluate the susceptibility of melanoma cells towards NK cells. In comparison to other established cytotoxicity assays, it allows a kinetic resolution of the killing process (Kummerow et al., 2014). The cytotoxic assay is based on the detection of calcein-AM labeled target cells that release the fluorescent dye during the killing process (Figure 8). Although NK cells preferentially lyse target cells, a part of the targets are also killed via apoptosis or even via a mixture of both killing types (Backes et al., 2018). The time course of NK cell-induced target cell apoptosis can vary but was shown to last around 38 min on average. In contrast, target cell lysis required only ~7 min (Backes, 2016). Therefore, NK cell-mediated apoptosis might be not detected at the initial phase of the assay but in its further course. Nevertheless, the real-time killing assay is a suitable method to investigate the principles of the NK cell-induced cytotoxicity against melanoma cells (NKiToxMel).

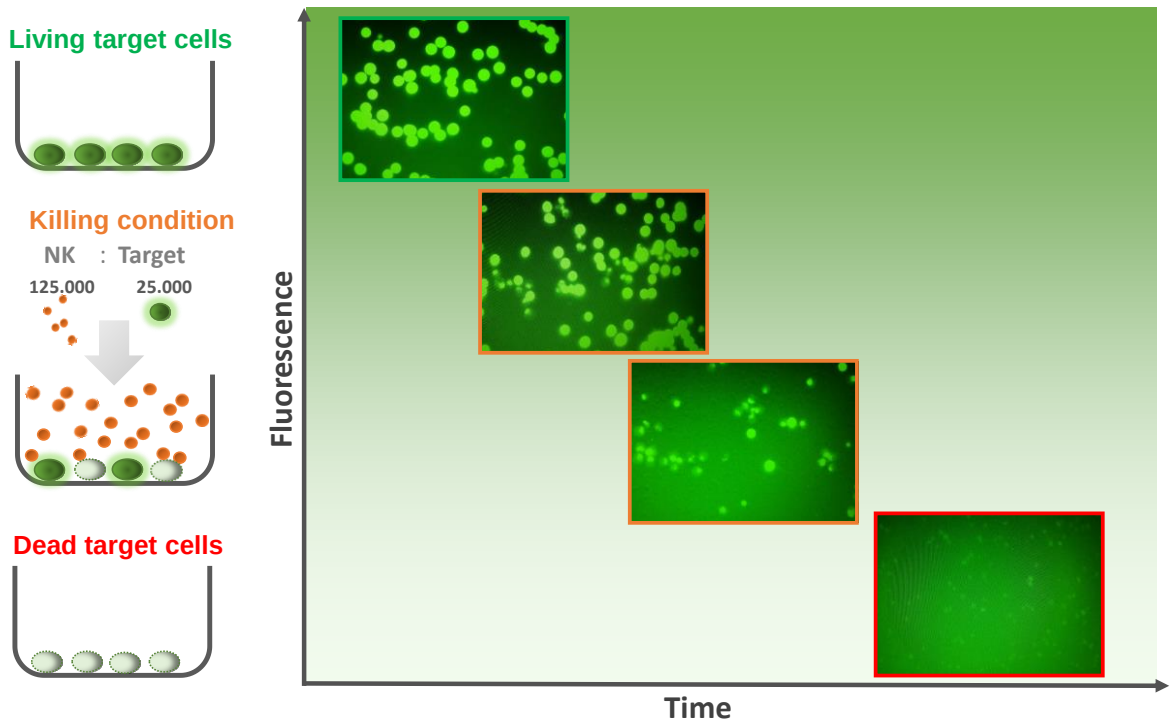

Figure 8. Real-time killing assay. Target cells were loaded with 0.5 µM calcein-AM and seeded in a 96-well plate (25,000 / well). After target cells were settled, NK cells (125,000 NK cells; E:T ratio of 5:1) were added to the destined wells. The NK cell-mediated killing of melanoma cells was detected and recorded by the decrease of fluorescence signal. Living target cells and Triton X-100 lysed cells were used as controls.

The target cells were loaded with 0.5 µM calcein-AM for 15 min under continuous rotation and darkness. The acetoxymethyl ester (AM) group allows the passive diffusion of the dye into the cell. The cellular esterases cleave the AM group from the dye and prevent the leakage from the cell. To remove remaining fluorescence solution, the cells were washed with AIMV* (AIMV with 10 mM HEPES). Then the cell number was determined and the target cells were seeded (25.000 cells in 200 µL / well) into a black, clear bottom 96-well plate (BD, 353219). After at least 20 minutes at room temperature, the target cells were settled and the effector cells (125,000 NK cells/ 50 µL) were slowly added to the destined wells. During NK cell-mediated lysis of the target cells, calcein-AM is released into the supernatant. The decrease of fluorescence signal can be detected by plate readers. Immediately after the effector cells were added, the fluorescence was measured. To determine the cytotoxicity, additional controls were needed. Target cells lysed by 20 µL lysis buffer (AIMV*+10 % triton X) were used as a positive control (100 % killing), whereas non-treated living target cells were used as a negative killing control. Corresponding background controls used were 250 µL AIMV* medium and 250 µL AIMV* medium with 20 µL lysis buffer. The single conditions were pipetted in triplicates to minimize variance of fluorescence during the 4 h measurement. To record the fluorescence over time (4 h, every

10 min) the plate readers infinite M200 Pro from Tecan (AG Hoth, Universität des Saarlandes) and the CLARIOSTAR® from BMG labtech were used.

Reader conditions:

M200 Pro:

Kinetic measurement; Kinetic cycles: 25; Interval time: 10 min
Mode: Fluorescence Bottom Reading
Target Temperature: 37 °C; CO_2 concentration: 5 %
Excitation Wavelength: 485 nm
Emission Wavelength: 535 nm
Excitation Bandwidth: 9 nm; Emission Bandwidth: 20 nm
Gain: Optimal Gain; Number of Flashes: 24
Integration Time: 40 µs; Lag Time: 0 µs; Settle Time: 0 ms

CLARIOSTAR®

Measurement type: Fluorescence; Bottom optic used
Target Temperature: 37 °C; CO_2 concentration: 5 %
Plate mode settings
Number of cycles: 25; Cycle time: 600 s; Number of flashes per well: 8
Scan mode: orbital averaging; Scan diameter: 3 mm
Optic settings
Excitation Wavelength: 483-14 nm
Dichroic filter: auto 502.5
Emission Wavelength: 530-30 nm
Gain: adjusted from full plate; Focal height: 4.2 mm

The means of the triplicates were determined for every measured point in time t. After subtraction from the averaged corresponding background control, the cytotoxicity (%) was quantified with the following equation:

$$\text{Killing (\%)} = \frac{Y-(NC \times I)}{I \times (PC-NC)} \times 100$$

Y: Fluorescence of the sample (killing condition) at point in time t
NC: Fluorescence of the negative control at the corresponding time t
PC: Fluorescence of the positive control at the corresponding time t

Since the killing condition and the negative control do not inevitably have the same starting fluorescence, the difference was corrected using the following index (I): $I_{t=0} = Y_{t=o}/NK_{t=0}$)
Experiments with index ≤ 0.95 were excluded.

3.10 Determination of mRNA expression

3.10.1 RNA isolation

Total RNA from melanoma cells was isolated with TRIzol® reagent from Invitrogen. The main components of TRIzol™ Reagent are phenol and guanidine isothiocyanate. Guanidine isothiocyanate lyses the cells and prevents RNA degradation by inhibiting RNase activity. Fresh cell pellets were homogenised in 800 µL TRIzol® reagent and were stored at -80 °C until further use. Further RNA isolation was based on a phenol-chloroform extraction (Chomczynski and Sacchi, 1987). First, the samples were centrifuged (12,000 x g, 10 min, 4 °C) and the supernatant transferred to a fresh 1.5 mL reagent tube. After 5 min of incubation at room temperature 200 µL chloroform was added and mixed by vigorous shaking of the tube. The second centrifugation step (12,000 x g, 15 min, 4 °C) rendered the phase separation visible. The lower red organic layer contains denatured proteins, whereas RNA is dissolved in the upper aqueous layer. DNA can be found in the interphase between the distinct two layers. The aqueous phase was transferred to a new 1.5 mL reagent tube. RNA was precipitated from the aqueous layer by adding 500 µL isopropanol and 1 µL glycogen (5 µg/µL). The 10 min incubation was stopped with another centrifugation step (12,000 x g, 10 min, 4 °C). Afterwards the RNA pellet was washed in 1 mL 75 % ethanol (7,500 x g, 10 min, 4 °C) and dried. The complete dry RNA pellet was dissolved in 10-20 µL DEPC treated water.

An alternative to the TRIzol® based isolation of RNA is the NucleoSpin® RNA Plus kit from Macherey-Nagel. The cell pellet was resuspended and lysed in 350 µL LBP buffer. To remove the genomic DNA, the homogenized sample was transferred to a gDNA-removal column preassembled with a 2 mL collection tube. After centrifugation (11,000 x g, 30 s) the column was discarded. A volume of 100 µL binding solution was added to the flowthrough and mixed rigorously before transferring the whole lysate mix to a RNA binding column with collection tube. The flow-through was discarded following centrifugation (11,000 x g, 15 s). Then the column was washed once with 200 µL buffer WB1 (11,000 x g, 15 s) and a second time with 600 µL buffer WB2 (11,000 x g, 15 s). To dry the column membrane completely, an additional 250 µL WB2 was added and then centrifuged (11,000 x g, 2 min). Finally, the RNA was eluted by

adding 30 µL RNase-free water and centrifuging at 11,000 x g for 1 min. The RNA yield can be increased by repeating the elution step.

The RNA concentration was determined with the help of a spectrophotometer (NanoDrop). Isolated RNA was either used directly for cDNA synthesis or was stored at -80 °C until further use.

3.10.2 Reverse transcription for cDNA synthesis

The isolated RNA was used as a template to synthesise DNA via reverse transcription. This process produces complementary DNA (cDNA), which can be used in later polymerase chain reactions (PCR) and also later help to quantify mRNA levels. The cDNA synthesis was performed by Andrea Paluschkiwitz.

For this purpose, 800 ng RNA was mixed with 50 µM Oligo-$(dT)_{20}$ primers as well as 10 mM dNTP-Mix in a final volume of 13 µL. This RNA-primer mixture was heated up to 65 °C for 5 min and then incubated on ice for 1 min. Then the RT reaction mix was prepared. For one reaction 4 µL 5x SSIV Buffer, 1 µL 100 mM dithiothreitol (DTT), 1 µL ribonuclease inhibitor and 1 µL SuperScript™ IV Reverse Transcriptase (200 U/µL) was mixed. The prepared RT reaction mix was combined with the annealed RNA. For optimal reaction, the mixture was incubated at 50-55 °C for 10 min. Finally, the incubation at 80 °C for 10 min inactivated the reaction. The synthesized cDNA was either used immediately for PCR amplification or was stored at -20 °C until further use.

3.10.3 Quantitative real-time polymerase chain reaction (qRT-PCR)

To quantify and compare the gene expression of melanoma cells, quantitative real-time polymerase chain reaction (PCR) was used. The shown qRT-PCRs were performed by Andrea Paluschkiwitz. This method allows the detection as well as the quantification of the cDNA amplification with the aid of a fluorescence dye that reversibly intercalates with double-stranded DNA. With every PCR cycle, more dsDNA is synthesized and the fluorescence signal increases. For this purpose, we used the GoTaq®qPCR Master Mix of Promega that contains not only the BRYT Green® Dye (Ex: 493 nm; Em: 530 nm) but also all components for qPCR except cDNA, primers and water. The following qRT-PCR reaction mix (1 x) was used:

Table 17. qRT- PCR reaction mix

Reagent	Volume (µL)
2x GoTaq qPCR Master Mix	25
Primer forward 10 µM	1.5
Primer reverse 10 µM	1.5
$H_2O_{dest.}$	12
1:10 cDNA (<500 ng)	10
Total volume	**50**

Mastermix (40 µL) was pipetted into each well of a 96 PCR-plate (Sarstedt 72.1978.202) and 10 µL of the 1:10 prediluted cDNA (<500 ng). To avoid evaporation during the cycling heating, the plate was covered with an adhesive seal (4titude, 0560). After spinning down, the plate was placed in an Agilent Mx3005P qPCR instrument using the following cycling program (Table 18).

Table 18. qPCR Cycling Program

Cycles	Temperature (°C)	Time (min)	Stage
1	95	15:00	Initial polymerase activation
35-45	95	00:15	Denaturation
	58	00:30	Annealing
	72	00:30	Elongation and measurement
1	95	1:00	Final elongation and Melting curve
	58	00:30	
	95	00:30	

The further analysis of the gene expression levels was done with the MxPro software. The different melanoma cell lines were compared by analyzing the CT values that represent the PCR cycle after which the fluorescent signal reaches a fluorescent threshold (background). The target gene expression was normalised to the housekeeping gene TATA-binding protein (TBP). The ΔCT (CT gene of interest - CT housekeeping gene) was inserted in the formula $2^{-\Delta CT}$ to calculate the relative expression fold change and facilitates the comparative analysis.

3.11 Melanoma-NK cell-co-culture

Initially, 2-5 x 10^5 melanoma cells were seeded in a 25 cm^3 cell culture flask. After 4 h, melanoma cells settled down and were challenged with either IL-2 activated primary NK cells or the cell line NK-92. After 3-4 days, melanoma cells that survived NK cell killing were split and exposed to a new NK cell donor. Remaining NK cells from the previous co-culture were removed by two PBS washes. This co-culture cycle was repeated over several weeks. During these cycles, the effector-target ratio was increased from 1:2 to 4:1 with primary NK cells and from 1:2 to 7:1 with NK-92. Untreated melanoma cells with the same culture and splitting conditions were used as a control. The melanoma cells of the co-cultures were further characterised using RNA sequencing. For that purpose, the isolated RNA requires high purity. To reduce the contamination with RNA of NK cells, irradiation (30 Gy) of NK cells right before co-culture experiments induces NK cell apoptosis after 6 hours (Seki et al., 1994) and hence limits their survival. Unfortunately, the radiation in this dosage has also shown to partially impair the cytotoxic potential of resting NK cells (Rana et al., 1990). However, IL-2 stimulated NK cells showed mainly to retain their ability to kill K562 and WM3734 (Figure 37). At regular intervals, the susceptibility of to the surviving melanoma cells to NK cells were determined.

3.12 mRNA sequencing of melanoma-NK cell-co-culture

3.12.1 Sample preparation

The melanoma cell line WM3734 that have been co-cultured with primary NK cells/NK-92 was harvested and their RNA was isolated via phenol-chloroform extraction (see 3.10.1). Isolated RNA of two melanocyte cell lines Mel B and Mel W were used as healthy controls. The RNA of WM3734 co-cultured with primary NK cells were isolated by Gertrud Schwär. The following table shows the collected samples for the performed mRNA sequencing.

Table 19. mRNA sequencing melanoma samples under specification of co-culture (I -IV indicate different starting points of co-culture), E:T ratio and recovery time

Sample	Co-cultured with	E:T Ratio	Recovery time
WM3734 (I)	Primary NK cells	2 :1	none
	/	Control	/
WM3734 (II)	Primary NK cells	4 : 1	none
	/	Control	/
WM3734 (III)	Primary NK cells	4 : 1	none
	Primary NK cells	5:1	none
	/	Control	/
WM3734 (IV)	NK-92	1:7	none
	NK-92	1:7	3 days
	NK-92	1:3	none
	NK-92	1:3	3 days
	/	Control	/
Mel B	/	/	/
Mel W	/	/	/

3.12.2 mRNA-Seq library preparation

Further sample preparation, data procession and analysis was done by the epigenetics group of Prof. Dr. Jörn Walter of Saarland University in Saarbrücken. mRNA- Seq library preparation and the subsequent sequencing was performed by Dr. Gilles Gasperoni as follows. To purify the isolated melanoma RNA, the samples were additionally treated with DNaseI to minimize DNA contamination. From ~ 200 ng total RNA, mRNA was captured by using streptavidin coated tubes (mRNA Capture Kit, Roche). Remaining DNA and ribosomal RNA was removed by washing the tubes three times. After that, the first-strand cDNA synthesis was performed by adding M-MLV Reverse Transcriptase (Promega) at 37 °C for 1.5 h. Subsequent degradation of the RNA template by 5 U RNase H allowed the generation of the double stranded cDNA. For this purpose, 10 U DNA Polymerase I (Thermo Fisher Scientific) and 200 U T4-Ligase (NEB) were added and incubated for 2.5 h at 16 °C. After another washing step, the cDNA was fragmented using the Tn5 transposase from the Nextera Library Preparation kit (Illumina) for 5 min at 55 ° C. Before fragments were enriched by PCR amplification (9-12 cycles) with the

NEB Next PCR Master mix, the samples were purified using the MinElute PCR purification kit (Qiagen). The last step before sequencing is the final mRNA-Seq library purification with 0.8 x Agencourt AMPure XP beads (Beckman Coulter). Then the libraries were sequenced for 100 basepairs using a V3 single read flow-cell on a HiSeq 2500 (Illumina).

3.12.3 mRNA data analysis

The mRNA sequencing data were further processed and analysed by Dr. Karl Nordström. Low quality sequence reads (Q<30) were excluded and adapter sequences were trimmed with TrimGalore! (http://www.bioinformatics.babraham.ac.uk/projects/trim_galore/). The remaining reads were then aligned to the hg19 reference genome using STAR aligner (Dobin et al., 2013). PCR duplicates were detected with the help of the MarkDuplicates function from Picard tools (http://broadinstitute.github.io/picard/). In a last step, the reads were summarised with featureCounts (Liao et al., 2014) and a differential analysis via edgeR was performed.

3.13 Flow cytometry

Flow cytometry allows the examination of different cell parameter such as size, granularity and surface as well as intracellular protein expression. In this study, the expression profile of ligands and receptors involved in the melanoma NK cell interaction were determined. All used fluorochrome conjugated antibodies are listed in Table 3.

To stain the NK cell receptors and their ligands on the melanoma cell surface the following protocol was used. 1x 10^6 cells were washed (300 x g, 4 min, RT) and resuspended in 100 µl staining buffer (1x DPBS + 5 % FCS). NK cells express Fc gamma R III/II that could lead to non-specific antibody binding. Therefore, 5 µL of Human TruStain™ (BioLegend 422302), an Fc receptor blocking solution, was added to the NK cell suspensions and was incubated for 10 min on ice. Melanoma cells do not express this receptor and do not need this blocking. After an additional washing step, the staining of NK cells and melanoma cells followed the same protocol. 5 µL of each antibody was added to 100 µL of the cell suspensions of each sample and was incubated at 4 °C, for 25 minutes in the dark. To reduce unspecific binding of the remaining antibody, the cells were washed with 1 mL staining buffer (300 x g, 4 min, RT). Afterwards, the cells were resuspended in 200-500 µL staining buffer and transferred to a 5 mL tube. For intracellular staining, the cells needed to be fixed and permeabilised after the first staining. Therefore, the cells were washed for a second time and resuspended in 100 µL staining buffer containing 4 % paraformaldehyde. After 20 minutes of incubation, the cells were washed twice

with staining buffer to remove the PFA. To permeabilise the cell membrane, the cell pellet was resuspended in 200 µL permeabilisation buffer solution, containing 0.1 % saponin. The following incubation of 10 min at 4 °C was stopped by another centrifugation (300 x g, 4 min, RT). To ensure the permeability of the cell membrane, the subsequent intracellular staining was performed in 100 µL permeabilsation buffer with 5 µL antibody. After 20 min at 4 °C, 500 µL permeabilisation buffer was added to remove unbound antibody. In a final step, cells were centrifuged (300 x g, 4 min, RT) and were resuspended in 200 µL staining buffer.

For subsequent analysis unstained controls, corresponding isotype controls as well as fluorescence minus one (FMO) controls in case of multicolour staining were used.

To ensure the fluorochrome stability, the tubes were stored in the dark at 4 °C. The fluorescence measurements were performed with the FACS Verse of BD (AG Prof. Markus Hoth, Saarland University) and FACS Canto II of BD (AG Prof. Schwappach, University Göttingen).

Analysis:

For analysis the softwares FlowJo Version 10 and FACS Diva were used.

Cell debris was excluded by low forward scatter (FSC) and sideward scatter (SSC). The fluorescence signal of the remaining cells was detected and quantified. For the quantification and statistical analyses, the background fluorescence of the isotype controls were subtracted from the signal obtained by stained cells.

3.14 Determination of protein expression level

The mRNA levels do not always represent the actual intracellular protein level. Protein biosynthesis is a highly regulated process, which involves different control steps where the translation can be prematurely terminated. Additionally, the protein half-life can be influenced by degradation processes. Therefore, the expression of protein levels can give more information about the actual effect of the investigated protein.

3.14.1 Protein extraction

Melanoma cells were lysed with the freshly prepared TGH lysis buffer (see chapter 2.2.2). The cell lysates were prepared on ice to reduce protein degradation. Before lysis buffer was added the cell plates or flasks were rinsed twice with cold 1x DPBS to remove medium residues. Depending on plate size and cell confluence, a certain volume of TGH lysis buffer was added. Then the cells were scraped off the plates with the help of a rubber cell scraper. The cell solution was

resuspended and collected in a 1.5 mL tube. After 10 min of incubation on ice, the cell lysates were shortly resuspended again and incubated for another 10 min on ice. To remove cell fragments, the cell lysates were centrifuged (11,000 x g, 10 min, 4 °C) and only the clear supernatant containing the cell proteins was transferred to a new 1.5 mL tube. The protein samples were frozen at – 80 °C until further use.

3.14.2 Bradford Assay

To determine the protein concentration of melanoma cell lysates, the Bradford reagent was used. The basis of this reagent is Coomassie Brilliant Blue G-250 that shows an absorbance shift (465 nm to 595 nm) after binding to protein. A volume of 1 µL of protein lysate was mixed with 200 µL Bradford reagent and 799 µL $H_2O_{dest.}$. Next, 200 µL of each sample were loaded on a 96 well plate in triplicates. The absorbance at 595 nm was detected with the Mithras LB940 plate reader. The total protein concentration was calculated with the help of a BSA-based standard curve (0.5 -20 µg/mL).

3.14.3 SDS-PAGE

Sodium dodecyl sulphate polyacrylamide gel electrophoresis (SDS-PAGE) was used to separate the proteins of the prepared lysates by their molecular weight. After applying a voltage, the proteins move through a discontinuous polyacrylamide matrix in the direction of the anode. The negative charged SDS functions as a surfactant and binds to the amino acids of the proteins. The size of the protein correlates with the SDS binding and the resulting negative charge. The matrix consists of a stacking gel (5 %) and a separation gel (10 %) as shown in Table 20.

Table 20. SDS matrix. Composition of stacking and separation gel

Component	5 % Stacking gel	10 % Separation gel
$H_2O_{dest.}$	3.08 mL	4.91 mL
4x TG-buffer	1.25 mL	2.5 mL
40 % Acrylamide	0.63 mL	2.5 mL
10 % APS	37.5 µL	75 µL
TEMED	7.5 µL	15 µL

The protein lysates were mixed with 4x LaemmLi Sample Buffer (with 355 mM beta-mercaptoethanol) and denatured at 95 °C for 3 min. Then the samples were loaded into the cavities of the gels and a voltage of 80 V was applied. After entering the separation gel, the

voltage was increased to 100 V. To determine the protein size the Precision Plus Protein™ Dual Color Standard (Bio-Rad, 1610374) was used.

3.14.4 Immunoblot (Western Blot)

Following SDS-PAGE, the separated proteins were transferred onto a nitrocellulose membrane by using a semi-dry Trans-Blot® Turbo™ Transfer System from Bio-Rad. Before the transfer, the nitrocellulose membrane was equilibrated for 3 min in Turbo transfer buffer. At the same time, the paper stacks that were used as ion reservoirs were soaked with the same transfer buffer. Then the transfer pack was assembled in the following order: bottom ion reservoir stack, nitrocellulose membrane, gel and top ion reservoir stack. This transfer pack was placed on the bottom (+) cassette and closed with the top (-) cassette. After applying 2.5 A, up to 25 V for 10 min, the negatively charged proteins were transferred to the nitrocellulose membrane. Following this, the membrane was blocked in 1 x TBS + 5 % BSA % at RT for 1 h to prevent unspecific antibody binding. Primary antibodies were diluted in 1 x TBS solution supplemented with 1 % BSA according to Table 1. After incubation overnight at 4 °C, the membrane was washed three times with 1x TBST for 5 min to remove remaining unbound primary antibody. In the next step, the IRDye® secondary antibodies were diluted 1:10,000 in 1 x TBST buffer and incubated for 1h at RT on a rocker. These secondary antibodies are labelled with a fluorescent dye that allows detection by a fluorescent imaging system. Subsequently, remaining secondary antibody was removed by washing three times with 1x TBST for 10 min. To visualise the protein bands, the membrane was scanned with the Odyssey® CLx Imager from Li-cor.

3.15 Reverse Phase Protein Array (RPPA)

The reverse phase protein array (RPPA) is a high throughput approach that allows the simultaneous detection and quantification of hundreds of proteins expressed in cells and tissues. (Tibes et al., 2006). Therefore, protein lysates were immobilised on nitrocellulose-coated slides and probed with primary antibodies. Subsequently, biotinylated secondary antibodies allow the detection and quantification of the protein expression (Figure 9).

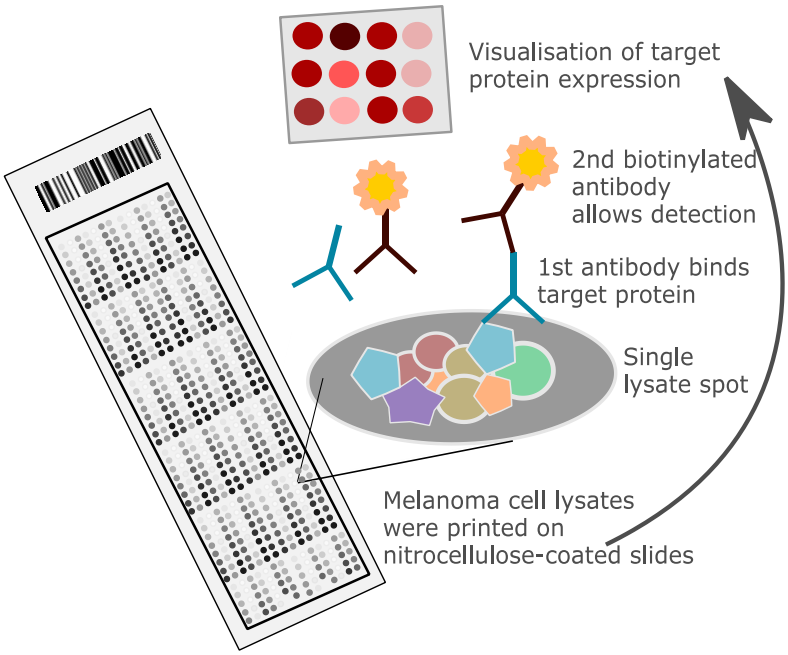

Figure 9. Principle of the Reverse Phase Protein Array (RPPA). Serial diluted cell lysates were arrayed on nitrocellulose-coated slides. Specific primary antibody binds target proteins of the lysate spots followed by a secondary biotinylated antibody for detection and later visualisation of the protein expression.

The lysates from different melanoma cell lines were prepared by The Wistar Institute (Philadelphia, USA). The RPPA and data processing were performed by the MD Anderson Center RPPA core facility (Houston, TX, USA). First, serial-diluted lysates (prepared by Tecan Robotic Liquid Handling System) of every melanoma cell line were printed on nitrocellulose-coated slides using a 2470 Microarray printer of Aushon Biosystems. The small size of the lysate spots allows the printing of more than 5000 array spots per slide. To ensure the quality of the RPPA, control lysates were placed on each slide. The DAKO Universal Staining System probed each slide with a different validated primary antibody under appropriate conditions. Then the slides were probed with the corresponding biotin-conjugated secondary antibody to allow the signal amplification by forming an avidin-biotin-complex using the Vectastain Elite ABC kit (Vector Lab). The visualisation of the signals were achieved by a secondary streptavidin-conjugated HRP and following DAB colorimetric reaction. After scanning of the slides, the spot intensities were generated by further data analyses and quantification using Array-Pro Analyzer software (MediaCybernetics). The different signal intensities of the dilution series of every sample were used to create a supercurve fitting (Hu et al., 2007) and increase accuracy of the protein concentration determination (in log2 scale). In a last step, the data were normalised by using median-centering across antibodies (MD Anderson, 2019).

3.16 Inhibitor treatment of melanoma cells

Melanoma cells (7 x 10^5) were seeded into 60 mm cell culture dishes 4 hours before inhibitor treatment. After the cells settled, the melanoma cells were treated with inhibitors targeting PI3K-AKT-mTOR pathway (Table 7). Dimethyl sulfoxide (DMSO) was used as a control since all the inhibitors were dissolved in DMSO. During the treatment (24 h or 96 h), the cell culture dishes were incubated at 37 °C and in 5 % CO_2 atmosphere.

3.17 Statistics

Data were analysed using Microsoft Excel 2016. Unless noted otherwise, experiments are shown as means ± SEM. Statistical significance was determined by two-tailed unpaired or paired Student's *t*-test as indicated. Significance is marked with * for $p < 0.05$, ** for $p < 0.01$ and *** for $p < 0.001$.

4 Results

4.1 Effector-to-Target ratio determines effect size of NK cell killing

The number of tumour infiltrating lymphocytes were associated with enhanced patient survival (Cursons et al., 2019; Fortes et al., 2015; Thomas et al., 2013). In this regard, effector-to-target ratios (E:T ratios), which represent the NK cell tumour infiltration in a real setting are from major biological interest. In a study from 2012, Balsamo and colleagues investigated the NK cell infiltration of primary cutaneous melanoma and found that the E:T ratio ranged between 0.03:1 and 0.5:1 (Balsamo et al., 2012). Based on this knowledge and the most frequently used E:T ratios in other studies that used *in vitro* cytotoxicity assays, four E:T ratios between 0.5 to 1 and 10 to 1 were tested in two cancer cell lines, K562 and WM3734 (see Figure 10).

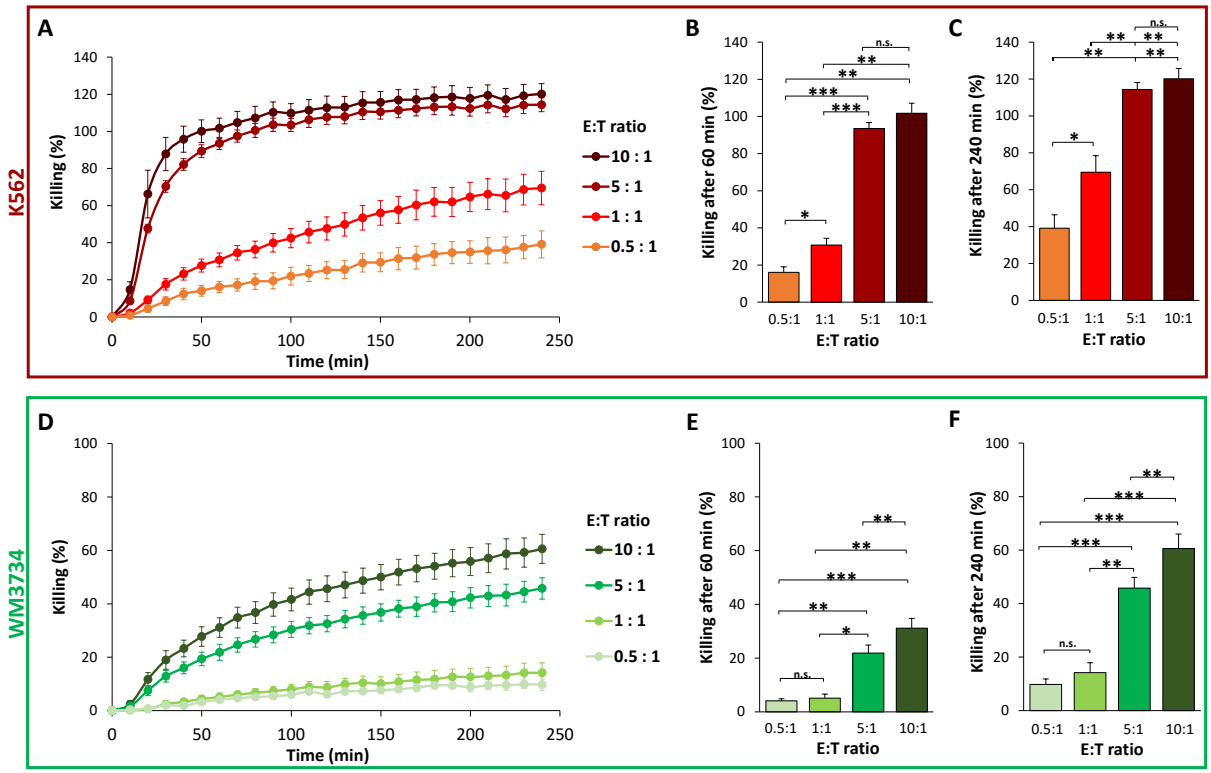

Figure 10. Effector-to-target ratio determines effect size of NK cell killing. Calcein-AM (0.5 µM) loaded target cells were analysed in four 240 min cytotoxic assays (A and D) with the following E:T ratios: 0.5:1, 1:1, 5:1 and 10:1. Effector cells were IL-2 stimulated NK cells. K562 (red) and WM3734 (green) were used as target cells. For further statistical analysis, the killing after 60 min (B and E) as well as the killing after 240 min (C and F) were used. Bars and graphs indicate means ± SEM. Statistical significance of paired, two-tailed Student's *t*-test is indicated with * for p <0.05, ** for p <0.01 and *** for p <0.001.

K562 cells were used as a positive control to evaluate the cytotoxicity of the used NK cell donors as they showed to be highly susceptible to NK cells due to their ligand profile (Tremblay-McLean et al., 2019). As shown in Figure 10 A, this cell line was highly susceptible to NK cells as

expected, and target cells were killed to 100 % after 80 min in E:T ratios higher than 5:1. During the initial killing phase, shown in Figure 10 B, the lower E:T ratios showed a much lower killing (±16 %) in comparison to the higher E:T ratios (5:1 or 10:1) (±30 %). After 240 min (see Figure 10 C), the lower E:T ratios only reached a killing of ~39 % and ~69 % at the 0.5:1 and 1:1 ratio, respectively. The cytotoxic efficiency of the 5:1 and 10:1 ratios did not differ dramatically in K562. In contrast, the melanoma cell line WM3734 was less susceptible to NK cells (Figure 10 D). Even the highest E:T ratio did not exceed a killing of ~31 % (Figure 10 E) after 1 h and ~61 % after the 4 h measurement (Figure 10 F). Half the amount of NK cells (E:T ratio of 5:1) were still able to kill ±46 % of WM3734 after 240 min. The lowest E:T ratios showed similar flat killing curves with an initial killing of ~5 % that increased to ~10-15 % until the end of the experiment.

The cytotoxicity assay requires an adequate dynamic range to detect both an increase as well as a decrease of the cancer cell susceptibility to NK cells after treatment with different pharmaceutical substances or genetic manipulation. Lower E:T ratios that represent the real intratumoral NK cell infiltration were not sufficient to detect smaller differences of melanoma killing in the used cytotoxicity assay. In an E:T ratio of 5:1, NK cells kill ~50 % of WM3734 cells and allow the adequate detection of an increase as well as a decrease of NK cell-induced cytotoxicity against melanoma cells (NKiToxMel). Furthermore, this ratio is sufficient to eliminate 100 % of K562 cells that serve as a positive control for NK cell cytotoxicity. If not stated differently, an E:T ratio of 5:1 was used for subsequent experiments.

4.2 Interleukin-2 stimulation increases NK cell cytotoxicity

Interleukin-2 regulates NK cell activity and can increase their cytotoxicity (Henney et al., 1981; Lehmann et al., 2001). To investigate if and how IL-2 stimulation affects NKiToxMel, non-stimulated and IL-2 stimulated (0.05 µg/mL) NK cells from the same donor were used in cytotoxic assays. In Figure 11, the results depicting NK cell cytotoxicity against three different melanoma cell lines, as well as the control K562, are summarised. In all cell lines, the non-stimulated NK cells showed significantly lower cytotoxicity than the IL-2 stimulated NK cells (see Figure 11 A). This was not only visible at the initial phase of the experiment (Figure 11 B), but it also appears at the endpoint of the killing assay (Figure 11 C). Non-stimulated NK cells were still able to kill all K562 cells during the observation time of the cytotoxic assay, but they needed 2 hours longer than stimulated NK cells (~80 min). Among the investigated melanoma cell lines, 1205Lu cells showed the highest susceptibility towards IL-2 stimulated NK cells and had an almost identical time course compared with K562-killing by non-stimulated NK cells. In

the first hour (Figure 11 B) more than half (~56 %) of the 1205Lu were eliminated. At the end of the assay, all 1205Lu were killed by stimulated NK cells (see Figure 11 C). Non-stimulated NK cells only killed ~10 % after 60 min and reached a killing plateau of ~34 % after 220 min. WM3734 had an intermediate susceptibility to NK cells. Figure 11 C shows that IL-2 stimulated NK cells killed ~42 % of WM3734 cells, whereas their susceptibility to non-stimulated NK cells is reduced to ± 12 %. WM88 are the least susceptible melanoma cells among those that were tested, as non-stimulated NK cells were not able to kill WM88 to any detectable amount. Even after stimulation, NK cells only marginally killed this melanoma cell line (12 %).

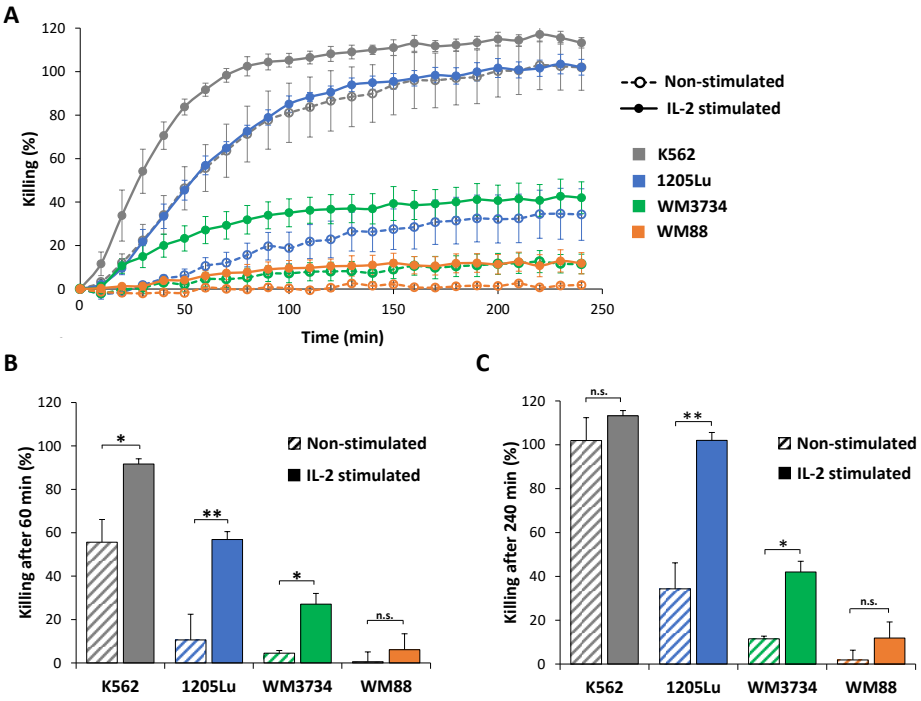

Figure 11. Interleukin-2 stimulation increases cytotoxicity against cancer cells. NK cell-mediated killing of the melanoma cell lines 1205Lu, WM3734 and WM88 as well as the control cell line K562 was determined in 4 h a cytotoxic assay (A). NK cells from four different donors either IL-2 stimulated (1-2 days) or non-stimulated were used as effector cells. For further statistical analysis the killing after 60 min (B) as well as the killing after 240 min (C) were used. Bars and graphs indicate means ± SEM. Statistical significance of paired, two-tailed Student's *t*-test is indicated with * for $p<0.05$ and ** for $p<0.01$.

As previously shown (Cappello, 2015), the difference between non-stimulated and IL-2 stimulated NK cells are due to alterations in the NK cell receptor profile and differences in the content of lytic granules before and after stimulation. The representative histograms (Figure 12 A) depict altered expression levels of the NK cell receptors CD16, NKp30, NKG2D, the adhesion molecule CD56 as well as perforin and granzyme B. The median fluorescence intensity (MFI) was used to compare the expression profile of non-stimulated and IL-2 stimulated NK cells (see Figure 12 B). To exclude fluorescence signals, which were caused by non-specific antibody binding, the MFI of the corresponding isotype controls were subtracted. In comparison to the other analysed parameters, the median fluorescence intensities (MFIs) of the activating receptors NKp30 and NKG2D were low (Net MFI of 50 and 187, respectively) in non-stimulated NK cells. After IL-2 stimulation, the MFI increased to 154 for NKp30 and 908 for NKG2D. The detected amount of CD56 expression on the NK cell surface increased almost fourfold (MFI of 882 to MFI of 3215) after stimulation. The CD16 surface expression showed only a small increase from MFI of 3600 to 4800 after IL-2 stimulation. In addition to the higher expression of activating NK cell receptors, the NK cells tended to have a higher content of intracellular granzyme B and perforin (from 2822 to 5642 and from 6264 to 9120, respectively). These findings are also in agreement with observations from other groups (Balsamo et al., 2013) and partially explain the lower cytotoxicity of non-stimulated NK cells to melanoma cells.

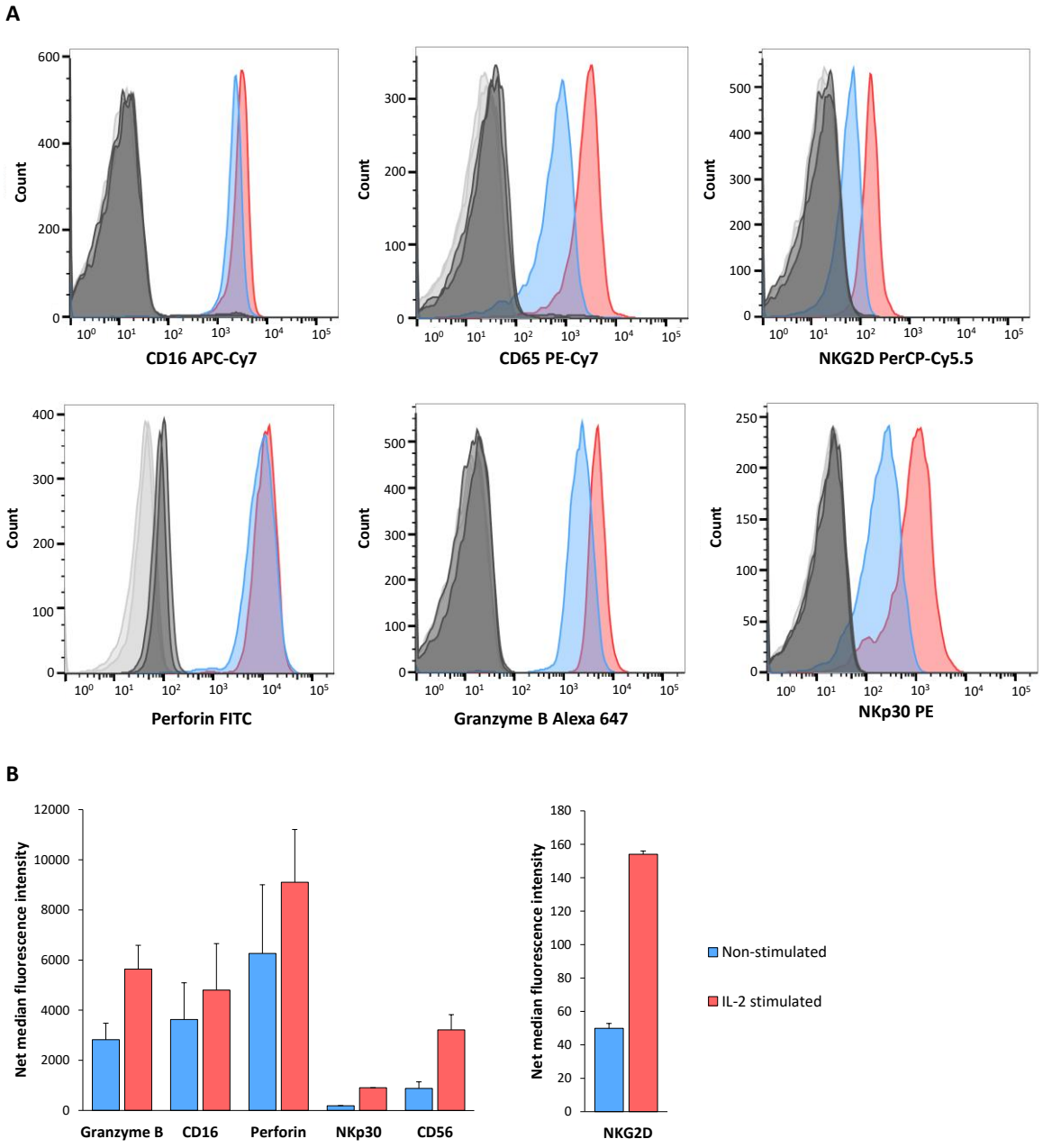

Figure 12. Interleukin-2 stimulation alters expression profile of NK cells. The expression levels of CD16, NKp30, NKG2D, CD56, perforin and granzyme B were analysed with flow cytometry. (A) Histograms show the cell distribution according to the emitted fluorescence of the indicated fluorochrome conjugated antibodies (see Table 3). The following colour code was used: light grey: non-stained samples; dark grey: corresponding isotype controls; blue: non-stimulated NK cell samples; red: IL-2 stimulated NK cells (B) The bar graphs show the net median fluorescence intensity (MFI) (minus MFI of corresponding isotype control). Bars indicate SEM of 3 NK cell donors. Data were analysed with Flow Jo software Version 10. Data were previously shown in (Cappello, 2015)

The NK cells were used on different days after IL-2 stimulation. Therefore, it was important to estimate the dependence of NK cell cytotoxicity towards melanoma in relation to the duration of IL-2 stimulation. As depicted in Figure 13 A, the duration of IL-2 stimulation influenced the NK cell cytotoxicity towards cancer cells only marginally. Figure 13 B shows that NK cells after 1-3 days of IL-2 stimulation had significant higher cytotoxicity (~73 % and ~54 % after 60 min) towards the cell lines K562 and 1205Lu. WM3734 cells and WM88 cells were best eliminated by NK cells stimulated for 4-7 days with IL-2 (compare Figure 13 C). Nevertheless, these minor alterations in NK cell cytotoxicity in the course of IL-2 stimulation can be neglected as the general susceptibility of melanoma cells to NK cells is unchanged.

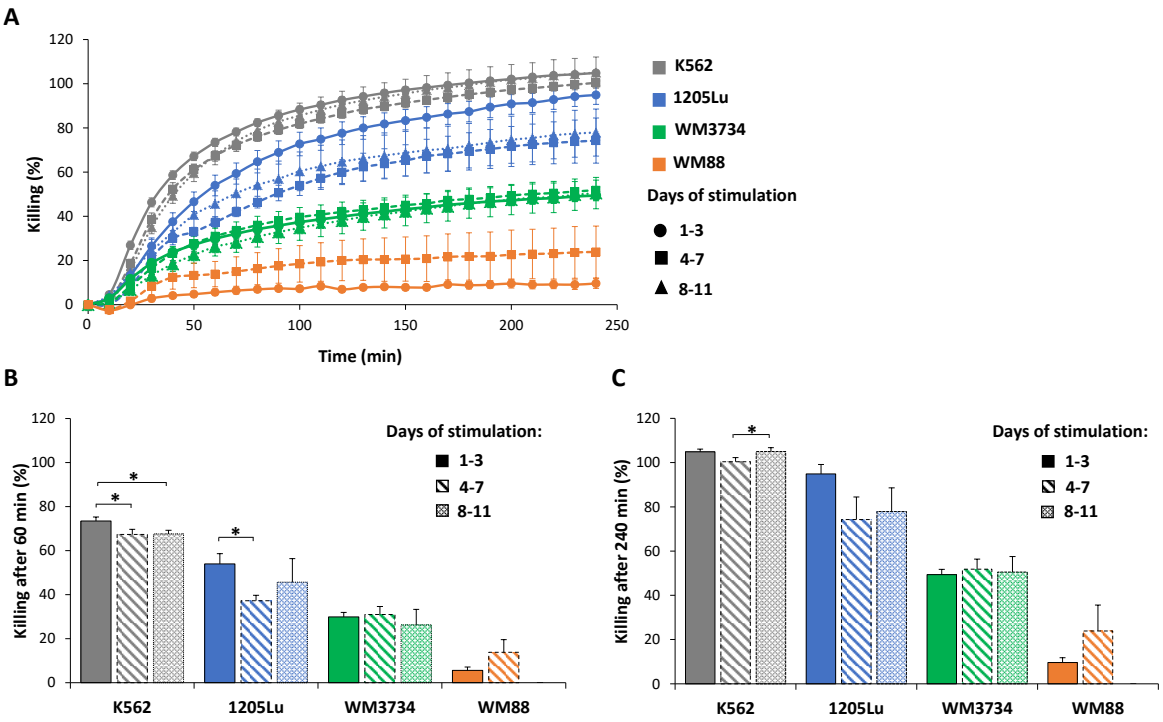

Figure 13. NK cell cytotoxicity stays nearly unchanged in the course of Interleukin-2 stimulation. The susceptibility of the melanoma cell lines to NK cells that were stimulated with IL-2 over multiple days: K562 1-3 d (n=84), 4-7 d (n=39), 8-11 d (n=33); 1205Lu 1-3 d (n=15), 4-7 d (n=2), 8-11 d (n =5); WM3734 1-3 d (n=50), 4-7 d (n=21), 8-11 d (n=8); WM88 1-3 d (n=5), 4-7 d (n=8). (A) Kinetics of 4 h cytotoxic assay. For further statistical analysis the killing after 60 min (B) as well as the killing after 240 min (C) were used. Bars and graphs indicate means ± SEM. Statistical significance of unpaired, two-tailed Student's *t*-test is indicated with * for $p<0.05$.

Altogether, the data presented here indicate that IL-2 stimulation increased the NK cell cytotoxicity against cancer cells. This increase could be partly explained by the IL-2 induced upregulation of activating NK cell receptors that were required for detection of tumour cells. Since the duration of the IL-2 stimulation marginally altered the general NK cell cytotoxicity against tumour cells; isolated NK cells were used for cytotoxicity assays between one and 11 days after stimulation.

4.3 Heterogeneous susceptibility of melanoma cells to primary NK cells

To reveal the therapeutic potential of NK cells in melanoma treatment, we initially assessed the susceptibility of eight genetically diverse melanoma cell lines to primary NK cells (Figure 14). As seen in Figure 14 A, the performed cytotoxic assays revealed heterogeneous susceptibility of the different melanoma cell lines to primary NK cells. The most susceptible melanoma cell line was 1205Lu that was killed to ~91 %, whereas WM88 was largely resistant (14 %) to the NK cell-mediated killing (Figure 14 B). These differences were already visible after 60 min (Figure 14 C), where the cell lines 1205Lu and WM88 also showed the highest (52 %) and lowest (8 %) killing, respectively. The endpoint killing of the other investigated melanoma cell lines ranged from 31 % (WM1366) to 68 % (WM3918) although the killing after 60 min showed similar results (26 % and 20 %, respectively). This can be partially explained by a different shape of the killing curves. As seen in Figure 14 A, the killing of WM1366 cells stagnated after 1 hour of the experiment while the killing of WM3918 cells showed a more linear progression. A similar pattern of linear progression was found in the cell lines WM9 and WM983B. Both cell lines were initially killed to less than 18 % and reached maximal killing values of 42 % and 46 % after 4 h. WM3734 cells showed an initial susceptibility to NK cells of 31 % and stagnated in the next two hours to about 50 %. A slower stagnation of the killing was visible in the cell line 451Lu, which showed at the first half of the measurement a comparable killing curve to WM3734 with also 31 % killed after 60 min but reached an endpoint killing of 62 %. The heterogeneity between the different cell lines after 60 min were much smaller and less statistically significant (Figure 14 D) compared to the killing results after 240 min (Figure 14 E).

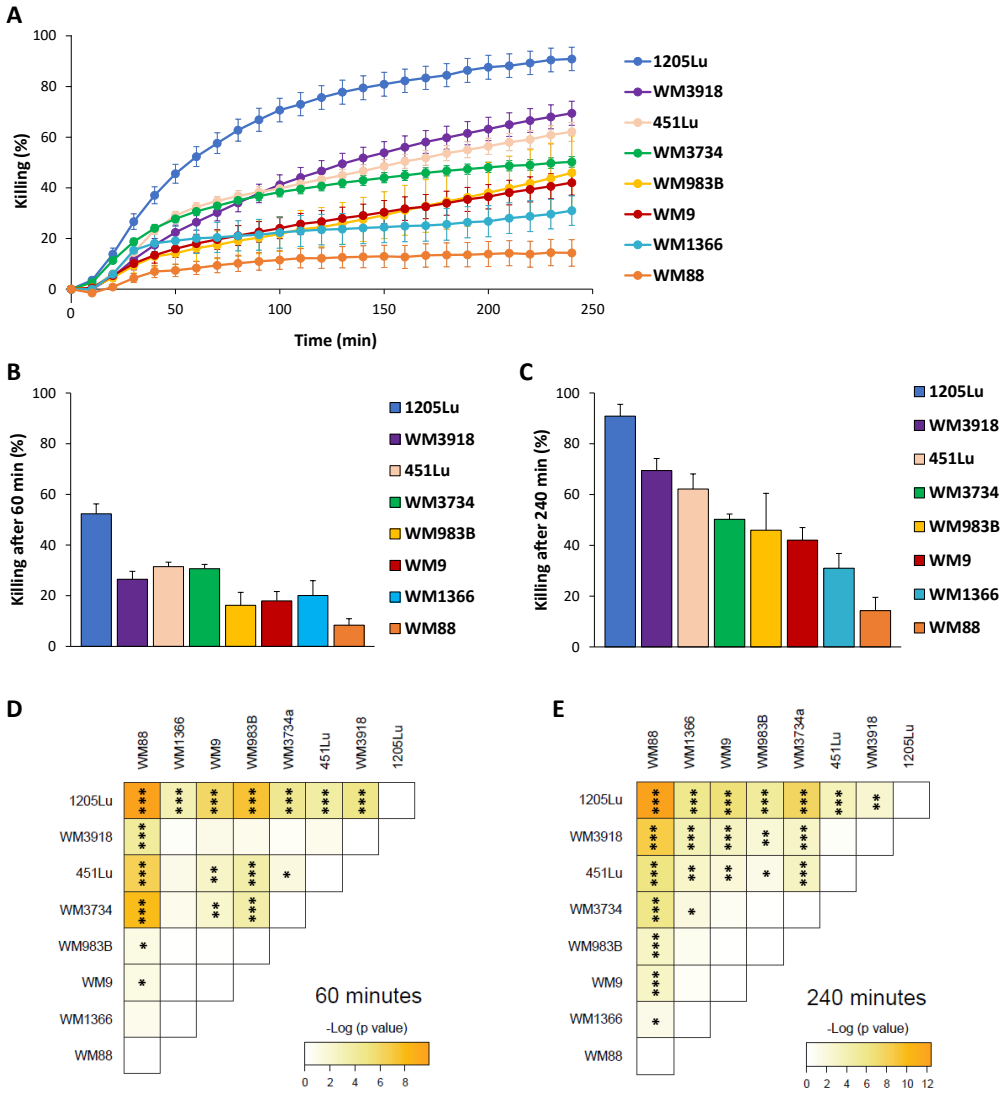

Figure 14. NK cell-mediated killing of melanoma cell lines is heterogeneous. Melanoma cells are loaded with calcein-AM (0.5 µM) and exposed to NK cells (E:T ratio of 5:1) for 4 h. Melanoma cells in the cytotoxic assays are: n (1205Lu): 19; n (WM3918): 20; n (451Lu): 6; n (WM3734): 79; n (WM983B): 10; n (WM9): 11; n (WM1366): 7 and n (WM88): 20. (A) Killing kinetics of 4h cytotoxic assay. Quantification of killing efficiency after 60 min (B) and after 240 min (C) were used to perform Student's *t*-tests (D+E). Bars and graphs indicate means ± SEM. Statistical significance of unpaired, two-tailed Student's *t*-test is indicated with * for $p<0.05$, ** for $p<0.01$ and *** for $p<0.001$. Data was partially obtained from (Cappello, 2015).

The NK cell cytotoxicity is determined in part by the engagement of NK cell receptor with their corresponding ligands (Long et al., 2013). One of the best investigated inhibitory ligands are MHC class I molecules (HLA-A,B,C) that protect target cells against NK cell killing (Karre, 2002). To estimate if and how MHC class I surface expression affect the susceptibility of melanoma cells to NK cells, the expression of this inhibitory ligand in selected cancer cell lines was further analysed by flow cytometry. Figure 15 A shows that the expression of MHC class I molecules in melanoma cell lines (coloured histograms) was more dominant compared to the cell line K562 (dark grey histogram). This leukaemia cell line only marginally showed MHC class I

antigens (Net MFI of ~300) on their cell membranes, whereas the melanoma cell lines expressed much higher levels of MHC class I (Net MFI < 10000) (see Figure 15 B). In comparison to WM88 and 1205Lu (both around ~ 18,000), the expression level of this inhibitory ligand in WM3734 cells (~ 38,000) was slightly increased. Hence, there was no linear correlation between NK cell susceptibility of melanoma cells and their levels of MHC class I expression.

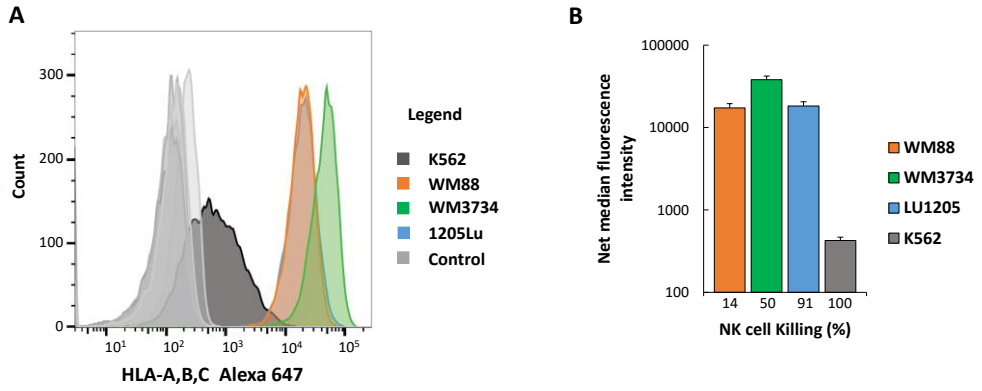

Figure 15. MHC class I expression does not explain the susceptibility of melanoma cells towards NK cell killing. The expression levels of MHC class I (HLA-A,B,C) in WM88 (orange, n=4), WM3734 (green; n=3), 1205Lu (blue; n=4) as well as K562 (dark grey; n=4) were determined by flow cytometric analysis. (A) Representative histogram shows the cell counts according to the emitted fluorescence signal of the HLA-A,B,C Alexa 647 antibody coated target cells. Controls were unstained samples as well as isotype controls. (B) The bars show the net median fluorescence intensity (MFI) (minus MFI of corresponding isotype control) in correlation to the NK cell-mediated killing. Bars indicate means ± SEM. Data were analysed with Flow Jo software Version 10.

However, the inhibitory ligands alone do not determine the NK cell activation (Karre, 2002). In addition, the stimuli received by activating NK cell receptors are needed for the initiation of NK cell killing. The ligands for the activating NKG2D receptor MICA/MICB (80 %) and ULBPs (15-25 %) are frequently expressed in melanoma (Casado et al., 2009). Furthermore, NCRs (in particular NKp30 that targets among others B7-H6 molecules) were shown to be important for the NK cell-induced toxicity against melanoma cells (NKiToxMel) (Morgado et al., 2011). To test if activating ligands on the melanoma surface affect the susceptibility to NK cells, the expression profile of MICA/MICB, ULBP-2/-5/-6 and B7-H6 in three melanoma cell lines were determined using multicolour staining. Figure 16 A shows that ULBPs and B7-H6 were only marginally expressed in the analysed melanoma cell lines. Only MICA/MICB expression were visibly heterogeneous in the distinct melanoma cell lines. However, additional flow cytometric analysis showed that the expression levels of all activating ligands increased with higher susceptibility of melanoma cells to NK cells (Figure 16 B). WM88 cells had the lowest expression of activating ligands (Net MFI <10), whereas the cell line WM3918 showed the highest levels of MICA/MICB (Net MFI >103), ULPBs (Net MFI ~17) and B7H6 (Net MFI~8). WM3734 cells

had moderate MICA/MICB levels (net MFI of 60). ULBPs and B7-H6 were only marginally expressed (Net MFI <10). In conclusion, the expression profile of the activating ligand MICA/MICB were in line with the measured susceptibility of melanoma to NK cells. Since the other activating ligands were only marginally expressed, no further conclusions about their role in the NK cell-mediated killing could be drawn.

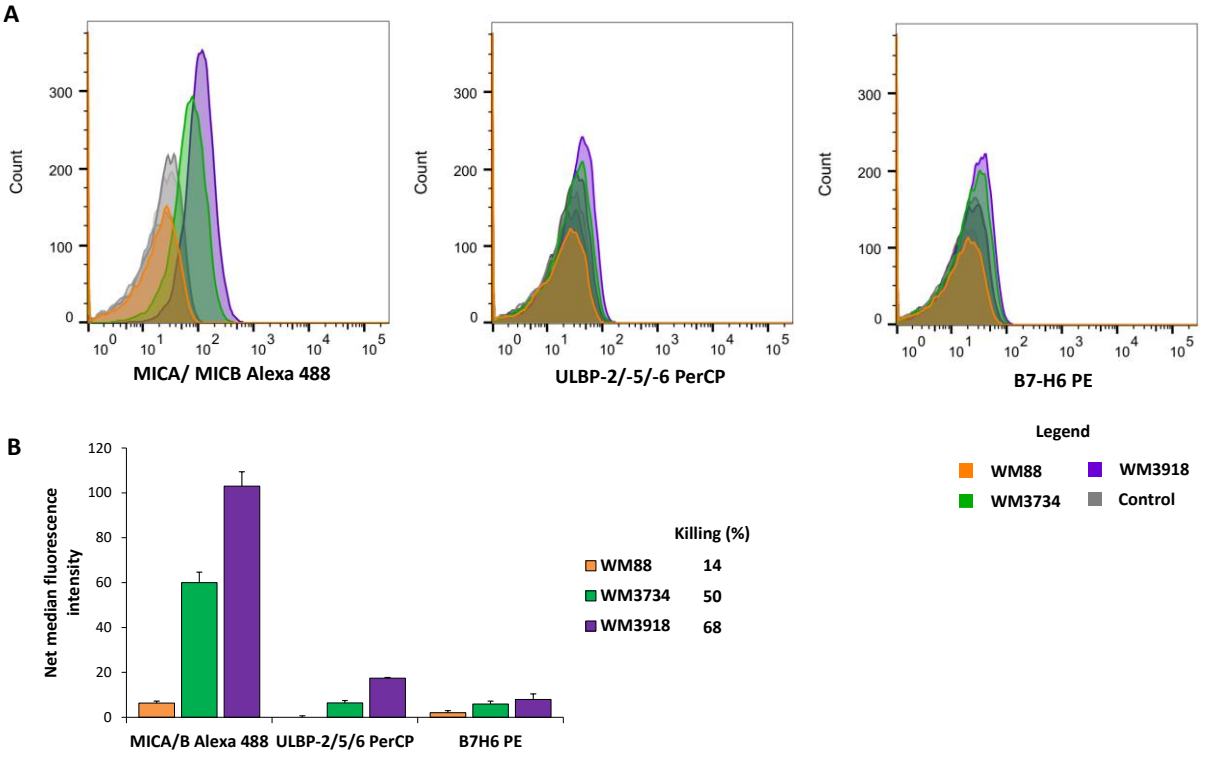

Figure 16. Activating ligands partially explain the susceptibility of melanoma cells towards NK cells . Flow cytometric analysis of the expression levels of MICA/MICB, ULB-2/-5/-6 and B7-H6 in WM88 (orange, n=3), WM3734 (green; n=3), WM3918 (purple; n=3). (A) Representative histograms show the cell counts according to the emitted fluorescence signal of the indicated antibody coated target cells. Controls were unstained samples, isotype controls as well as FMO controls. (B) The bar graphs show the net median fluorescence intensity (MFI) (minus MFI of corresponding isotype control) in correlation to the NK cell-mediated killing. Bars indicate means ± SEM. Data were analysed with Flow Jo software Version 10.

In conclusion, the obtained data shows that the susceptibility of melanoma cells to NK cells was highly heterogeneous. There were some indications that this heterogeneity was partially caused by a distinct activating ligand profile on the surface of melanoma cells. However, MHC class I molecules as an inhibitory NK cell ligand were not associated with the NKiToxMel.

4.4 Reverse phase protein array reveals proteins correlating with susceptibility to NK cells

The investigated melanoma cell lines were derived from different disease stages and have different genetic backgrounds. Therefore, the factors determining the observed heterogeneity in susceptibility to NK are rather complex. As flow cytometry only allows the investigation of a limited number of proteins, we used reverse phase protein array (RPPA) (see page 50) to identify melanoma proteins correlating with the observed NK cell killing. This method allows the simultaneous detection and quantification of more than 300 cancer related proteins (Tibes et al., 2006). The melanoma protein lysates were arrayed on slides and probed with primary antibodies that were detected with biotinylated, secondary antibodies (MD Anderson, 2019). After the quantification of the signal intensities, the protein expression data were normalised by using median-centering across antibodies. In Figure 17, all proteins that showed high Pearson correlation coefficient ($>\pm0.7$) between protein expression and NK cell-mediated killing were summarized in a heat map. For better visualisation of the heat map, the log2MedCen intensities values were transformed into the standard scores (z-score) scaled by individual gene (row). As seen in the heat map (Figure 17), melanoma cell lines that have a higher susceptibility to NK cells showed an opposed expression profile to the melanoma cells with higher NK cell resistance. Using this analysis, we identified a number of proteins that positively (yellow) or negatively (purple) correlate with the killing efficiency. Interestingly, SNAI1, a transcription factor that promotes EMT (Poser et al., 2001), showed a strong association with NK cell mediated killing of melanoma. Other EMT related proteins that were identified were TWIST2 (Kang and Massague, 2004; Mao et al., 2012), protein tyrosine kinase 2 (PTK2) (Giehl and Menke, 2008) and Napsin A Aspartic Peptidase (NAPSA) (Zhou et al., 2018a). Surface receptors such as transferrin receptor (TFRC), platelet derived growth factor receptor beta (PDGFRB), progesterone receptor (PGR) were part of the heat map as well. In addition, several proteins involved in the regulation of general cell metabolic processes were identified as possible regulators of NKiToxMel. Among them, hexokinase (HK2) and glyceraldehyde-3-phosphate dehydrogenase (GAPDH) are important glycolytic enzymes (Lunt and Vander Heiden, 2011), while RPTOR Independent Companion Of MTOR Complex 2 (RICTOR) and proline-rich Akt substrate of 40 kDa (PRAS40) (Saxton and Sabatini, 2017) are regulating components of the mTOR signalling axis. DIABLO, an mitochondrial protein that promotes the initiation of apoptosis (Du et al., 2000) was the top hit of the negative correlated proteins. Additional identified proteins involved in programmed cell death were BAD and CASP3 (Elmore, 2007).

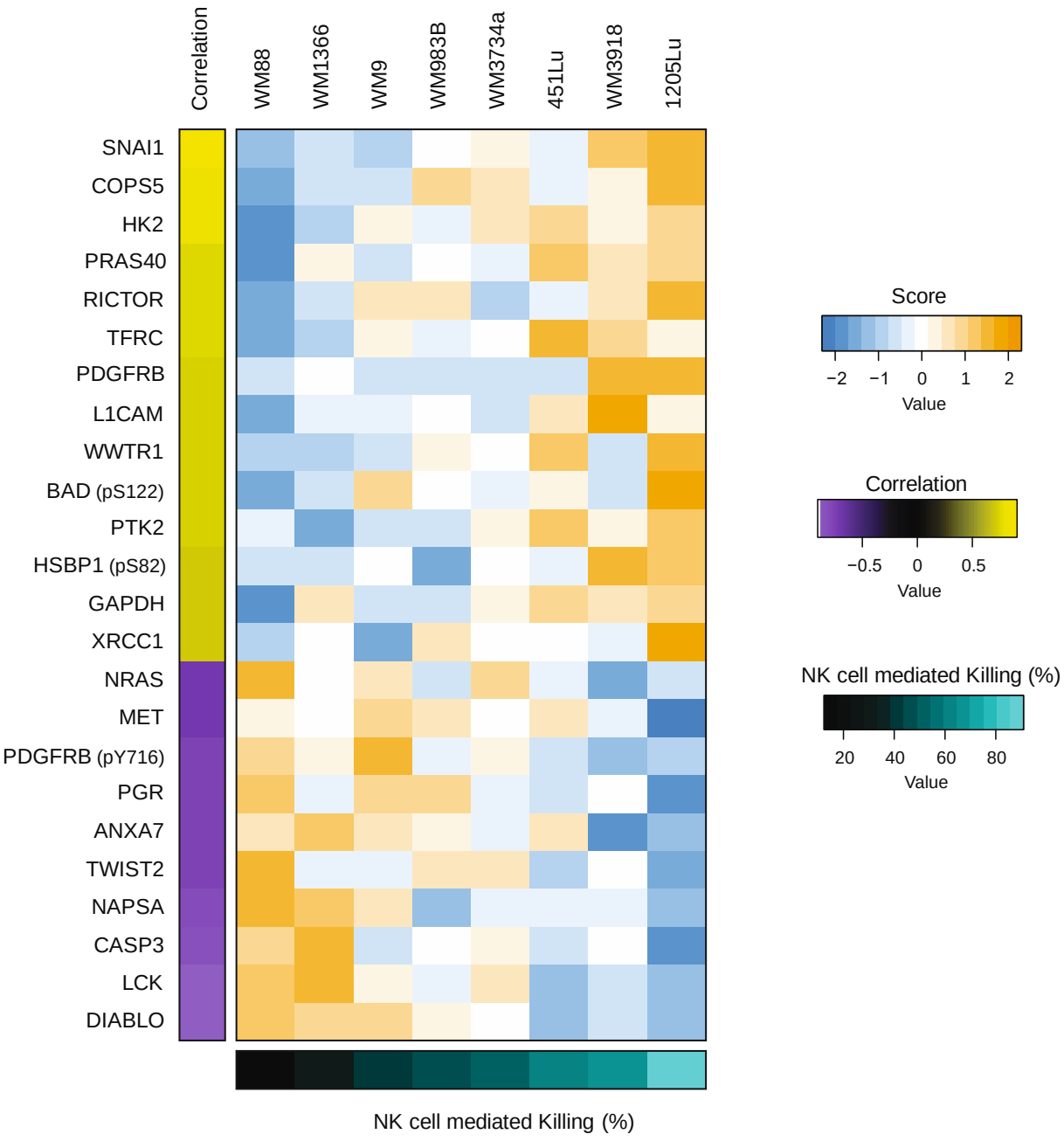

Figure 17. Melanoma protein signature determines susceptibility to primary NK cells. Heat map of the protein expression profile of eight melanoma cell lines shown in Figure 14. Protein expression of the RPPA are given as median centered log2 intensities. The correlation between NK cell killing and protein expression was determined by the Pearson correlation coefficient. For better visualisation of the heat map the log2MedCen intensities values were transformed into the standard scores (z-score) scaled by individual gene (row). Proteins that correlated directly (yellow) with the killing efficiency were: SNAI1, COP9 signalosome subunit 5 (COPS5), HK2, PRAS40, RICTOR, TFRC, PDGFRB, L1 Cell Adhesion Molecule (L1CAM), WW Domain Containing Transcription Regulator 1 (WWTR1), BAD (pS122), PTK2, Heat Shock Factor Binding Protein 1 (HSBP1), GAPDH and X-Ray Repair Cross Complementing 1 (XRCC1). A negative correlation was observed in the case of NRAS, MET, PDGFRB (pY716), PGR, Annexin A7 (ANXA7), (TWIST2), NAPSA, CASP3, Lymphocyte Cell-Specific Protein-Tyrosine Kinase (LCK) and DIABLO. The heat map was generated by using the gplots package in R.

As discussed above, melanoma proteins that highly correlated with NK cell killing are involved in several distinct cellular processes. The expression pattern of these identified molecular

determinants of melanoma susceptibility towards NK cell killing was named 'melanoma killing signature' and was applied to predict NK cell-induced cytotoxicity against different untested melanoma cell lines.

4.5 Melanoma killing signature allows the prediction of susceptibility to NK cells

The prediction of treatment success is a crucial part in developing a proper therapeutic strategy. Since *in vitro* studies could give indications about the success of treatment, the protein expression profile of the different melanoma cell lines was used to develop a simple prediction model. The original median centered log2 intensities (Log2MedCen) of all proteins that showed a higher Pearson correlation coefficient than ±0.7 are depicted in Table 21. The intensity values of negatively correlated proteins (highlighted in grey) were inverted and the average expression of the melanoma killing signature was determined for each melanoma cell line for later linear regression analysis.

Table 21. Correlation of melanoma protein expression with NK cell susceptibility

	Cell line	WM88	WM1366	WM9	WM983B	WM3734	451Lu	WM3918	1205Lu	Correlation
	Killing (%)	14.3	31.0	42.1	45.0	50.3	62.0	69.4	90.9	
Log2MedCen of the indicated protein	SNAI1	-0.07	-0.005	-0.035	0.119	0.129	0.064	0.255	0.328	0.906
	COPS5	-0.044	0.03	0.043	0.142	0.116	0.049	0.1	0.204	0.825
	HK2	-0.241	-0.101	0.144	0.042	0.146	0.244	0.102	0.212	0.825
	BAD (pS112)	-0.352	-0.152	0.18	-0.015	-0.108	0.031	-0.132	0.334	0.73
	RICTOR (pT1135)	-0.488	-0.138	0.266	0.371	-0.308	-0.041	0.304	0.65	0.75
	PRAS40	-0.395	0.161	-0.101	0.039	0.024	0.34	0.196	0.242	0.76
	GAPDH	-0.859	0.369	-0.296	-0.176	0.231	0.453	0.299	0.411	0.717
	TFRC	-0.584	-0.226	0.191	-0.034	0.084	0.802	0.491	0.246	0.746
	WWTR1	-0.052	0.03	0.166	0.605	0.462	1.238	0.062	1.386	0.731
	L1CAM	-1.726	-0.365	-0.51	0	-0.715	0.535	1.701	0.252	0.739
	PDGFRB	-0.173	0.371	-0.203	-0.029	-0.016	-0.2	2.081	2.223	0.745
	XRCC1	-0.296	-0.101	-0.45	0.069	-0.048	-0.064	-0.129	0.432	0.709
	HSBP1 (pS82)	-0.359	-0.376	-0.234	-0.659	-0.22	-0.269	0.303	0.218	0.719
	PTK2	-0.086	-0.606	-0.201	-0.276	0.05	0.429	0.055	0.455	0.723
	NRAS	-0.078	0.033	-0.025	0.079	-0.045	0.049	0.144	0.088	0.706

	Cell line	WM88	WM1366	WM9	WM983B	WM3734	451Lu	WM3918	1205Lu	Correlation
	Killing (%)	14.3	31.0	42.1	45.0	50.3	62.0	69.4	90.9	
	PDGFRB (pY716)	-0.079	0	-0.205	0.14	0.04	0.191	0.281	0.239	0.755
	MET	-0.015	0.018	-0.064	-0.029	0.043	-0.051	0.065	0.317	0.707
	ANXA7	-0.166	-0.213	-0.165	-0.133	-0.088	-0.163	0.059	0.006	0.76
	PGR	-0.104	0.054	-0.076	-0.093	0.028	0.081	0.013	0.178	0.757
	NAPSA	-0.124	-0.077	0.006	0.223	0.122	0.099	0.104	0.243	0.805
	TWIST2	-0.128	0.019	0.018	-0.054	-0.059	0.055	-0.004	0.111	0.768
	CASP3	-0.057	-0.101	0.065	0.007	-0.001	0.065	0.019	0.153	0.828
	LCK	-0.256	-0.323	-0.094	0.02	-0.137	0.194	0.127	0.225	0.885
	DIABLO (Smac)	-0.129	-0.035	-0.056	0.082	0.187	0.468	0.266	0.47	0.9
	Average	-0.286	-0.072	-0.068	0.018	-0.003	0.192	0.282	0.401	

Simple linear regression analysis showed a strong correlation ($r > 0.96$) between this average expression (log2MedCen) of the melanoma killing signature and the NK cell-mediated killing of the same melanoma cell lines (Figure 18).

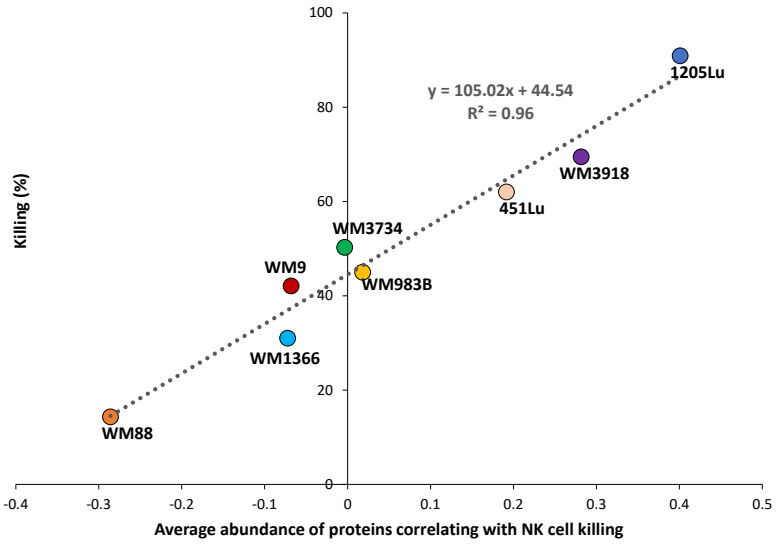

Figure 18. Linear regression analysis of the melanoma killing signature is used to establish a killing prediction model. The average expression of the melanoma killing signature (Table 21) correlates with NK cell-induced cytotoxicity against melanoma cells.

Given the high correlation, we postulated that we could use the average expression of the melanoma killing signature to predict the NK cell-induced cytotoxicity against additional

melanoma cell lines. To validate this prediction model, we calculated the expected NK susceptibility of eight additional, previously untested melanoma cell lines with the help of the simple linear regression equation (Figure 19 A). Subsequently, the susceptibility of these eight melanoma cell lines was determined experimentally using the above-described killing assay (Figure 19 B). As expected, the new panel of melanoma cell lines were killed to varying amounts by primary NK cells. The most resistant melanoma cell line was WM3268 that was only killed about 23 % after 4 h, whereas WM3682 was highly susceptible (~81 %) to primary NK cells. In addition, the endpoint killing of WM858 cells (~71 %) was comparable to the susceptibility results of the cell line WM793 (~69 %), whereas WM858 cells were initially killed faster. In comparison to WM3482 cells that show a stagnant course of killing curve with a maximal killing of 33 %, the cell line WM902B has a linear course of killing that reached after 240 min almost 47 %. Furthermore, WM164 cells and WM47 cells were eliminated to ~55 % and ~62 %, respectively. In Figure 19 C, the experimental data of the cytotoxic assays are compared to the melanoma susceptibility of the prediction model. Although, the NK cell-mediated killing of WM3682 and WM3268 was predicted to be similar (35 % and 39 %, respectively), only the low susceptibility of WM3268 (~23 %) to NK cells was experimentally validated. A better match was achieved with WM47 (~61 %) that was predicted to be eliminated about 53 % after 4 h. The experimental data of WM902B (~47 %) and WM164 (~55 %) were a slightly lower than the predicted killing (~62 %, ~69 %), but showed good correlation. The predicted susceptibility of WM858 (~70 %), WM793 (~64 %) and WM3482 (~33 %) almost matches the results of the killing assays (66 %, 65 %, 38 %). WM3682 was the only cell line that showed immense aberration between predicted and experimental killing. The susceptibility of WM3682 might have other genetically reasons and be dominated by distinct proteins than the majority of the investigated melanoma cell lines. Therefore, this cell was excluded from subsequent linear regression analysis. Although the prediction model sometimes over- or underestimated the experimental NK cell-mediated killing of the seven melanoma cell lines, Figure 19 D shows that the correlation of predicted and validated killing was relatively high (0.67).

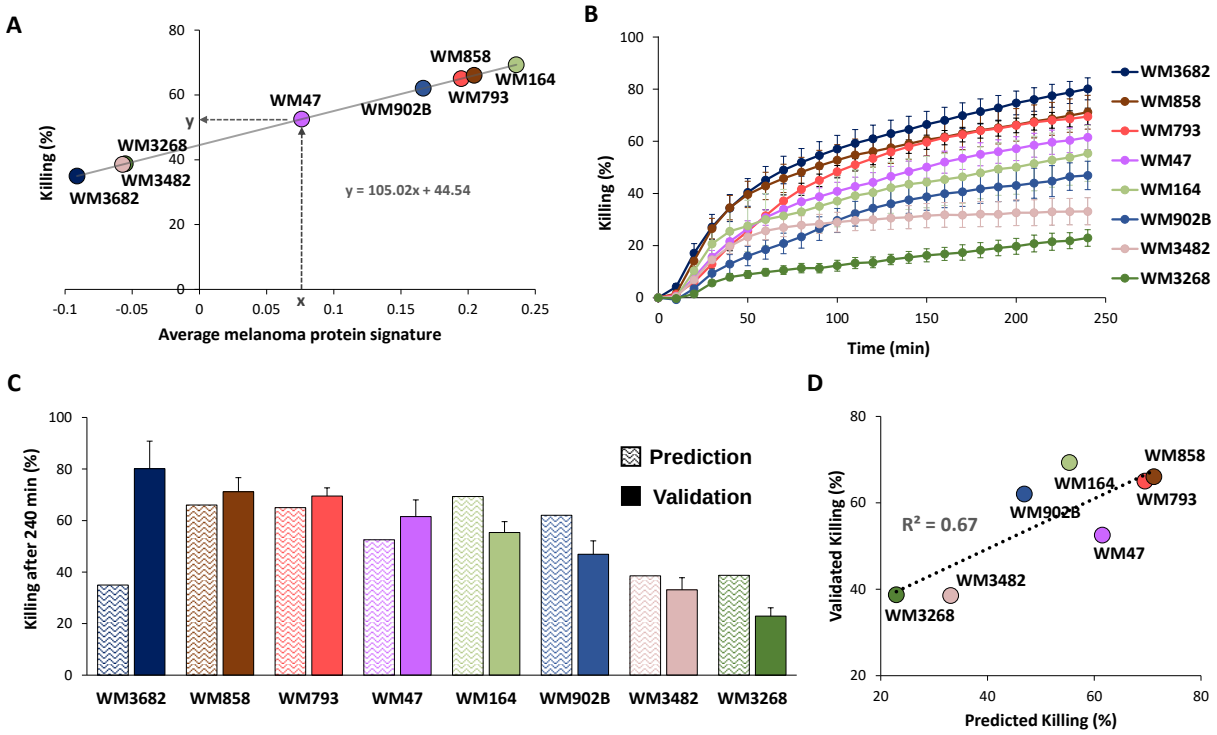

Figure 19. Validation of the prediction model. (A) The susceptibility of eight additional melanoma cell lines was calculated with the help of their protein signature. (B) Subsequent cytotoxicity assays with the tested melanoma cell lines: n (WM3682): 10; n (WM858): 10; n (WM793): 7; n (WM47): 9; n (WM164): 3; n (WM902B): 3; n (WM3482): 8 and n (WM3268): 3. Effector cells were IL-2 activated primary NK cells. Graphs indicate means ± SEM (C) Predicted as well as validated killing after 240 min. Bars of the validation indicate means ± SEM. (D) Correlation of predicted and validated end killing (240 min) of all investigated cell lines with trend line and under specification of their correlation (with exclusion of WM3682).

These data clearly indicated that this model can be used to predict the rough NK cell cytotoxicity against melanoma cells and might help in estimating if a patient would benefit from a NK cell-based therapy.

4.6 Single regulators of the melanoma cell susceptibility to NK cell killing

The killing data of the additional validated melanoma cell lines was further used to identify the pivotal proteins involved in the susceptibility of melanoma to NK cell killing. Therefore, the additional seven melanoma cell lines were included in the previously described RPPA analysis (chapter 4.4). This additional analysis identified the proteins SNAI1 and DIABLO with Pearson correlation coefficients $<\pm 0.7$ as the most important determinants of NKiToxMel. All other proteins of the melanoma killing signature showed lower correlation with NK cell killing.

In order to validate SNAI1 and DIABLO as regulators of melanoma cell susceptibility to NK cells the expression levels of individual proteins were altered by genetic manipulation.

4.6.1 DIABLO is a potential negative regulator of NK cell-mediated killing

DIABLO is a mitochondrial protein that promotes apoptosis by binding inhibitors of apoptosis proteins (Verhagen et al., 2000). Taken that the expression levels of DIABLO showed highest inverse correlation with NKiToxMel (Table 21), the role of DIABLO in melanoma susceptibility to NK cell killing was investigated in more detail.

To examine the expression of DIABLO in melanoma cell lines, the initial 'prediction model cell panel' melanoma cell panel was analysed using immunoblot analyses. In Figure 20, the protein abundance of DIABLO in 8 different melanoma cell lines (training panel) is shown. The expression was normalised to the reference protein calnexin. Similar to the RPPA data, the expression of DIABLO decreased with increasing susceptibility to NK cells. For example, WM88 cells expressed double the amount of DIABLO (0.77) in comparison to 1205Lu (0.38).

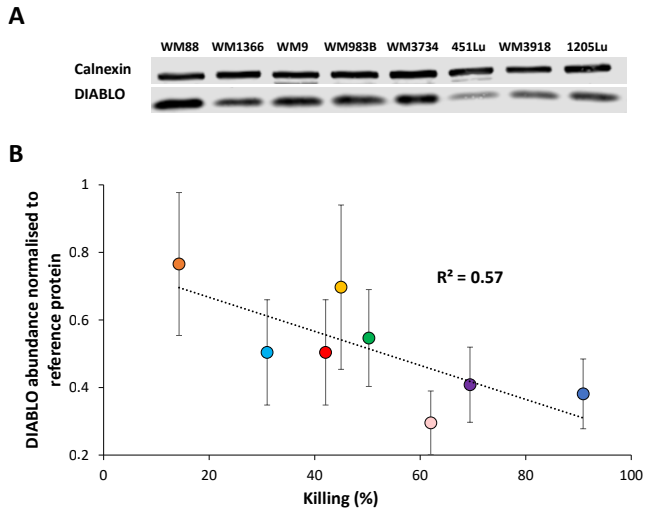

Figure 20. DIABLO abundance in melanoma correlates with their susceptibility to NK cells(A) Representative immunoblot. (B) Mean and SEM of five analysed immunoblots under specification of the protein expression normalised to the loading control Calnexin. The coloured dots correspond to each cell line presented in (A) in order of appearance from left to right.

After validation of the endogenous protein abundance, the expression of DIABLO was genetically altered to examine if and how DIABLO abundance affects NKiToxMel. Transient overexpression of a gene of interest with a plasmid construct is an established approach to investigate a functional role of a given protein. The use of a GFP labelled plasmids allows an easy validation of transfection efficiency. Hence, melanoma cells were transfected with pmax GFP, a plasmid with high transfection efficiency and GFP signal intensity. After 24 h, the targets cells showed a strong GFP signal and were used in our future cytotoxic assays. Because it was possible that GFP may interfere with the fluorescence signals from calcein-AM also used in the cytotoxic assay, we tested the possible interference. As seen in Figure 21 (A+B), pmax GFP transfected

and non-transfected WM88 cells (A) and WM47 (B) show almost identical killing curves. Therefore, the interference of the much weaker GFP signals in the calcein-AM based cytotoxic assay could be excluded.

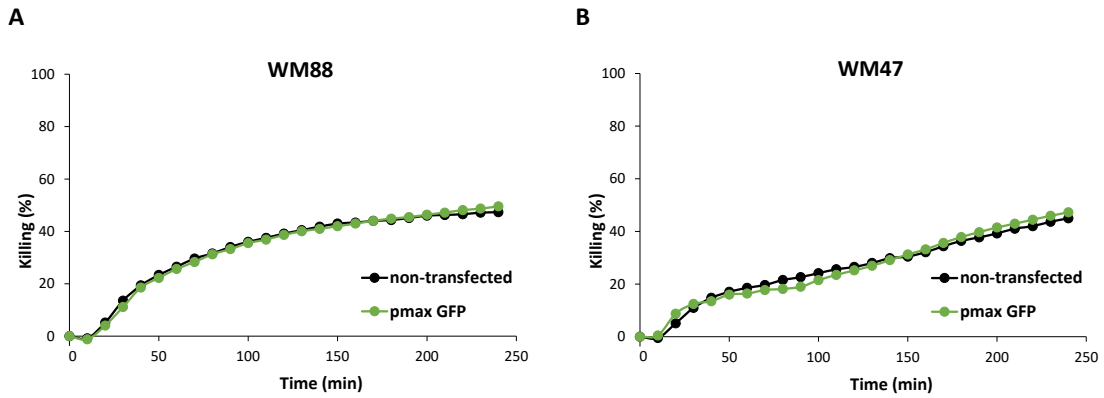

Figure 21. GFP signal does not interfere with calcein-AM detection. WM88 (A) and WM47 (B) were transfected with pmax GFP. After 24 h transfected as well as melanoma cells were challenged with one primary NK cell donor (A) and NK-92 cell line (B) in a 4 h real-time killing assay.

The 1205Lu line has one of the lowest DIABLO expression and was thus used to test if and how DIABLO-GFP overexpression affects NKiToxMel. The GFP construct allowed monitoring of the DIABLO expression and determination of the harvesting time after transfection. The overexpression of DIABLO after 24 h of the performed transfection showed an almost 30-fold increased expression of DIABLO-GFP (Figure 22 A-B). Notably, in the cells overexpressing DIABLO-GFP, the endogenous expression of DIABLO was reduced by about 20 %. However, despite the validated overexpression, the susceptibility of 1205Lu was not influenced by the higher protein abundance of DIABLO. As seen in Figure 22 C, the killing curve of DIABLO-GFP transfected 1205Lu cells was almost congruent with the killing curve of the peGFPC1 control. Both curves showed an initial killing of ~30 % (Figure 22 D) that increased to a value of about 70 % after 4 hours (Figure 22 E).

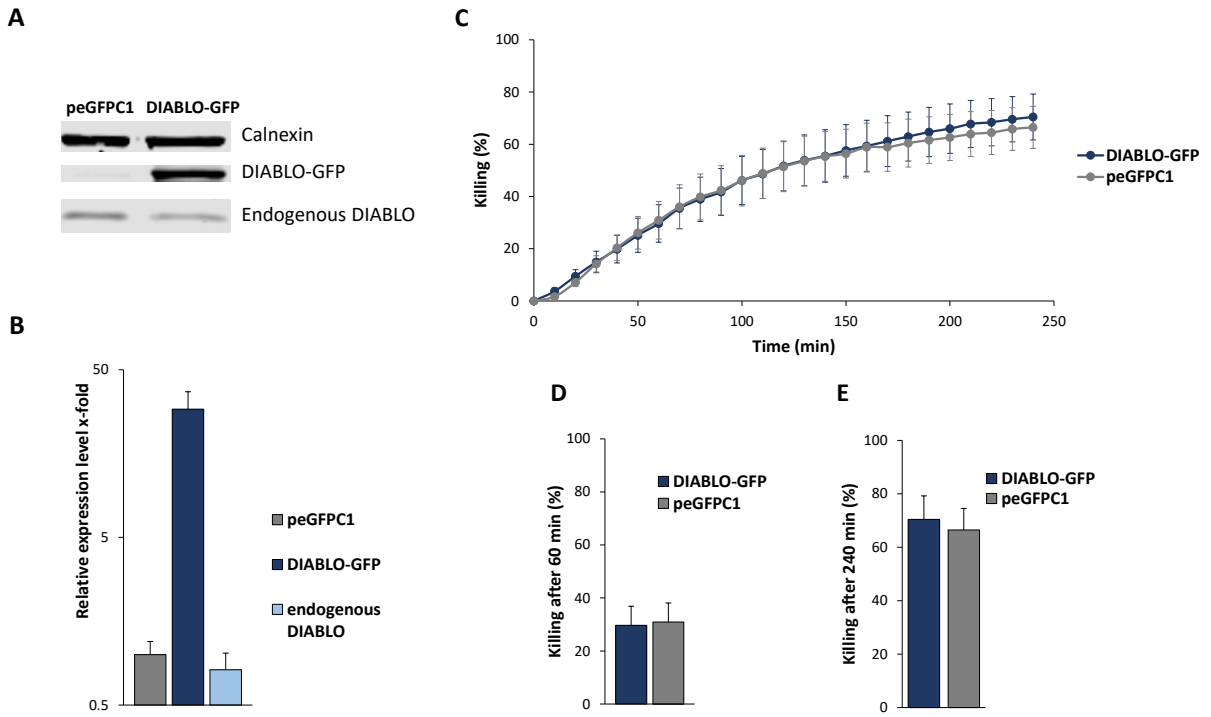

Figure 22. Overexpression of DIABLO does not change susceptibility of melanoma towards NK cells. 1205Lu cells were transfected with a DIABLO-GFP construct or with the control plasmid peGFPC1. After 24 h cells were harvested and the DIABLO expression was analysed. (A) Representative immunoblot (B) The band intensities of 3 immunoblots were quantified with Image Studio™ Lite Software. The band intensities of DIABLO (DIABLO-GFP; endogenous DIABLO) were normalised to the band intensities of the loading control Calnexin. (C-E) The susceptibility of DIABLO overexpressing 1205Lu cells were determined in 4 h real-time killing assays. 1205Lu cells transfected with DIABLO-GFP or with the empty plasmid peGFPC1 were exposed to primary NK cells (n=6) in E:T ratio of 5:1. (C) Killing kinetics of 4 h cytotoxic assay. (D) Killing after 60 min and (E) killing after 240 min. All bars and graphs indicate means ± SEM.

Given the fact that DIABLO interacts with other proteins such as XIAP, increasing levels of DIABLO alone, without changing expression levels of its interaction partners might not affect the NKiToxMel. That is why the downregulation of DIABLO was tested next. For this purpose, the WM3734 cells that showed higher expression of DIABLO were transfected with two different siRNAs (#1, #2). One day after the initial transfection, the transfection procedure was repeated. After additional 24 h, WM3734 cells were harvested and further analysed. As shown in Figure 23 A and B, the protein abundance of DIABLO after 24 h of double transfection was reduced by 22 % (#2) and 41 % (#1). The transfection with DIABLO #2 was not sufficient to alter the NKiToxMel whereas DIABLO #1 siRNA slightly increased the susceptibility of WM3734 to primary NK cells (Figure 23 C). The initial killing (Figure 23 D) could be significantly increased from 47 % to 53 % after DIABLO knockdown. This increased susceptibility to NK cells of about 6 % was also detectable 4 h after the NK cell treatment (68 % to 74 %) (Figure 23 E).

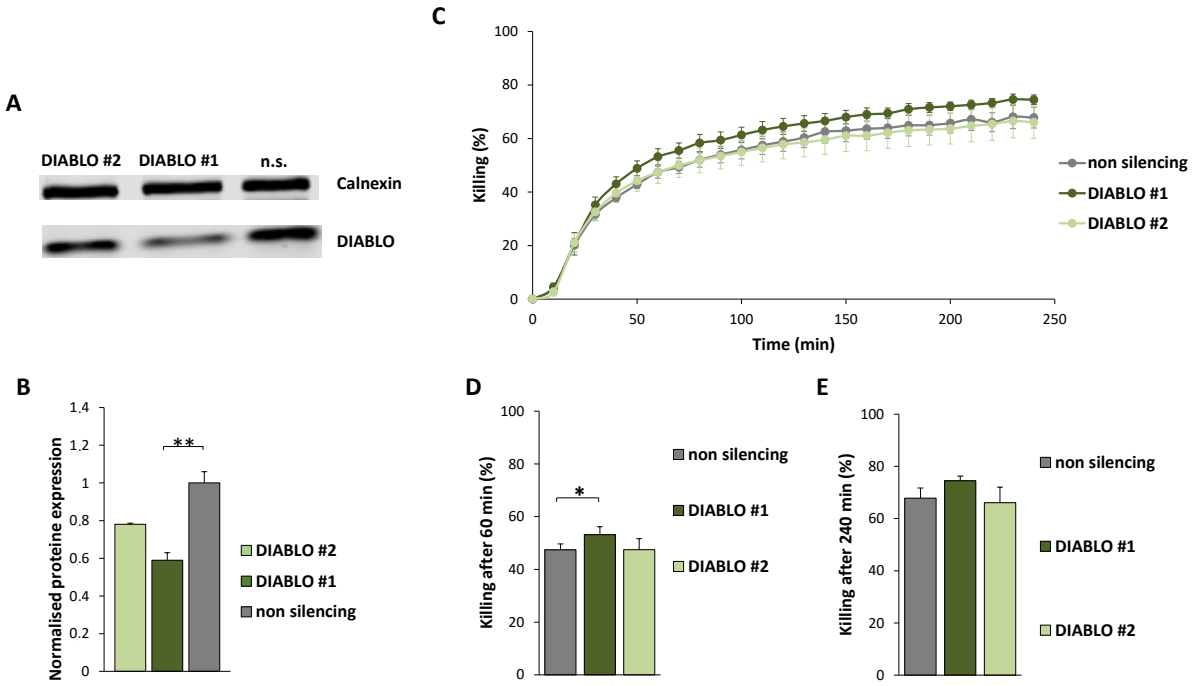

Figure 23. DIABLO knockdown slightly increases susceptibility of melanoma towards NK cells. WM3734 cells were transfected with non-silencing RNA or with two different siRNA (#1 and #2) targeting DIABLO. The next day, the procedure was repeated and WM3734 cells were harvested and further analysed after additional 24 h. The DIABLO expression of WM3734 after DIABLO knockdown was analysed. (A) Representative immunoblot. (B) The band intensities of 4 immunoblots were quantified with Image Studio™ Lite Software. The band intensities of DIABLO were normalised to the band intensities of the loading control Calnexin. (C-E) The susceptibility of WM3734 after DIABLO knockdown was determined in 4 h real-time killing assays. Target cells were exposed to primary NK cells (n=4) in E:T ratio of 5:1. (C) Killing kinetics of 4 h cytotoxic assay. (D) Killing after 60 min and (E) killing after 240 min. All bars and graphs indicate means ± SEM. Statistical significance of unpaired (B) or paired (D), two-tailed Student's *t*-test is indicated with * for $p<0.05$ and ** for $p<0.01$

Although the abundance of DIABLO showed the expected heterogeneity in the melanoma cell lines and was even associated with their susceptibility to NK cells (Figure 20), short-term altered expression level of DIABLO did not resulted in dramatic changes in NKiToxMel. These data do not exclude the potential role of DIABLO in susceptibility of melanoma to NK cell killing. Longer overexpression times or the stable knockdown of DIABLO might be needed to alter NKiToxMel more efficiently.

4.6.2 SNAI1 is a positive regulator of NK cell-mediated killing of melanoma

Contrary to DIABLO, previous data (see above) indicated that the protein SNAI1, also known as Snail, positively influences the susceptibility of melanoma cells towards primary NK cells. SNAI1, a zinc finger protein, is a key regulator of EMT by repressing E-cadherin expression (Kaufhold and Bonavida, 2014; Wang et al., 2013). To test the expression of *SNAI1* in the investigated melanoma cell lines, quantitative PCR (qPCR) with the initial "training" melanoma panel was

performed. Figure 24 shows that, the mRNA levels of *SNAI1* in eight melanoma cell lines were associated with their susceptibility to primary NK cells. The $2^{-\Delta\ Cq}$ expression values were normalised to the housekeeping gene TBP. The melanoma cell lines WM88 and WM1366 with lowest susceptibility to NK cell killing did not express *SNAI1*. The majority of the other melanoma cell lines showed mRNA levels of *SNAI1* higher than 0.8. Only WM3918 revealed low *SNAI1* mRNA level (0.22) that mismatched with their high NK cell susceptibility. Nevertheless, increasing *SNAI1* mRNA level was associated with higher NKiToxMel.

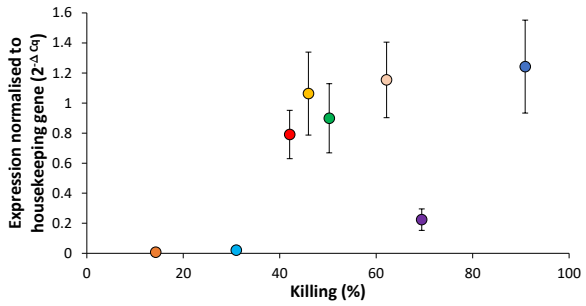

Figure 24. The expression of *SNAI1* in melanoma cells is associated with their susceptibility to NK cells. The mRNA expression levels ($2^{-\Delta\ Cq}$) of 8 melanoma cell lines were normalised to the housekeeping gene TBP. The melanoma cell lines used were WM88 (orange, n=5), WM1366 (light blue, n=5), WM9 (red, n=5), WM983B (yellow, n=5), WM3734 (green, n=5), 451Lu (rosé, n=5), WM3918 (purple, n=4) and 1205Lu (dark blue, n=5).

As WM88 cells were shown to be *SNAI1* negative, this cell line was used for further overexpression experiments. Hence, WM88 was transfected with a SNAI1-GFP construct or the corresponding empty plasmid peGFPC1. As seen in Figure 25 A, WM88 cells already showed a stable GFP signal after 24 h. Additionally, the overexpression was validated by immunoblot analysis (Figure 25 B). The SNAI1 expression in WM88 could be significantly increased more than 50 times (Figure 25 C). Subsequent real-time killing assays depicted in Figure 25 D showed that the SNAI1 overexpression led to a higher NKiToxMel. The initial killing (Figure 25 E) of SNAI1-GFP transfected WM88 was almost doubled in comparison to the control plasmid. This trend continued and strengthened during the whole course of the cytotoxic assay. After 240 min, the killing of WM88 was significantly increased from ~12 % (peGFPC1 plasmid) to 23 % (Figure 25 F).

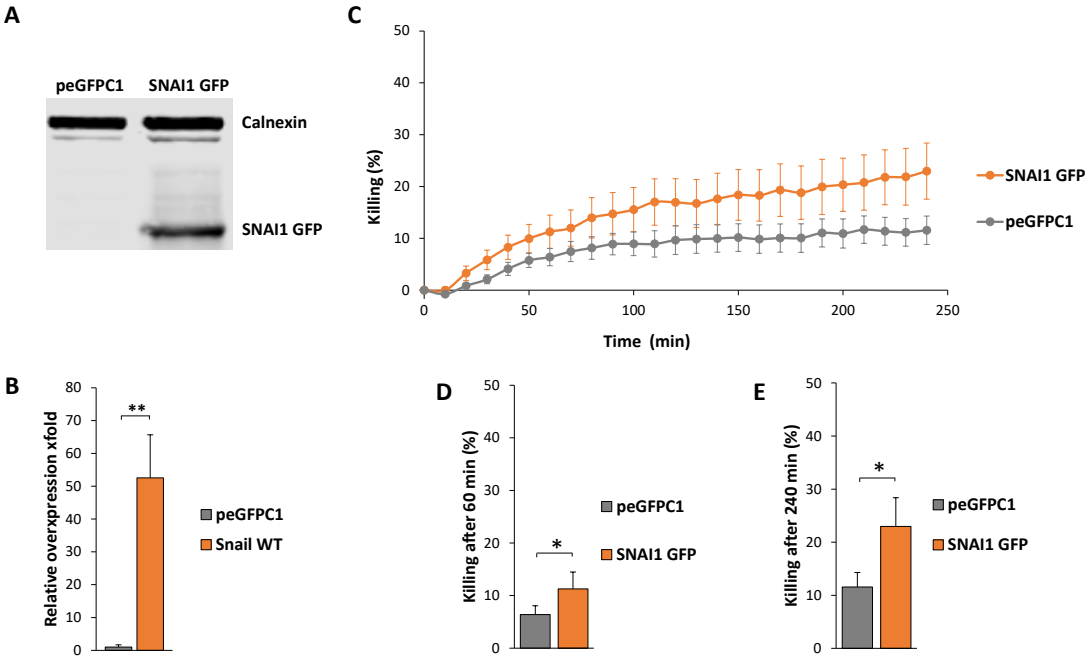

Figure 25. Overexpression of SNAI1 increases the susceptibility of melanoma cells towards NK cells. WM88 was transfected with a SNAI1-GFP construct or with the control plasmid peGFPC1. After 24h cells were harvested and SNAI1 expression was analysed. (A) Representative immunoblot. (B) The band intensities (n=6) of immunoblots were quantified with Image StudioTM Lite Software. The band intensities of SNAI1 were normalised to the band intensities of the loading control Calnexin. (C-E) The susceptibility of SNAI1 overexpressing WM88 cells was determined in 4 h real-time killing assays. WM88 cells transfected with SNAI1-GFP or peGFPC1 control plasmid were exposed to primary NK cells (n=10) in E:T ratio of 5:1. (C) Killing kinetics of 4 h cytotoxic assay. (D) Killing after 60 min and (E) killing after 240 min. All bars and graphs indicate means ± SEM. Statistical significance of paired (D+E) and unpaired (B), two-tailed Student's *t*-test is indicated with ** for $p<0.01$.

SNAI1 was validated as a positive regulator of the NK cell-mediated killing of melanoma cells since elevating *SNAI1* expression was associated with higher susceptibility of melanoma cells to NK cell killing and the overexpression of SNAI1 increased NKiToxMel.

4.7 Susceptibility of melanoma cells towards NK-92 killing shows heterogeneity similar to primary NK cells

The use of primary NK cells in clinical applications can be challenging since NK cell proliferation and reliable NK cell cytotoxicity are limiting factors. Therefore, the use of NK cell lines or iPSC-derived NK cells as an 'off-the-shelf therapeutic' with enhanced cytotoxicity by genetic modifications as well as increased expansion potential are attractive alternatives in adoptive cell transfer (Suck et al., 2016). For this reason, the cytotoxicity of the NK cell line NK-92 against nine different melanoma cell lines and the control cell line K562 was tested. Figure 26 A shows that also NK-92 induced heterogeneous melanoma killing, with a pattern similar to the one of the primary NK cells. Nevertheless, the cytotoxicity of NK-92 against melanoma after 4 h (Figure

26 B) is in average lower when compared to the primary NK cells. Even the positive control cell line K562 was only killed to 88 % after 240 h. Comparable to the primary NK cells, the melanoma cell line 1205Lu showed the highest (~64 %) susceptibility to NK-92, whereas WM88 was resistant (1 %) against NK-92 killing. In addition, Figure 26 C shows that the initial NK-92 killing of melanoma was lower on average than primary NK cell killing (7 %). The susceptibility of the other cell lines ranged between 11 % (WM3482) and 52 % (WM3682). WM983B and WM3734 were again in the middle range (29 % and 25 %, respectively) of the determined effector killing. One group of melanoma cells consisting of WM47, WM3918 and WM858 showed much lower susceptibility (< 25 %) towards NK-92 than expected from the previous experiments with primary NK cells. Despite this discrepancy, the cytotoxicity of primary NK cells and NK-92 against melanoma cells showed a good correlation (Figure 26 D), although the cytotoxic potential of NK-92 against melanoma cells was lower.

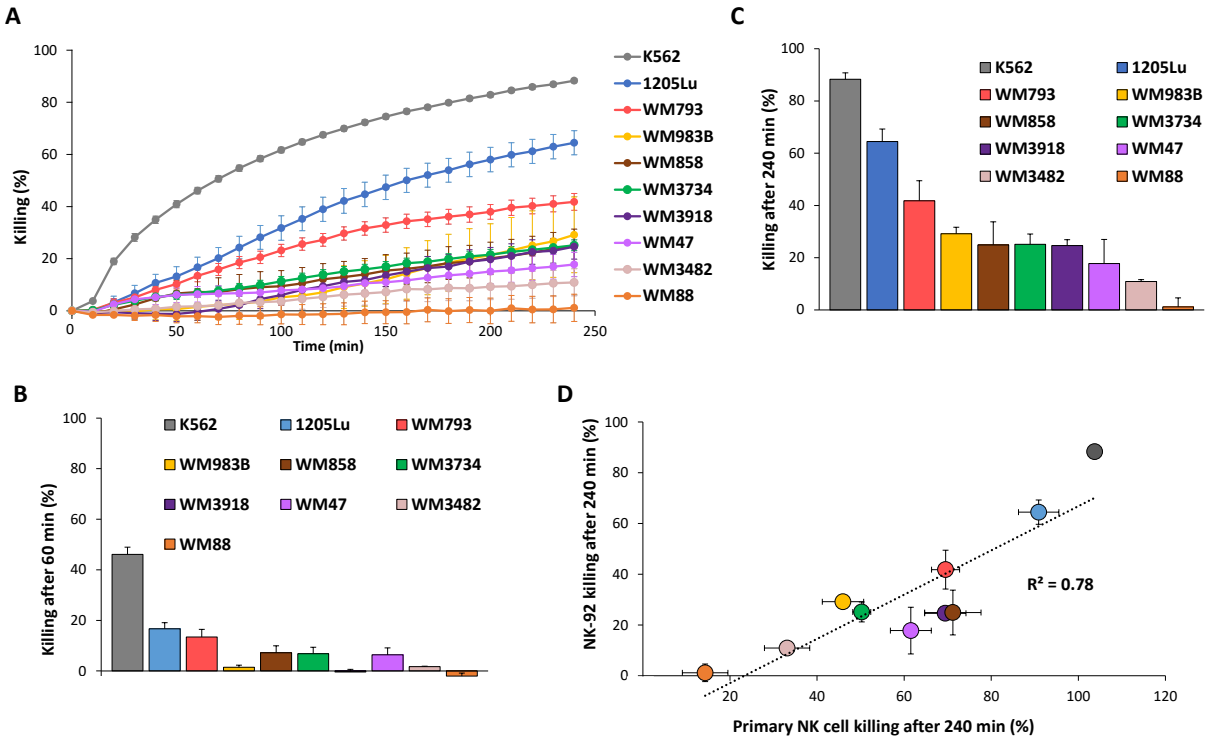

Figure 26. Susceptibility of melanoma cell lines to NK-92 is heterogeneous. The melanoma cell lines used in the 4h real-time killing assays were: 1205Lu (n=5), WM793 (n=3), WM983B (n=4), WM3734 (n=16), WM858 (n=4), WM3918 (n=4); WM47 (n=5), WM3482 (n=3) and WM88 (n=11). As a positive killing control, K562 (n = 43) was used. (A) Killing kinetics of 4 h cytotoxic assay. (B) Killing after 60 min and (C) killing after 240 min. (D) Correlation of primary NK cell and NK-92 mediated end killing (240 min) of all investigated cell lines with trend line and under specification of their correlation. Bars and graphs indicate means ± SEM.

Since the pattern of the NK-92 and primary NK cells showed similarities, the investigation of the proteins that are involved in the susceptibility of melanoma towards NK-92 could provide a more detailed insight into the complexity of NK cell cytotoxicity against melanoma cells.

Accordingly, the RPPA data was correlated with the NK-92 killing results of the nine tested melanoma cell lines. The proteins with high Pearson correlation coefficients (> ± 0.7) were termed 'melanoma-NK-92 killing signature' and are summarised in Table 22.

Table 22. Correlation of melanoma protein expression with NK-92 cell susceptibility

	Cell line	WM88	WM3482	WM47	WM3918	WM858	WM3734	WM983B	WM793	1205Lu	Correlation
	Killing (%)	3.2	10.9	17.8	24.6	24.9	26.6	29.1	41.8	64.5	
Log2MedCen of the indicated protein	PEA15 (pS116)	-0.03	-0.08	-0.03	-0.09	-0.03	0.02	0.01	0.19	0.23	0.85
	BAD (pS112)	-0.35	-0.05	-0.03	-0.13	-0.26	-0.11	0.102	0.28	0.33	0.84
	XRCC1	-0.30	-0.01	-0.10	-0.13	-0.30	-0.05	0.07	0.44	0.43	0.82
	RPS6K (pT573)	-0.51	-0.20	0.08	-0.44	0.00	0.29	-0.07	0.67	0.62	0.82
	TGM2	-0.08	-0.14	-0.05	0.07	0.45	0.31	0.08	0.30	0.55	0.81
	HK2	-0.24	-0.16	-0.23	0.10	-0.18	0.15	0.04	0.13	0.21	0.80
	SNAI1	-0.07	-0.07	0.08	0.26	0.32	0.13	0.12	0.33	0.33	0.79
	RPS6KB1 (pT389)	-0.49	0.30	-0.22	0.07	0.40	0.22	1.26	2.36	1.33	0.74
	MEK1 (pS217)	-0.15	-0.01	0.69	-0.48	0.12	0.07	0.20	0.68	0.59	0.73
	YBX1	-0.22	-0.07	-0.07	-0.10	0.15	0.39	-0.08	0.31	0.33	0.73
	CDKN1B	-0.04	-0.05	0.00	0.03	0.03	-0.05	0.14	0.45	0.23	0.72
	XBP1	0.04	-0.18	0.12	-0.16	-0.06	0.58	1.47	2.59	1.57	0.72
	EGFR	-0.16	-0.13	-0.08	0.49	1.54	0.43	2.12	3.34	1.88	0.71
	PGR	0.10	0.03	0.23	-0.01	0.05	-0.03	0.09	-0.26	-0.18	- 0.73
	PIK3R1	0.28	-0.11	0.27	0.05	-0.26	0.21	-0.45	-0.28	-0.56	- 0.73
	MET	0.02	-0.11	0.05	-0.06	0.02	-0.04	0.03	-0.25	-0.32	- 0.77
	BCL2	0.45	0.45	0.02	0.04	-0.27	-0.06	0.21	-0.03	-0.37	- 0.78
	HSP70	0.91	0.77	0.09	0.09	-0.11	0.06	0.07	-0.73	-0.29	- 0.79
	DVL3	0.38	0.42	0.01	-0.09	0.15	-0.02	-0.18	-0.25	-0.25	- 0.82
	DIABLO	0.13	-0.15	-0.09	-0.27	-0.07	-0.19	-0.08	-0.27	-0.47	- 0.87

In addition, the results of this RPPA analysis were visualised in a heat map (Figure 27). The top positive regulator of NK-92 cytotoxicity against melanoma cells were phosphorylated (S116) proliferation and apoptosis adaptor protein 15 (PEA15), whereas DIABLO showed again the highest negative killing correlation. In addition, the identified proteins HK2, SNAI1, BAD (pS112), XCCR1, MET and PGR were also part of the previous presented melanoma killing

signature (Figure 17). Furthermore, ribosomal protein S6 kinase (RPS6K) (pT573), ribosomal protein S6 kinase B1 (RPS6KB1) (pT389) and phosphatidylinositol 3-kinase regulatory subunit alpha (PIK3R1) indicate the involvement of PI3K-AKT-mTOR signalling in melanoma susceptibility to NK-92 killing.

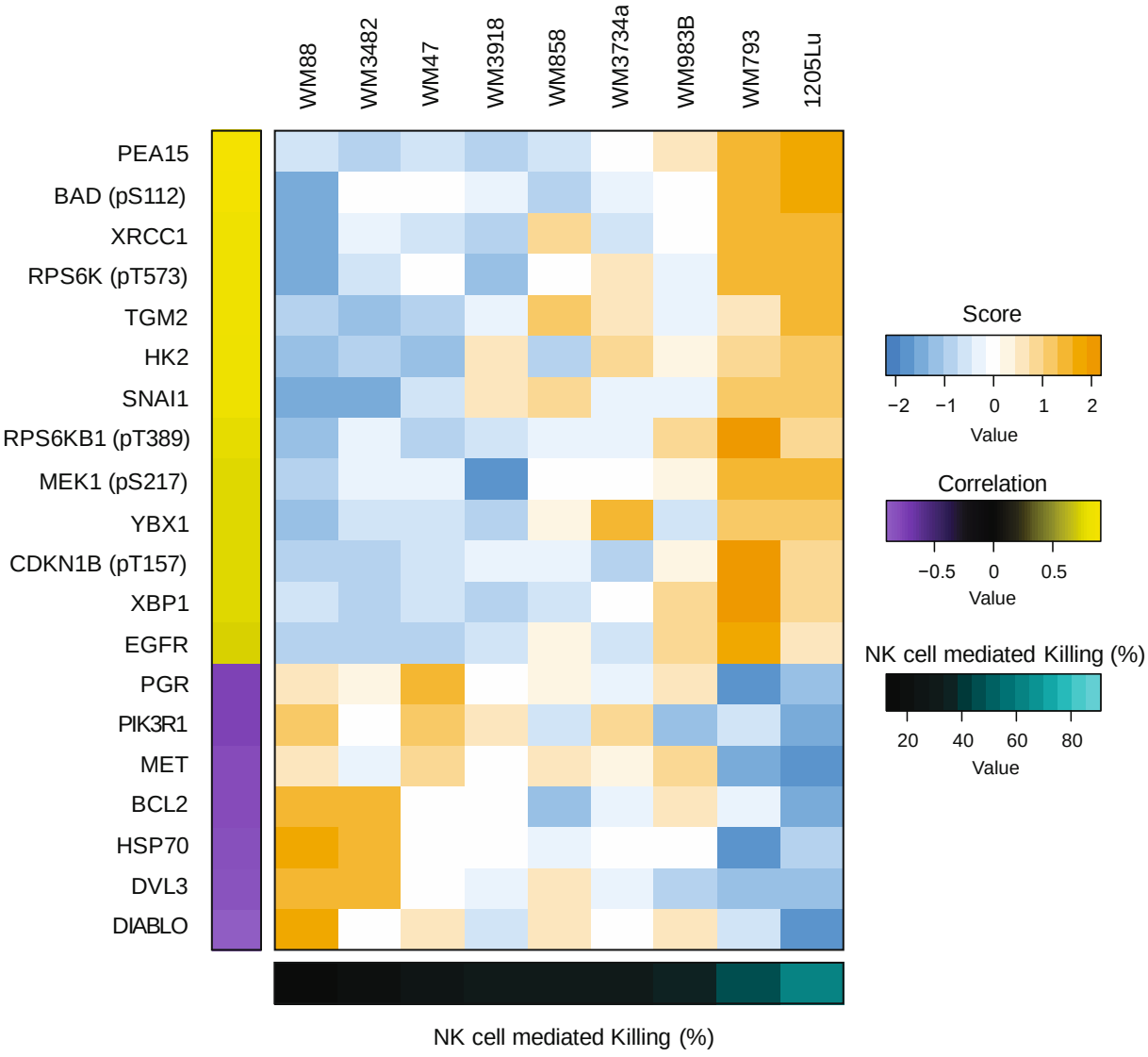

Figure 27. Melanoma NK-92 killing signature determines susceptibility to NK-92 cells. Heat map of the protein expression profile of nine melanoma cell lines differing in their susceptibility to NK-92. Protein expression of the RPPA were median centered log2 intensities. The correlation between NK-92 killing and protein expression was determined by the Pearson correlation coefficient. The increased expression of PEA15, BAD (pS112), XRCC1, RPS6K (pT573), Transglutaminase-2 (TGM2), HK2, SNAI1, RPS6KB1 (pT389), MEK1 (pS217), Y-box-binding protein 1 (YBX1), Cyclin-dependent kinase inhibitor 1B (CDKN1B), X-Box Binding Protein 1 (XBP1) and EGFR were associated with a higher susceptibility of melanoma towards NK-92. Inverse correlation (purple) of protein abundance and NK-92 killing was found in PGR, phosphatidylinositol 3-kinase regulatory subunit alpha (PIK3R1), MET, BCL2 apoptosis regulator (BCL-2), heat shock protein family A (HSP70), dishevelled segment polarity protein 3 (DVL3) and DIABLO. For better visualisation of the heat map the log2MedCen intensities values have been transformed by row (gene) using z-score. The heat map was generated by using the gplots package in R.

The comparison of melanoma NK-92 killing signature (Figure 27) with the previous melanoma killing signature derived from primary NK cell killing (Figure 17) showed a protein overlap of 35 %. The RPPA analysis of primary NK cell killing and NK-92 killing revealed only partial overlap of proteins involved in melanoma susceptibility to NK cell killing. Nevertheless, it identified that the same cell processes such as EMT and apoptosis as well as pathways such as PI3K-AKT-mTOR or RAS-RAF-MEK are involved in the melanoma killing by both NK cell types.

4.8 Inhibition of the PI3K-AKT-mTOR signalling pathway decreases melanoma susceptibility to NK cells

Although the molecular manipulation of the single top hits could alter the susceptibility of melanoma to NK cells, the effects were only partly significant. The reason might be that the effects on NK cell killing were dependent on the stability as well as the efficiency of the transient transfection. Furthermore, the previous RPPA analyses only takes into consideration the mere existence of a correlation between melanoma killing and protein expression into account. How strong the protein expression (fold-change) influenced the susceptibility of melanoma was however, not taken into consideration. Therefore, we reused the information from the RPPA to determine the magnitude of this influence. The correlation of the primary NK cell killing and the protein level (log2MedCen) allowed the creation of a linear trend graph with known intercept and slope for each protein in the RPPA panel. The graphs of the top hits DIABLO and SNAI1 are shown as examples in Figure 28 A+B. The slope of the graphs can be interpreted as the magnitude of change in NK cell-mediated killing as a function of the expression level of the protein of interest. The values of the slope together with the already determined Pearson correlation coefficients were further used to create a volcano plot (Figure 28 C) that visualised the statistical significance versus the effect size and allowed the identification of proteins with large fold-change and high statistical significance at the same time. The volcano plot shows that DIABLO and SNAI1 were the proteins with highest Pearson correlation coefficient but did not have the highest slope. In contrast, the protein abundance of CASP3 or COPS5 could alter the NK cell-mediated killing stronger, although their Pearson correlation coefficient is smaller. The lower effect size might partially explain the modest success in manipulating DIABLO, even though it was the top negative regulator of primary NK cell- and NK-92-mediated killing of melanoma cells. The manipulation of a single individual protein neglects the synergic effects of several proteins working together on the NKiToxMel. This protein interaction could enhance the actual effect on NK cell-mediated killing even if the expression level of the individual proteins involved are only slightly changed. Therefore, further investigations were focused on identifying

and manipulating signalling pathways i.e. functional characterisation rather than altering the expression levels of single proteins. In order to choose the most promising pathway, the RPPA analyses of primary NK cell killing and NK-92 killing were compared. In particular the melanoma NK-92 killing signature showed a clear indication of the involvement of the PI3K-AKT-mTor pathway in the NKiToxMel since RPS6K, RPS6KB1 and PIK3R1 were identified as hits (Figure 27). Interestingly, RICTOR and PRAS40, other components of this pathway, were found to correlate with primary NK cell killing (Figure 17). In addition, several other PI3K-AKT-mTor connected proteins, such as RPS6K (pT573), RPS6KB1 (pT389) and phosphorylated 40S ribosomal protein S6 (RPS6) considerably correlated with the melanoma susceptibility to NK cell killing (Figure 28). Moreover, also mTOR and PIK3R1 showed association with primary NK cell killing.

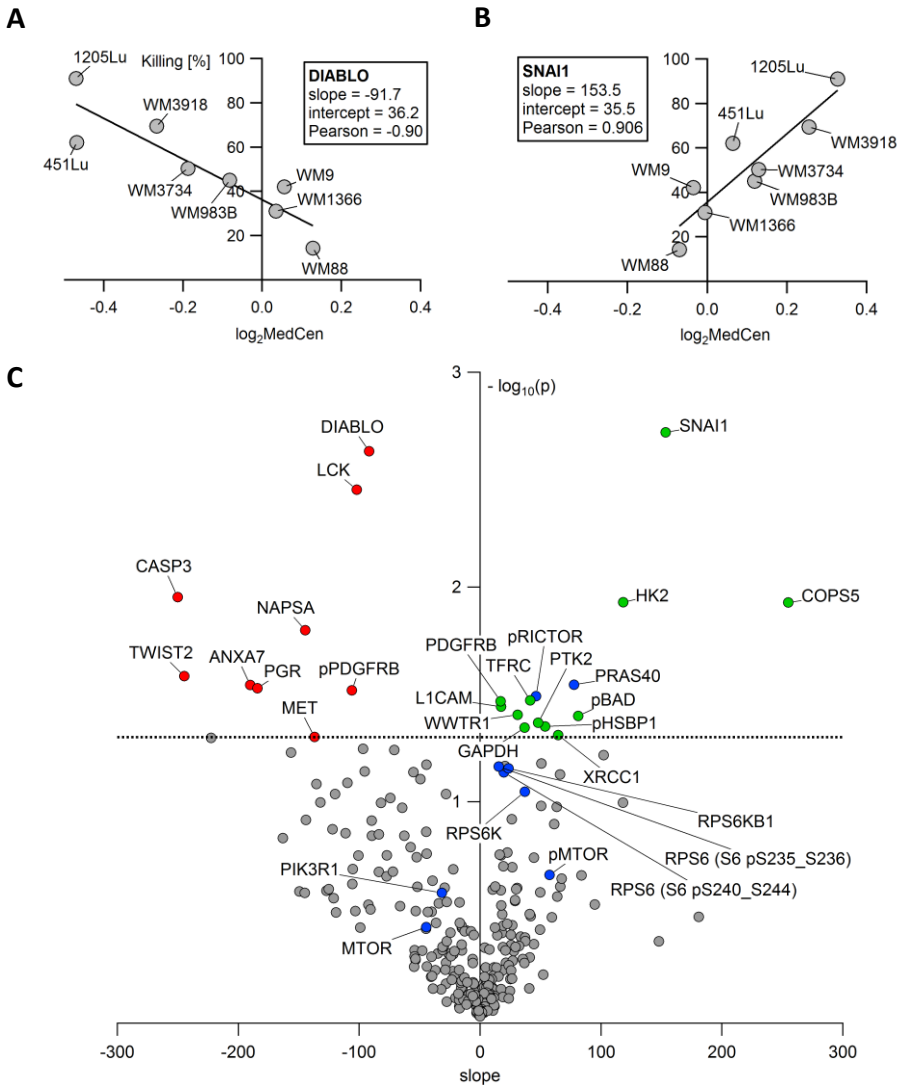

Figure 28. Effect size of the individual proteins from the melanoma killing signature might limit success of manipulating single hits . (A-B) Plot of NK cell-mediated killing versus the expression level (log2MedCen) of (A) DIABLO and (B) SNAI1 (C) Volcano plot visualises the p ($-\log_{10}$) value as measuring unit of statistical significance versus the fold-change. The effect size was determined by the slope of the linear trend graphs after plotting the NK cell killing versus the log2MedCen of the individual proteins. Left side (proteins marked in red) showed proteins that negatively influence NK cell killing, whereas proteins with direct correlation to NK cell killing were marked in green (right side). Proteins involved in PI3K-AKT-mTOR pathway are marked in blue. The dashed line shows the significance threshold of $p = 0.05$ with points above the line having $p < 0.05$ and points below the line having $p > 0.05$. The volcano plot is generated by using IGOR Pro.

Based on these findings, the role of the PI3K-AKT-mTor pathway on NK cell susceptibility of melanoma was examined in more detail. Given that the activation of this pathway is correlated with cell survival and proliferation (Saxton and Sabatini, 2017), there are already multiple drug inhibitors targeting various components.

In Figure 29, the inhibitors used in the later experiments are presented together with their effects on the cell viability of WM3734 cells. BKM120 is a selective inhibitor of PI3K (Koul et al., 2012)

and showed a cytotoxic effect on WM3734 cells, especially at higher concentrations (>= 1 μM) and longer treatment periods (>48 h) (Figure 29 A). The cell viability decreased from 61 % to 45 % after doubling the concentration (1 μM to 2 μM) after longer treatment. Short-term treatment only marginally reduced cell viability. After 24 h, 1 μM BKM120 seemed to increase cell viability while 2 μM BKM120 treatment caused a reduction of cell viability of about 20 %.

A selective inhibitor for AKT is MK2206 (Nitulescu et al., 2016). As shown in Figure 29 B even after 72 h treatment with the highest concentration the viability of WM3734 was only marginally affected by this drug.

Rapamycin is a potent inhibitor of the mTOR complex 1 (Saxton and Sabatini, 2017). However, only lower concentrations of rapamycin seemed to decrease the viability of WM3734 to maximum 77 % (2 μM, 24h), whereas cell viability was only marginally affected by higher concentrations (Figure 29 C). Although these inhibitors as single agents show only minor direct effects on cell viability according to the CellTiter-Blue® viability assay, the subsequently used concentrations of BKM120 (Niessner et al., 2016), MK2206 (Rebecca et al., 2014) and rapamycin (Molhoek et al., 2005; Rosenberg et al., 2015) were shown to affect melanoma cell proliferation and melanoma invasion or metastasis. Since the drugs were dissolved in DMSO, possible side effects of the solvent need to be considered and minimised. DMSO not only decreased melanoma cell proliferation and metabolic activity at high dosages (<1 %) (Ferk and Daris, 2018; Huberman et al., 1979) but also lower concentrations (>0.1 %) affected cytoskeleton organization and adhesion of mouse B16 melanoma cells (Lampugnani et al., 1987). In order to decrease undesirable effects, the drug concentrations were chosen in a way that DMSO effects are minimised but drug concentration is high enough to get a visible melanoma phenotype.

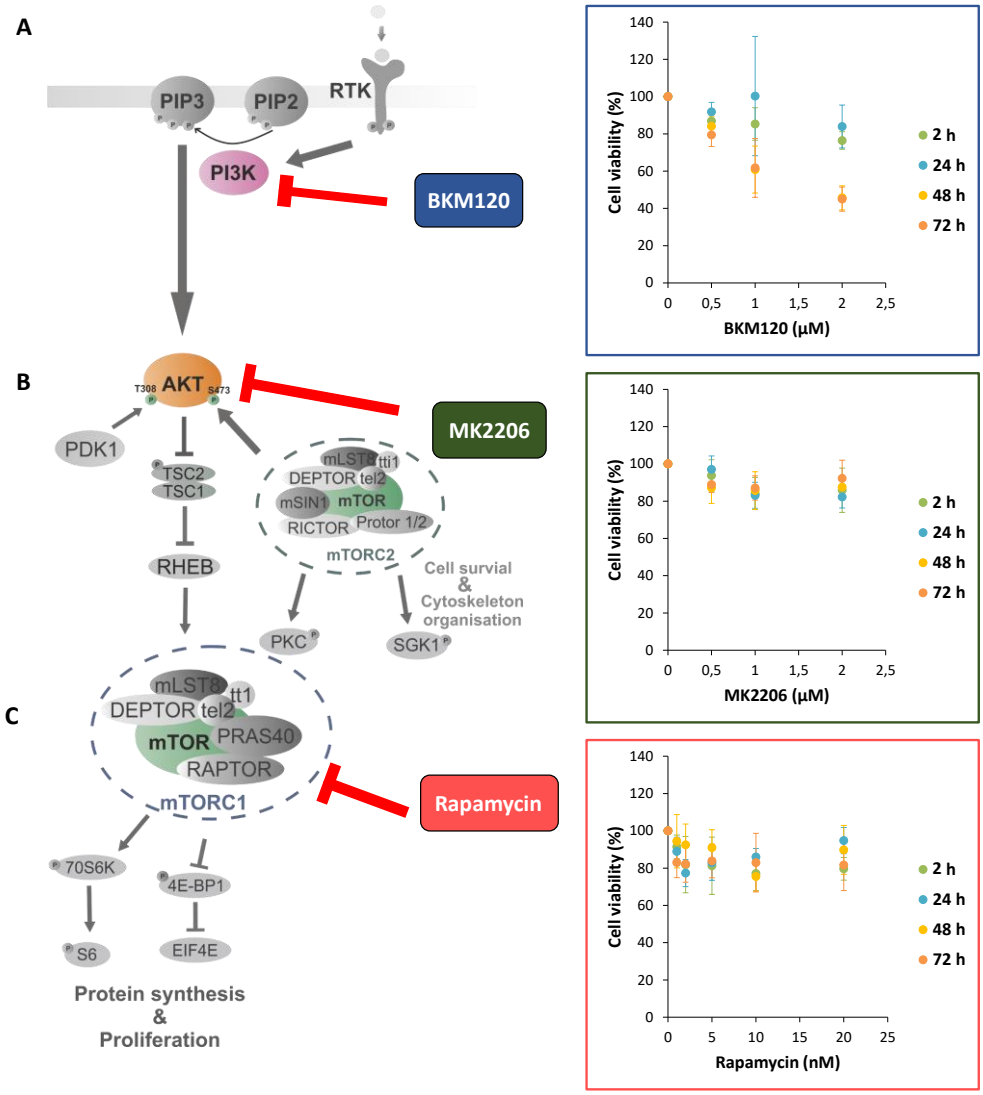

Figure 29. The effect of drugs targeting the PI3K-AKT-mTOR pathway on melanoma cell viability. WM3734 were treated with different concentrations of (A) BKM120 (n=4), a selective inhibitor of PI3K, (B) MK2206 (n=4), a selective inhibitor of AKT and (C) rapamycin (n=3), an inhibitor of mTOR over a period of 3 days. Melanoma cell viability was determined using the CellTiter-Blue® viability assay.

To investigate if we could affect the NK cell-mediated killing of melanoma by manipulating the PI3K-AKT-mTOR pathway, melanoma cells were treated with different drug inhibitors (Figure 29). WM3734 cells and 1205Lu cells have distinct NK cell susceptibility (50 % and 90 %, respectively) and should have a different PI3K-AKT-mTOR status according to the RPPA data. Besides short-term treatments with PI3K-AKT-mTOR inhibitors, additional investigations of longer treatment periods can give further information about the kinetics of drug action and could shed new light on the effects of these drugs on patient therapy. Figure 30 A shows that 24 h treatment of WM3734 cells with 2.5 nM rapamycin reduced the NK cell susceptibility significantly. The killing curves of rapamycin treated and DMSO treated cells started to separate after 30 min and the reduced killing of the treated cells was more visible during the experiment.

As seen in Figure 30 B, the rapamycin treatment decreased the susceptibility of WM3734 from 31 % to 26 %, already after 1 h. During the course of the experiment, this trend continued and reached a significant maximal reduction in NKiToxMel of ~10 % (Figure 30 C). Longer treatment periods (96 h) resulted in similar killing curves of WM3734 cells (Figure 30 D) and decreased the susceptibility to NK cells after 1 h (Figure 30 E) as well as after 4 h of killing (Figure 30 F) about 10 %.

As shown in Figure 30 G, the effect of short-term treatment with rapamycin were validated in 1205Lu cells that also showed a reduced susceptibility to NK cells after drug treatment. In this cell line the killing mediated by primary NK cells was reduced in the initial phase of about 5 % (Figure 30 H) and in the end phase of about 10 % (Figure 30 I). The decreased NK cell susceptibility of 1205Lu cells was even more pronounced after 96 h drug treatment (Figure 30 J). The initial killing of pre-treated 1205Lu cells, as shown in Figure 30 K, was significantly reduced about 19 % in comparison to the DMSO control (33 %). During the course of the killing assay, this trend continued and reached a significant maximal reduction in NK cell-mediated killing of ~28 % after 240 min (Figure 30 L).

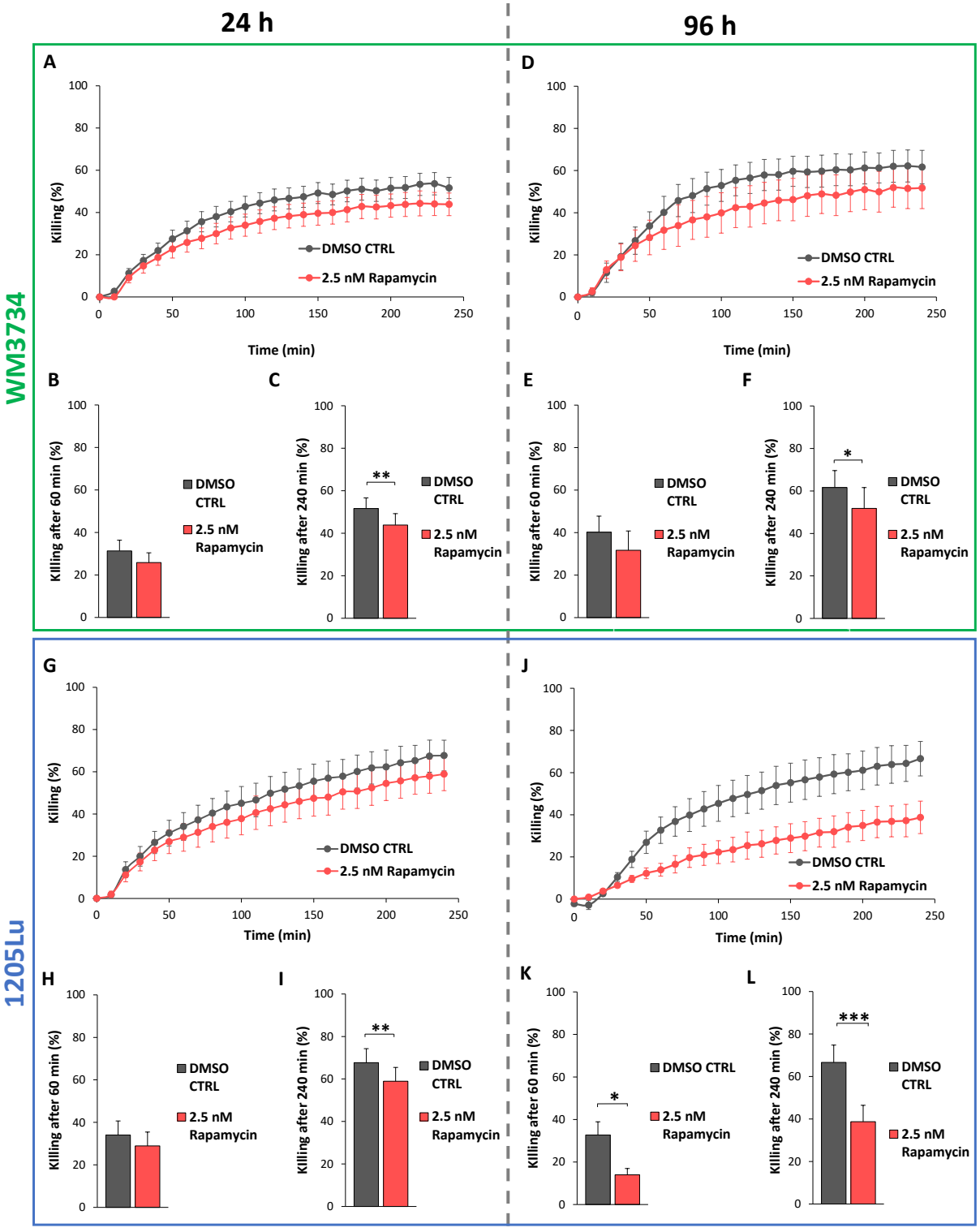

Figure 30. Rapamycin decreased the susceptibility of melanoma cells to primary NK cells. WM3734 (green rectangle) and 1205Lu (blue rectangle) were pre-treated with 2.5 nM rapamycin or the corresponding DMSO control for 24 h (n (WM3724)=12; n (1205Lu)=6) and 96 h (n (WM3724)=6; n (1205Lu)=3). Afterwards cells were loaded with calcein-AM (0.5 µM) and were exposed to NK cells (E:T ratio of 5:1) for 4h. (A,D,G,J) Killing kinetics of 4h cytotoxic assay. For statistical analysis the killing after 60 min (B,E,H,K) and after 240 min (C,F,I,L) were used. Bars and graphs indicate means ± SEM. Statistical significance of paired, two-tailed Student's *t*-test is indicated with * for $p<0.05$, ** for $p<0.01$ and *** for $p<0.001$.

Altogether, short-term as well as long-term treatment of rapamycin significantly decreased the susceptibility of melanoma cells. These findings further support the hypothesis that PI3K-AKT-mTOR signalling in melanoma cells is a determining factor of NKiToxMel.

The drug inhibitors BKM120 and MK2206 are known to target PI3K and AKT, respectively, more upstream in the PI3K-AKT-mTOR pathway than rapamycin (Niessner et al., 2016). As shown in Figure 31 A-C, the NK cell susceptibility of WM3734 cells was not affected by the short –term treatment (24 h) with 1 μM MK2206 nor 1 μM BKM120. However, 96 h BKM120 treatment decreased the susceptibility of WM3734 cells to NK cells significantly (Figure 31 D). After 60 min of the assay (Figure 31 E), the killing was decreased about 16 % and about 9 % after 240 min (Figure 31 F). On the other hand, long-term treatment with MK2206 did not affect the initial killing of WM3734 cells (Figure 31 E) and even increased the killing about 13 % at the end of the experiment (Figure 31 F). In the other melanoma cell line 1205Lu, 24 h treatments with both drugs reduced the susceptibility of this cell line to NK cells significantly (Figure 31 G). As shown in Figure 31 H, already after 60 min the pre-treatment of 1205Lu cells with either MK2206 or BKM120 significantly decreased their NK cell susceptibility by about 5 %. These effects were even more dominant during the following course of the cytotoxic assay. The killing of BKM120 pre-treated 1205Lu cells were reduced on average by about 10 %, whereby this reduction was not statistically significant for all time points. MK2206 treated 1205Lu cells showed a significantly reduced NK cell-mediated killing of 19 % after 240 min (Figure 31 I). Figure 31 J shows that 96 h pre-treatment of 1205Lu with BKM120 and MK2206 decreased the susceptibility of 1205Lu drastically. In comparison to the DMSO control (~74 %) primary NK cells killed the drug pre-treated melanoma cells only to ~58 % (MK2206) and to ~43 % (BKM120) after 4 h (Figure 31 L). This reduced susceptibility was already been observed after 60 min (Figure 31 K) where the treatment with MK2206 and BKM120 reduced the killing of melanoma by 10 % and 22 %, respectively.

In summary, it can be stated that 96 h treatment of melanoma cells with PI3K inhibitor BKM120 decreased the NKiToxMel, whereas short-term treatment only affected the susceptibility of 1205Lu cells to NK cell killing. Similar observations were made with the AKT inhibitor MK2206 that reduced the NK cell meditated killing of 1205Lu cells. However, MK2206 treatment of WM3734 cell line increased its susceptibility to NK cell killing.

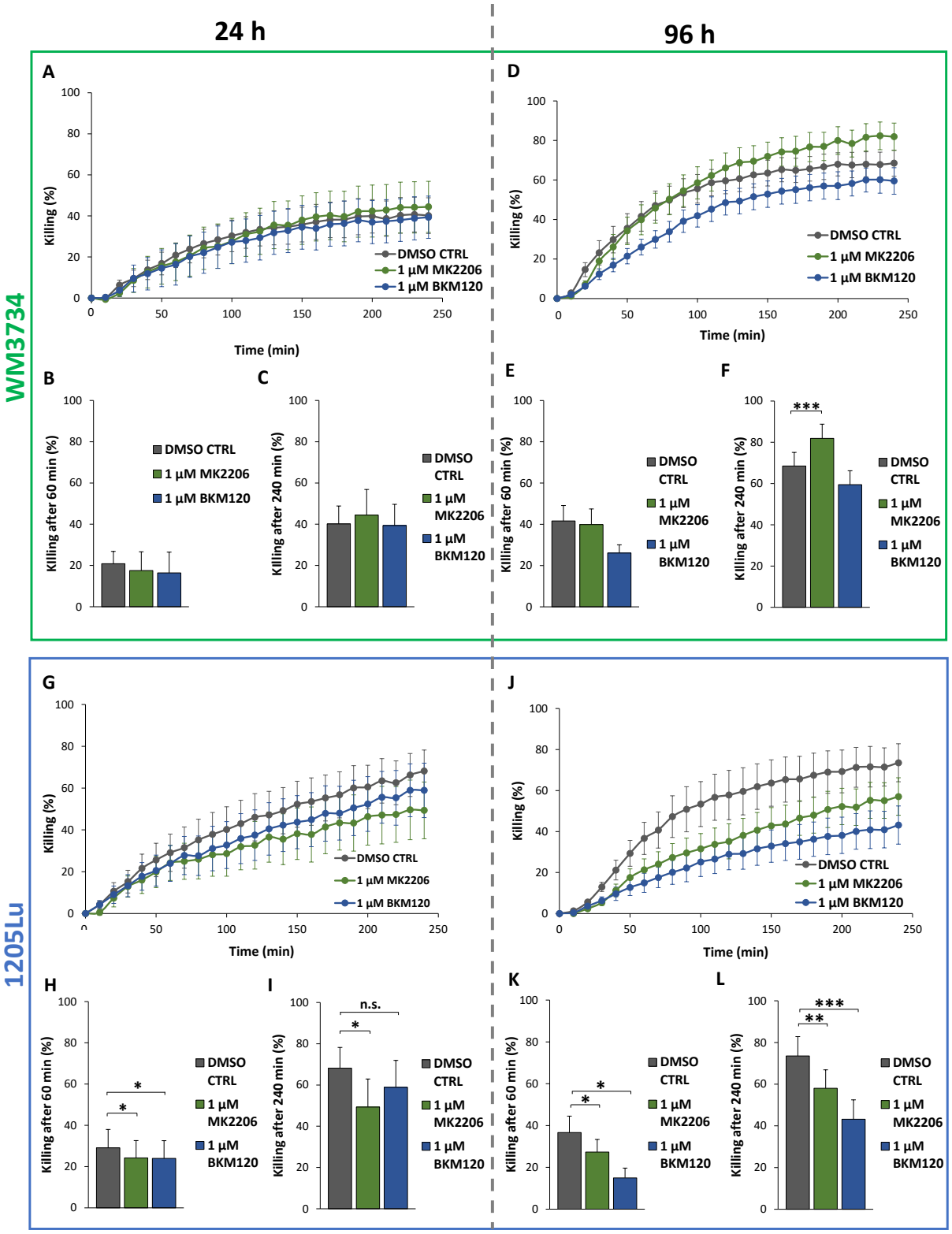

Figure 31. MK2206 and BKM120 partially decreased melanoma cell susceptibility to NK cells. WM3734 (green rectangle) and 1205Lu (blue rectangle) were pre-treated with 1 µM BKM120 (blue) or 1 µM MK2206 (green) and the corresponding DMSO control for 24 h (n (WM3724)=3; n (1205Lu)=4) and 96 h (n (WM3724)=6; n (1205Lu)=3) . Then cells were loaded with calcein-AM (0.5 µM) and exposed to NK cells (E:T ratio of 5:1) for 4 h. (A,D,G,J) Killing kinetics of 4 h cytotoxic assay. For statistical analysis the killing after 60 min (B,E,H,K) and after 240 min (C,F,I,L) were used. Bars and graphs indicate means ± SEM. Statistical significance paired, two-tailed Student's *t*-test is indicated with * for $p<0.05$, ** for $p<0.01$ and *** for $p<0.001$.

A critical point of the performed experiments is that leftovers of the drug inhibitors might diminish NK cell cytotoxicity. In the course of the assay preparation, the target cells were carefully washed several times and resuspended in a fresh culture medium. This procedure removed residual drug so that the highest remaining drug concentration in the assay could not exceed pM range. Nevertheless, there is the possibility that melanoma cells internalise the drug and release it during the cytotoxic assay, hence affecting NK cell effector function. Active mTOR signalling is important for NK cell development (Marcais et al., 2017; Yang et al., 2018). Although longer rapamycin treatments (5 days) impaired NK cell cytotoxicity (Eissens et al., 2010), short exposure (4 h) to even 100 nM rapamycin did not alter NK cell cytotoxicity to sensitive target cells (Yang et al., 2018). The other drug inhibitors MK2206 and BKM120 decreased the cell proliferation of distinct immune cell populations (Abu-Eid et al., 2014; Ding et al., 2014) and impaired the cytotoxicity of NK-92 cells (Jiang et al., 2000; Yea et al., 2014). In order to test if these drugs could impair primary NK cell cytotoxicity against melanoma cells directly, several control experiments were performed.

As depicted in Figure 32, the treatment of K562 cells with 2.5 nM rapamycin for 24 h did not impair the NK cell-mediated killing of K562. This observation thus indicated that it is unlikely that drug remaining in the medium or released from target cells after internalisation would inhibit the cytotoxicity of the NK cells.

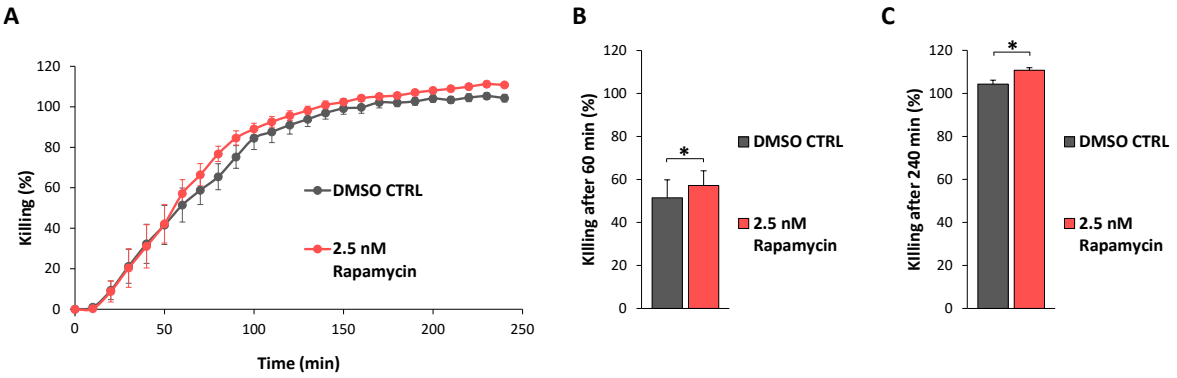

Figure 32. Rapamycin treatment does not affect susceptibility of K562 to NK cells. K562 cells were pre-treated with 2.5 nM rapamycin or the corresponding DMSO control for 24 h. Afterwards cells were loaded with calcein-AM (0.5 µM) and exposed to NK cells (E:T ratio of 5:1) for 4 h (n=5). (A) Killing kinetics of 4 h cytotoxic assay. For statistical analysis the killing after 60 min (B)) and after 240 min (C) were used. Bars and graphs indicate means ± SEM. Statistical significance of paired, two-tailed Student's *t*-test is indicated with * for $p<0.05$.

In another experimental setting (Figure 33), the susceptibility of non-treated and drug pre-treated melanoma cells to NK cell killing was tested in the absence or presence of drug inhibitors or DMSO controls. Therefore, drug inhibitors and corresponding DMSO controls were added right before the beginning of the killing assay. As seen in Figure 33 A+B, the NK cell-induced killing

of WM3734 cells was not affected in the presence of rapamycin or the corresponding DMSO control independent of the pre-treatment of the melanoma cells. The presence of MK2206 reduced the initial killing of non-pretreated WM3734 cells by ~ 8 % in comparison to the DMSO control (Figure 33 C). However, in the course of the assay the difference between MK2206 and the DMSO control was reduced by ~5 %. In addition, Figure 33 D shows that MK2206 pre-treated WM3734 cells were not affected by additives during the killing assay. As seen in Figure 33 E+F, the presence of BKM120 reduced the NK cell-mediated killing of non-pre-treated WM3734 cells by ~8 % and the killing of BKM120 by about 10 %. However, BKM120 pre-treated WM3734 cells were less killed (~36 %) than non-treated melanoma cells (~46 %).

Taken together, rapamycin did not show inhibitory effects on NK cell cytotoxicity in the used cytotoxicity assays, whereas the possible impairment of NK cells by the other drug inhibitors could not be completely excluded. However, the results indicate that MK2206 affects melanoma cells rather than NK cells since MK2206 treatment of WM3734 did not decrease NKiToxMel (Figure 31). Besides, MK2206 only reduced the NK cell-mediated killing of non-pre-treated WM3734 (Figure 33 C+D). Assuming that MK2206 impairs NK cell cytotoxicity, the killing of MK2206 pre-treated WM3734 cells should also be reduced in the presence of MK2206. Similar considerations lead to the assumption that 1 μM BKM120 during the assay impairs NK cell cytotoxicity. Nevertheless, the residual concentrations of BKM120 during the cytotoxicity assay should be considerably lower. Furthermore, it should be noted that the BKM120 pre-treatment of melanoma cells alone drastically decreased NKiToxMel.

In sum, it can be concluded that the effects of the used drug inhibitors are mainly caused by altered susceptibility of melanoma cells to NK cells rather than the impairment of NK cell cytotoxicity.

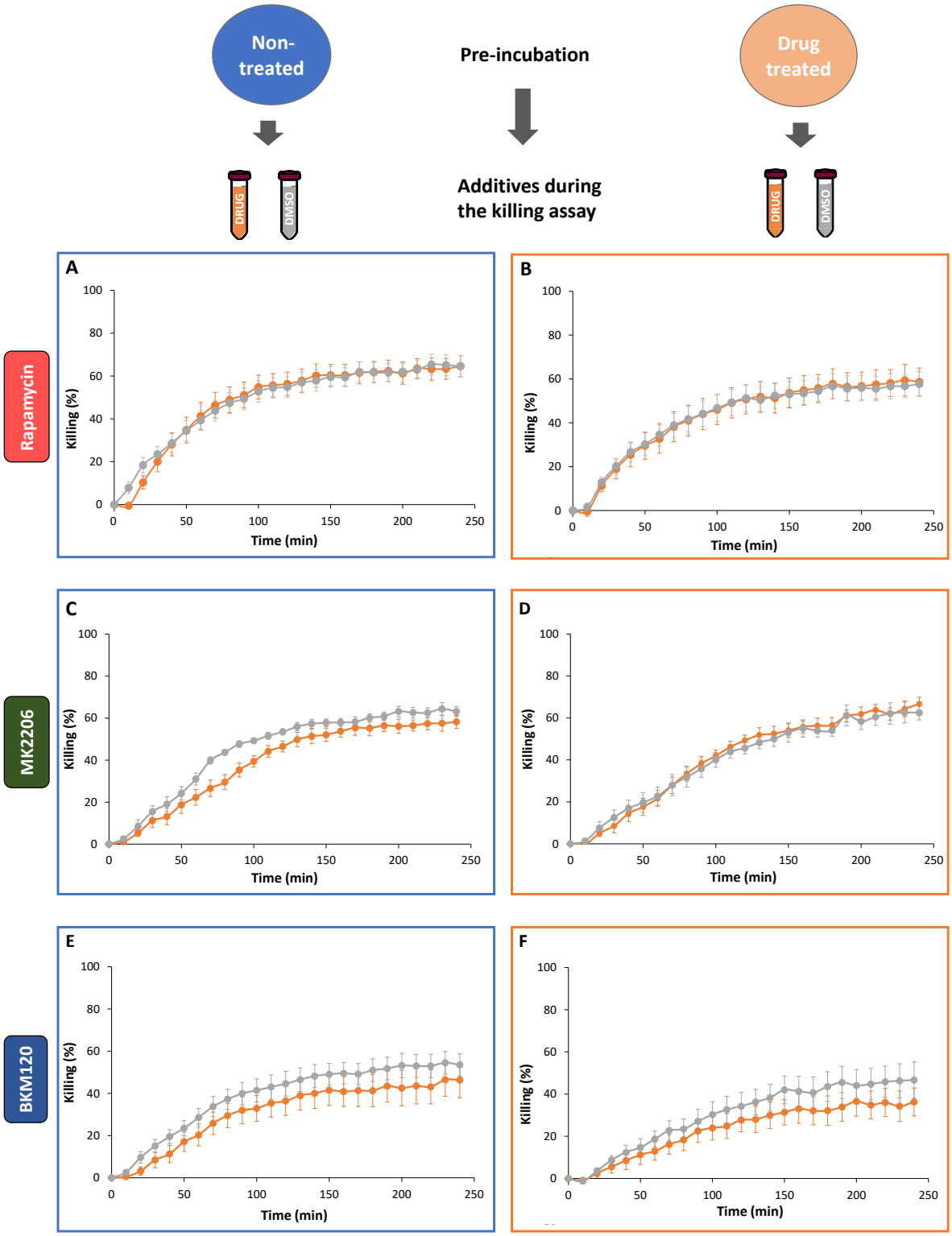

Figure 33. Control experiments support altered melanoma cell susceptibility to NK cells after inhibitor treatments. WM3734 were pre-treated with three drug inhibitors or solvent control 24 h after treatment cytotoxicity assays were performed. In this killing assay either no additives, one of the used drugs or DMSO was added. Afterwards cells were loaded with calcein-AM (0.5 µM), washed and resuspended in the appropriate volume of AIMV medium. This medium contained either no additives, 2.5 nM rapamycin (n=7); 1 µM MK2206 (n=4); 1 µM BKM120 (n=4) or the corresponding DMSO control. After seeding and settling of the melanoma cells, primary NK cells (E:T ratio of 5:1) were added and the cytotoxic assay was recorded for 4 h. (A) Killing kinetics of non-pre-treated WM3734 under the influence of different additives. Bars and graphs indicate means ± SEM.

4.9 Other parameters influencing the NK cell-mediated killing of melanoma

Given that several proteins involved in cell survival and metabolism affected the NK cell susceptibility of melanoma, the proliferation status of seven melanoma cells was tested. Therefore, the same melanoma cell number was seeded and the percentage proliferation was determined after counting the total number of cells. Figure 34 A shows that the proliferation of seven melanoma cell lines is heterogeneous. WM88 cells were the least proliferative as this cell line only doubled their cell number after 72 h. The highest proliferation status was displayed by WM3918 cells that more than triplicated after 24 h and showed a mean cell proliferation of around 600 % after 72 h. The growth rate of WM983B and 1205Lu cell lines was slower as the cell number was not even doubled after 24 h. However, after 72 h the cell proliferation was more than 500 % in both cell lines. The other three cell lines 451Lu, WM1366 and WM3734 showed a median proliferation that was also characterised by a slow increase in cell number (<200 % proliferation) after 24 h but did not exceed 400 % after 72 h. As seen in Figure 34 B, the melanoma cell proliferation after 72 h correlates with the NK cell-mediated killing of melanoma.

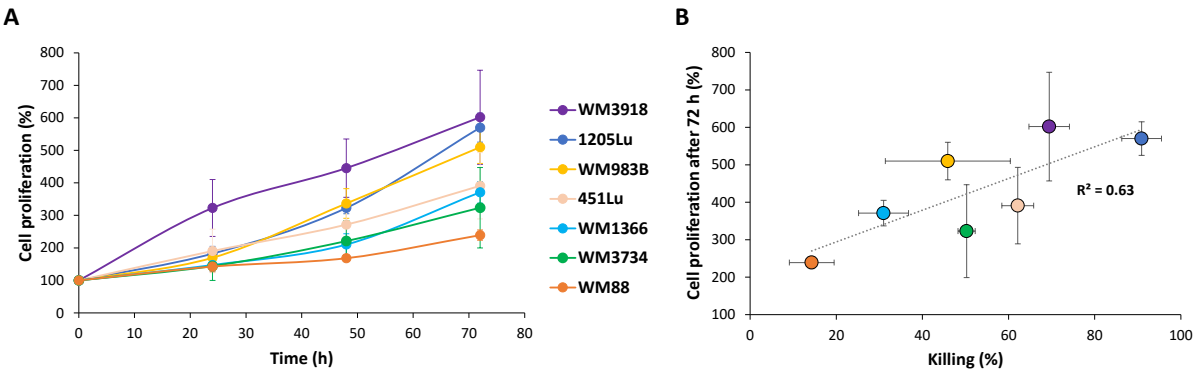

Figure 34. Melanoma cell proliferation correlates with NK cell susceptibility. (A) Same melanoma cell number of 1205Lu (n=4), WM3918 (n=4), WM983B (n=4), 451Lu (n=3), WM1366 (n=4), WM3734 (n=3) and WM88 (n=3) was seeded and percentage proliferation was determined by counting the cells after 24 h, 48 h and 72 h. (B) Melanoma cell proliferation after 72 h was correlated with the susceptibility of these melanoma cells to NK cell killing.

These findings support the hypothesis that the more proliferative melanoma cells present a better target for NK cell killing.

Melanoma staging is not only associated with increasing mutation burden but it also influences therapeutic approaches. The mutation status of certain proteins such as BRAF, NRAS or PTEN did not indicate a link with the susceptibility of melanoma to NK cells. Nevertheless, the tested primary melanoma cell lines WM1366 and WM3268 with non-mutated BRAF were more resistant to NK cells than the other primary cell lines WM793 and WM902B. In order to see if and how the melanoma stage affects the susceptibility of melanoma towards NK cells, all tested

melanoma cells with a clear indication of isolation site were categorised in primary tumours (VGP), lymph node metastasis and distant metastasis (e.g. brain, lung etc.). As depicted in Figure 35, increasing melanoma stage seems to be associated with higher melanoma susceptibility to NK cells. On average, primary melanoma cells were killed to ~43 % whereas melanoma cells of lymph node metastasis were more susceptible to primary NK cells (~60 %). Melanoma cells of distant metastasis were on average killed up to 68 % and showed the highest susceptibility to NK cells. Nevertheless, the variation of melanoma susceptibility within the stages was considerably high. In addition, the samples size might not be sufficient to represent the distinct melanoma stages and did not allow statistical analysis.

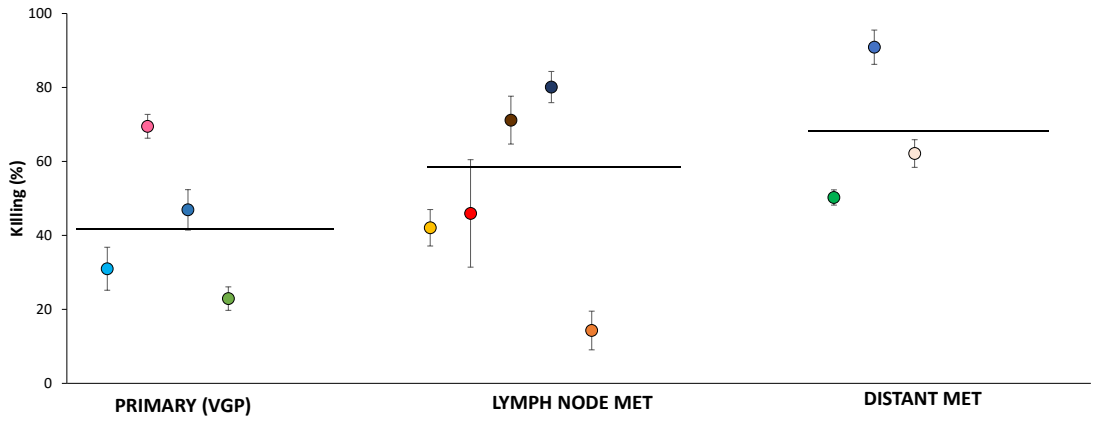

Figure 35. Melanoma staging is associated with increasing susceptibility of melanoma cells to NK cells. NK cell-mediated killing of primary tumours/skin metastasis: WM3268 (green, n=3)WM1366 (light blue, n=7); WM902B (blue, n=3) WM793 (red, n=7) lymph node metastasis: WM88 (orange, n=20), WM983B (red, n=10), WM9 (yellow, n=11), WM858 (brown, n=10), WM3682 (dark blue, n=10) and distant metastasis: 451Lu (light rose, n=6), WM3734 (green, n=79) and 1205Lu (blue, n=19) after 4 h real-time killing assay are shown; E:T ratio of 5:1 are used.

4.10 Melanoma-NK cell-co-culture

The previous experiments showed that melanoma cells have an intrinsic susceptibility to NK cell killing. This susceptibility depends on the protein signature of the melanoma cells and can be pharmacologically as well as genetically manipulated. Given that melanoma phenotypes are often dynamic, the successes of immune-based therapies are not only dependent on the initial positive clinical effect but also on the prevention of therapy resistance. Therefore, melanoma-NK cell-co-cultures were established to investigate if and how melanoma cells evade NK cell-mediated immunosurveillance.

4.10.1 Co-culture with primary NK cells

For the establishment of NK-melanoma cell-co-culture, we used WM3734 cells that showed an average killing rate of around 50 % after 4 h. This was needed on the one hand to ensure survival during co-culture and on the other hand to allow possible shifts of NK cell susceptibility of melanoma in both positive and negative direction. Seeded melanoma cells were challenged with activated NK cells for 3-4 days. Surviving melanoma cells were subcultured and exposed to fresh NK cells again, a procedure that was repeated for 30 weeks. During this co-culture process, the effector-target ratio was constantly increased (Cappello, 2015). The susceptibility of the melanoma cells during the co-culture was monitored by real-time killing assays. The NK cell-mediated killing of all WM3734-NK cell-co-cultures declined over time as initially susceptible melanoma cells acquired resistance. Figure 36 A shows an example of a long-term WM3734-NK cell-co-culture. With increasing E:T ratio and co-culture time, the susceptibility of WM3734 to NK cells decreased. The performed killing assays showed that the initial NK cell-mediated killing of 35 % in the second week was reduced to 20 % and 12 % in week 9 and 11, respectively. After 29 weeks of co-culturing the WM3734 was resistant to NK cells (3 % killing). During the long culture period, also the non-treated control showed a decreased susceptibility to NK cells. Therefore, the ratio of reduction was calculated by the quotient of killing from co-culture and untreated control (Figure 36 B). In comparison to the non-treated control, the killing of co-cultured WM3734 could be reduced from an initial 25 % to over 50-70 % between week 9 and 11, to almost 85 % after 29 weeks of co-culture.

The ratio of reduction is calculated by the following formula:

$$Ratio\ of\ reduction = 1 - \frac{Killing\ of\ co{-}culture\ (\%)}{Killing\ of\ non{-}treated\ control\ (\%)}$$

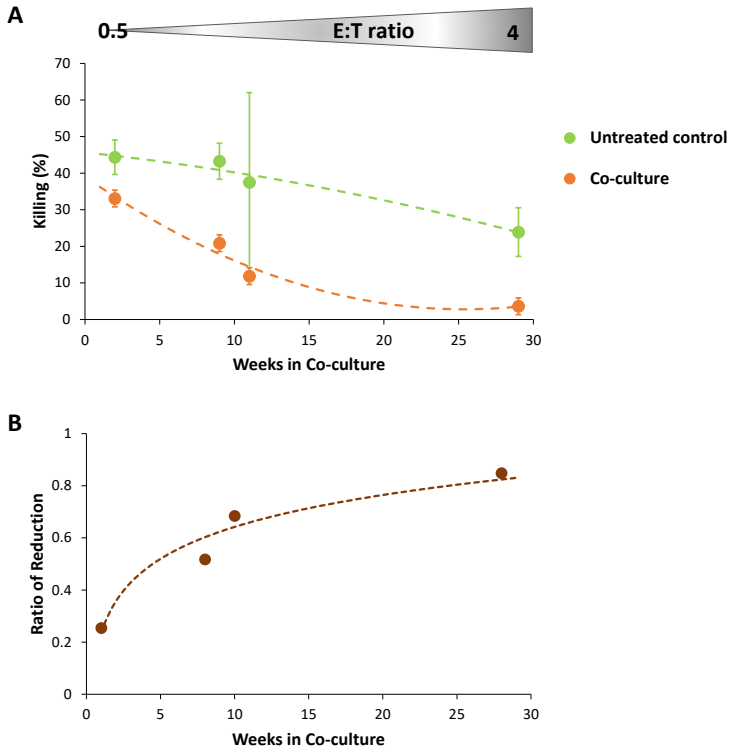

Figure 36. Development of NK cell resistance during melanoma-NK cell-co-cultures.(A) Endpoint killing of untreated WM3734 and a WM3734-NK cell-co-culture at indicated times during co-culture. In the real-time killing assay an E:T ratio of 5:1 was used. The displayed dashed line indicates the polynomial fit of susceptibility to NK cell during co-culture process with increasing E:T ratio.(B) Ratio of reduction (for calculation see equation above). Data were previously shown in (Cappello, 2015).

After sufficient reduction of melanoma susceptibility to NK cell killing, subsequent RNA sequencing of the co-cultured melanoma cells revealed genes involved in the NK cell evasion process. RNA sequencing is a very sensitive method and requires a high purity of the RNA material of interest. As the melanoma cells are co-cultured with NK cells, the contamination with RNA of NK cells needed to be minimised. Therefore, before being added to the co-culture, NK cells were irradiated (30 Gy, Cs 137 γ-emitter) to induce delayed NK cell death and prevent NK cell proliferation. Furthermore, several washing steps before harvesting of melanoma cells ensured the purity of the melanoma co-culture.

To estimate the effect of the irradiation on NK cell cytotoxicity, irradiated and non-irradiated NK cells of the same donor were used to kill the cell lines K562 and WM3734. As seen in Figure 37, the irradiation seemed to reduce the cytotoxicity of the NK cells. The NK cell-mediated killing of K562 delayed elimination at the initial phase of the killing. Nevertheless, the irradiated NK cells were able to kill almost all K562 cells during the cytotoxic experiment. The killing of WM3734 cells seemed to be reduced during the whole course of the experiment. Even though this effect is more dominant in K562 cells, it was not statistically significant (by paired Student's

t-test) in both cell lines. These impairments of the NK cell cytotoxicity were acceptable to guarantee RNA purity.

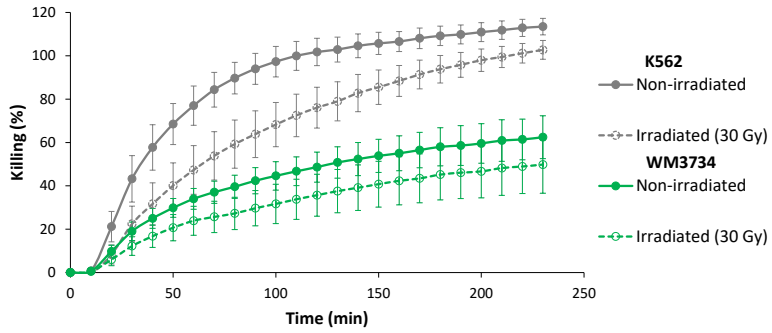

Figure 37. Irradiated NK cells showed reduced but sufficient cytotoxicity against cancer cells. Primary IL-2 stimulated NK cells (n=5) were irradiated with 30 Gy and immediately added to calcein-AM-loaded K562 or WM3734 (E:T ratio of 5:1). Non-irradiated NK cells were used as controls. The graphs of the 4 h real-time killing assay are shown as means ± SEM. Data were previously shown in (Cappello, 2015).

4.10.2 Co-culture with NK-92

NK-92 is a NK cell line that is already used in several clinical trials (Arai et al., 2008; Klingemann et al., 2016) and is a promising tool for immunotherapies. Furthermore, NK-92 cell line shows more constant cytotoxicity than differing primary NK cells donors, so that the development of resistance is not subject to variation. This allowed comparable NK cell cytotoxicity over the duration of the co-culture experiment and higher E:T ratios.

To compare the results of the co-culture experiments with primary NK cells, the same cell line WM3734 was used. The lower susceptibility of WM3734 to NK-92 (see chapter 4.5.) as well as the abundance of effector cells allowed the parallel establishment of WM3734-NK-92 co-cultures with different E:T ratios (1:1, 1:3, 1:7). Over a period of two weeks, the irradiated effector cells were freshly added two times a week. Before the last exposure to NK-92, the co-cultures were subcultured. One half was re-treated with NK-92, whereas the other half was not treated for 3 days (recovery) before the cytotoxicity experiment. Figure 38 A depicts the NK-92-mediated killing of the three co-cultures as well as their corresponding recovery conditions in comparison to the untreated control. The susceptibility of WM3734 cells was reduced from ~22 % (untreated control) to less than 10 % after co-culture with NK-92 (Figure 38 B). With increasing E:T ratio in the co-culture, the susceptibility decreased from ~ 9 % (1:1) to over ~6 % (3:1) and ~3 % (7:1). Already after 3 days without NK-92 exposure the susceptibility (240 min) of the co-cultures increased by ~6 % in all E:T ratios.

These co-culture conditions were also harvested and used for further RNA sequencing analysis.

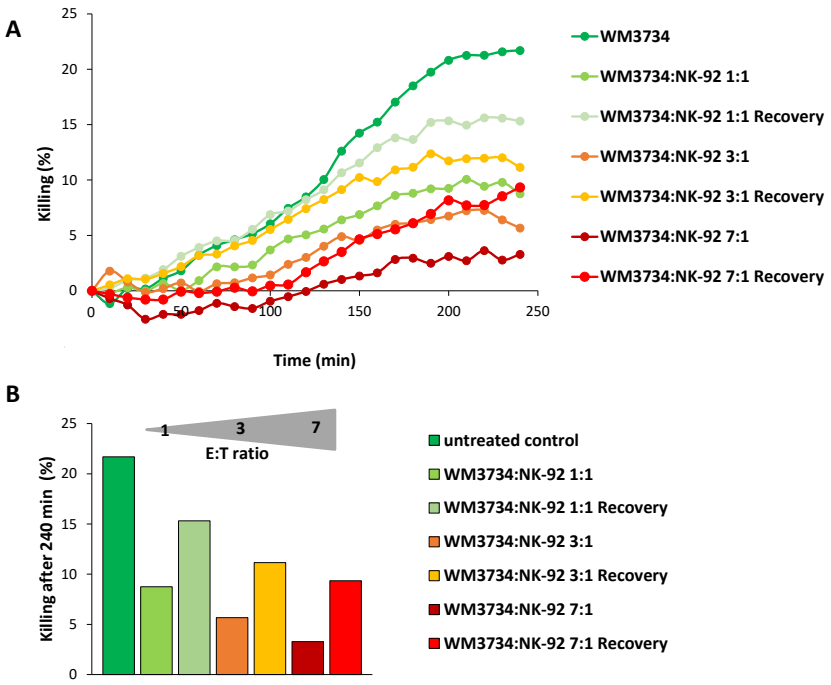

Figure 38. WM3734-NK-92-co-cultures have reduced susceptibility to NK-92 cells. WM3734 cells were co-cultured with NK-92 cells at different E:T ratios (1:1, 3:1, 7:1) for 2 weeks. Two times per week NK-92 were replaced. After the last NK-92 exposure, only one half of the subcultured co-culture was re-treated with NK-92. The other half was non-treated for three days (Recovery) before cytotoxicity experiment. Afterwards melanoma cells of the co-cultures as well as untreated control cells were used in real-time killing assays with NK-92 (E:T ratio of 5:1). (A) Killing kinetic of 4 h cytotoxic assay. (B) Killing after 240 min.

To test how fast the resistance of melanoma to NK-92 cells developed, short-term co-cultures of 24 h were analysed. After one day, the surviving melanoma cells were exposed to NK-92 but also to primary NK cells (E:T ratio of 5:1). Figure 39 A shows that WM3734 cells co-cultured with NK-92 for 24 h have reduced susceptibility to NK-92 (reduction of ~12 %) comparable to co-culture results with primary NK cells. Given that WM3734 cells are less susceptible to NK-92 compared to primary NK cells, no killing was detectable after 60 min (Figure 39 E) but showed a reduced NK-92 killing after co-culturing after 240 min (Figure 39 F). In addition, the NK-92 co-cultured melanoma cells are also less susceptible to primary NK cells (Figure 39 A). Figure 39 C shows that this cross-resistance of 8 % was already significant at the initial phase of the cytotoxic assay. After 240 min, the susceptibility of WM3734 decreased significantly from 54 % (control) to 42 % (co-culture) (Figure 39 D).

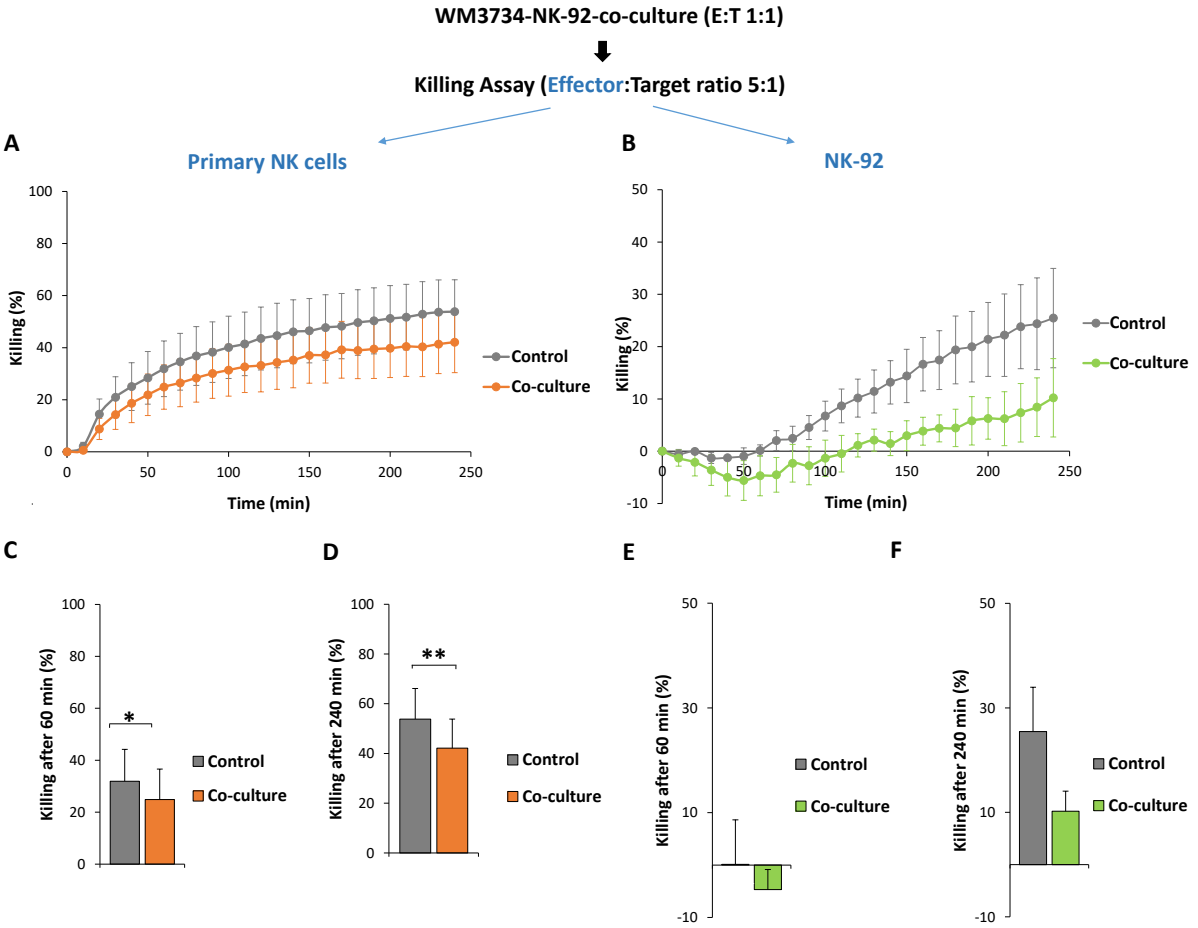

Figure 39. Short-term (24 h) co-cultures with NK-92 reduces the susceptibility of melanoma cells to NK-92 and induce cross-resistance to primary NK cells. WM3734 were co-cultured with NK-92 in an E:T ratio of 1:1 for 24 h. Then, melanoma cells of the co-cultures as well as corresponding controls were loaded with 0.5 µM calcein-AM and exposed to the effector cells NK-92 (right; n=3) or primary NK cells (left; n=5) (E:T ratio of 5:1). (A+B) Killing kinetic of 4 h cytotoxic assay. For statistical analysis, killing after 60 min (C+E) and after 240 min (D+F) were used. Bars and graphs indicate means ± SEM. Statistical significance of unpaired, two-tailed Student's *t*-test is indicated with * for $p<0.05$ and ** for $p<0.01$.

The observations made with WM3734-NK-92-co-cultures were also confirmed with 1205Lu-NK-92-co-cultures. As seen in Figure 40 B, high E:T ratios of 3:1 or 7:1 during NK-92 co-culture induced resistance of 1205Lu cells to NK-92 (killing less than 6 %). After a short recovery time, the 3:1 NK-92-melanoma-co-culture reached the susceptibility of the non-treated 1205Lu control (~47 %). Additionally, the 7:1 NK-92-melanoma-cell co-cultures were killed to ~40 %. Furthermore, Figure 40 A shows that the susceptibility of 1205Lu towards primary NK cells was strongly reduced after co-culturing with NK-92. The control was killed to ~ 80 % whereas both co-cultures (3:1 and 7:1) were only killed to ~40 % by primary NK cells. This developed resistance was reversible after three days and a susceptibility to NK cells of more than 71 % was recovered.

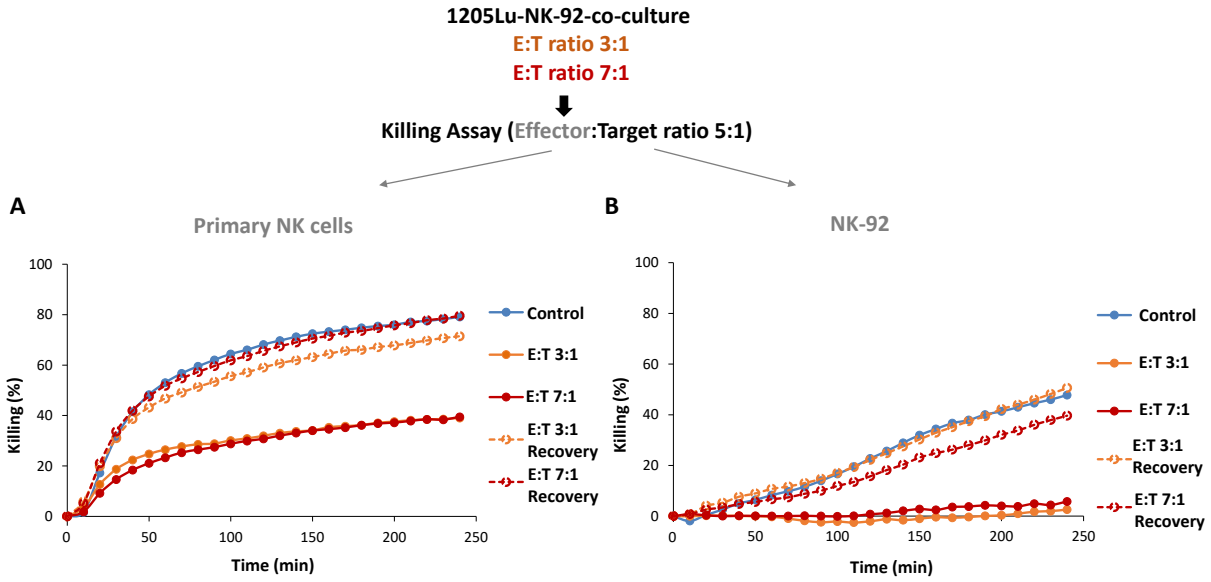

Figure 40. 1205Lu-NK-92-co-cultures and cross-resistance to primary NK cells. 1205Lu were co-cultured with NK-92 in E:T ratios of 3:1 and 7:1 for 2 weeks. Thereby, NK-92 were renewed two times a week. Before the last NK-92 exposure the co-cultures were subcultured. One half was re-treated with NK-92, whereas the other part was non-treated for three days (Recovery) before cytotoxic experiment. Then, melanoma cells of the co-cultures as well as corresponding control were loaded with 0.5 µM calcein-AM and exposed to primary NK cells (A) or NK-92 (B) (E:T ratio of 5:1). The 4 h killing kinetic of one performed real-time killing assay with NK-92 and one primary NK cell donor is shown.

4.10.3 RNA sequencing reveals proteins involved in NK cell-mediated immune escape

To investigate which genes are involved in the process of immune escape, total RNA of melanoma cells of different WM3734-NK cell-co-cultures and healthy melanocytes (Table 19) was sequenced using Illumina HiSeq 2500. The analysis showed that the samples clustered differently according to principal component analysis (PCA) (Lever et al., 2017). As shown in Figure 41 A, melanocytes were separated from the melanoma sample set. Within the melanoma samples, Figure 41 B showed that WM3734-NK cell-co-cultures and the corresponding controls clustered differently compared to WM3734-NK-92-co-cultures and their corresponding controls.

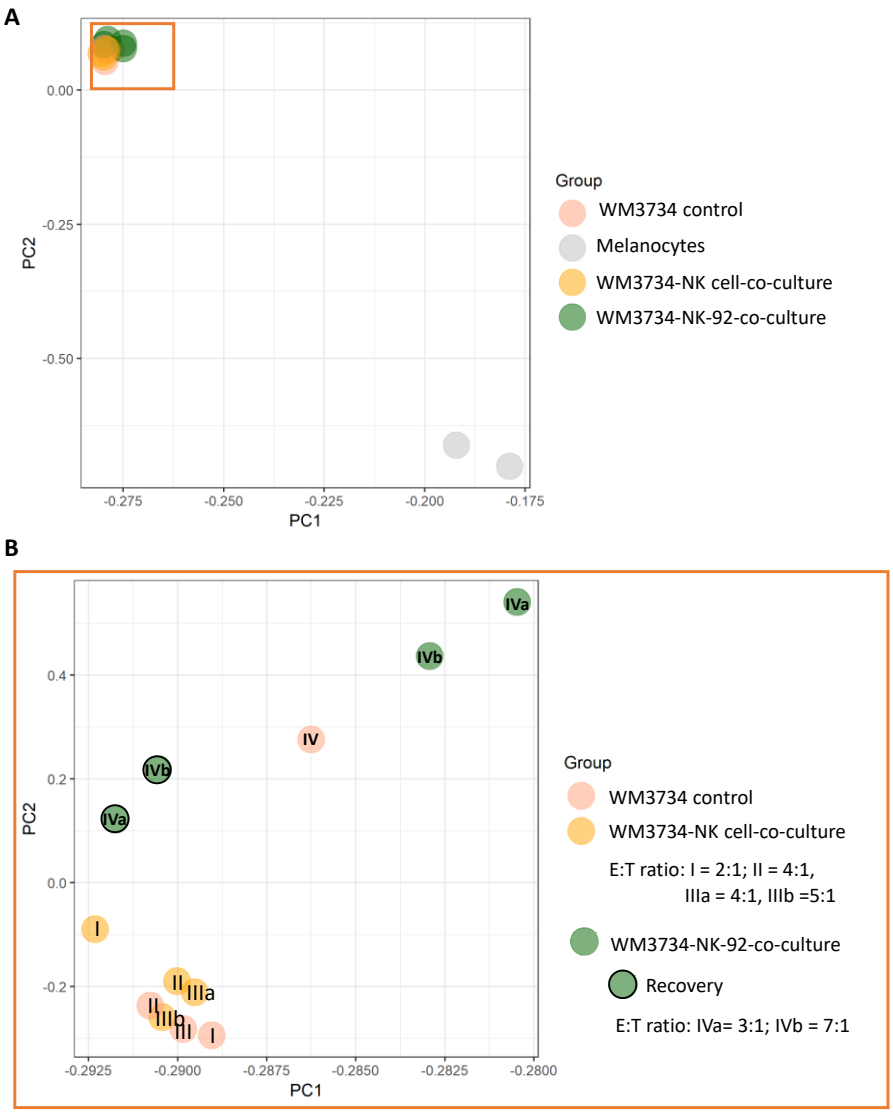

Figure 41. Principal component analysis (PCA) of WM3734-NK cell-co-cultures. Samples are grouped (A) by cell type (melanocytes vs. melanoma) and (B) by co-culture treatment. Non-treated WM3734 (control) are coloured pink; co-culture with primary NK cells are coloured orange, co-culture with NK-92 cell line are coloured green; black circled = Recovery.

Due to the restricted sample number, different E:T ratios of the co-cultures and the respective controls were pooled (Figure 42) to allow differential gene expression (DGE) analysis.

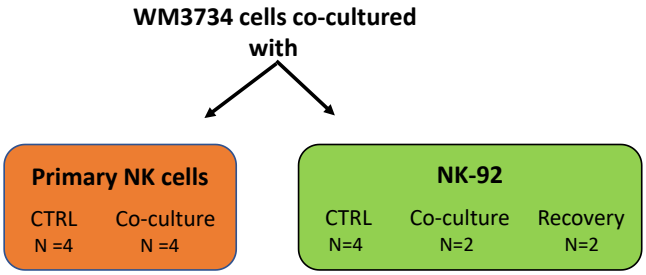

Figure 42. Pooling of samples for RNA sequencing analysis. WM3734 were co-cultured with primary NK cells (orange) or NK-92 (green).

This analysis revealed that about 100 genes were differently expressed after the co-culturing process with primary NK cells (see table A1 in the appendix) and NK-92 cells (see table A2 in the appendix). To identify genes that play a central role in the susceptibility of melanoma cells to NK cells, only the overlap of differentially expressed genes in both data sets were further analysed. The comparison of both data sets identified 13 common differently expressed genes of WM3734 cells co-cultured with primary NK cells and NK-92 (see Table 23). Ten out of 13 genes were coding directly for MHC molecules or were associated with these molecules. MHC class I molecules were represented by HLA-B, beta-2-microglobulin (*B2M*) as well as HLA complex 5 (*HCP5*). Most of the identified genes belong to the group of MHC class II molecules. Among them *HLA-DMB, HLA-DPA1, HLA-DPB1, HLA-DQA1, HLA-DQB1, HLA-DRA*. *CD74* also known as *HLA-DR* antigens-associated invariant chain were coding for a polypeptide, which help to form and transport MHC class II molecules. The other genes: absent in melanoma 2 (*AIM2*), complement component 1 subcomponent (*C1S*) and the transmembrane protein 158 (*TMEM158*) were in the broadest sense associated with the proliferative/invasive status of the melanoma cells. Differently expressed genes of WM3734-NK-92 co-culture had approximately 3 times higher fold change (logFC) and much higher false discovery rate (FDR) values compared to differently expressed genes of the primary NK cell co-culture.

Table 23. Common differentially expressed genes of WM3734 co-cultured with primary NK cells and NK-92 under specification of logFC, FDR and association with cellular processes . For comparison analysis Notepad ++ was used.

Gene	logFC		FDR		Gene associated with
	NK-92	Primary	NK-92	Primary	
AIM2	6.88	4.45	1.00E-06	7.27E-48	Phenotype switch
B2M	2.74	0.65	0.006	0.003	MHC class I
C1S	4.79	1.42	1.12E-05	0.001	Phenotype switch
CD74	2.42	0.62	0.0002	0.0003	MHC class II
HCP5	8.19	2.42	2.62E-08	0.006	MHC class I
HLA-B	3.97	0.77	1.33E-08	1.49E-05	MHC class I
HLA-DMB	2.47	1.11	0.0033776	7.93E-13	MHC class II
HLA-DPA1	2.63	0.91	0.0011175	6.21E-11	MHC class II
HLA-DPB1	2.48	0.88	0.0001648	1.03E-09	MHC class II
HLA-DQA1	7.42	2.98	1.394E-15	2.69E-20	MHC class II
HLA-DQB1	3.27	1.09	5.155E-07	1.14E-11	MHC class II
HLA-DRA	2.49	0.9	0.0016177	6.21E-11	MHC class II
TMEM158	2.74	2.02	0.0003767	2.69E-20	Ras activation

In addition, the gene expression of the co-culture was compared with the expression profile of the co-culture after removal of the NK-92 for 3 days. This short recovery time changed the expression of 103 genes (see table A3 in appendix), where 59 of these genes were also

differentially expressed in the previous comparison. Hence, after NK-92 cells were removed, the expression profile of the recovered melanoma cells equalled the control again. This was further supported by the marginal DGE (see table A4 in the appendix) of these cells in comparison to the untreated WM3734 cells.

Taken together, melanoma cells developed resistance to primary NK cells as well as NK-92 cells during long-term and short-term co-cultures. Subsequent RNA sequencing of melanoma co-cultures revealed a limited number of common differentially expressed genes of WM3734 co-cultured with primary NK cells and NK-92. These genes are mainly associated with MHC class I and II molecule expression and might explain the induced a cross-resistance of melanoma-co-cultures with NK-92 cells to primary NK cells. In addition, the results of this study indicate that the resistance to NK cells is reversible and melanoma cells get susceptible again after short recovery time.

5 Discussion

Melanoma is the most lethal form of skin cancer with increasing incidence worldwide (World Health organization, 2020). In addition to its high metastatic potential, the treatment of this cancer is challenged by its heterogeneity and adaptability to therapies. During the last years, targeted therapies in combination with immunotherapies showed most clinical success (Seidel et al., 2018). Nevertheless, the development and improvement of anti-melanoma therapies are required to prevent therapy resistance and relapses. In this study, the potential of NK cells to improve and complement current melanoma therapy was investigated.

5.1 Effector-to-Target ratio determines effect size of NK cell killing

Therapy success is not only dependent on persistent immunogenicity of melanoma cells but also on tumour infiltrating lymphocytes (Cursons et al., 2019; Fortes et al., 2015; Thomas et al., 2013). NK cell infiltration of primary melanoma tumours ranged between E:T ratios 0.03:1 and 0.5:1 (Balsamo et al., 2012). In order to consider E:T ratios, which resemble intratumoural NK cell infiltration four different E:T ratios were tested. The lower E:T ratios 0:5:1 and 1:1 showed only marginal NK cell-mediated killing of the melanoma cell line WM3734 and revealed that even high NK cell infiltration might only induce small reduction of the tumour burden. Only significantly higher NK cell numbers (5:1 and 10:1) showed a potent cytotoxic effect (Figure 10). Although these ratios do not correspond to the NK cell infiltration into melanoma tumours, the cytotoxicity assay requires a dynamic range to investigate parameters influencing the NK cell-induced cytotoxicity against melanoma cells. In contrast to WM3734 cells, the initial NK cell cytotoxicity to the leukemia cell line K562 was not only considerably higher but also increased almost proportional to the used NK cell number until reaching 100 % maximum. This is explainable by the low expression of the inhibitory MHC class I molecules with simultaneous presence of NK cell activating ligands (Tremblay-McLean et al., 2019). Moreover, it was shown that the NK cell detachment from a target was retarded or even inhibited after unsuccessful killing, hence reducing the serial killing of NK cells (Anft et al., 2020). This might contribute to the observed differences between the cell lines K562 and WM3734. Although the killing of melanoma was increased with higher E:T ratios, the killing was not much increased after doubling the NK cell numbers from E:T ratio 5:1 to 10:1. One possible explanation could be that a certain subpopulation of WM3734 cells is intrinsically less susceptible to NK cells and evade elimination. Besides that, also the challenging of melanoma cells with NK cells could induce rapid adaptions of the melanoma cell phenotype that might diminish the NK cell-mediated

killing. However, the questions if and how such adaptions affect melanoma susceptibility to NK cells in the relative short time of the experimental set up remain open.

5.2 Interleukin-2 stimulation increases NK cell cytotoxicity

Already in the early days of NK cell studies the stimulating character of certain cytokines on the cytotoxicity of NK cells was discovered and further used to increase the capability of the effector cells (Wu et al., 2017). Several studies showed that IL-2 stimulation increased NK cell cytotoxicity against cancer cells (Balsamo et al., 2013; Henney et al., 1981; Huenecke et al., 2010; Lehmann et al., 2001). Also in this study, it was shown that IL-2 stimulation is crucial to enhance NK cell cytotoxicity against melanoma cell lines and to a lower extend against K562 cells (Figure 12). The killing capability of NK cells is among others determined by the expression profile of activating and inhibitory receptors on the cell surface as well as the intracellular content of the lytic granules. Flow cytometric analysis of IL-2 stimulated NK cells showed an upregulation of the activating receptor NKp30 and NKG2D as well as higher levels of CD16. Furthermore, an increased intracellular content of perforin and granzyme B was observed (Figure 12). These alterations of the NK cell phenotype were also observed by other groups, which reported an upregulation of the natural cytotoxicity receptors (NCRs) NKp30 and NKp46 as well as the *de novo* expression of NKp40 following IL-2 stimulation (de Rham et al., 2007; Pietra et al., 2012a). Moreover, the density of NCRs on the effector surface has been shown to directly correlate with the NK cell-mediated killing of certain tumour cells (Pende et al., 2002). Similar observations have been made with the expression level of NKG2D and the NKG2D-mediated killing of melanoma (Morgado et al., 2011). Hence, a crucial role of these activating receptors in NK cell recognition of melanoma can be assumed. In addition, higher levels of perforin and granzyme B in NK cells subsequent to IL-2 stimulation were described by other scientific reports (DeBlaker-Hohe et al., 1995; Salcedo et al., 1993; Zhang et al., 2008). All of these alterations in the NK cell phenotype can at least partly explain the IL-2 induced increase in NK cell cytotoxicity. The different susceptibility of K562 cells and WM3734 cells could be explained by a distinct ligand profile. In comparison to melanoma cell lines, the cell line K562 lacks MHC class I molecules (Garson et al., 1985) and has thereby a lower activation threshold for NK cell cytotoxicity. Consequently, the NK cell-mediated killing of K562 cells should be less dependent on the expression of activating ligands, an aspect that might explain the lower effect of IL-2 stimulation. Nevertheless, the correlation of MHC class I expression and NK cell susceptibility of K562 is controversial as several studies showed no direct connection of these parameters (Nishimura et al., 1994; Reiter et al., 1991). Due to the higher expression levels of activating

receptors, IL-2 stimulated NK cells could overcome inhibitory stimuli (e.g. HLA-A,B,C expression) and have a lowered activation threshold enhancing target cell elimination. Although other reports showed that longer stimulation periods slightly reduced activating receptors (Balsamo et al., 2013) or even led to NK cell exhaustion (Huenecke et al., 2010), the experimental data of this thesis did not support these findings. The duration of this stimulation only marginally affected the general NK cell cytotoxicity towards cancer cells independent of their NK cell susceptibility (Figure 13). Smaller observed differences in NK cell cytotoxicity can be explained by different temporal upregulation of individual NK cell receptors and their distinct involvement in the killing process of specific cancer cell lines. Nevertheless, IL-2 stimulation increases the NK cell cytotoxicity against melanoma cells by upregulation of activating receptors and reveals distinct susceptibility of melanoma towards NK cells.

5.3 Heterogeneous susceptibility of melanoma cells to primary NK cells

Melanoma is an immunogenic cancer as it was shown to express several ligands that bind activating immune receptors (Casado et al., 2009; Chan et al., 2010; O'Donnell et al., 2019). Within this thesis, the susceptibility of 20 melanoma cell lines with distinct genetic backgrounds and development stages to NK cells were analysed. The performed cytotoxic assays revealed a highly heterogeneous NK cell-mediated killing of melanoma cells (Figure 14). Distinct expression profiles that alter the number of activating and inhibitory ligands on the melanoma cell surface may be responsible for these results. One of the ligands are MHC class I molecules that are known to protect target cells against the NK cell-mediated killing according to the 'missing self' hypothesis of Kärre (Karre, 2002). However, the MHC class I molecules on the melanoma cell surface did not correlate with the measured susceptibility of distinct melanoma cell lines towards NK cells (Figure 15). These findings were in line with the reports of other groups who also failed to find a linear correlation of MHC class I expression and the NK cell-mediated killing of cancer cells, including melanoma (Andalib et al., 2000; Pena et al., 1990). A possible explanation for these observations might be a saturation of all KIR receptors, so that increased expression will only influence the NK cell-mediated killing of target cells with low or absent MHC class I expression. This hypothesis would support the findings that restoration of MHC I expression in K562 cells reduced their susceptibility to NK cells (Sarin et al., 1995; Tóth and Kubeš, 1993). Moreover, it is necessary to consider that the isolated NK cells were derived from donors with unknown HLA status. In this allogeneic setting, a KIR-HLA-class I-mismatch is quite likely and would explain the missing correlation of this inhibitory ligand and the susceptibility of melanoma cells towards "unlicensed" NK cells. Nevertheless, it has been shown that also autologous NK

cells were able to kill melanoma cells expressing matched MHC I molecules (Carrega et al., 2009). Therefore, the impact of MHC class I surface expression on the NKiToxMel is still controversially discussed.

The involvement of NKG2D/NKG2DL engagement in the NK cell-mediated killing of melanoma and other cancers seems to be more profound (Casado et al., 2009; Frazao et al., 2019; Morgado et al., 2011; Raulet, 2003) and was partly validated in the experimental data of this thesis. A higher abundance of MICA/MICB and ULBPs was associated with an increased NKiToxMel (Figure 16). These NKG2D ligands were commonly but heterogeneously expressed on melanoma cells (Casado et al., 2009; Vetter et al., 2002). Moreover, there are multiple indications that the expression levels of these ligands inversely correlate with tumour progression and patient survival due to an increase of soluble NKG2D ligands in the serum of cancer patients, including melanoma patients (Maccalli et al., 2017; Paschen et al., 2009; Shen et al., 2017; Vyas et al., 2017). This 'shedding' not only reduced density of these ligands on the cell surface but also induced the downregulation of surface NKG2D expression diminishing NK cell recognition even further (Salih et al., 2002). Experimental data obtained via flow cytometry only detect proteins expressed on the cell surface so that the shedding of ligands as well as intracellular molecules could not be inspected with this approach. Therefore, the NKG2D ligand expression shown in Figure 16 might be underestimated. In addition to the NKG2D receptor, also NCRs are important for melanoma detection by NK cells. One of them is Nkp30, whose known ligand B7-H6 has been shown to be expressed in about 20 % of cancer cell lines including melanoma (Bjornsen et al., 2019; Brandt et al., 2009). The abundance of B7H6 on the investigated melanoma cells was only marginal but showed the expected trend of higher B7H6 levels in the more susceptible melanoma cell lines (Figure 16). In sum, melanoma susceptibility to NK cells was associated with increasing activating ligands. However, the actual impact of individual ligands on the NK cell-mediated killing could only partially be resolved with the expression analysis obtained by flow cytometry. Additionally, the limited number of surface expressed ligands and the investigation of three cell lines, give only a limited view of the ligand profile of melanoma cells.

Despite the distinct NK cell detection, also the mode of melanoma cell death might be different. As already discussed, NK cells can kill tumour cells via necrosis and apoptosis (Backes et al., 2018). Taken that these processes have different kinetics, the observed killing curves could be partly a result of a heterogeneous preference to a distinct killing mode dependent on the melanoma cell line. Nevertheless, it is very plausible that universal protein expression patterns determine the heterogeneous NK cell-mediated killing of melanoma cells.

5.4 Reverse phase protein array reveals proteins correlating with susceptibility to NK cells

The flow cytometry-based analysis of a limited number of potential melanoma ligands was not sufficient to understand the heterogeneous susceptibility of the melanoma cell lines to NK cells. On the other hand, reverse phase protein array (RPPA) allows sensitive and high throughput detection of more than 300 cancer-related proteins (MD Anderson, 2019; Tibes et al., 2006). RPPA was performed to further characterise the melanoma cell lines used in this study and allowed the identification of melanoma proteins that correlate with the determined NK cell-mediated killing of melanoma cells. Intensive literature research for all proteins (marked in bold) of this melanoma killing signature revealed a melanoma phenotype switch determining the susceptibility to primary NK cell killing.

Tumour growth and survival are parameters, which are dependent on environmental signals such as growth factors and nutrients. The receptors sensing and transducing these signals are thus important regulators of cell survival, proliferation, but also invasion. Multiple surface receptors were identified within the melanoma killing signature (Figure 17). One of the receptors that positively correlated with the NK cell-mediated killing was the **transferrin receptor** (**TFRC**). This receptor is involved in iron uptake and therefore plays an essential role in the cellular iron metabolism (Shen et al., 2018). High expression of TFRC was associated with enhanced cell proliferation (Trowbridge and Omary, 1981) and tumour progression. (Jones et al., 2006; Shen et al., 2018). Another identified receptor was the **platelet derived growth factor receptor beta** (**PDGFRB**). A decreased PDGFRB protein level diminished proliferation rate and invasion potential in several cancers (Fujino et al., 2018; Melaiu et al., 2017). PDGFR signalling is positively controlled by AKT and mediates tumour glycolysis (Ran et al., 2013). Furthermore, this receptor was found to be co-expressed with genes involved in EMT and has shown to be a characteristic of a mesenchymal phenotype in colorectal tumour cells (Steller et al., 2013). However, in melanoma the expression of PDGFRB has been shown to correlate with lower metastatic potential (McGary et al., 2004) and resistance to vemurafenib (Shi et al., 2011). Interestingly, PDGF-DD, one of the four polypeptides of the platelet-derived growth factor (PDGF) is an identified ligand for NKp44 (Barrow et al., 2018). Therefore, the relation of soluble PDGF and receptor bound growth factors might affect NK cell killing. A receptor that correlated with higher NK cell resistance was **c-MET**, that is known to bind hepatocyte growth factor and leads to the activation of several pathways e.g. PI3K/AKT and MAPK (Zhang et al., 2018).

Accordingly, this transmembrane receptor has shown to have increased activity in several cancer types including melanoma (Gherardi et al., 2012; Zhang et al., 2018) and thus promote tumourigenesis and cancer progression (Demkova and Kucerova, 2018). Furthermore, c-MET signalling was shown to promote EMT by disrupting cadherin-based cell–cell contacts (Zhou et al., 2019b). Another receptor found to negatively influence the NK cell-mediated killing was the **progresterone receptor (PGR).** Its general role in cancer progression and prognostic value is still controversy discussed. In prostate cancer, PGR was associated with disease progression (Grindstad et al., 2018), whereas in breast cancer mainly the opposite was reported (Yeung et al., 2016). However, breast cancer patients expressing this receptor had better prognosis (Lim et al., 2016a). In melanoma, progesterone has shown to inhibit cell growth, whereby the progesterone receptor itself does not seem to be involved (Ramaraj and Cox, 2014). Nevertheless, in breast cancer there is evidence that progesterone receptor suppress tumour growth by reducing translation of certain proteins (Finlay-Schultz et al., 2017). Furthermore, it has been reported that PGR-positive tumours may escape immune surveillance by downregulation of STAT-1 mediated IFN-γ signalling (Goodman et al., 2019). Also in melanoma, tumour immune escape was shown to be controlled by STAT-1 (Cerezo et al., 2018; Osborn and Greer, 2015).

Another cell signal transducer found to be associated with increased NK cell resistance was the well-established oncogene **NRAS**. Although NRAS is highly mutated and constitutively active in melanoma (Davies et al., 2002), the investigated melanoma cell lines for establishing the melanoma killing signature are known as NRAS WT. However, its proliferative function is not only determined by the absolute expression level but also its activation status. The RAS activation is regulated by the adapter molecule growth factor receptor-bound protein 2 (GRB2). **PDGFRB (pY716)** mediates direct binding of GRB2 and decreased the RAS activity. (Arvidsson et al., 1994). As this protein is also inversely correlated to the killing, one could conclude that melanoma cells more susceptible to NK cells had also higher NRAS activity independent from its expression level and mutational status. In addition, there are several indications that NRAS mutated melanoma patients show a better response to immunotherapies (Johnson et al., 2015; Kirchberger et al., 2018; Munoz-Couselo et al., 2017). **COPS5** can affect several signalling pathways that are known to be involved in carcinogenesis. Furthermore, its overexpression was observed in many cancers (Liu et al., 2018).

The identified proteins downstream of this signalling cascade were part of the PI3K-AKT-mTor and Hippo pathways. Proline-rich Akt substrate of 40 kDa (PRAS40), also known AKT1 substrate 1, is part of the mTOR complex 1 and a known target of AKT. The phosphorylation of PRAS40 allows dissociation of the complex and hence releases the repression of mTORC1.

Based on these observations, it was proposed that elevated phosphorylation of PRAS40 is often associated with tumour progression. (Lv et al., 2017; Madhunapantula et al., 2007). However, only the total, non-phosphorylated PRAS40 was included in the RPPA-based melanoma killing signature. Threonine 246 is the only phosphorylation site of AKT1S1 included in the performed RPPA. Taken that PRAS40 has several phosphorylation sites, the RPPA cannot give a complete information about the phosphorylation status of this protein in the investigated melanoma cell lines. Furthermore, PRAS40 was shown to promote melanoma survival as it protects against apoptosis (Madhunapantula et al., 2007). **RICTOR** is a protein involved in assembly and function of mTOR complex 2 that regulates cytoskeleton remodelling and cell survival (Saxton and Sabatini, 2017). Although the mTORC1 dependent S6K1 was shown to phosphorylate RICTOR at T1135, the effect on the complex activity remains controversial. (Boulbes et al., 2010; Dibble et al., 2009). Nevertheless, there are indications that phosphorylation at this tyrosine residue might inhibit mTORC2 activity (Julien et al., 2010). The mTORC2 was also suggested to promote aerobic glycolysis i.e. the 'Warburg effect' via upregulation of c-Myc (Masui et al., 2014) In addition, RICTOR expression is associated with tumour growth, cell migration and invasion, and inversely correlated with patient survival (Liang et al., 2017; Schmidt et al., 2018). WW Domain Containing Transcription Regulator 1 (**WWTR1**) is one of the downstream effectors of the Hippo signalling pathway that controls organ size through strict regulation of apoptosis and cell proliferation (Zhao et al., 2010a). WWTR1 is upregulated in many solid tumours and is associated with elevated invasion, angiogenesis and metastasis, but also stemness maintenance in several cancers including melanoma (Boopathy and Hong, 2019; Chen et al., 2019a; Feng et al., 2018; Wei et al., 2019a). In addition, several proteins of the melanoma killing signature involved in metabolism suggested that melanoma cells with increased glycolysis were more susceptible to NK cells. Glyceraldehyde-3-Phosphate Dehydrogenase (**GAPDH**) is a crucial enzyme in glycolysis as it catalyses the conversion of glycerinaldehyde 3-phosphate to 1,3-bisphospho-glycerate (Nicholls et al., 2012). Moreover, GAPDH is involved in the regulation of mTORC1 activity as it prevents Rheb from binding to mTOR under low-glucose conditions (Lee et al., 2009). However, its role is not only restricted to its central role in cell metabolism (Nicholls et al., 2012). Several studies showed its involvement in other processes such as apoptosis through mitochondrial membrane permeabilization (Colell et al., 2009; Tarze et al., 2007) and EMT via SNAI1 upregulation (Liu et al., 2017a). As posttranslational modifications control the activity and function of GAPDH (Colell et al., 2009; Zhang et al., 2015), the RPPA failed to provide further information regarding a connection between GAPDH expression and its function in the context of NK cell-mediated killing of melanoma cells. Nevertheless, GAPDH was reported to be overexpressed in cancer and correlated with tumour progression in several cancers types

including melanoma (Hao et al., 2015; Ramos et al., 2015; Tang et al., 2012). Another important enzyme in the metabolic context is **Hexokinase 2** that catalyses the phosphorylation of glucose in the first step of glycolysis. It promotes tumour growth and increases the metastatic potential in numerous cancers (Anderson et al., 2017; Lee et al., 2019; Siu et al., 2019). In addition, HK2 binds voltage-dependent anion channels (VDACs) in the outer mitochondrial membrane. This suppresses the release of proteins such as cytochrome c or DIABLO, thereby inhibiting apoptosis and promoting cell survival (Pastorino and Hoek, 2003).

One essential hallmark of cancer is resisting cell death (Weinberg et al., 2019). As discussed above, NK cells are able to kill cancer cells in distinct modes. The activation of NK cells mediates the release of perforin that can lead to membrane disruption and necrotic cell death. **Annexin A7** (ANXA7) is part of the plasma membrane repair system (Sonder et al., 2019), so that increased level of ANXA7 might protect melanoma cells form NK cell killing. The role of ANAX7 in tumour progression seems to be dependent on the cancer type (Guo et al., 2013). However, in melanoma its expression was mainly connected to a less invasive phenotype (Kataoka et al., 2000). **BAD** is a pro-apoptotic protein that binds anti-apoptotic proteins such as Bcl-2 and allows the initiation of apoptosis (Anvekar et al., 2011). The activity of BAD is negatively regulated by phosphorylation at several residues. Several kinases including ribosomal protein S6 kinase alpha-1 (RPS6K1) phosphorylate BAD at serine residue 112 and prevent its pro-apoptotic activity (Stickles et al., 2015). Therefore, pBAD is associated with cancer development (Bui et al., 2018; Stickles et al., 2015) and therapy resistance (Chon et al., 2012; Marchion et al., 2011). Besides its role in apoptosis, there is evidence, that it is also involved in cell metabolism via the activation of glucokinase (Gimenez-Cassina et al., 2014). **CASP3** is a known executioner caspase in the apoptosis process. Nevertheless, melanoma cells expressing more CASP3 seem to be better protected against the NK cell killing. This might be a contra intuitive finding, but the result could be explainable by considering the non-apoptotic protein functions of CASP3. CASP3 mediates stem cell differentiation (Abdul-Ghani and Megeney, 2008), promotes cell migration as well as invasion of melanoma (Liu et al., 2013) and other cancers (Zhou et al., 2018b). **DIABLO** was shown to be the most negative regulator of NK cell-mediated killing of melanoma. DIABLO is a mitochondrial protein that acts pro-apoptotic by blocking the inhibitors of apoptosis (Du et al., 2000). Therefore, its decreased expression will inhibit apoptosis and promote cell survival (for more details see chapter 5.6.1). Heat shock protein beta 1 is a negative regulator of ferroptosis, an iron dependent programmed cell death (Sun et al., 2015). Furthermore, **HSPB1** is also involved in regulating tumour invasion, metastasis and survival (Arrigo and Gibert, 2014; Gibert et al., 2012; Straume et al., 2012). HSPB1 transfected melanoma cell showed increased expression of E-cadherin (Aldrian et al., 2002).

Taken together, the apoptosis-related proteins indicate that melanoma cells with lower apoptotic threshold show a higher susceptibility to NK cell killing. Nevertheless, this observation might also be a result of faster detection of necrotic cells than apoptotic cells, hence, negative correlation of apoptosis-related proteins with NKiToxMel.

In this study, melanoma cells susceptible to NK cells were not only characterised by a higher proliferation rate (Figure 34) but also by their staging (Figure 35) and invasion potential. Epithelial-mesenchymal transition plays a crucial role in cell invasion and tumour progression as it allows the generation of mesenchymal cells with motile properties to establish distant metastasis (Yeung and Yang, 2017). **SNAI1**, one of the top hits, is a known mediator of EMT (Kaufhold and Bonavida, 2014; Wang et al., 2013). This EMT-like phenotype switching has been also reported in melanoma (Li et al., 2015a). In addition to SNAI1, other proteins such as the adhesion molecules TWISTs also act as EMT promoters (Kang and Massague, 2004). **TWIST2** that was shown to be associated with NK cell resistance, is often overexpressed in human cancer, particularly in melanoma (Ansieau et al., 2008). Furthermore, it contributed to tumour progression in breast cancer (Fang et al., 2011) However, in breast cancer the differential cellular distribution of this protein determines its function regarding tumour progression. Nuclear TWIST2 initiates EMT and tumour invasion, whereas cytoplasmic TWIST2 maintains the epithelial-like and non-invasive cancer phenotype (Mao et al., 2012). Although TWIST1 and TWIST2 show structural homology and some functional redundancy, TWIST2 cannot be associated with cell invasion and patient survival in hepatocellular cancer patients (Sun et al., 2010). In prostate cancer, there is even evidence that TWIST2 could function as a tumor suppressor (Zhao et al., 2019). As the RPPA do not reveal information about the localization and function of TWIST2 in the investigated melanoma cells, the negative association to the NK cell-mediated killing may be a result of cytoplasmic localization and possible tumour suppressor function in melanoma. That mesenchymal phenotypes favour NK cell-mediated killing is further supported by the identification of **L1CAM** as a significant hit (Chen et al., 2018; Kiefel et al., 2012). In melanoma, it is involved in cell motility (Yi et al., 2014) as well as in metastatic spread in a xenograft model of human melanoma (Ernst et al., 2018). In addition, the **protein tyrosine kinase 2**, also known as focal adhesion kinase is involved in cellular adhesion and cytoskeleton organization (Mitra et al., 2005). It has been frequently overexpressed in cancers (Prickett et al., 2009; Zhou et al., 2019a) and is constitutively active in malignant melanoma (Kahana et al., 2002). Furthermore, it was shown that FAK inhibition reduces melanoma metastasis (Jeong et al., 2019; Kircher et al., 2019). This might be a result of a negative modulation of PTK2 in the E-cadherin dependent cell-cell-adhesion, leading to EMT (Giehl and Menke, 2008; Kleinschmidt and Schlaepfer, 2017). The reversion of EMT was followed by increased **Napsin A** expression (Zhou

et al., 2018a). Napsin A is a functional aspartic proteinase that is a known marker for primary lung adenocarcinoma (Ueno et al., 2003) and showed association with differentiation grade of adenocarcinoma. It was already shown to act as a suppressor of tumour growth (Ueno et al., 2008). An unexpected protein found in the melanoma killing signature was **LCK**. Beyond its function as a mediator of the TCR signalling, LCK seems to also play role in other cellular processes such as carcinogenesis and cancer cell phenotype switch (Bommhardt et al., 2019). In melanoma, it was shown that high LCK protein expression was associated with enhanced patient survival (Cancer Genome Atlas, 2015). The underlying molecular reasons are not known yet, but it might be connected to its repressing function in oxidative phosphorylation (Vahedi et al., 2015). One of the causes of melanoma is UV light exposure leading to DNA damage (Gandini et al., 2005b; Kulichova et al., 2014). The X-Ray Repair Cross Complementing 1 (**XRCC1**) is involved in DNA damage repair. Therefore, it is hardly surprising that the loss of XRCC1 was found to correlate with melanoma progression and poor patient survival (Bhandaru et al., 2014). In addition, single nucleotide polymorphisms (SNPs) in XRCC1 was also shown to increase cancer risk in some cancer types (Meng et al., 2017; Smolarz et al., 2019; Yin et al., 2007).

This newly established melanoma protein signature suggested that melanoma cells with a more invasive i.e. aggressive (mesenchymal) phenotype that rely more on aerobic glycolysis might pose a better target for NK cell killing. This hypothesis is summarised in Figure 43.

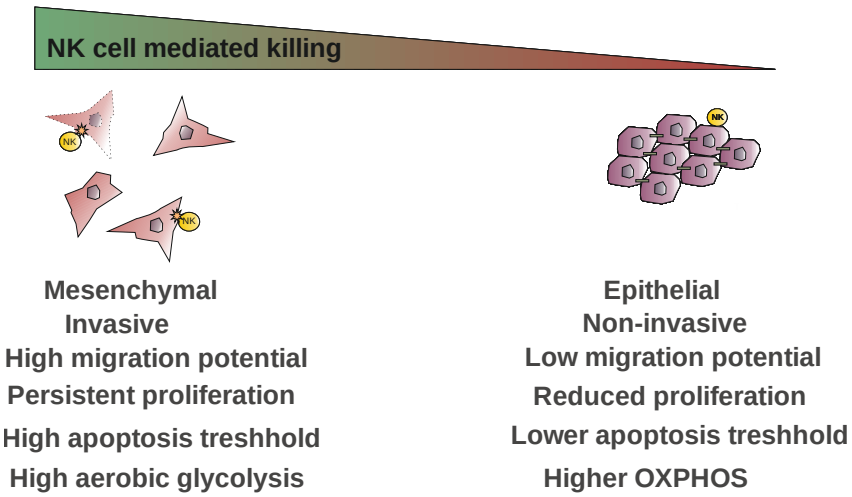

Figure 43. Melanoma cell phenotype determines susceptibility to NK cell killing.

This melanoma cell phenotype is also in line with the gene signature predicting NK cell infiltration and melanoma patients' survival (Cursons et al., 2019). According to this work, less mesenchymal melanoma tumours had a lower NK cell infiltration (NK score), whereas highly mesenchymal tumours had higher range in their NK cell score. Surprisingly, TGF-β specific EMT gene score did not correlate with the NK cell score. A number of studies reported

metabolic reprogramming of cancer cells during EMT (Kang et al., 2019). Melanoma cells with more invasive, mesenchymal properties tend to rely more on glycolysis than oxidative phosphorylation (OXPHOS) (Bettum et al., 2015). In addition, tumour progression was also associated with the aerobic glycolysis (Warburg effect) (Lee et al., 2018; Lu et al., 2015)

In sum, the RPPA based melanoma killing signature allowed the further characterisation of melanoma cells with higher susceptibility to NK cells. However, this method is limited by the restricted number of proteins selected due to their association with cancer. Therefore, RPPA can only provide a partial impression regarding the interconnection between melanoma phenotype and NK cell-mediated killing. Nevertheless, it allows the development of a limited but robust prediction model that can be extended and validated in further experiments.

5.5 Melanoma protein signature allows the prediction of susceptibility to NK cells

The expression levels of melanoma proteins correlating with the susceptibly to NK cells (protein signature) was used to predict the response to NK cell-mediated killing. A weak point of the prediction model is that the actual impact of the single proteins to the susceptibility were neglected and hence all proteins had an equal weight in the signature. To minimize the overfitting of the model, we refrained from weighting the single proteins according to the strength of their influence on the killing or their correlation. Trials to include this information to the model led to overfitting and impaired the prediction, so that this attempt was abandoned. The chosen prediction model is based on the linear correlation of the protein signature of the melanoma cell lines to their susceptibility to NK cells. The resulting equation of the linear regression analysis allowed prediction of eight additional, previously non-tested melanoma cell lines (Figure 18). Although the killing efficiency was not always fully fitting to the prediction, the actual susceptibility of the majority of tested melanoma cells corresponded to the predicted values (Figure 19) and only one cell line (WM3682) clearly failed the prediction. Notably, this cell line bears a NRAS mutation at codon 61 (Q61L), which might increase the susceptibility to NK cells as several studies showed that NRAS mutated tumours benefit from immunotherapies (Johnson et al., 2015; Kirchberger et al., 2018; Munoz-Couselo et al., 2017). This theory is, however, contradicted by the WM3268 cell, which harbors a common mutation at codon 61 (Q16K) (Dumaz et al., 2019), but showed low susceptibility to NK cells. The NRAS (Q61) variant showed pronounced MAPK signalling in comparison to NRAS (G12) variants (Posch et al., 2016). If the distinct substitution of glutamine (Q) to leucin (L) or lysine (K) affects this signalling behavior is not known. Taken together, NRAS mutation status does not provide a full

explanation of the failed prediction of WM3682 and this issue needs further experimental analysis.

The killing information of the additional melanoma cell lines was used to identify crucial proteins controlling the susceptibility of melanoma cells to NK cells. Therefore, the RPPA analysis was repeated including the additional seven melanoma cell lines. The distinct disease stages and genetic backgrounds of these melanoma cell lines may mask the similarities of the molecular determinants of the NK cell-mediated killing. Therefore, it was not unexpected that the inclusion of all melanoma cell lines reduced the number of identified proteins. Interestingly, SNAI1 and DIABLO remained as strongest positive and negative regulators of the NKiToxMel, respectively.

5.6 Single regulators of the melanoma cell susceptibility to NK cell killing

DIABLO and SNAI1 were the most promising regulators of the NK cell-mediated killing. Therefore, it was assumed that manipulation of these proteins should influence the melanoma killing.

5.6.1 DIABLO is a potential negative regulator of NK cell-mediated killing

In agreement with the RPPA data, the expression of DIABLO in the melanoma cell lines inversely correlated with their susceptibility to NK cells (Figure 20). This seemed contra intuitive as DIABLO promotes apoptosis by inhibiting iAPs. The mitochondrial release of DIABLO is the major initiator of the extrinsic apoptosis pathway (TRAIL) (Zhang et al., 2003). The progression in melanoma is associated with decreased expression of death receptors for tumour necrosis factor-related apoptosis-inducing ligands (Zhuang et al., 2006). This also fits to the finding that 1205Lu cells are TRAIL resistant. (Phipps et al., 2011). In sum, this knowledge suggests that the NKiToxMel is not mediated by the extrinsic pathway. Nevertheless, DIABLO was one of the strongest RPPA-identified hits (Figure 17). Depending on the cancer type, DIABLO abundance might promote or suppress tumour progression (Martinez-Ruiz et al., 2008). The decrease of DIABLO after knockdown augments the NKiToxMel (Figure 23). Given that in other biological contexts DIABLO is reported to promote apoptosis, which does not explain our observations regarding its negative correlation with melanoma susceptibility to NK cell killing, it is likely that the actual function of DIABLO in the NK killing context is not designated to affect apoptosis. Notably, DIABLO was shown to repress cell differentiation (Arbiser, 2018) and has an additional role in tumour formation by affecting phospho lipid synthesis (Paul et al., 2018). Indeed, a changed composition of the phospholipid layer might favour the NK cell detection or the general susceptibility to the lytic granules.

5.6.2 SNAI1- a positive regulator

SNAI1 is a known regulator of EMT and was shown to correlate with the susceptibility to NK cells (Figure 17). The RPPA data were confirmed by mRNA expression levels, which also correlate with NK cell killing (Figure 24). The here presented result that SNAI1 expression increases NK cell-mediated killing is supported by the findings of (Lopez-Soto et al., 2013). They overexpressed SNAI1 in HT29M6 colon cancer cells and could observe an upregulation of NKG2D ligands (mainly MICA/MICB and ULBP2/3). This increase in activating ligands also resulted in enhanced NK cell-mediated killing of these colon cancer cells. However, the authors failed to examine the mechanism by which SNAI1 upregulation alters cancer cell susceptibility towards NK cells. Moreover, it was shown that upregulation of SNAI1 represses the E-cadherin expression in melanoma (Poser et al., 2001). E-cadherin is mainly expressed in melanocytes and primary melanoma cell lines, whereas invasive metastatic melanoma cell lines lack it *in vitro* (Danen et al., 1996). The loss of E-cadherin is often accompanied by the gain of N-cadherin in melanoma (Hao et al., 2012; Lade-Keller et al., 2013; Marcelina et al., 2016). This so called 'cadherin switch' was shown to be associated with tumour progression (Yan et al., 2016) and enhanced invasion potential (Ciolczyk-Wierzbicka and Laidler, 2018; Li et al., 2001; Molina-Ortiz et al., 2009). E-cadherin is a known ligand for the inhibitory killer cell lectin-like receptor subfamily G member 1 (KLRG1) (Ito et al., 2006; Li et al., 2009). Therefore, a decreased E-cadherin expression should increase the NK cell activation threshold and protect melanoma cells against NK cells. This is in line with the study of (Shields et al., 2018) showing that exogenously expressed E-cadherin in a B16F10 melanoma mouse model enhanced melanoma immune surveillance and caused a higher susceptibility to immune checkpoint blockade therapies. In addition, the induction of EMT in lung cancer promoted the susceptibility to NK cell-mediated cytotoxicity (Chockley et al., 2018). The authors provide evidence that this is mainly caused by the downregulation of the KRLG1 ligand E-cadherin, but not by the observed increased expression of NKG2D ligands. Although EMT contributes to a metastatic phenotype (Alonso et al., 2007; Kudo-Saito et al., 2009) and a poor prognosis (Aruga et al., 2018; Yan et al., 2016), the susceptibility of melanoma cells with intrinsically higher mesenchymal properties to NK cells was increased (Figure 43). The *SNAI1* expression in melanoma was associated with NKiToxMel (Figure 24). Only WM3918 showed low *SNAI1* levels despite its high susceptibility. This is in line with its observed low invasive potential (Ma et al., 2011). As a transcription factor, the function of Snail is not restricted to inducing EMT. SNAI1 was shown to play an important role in the energy metabolism. Although SNAI1 suppressed aerobic glycolysis in breast cancer cells by repression of phosphofructokinase-1 and can act as metabolic switch to pentose phosphate pathway (Kim et al., 2017), it enhanced glycolysis during EMT in gastric cancer (Yu et al., 2017).

Furthermore, it should be noted that NK cells are able to kill cancer cells with cancer stem cell (CSC) characteristics (Ames et al., 2015; Pietra et al., 2009; Sultan et al., 2017) this was often associated with EMT (Liu and Fan, 2015; Singh and Settleman, 2010). Hence, NK cell based immunotherapy targeting of CSC might prevent tumour relapse and metastasis (Luna et al., 2017; Melaiu et al., 2019).

5.7 Susceptibility of melanoma cells towards NK-92 killing shows heterogeneity similar to primary NK cell killing

The NK cell line NK-92 revealed a lower cytotoxicity against melanoma cells in comparison to primary NK cells (Figure 26). Responsible for this difference is most likely the receptor profile of the cell line. Although NK-92 cells express several important activating receptors, including NKG2D, NKp30 and NKp46, other activating receptors such as NKp44 and CD16 are absent (Klingemann et al., 2016). In addition, the cell line NK-92 lacks most KIR receptors (with exception of KIR2DL4) (Suck et al., 2016). However, the cytotoxic potential seems to be determined by a repertoire of activating receptors. The relative cytotoxicity of primary NK cells and NK-92 cells against the cancer cell lines showed similar heterogeneity. These observations support the hypothesis that the heterogeneous susceptibility of melanoma to NK cells is not determined by the amount of MHC class I molecule on the melanoma cell surface. However, the NK-92 cell line shows the expression of the inhibitory receptor CD94/NKG2A (Suck et al., 2016). This receptor specifically binds to HLA-E, a non-classical MHC class I molecule (Brooks et al., 1999; Lee et al., 1998), that is also expressed by melanoma cells (Derre et al., 2006). Despite the lower cytotoxicity of NK-92, the susceptibility of melanoma cells to NK-92 strongly correlated to the data obtained with primary NK cells (Figure 26). Therefore, additional RPPA analysis with nine melanoma cell lines that were killed by NK-92, would support the identification of a universal protein signature that determines the melanoma cell phenotype and hence susceptibility to NK cells killing.

Although the melanoma NK-92 killing signature lacks some proteins of the protein signature correlating with primary NK cell killing, the top regulators SNAI1 and DIABLO as well as several other proteins were present in both signatures. A closer look at the additional identified proteins supports the previously described melanoma cell phenotype susceptible to NK cell killing. Melanoma cells with mesenchymal properties were more susceptible to NK cell killing. In addition to **SNAI1**, a potent EMT inducer (Kaufhold and Bonavida, 2014), also other proteins involved in EMT were identified as positive regulators of the NK 92-induced cytotoxicity against melanoma cells. **XBP1**, a transcription factor that promotes cell proliferation and tumour

progression in several cancers including melanoma was identified (Chen and Zhang, 2017; Shi et al., 2019). XBP1 is known to induce SNAI1 expression and hence promoting EMT resulting in increased cancer invasion and metastasis (Li et al., 2015b; Shi et al., 2019). In addition, XBP1 expression correlated with an upregulation of PI3K-mTOR signalling (Yang et al., 2015), which is also reflected in the protein signature by the activated ribosomal S6 protein kinases (**RPS6KB1** and **RPS6K**, also known as p70S6 kinase). Furthermore, phosphatidylinositol 3-kinase regulatory subunit alpha also referred as p85 alpha (**PIK3R1)** was identified as a negative regulator of NKiToxMel. PIK3R1 is a tumour suppressor gene that binds and stabilizes p110, the catalytic subunit of PI3K, hence maintaining PI3K in an inactive conformation (Cheung and Mills, 2016; Vallejo-Diaz et al., 2019) until growth factor stimulation activates it. PIK3R1 is frequently mutated in cancer and was shown to promote cell survival and proliferation (Jaiswal et al., 2009; Urick et al., 2011). This would explain why PIK3R1 was found to be upregulated in melanoma (Aziz et al., 2009) Another EMT inducer that is activated by MAPK and PI3K-AKT signalling, is the Y-box-binding protein 1 (**YBX1**) (Kosnopfel et al., 2018). The expression of YBXI is increased during melanoma progression and its nuclear localisation is associated with invasive and metastatic potential in melanoma (Schittek et al., 2007; Sinnberg et al., 2012). Transglutaminase (**TGM2**) is a transpeptidase that functions as a signal transducer and regulates extracellular matrix stability and cell adhesion (Akimov et al., 2000; Menter et al., 1991). In melanoma, higher levels of TGM2 were positively linked to tumour growth (Kozlowska et al., 1991) and metastasis (Fok et al., 2006; van Groningen et al., 1995; Xu et al., 2006). TGM2 was shown to activate PI3K-AKT signalling that leads to a SNAI1 induced EMT (Lin et al., 2011). Furthermore, TGM2 is involved in self-renewal (Eckert et al., 2015; Kang et al., 2018), chemoresistance (Verma and Mehta, 2007) and induces the activation of epidermal growth factor receptor (**EGFR**) (Eom et al., 2014) that was also identified as a positive regulator of NKiToxMel. EGFR transcription is additionally induced by YBX1(Stratford et al., 2007). EGFR is a growth-factor-receptor tyrosine kinase that positively regulates cell proliferation and survival after binding of EGFR (Herbst, 2004). In cancer, it is often associated with poor patient's survival (Nicholson et al., 2001), so that EGFR signalling was targeted in cancer therapy by specific monoclonal antibodies such as cetuximab or tyrosine inhibitors such as gefitinib (Seshacharyulu et al., 2012). Although EGFR is also involved in melanoma progression and metastasis, its prognostic significance in melanoma could not be validated (Boone et al., 2011). Its activation was shown to be associated with increased activation of AKT-PI3K-mTOR signalling and other pro-oncogenic signalling pathways (Wee and Wang, 2017). Moreover, it was shown to promote aerobic glycolysis (Lim et al., 2016b; Makinoshima et al., 2014) and initiate G1/S cell cycle progression (Baker and Yu, 2001; Lo and Hung, 2006). Cyclin-dependent kinase inhibitor 1B (**CDKN1B**) is another cell

cycle-related protein that is part of the melanoma NK-92 killing signature as well. CDKN1B is a tumour suppressor that arrest G1 cell cycle progression by binding to cyclin E-CDK2 or cyclin D-CDK4 complexes (Besson et al., 2008). However, elevated CDKN1B levels correlated with tumour progression in melanoma (Sanki et al., 2007). This can be explained by its dominant cytoplasmic localisation in melanoma (Chen et al., 2011; Denicourt et al., 2007) that increases migration potential and hence promotes metastasis (Wu et al., 2006). The cytoplasmic localisation seems to be determined by protein phosphorylation of CDKN1B tyrosine residues T157 and T198 (Larrea et al., 2009; Wander et al., 2011) and was regulated and stabilised by kinases such as RAS (Liu et al., 2000), AKT (Viglietto et al., 2002) and **MEK1** (Cheng et al., 1998). The dual specificity mitogen-activated protein kinase kinase 1 (MEK1) is not only associated with tumourigenesis (Govindarajan et al., 2003) but also part of the RAS-RAF pathway that was shown to be highly activated in melanoma (Davies et al., 2002).

Phosphorylated PEA15 (S116) showed the highest positive correlation to the NK-92-mediated killing. In contrast to its known tumour suppressor functions, the phosphorylation of PEA-15 has shown to increase MAPK signalling by allowing nuclear translocation of ERK (Mace et al., 2013). This tumour promoting function is further supported by its binding to FADD and by preventing the DISC assembly, thereby inhibiting apoptotic signalling (Sulzmaier et al., 2012). Furthermore, it was shown that PEA-15 and hexokinase 2, which is also highly correlated to the killing, act together as sensors of metabolic state determining cell fate (Mergenthaler et al., 2012).

The NK-92 derived killing signature also contains proteins involved in regulation of apoptosis. In addition to DIABLO, **BCL-2**, member of the anti-apoptotic Bcl-2 subfamily, is highly expressed in melanoma and shows the highest average expression for any cancer type other than leukemia (Placzek et al., 2010). How BCL-2 levels correlate with melanoma progression and metastasis is controversially discussed (Anvekar et al., 2011). Nevertheless, many studies are in line with our findings that BCL-2 expression decreases during melanoma progression (Divito et al., 2004; Saenz-Santamaria et al., 1994; van den Oord et al., 1994; Vlaykova et al., 2002). Although BCL-2 inhibits apoptosis initiation, the expression of BCL-2 alone does not determine the apoptotic threshold of the target cells. In addition, other pro-apoptotic as well as anti-apoptotic Bcl-2 family members regulate this process. In this regard, it was shown that BAX/BCL-2 ratio determines the susceptibility of human melanoma cells to CD95/Fas-mediated apoptosis (Raisova et al., 2001). Besides its role in apoptosis, BCL-2 was also shown to be involved in calcium homeostasis regulation (Bonneau et al., 2013). Another player in the NK-92 cell-mediated killing was the major stress-induced chaperone **HSP70.** It has been shown to be overexpressed in many cancers, including melanoma (Farkas et al., 2003; Sherman and Gabai,

2015). Its role in cancer progression seems to be dependent on the cancer type. In melanoma, the expression of HSP70 was associated with improved survival (Ricaniadis et al., 2001). This can be explained by an increased NK cell activity against HSP70 expressing and releasing tumours (Botzler et al., 1998; Elsner et al., 2007). However, the immune supporting effect was limited to tumour cells expressing NKG2D ligands (Elsner et al., 2007). These results seem to contradict our findings were melanoma cells with lower HSP70 were better NK cell targets. However, this expression pattern might be the result of the immunoediting process in the melanoma patients. The melanoma cell lines that were used in this study were established from patients at distinct melanoma stages. Melanoma cells that form distant metastasis have already evaded immune response and may express lower HSP70 level than the primary tumour. Besides its direct role in immune surveillance, HSP70 is involved in controlling the energy metabolism. To this end, overexpression of HSP70 in HeLa cells shifted the energy metabolism from (OXPHOS) to glycolysis (Wang et al., 2012). However, the results of (Leu et al., 2017) in melanoma cells draw the opposite picture. The treatment of melanoma cells with HSP70 inhibitors impaired OXPHOS accompanied by lowered oxygen consumption rate as well as adenosine triphosphate (ATP) production and reduced mitochondrial membrane potential (Leu et al., 2017). Furthermore, there is evidence that HSP70 silencing enhances metastatic potential by deregulation of E-cadherin expression and acquired a mesenchymal-like-phenotype (Kasioumi et al., 2019). However, it was also shown that HSP70 is overexpressed in metastatic melanoma and supports tumour progression by promoting FAK dependent invasion (Budina-Kolomets et al., 2016). Beside DIABLO, the most important negative regulator of the NK-92-mediated killing is **DVL3**. The dishevelled proteins are involved in the Wnt signalling pathway by preventing beta-catenin degradation in the cytoplasma (Kafka et al., 2014). This allows accumulation of beta-catenin and induction of EMT by upregulation of SNAI1 and SLUG (Gasior et al., 2017). Thus, the decreased expression of DVL3 would counteract the other EMT inducer. However, Dvl proteins, in particular DVL3, are also part of the non- canonical Wnt signalling and were shown to activate JNK (Li et al., 1999; Zhao et al., 2010b) that was shown to support cell survival and proliferation in melanoma (Alexaki et al., 2008; Jorgensen et al., 2006).

Although the identified proteins of the RPPA analysis of NK-92 cells were not completely identical to melanoma killing signature (primary NK cells), both analysis revealed a similar melanoma phenotype that determine susceptibility to these effector cells.

5.8 Inhibition of the PI3K-AKT-mTOR signalling pathway decreases melanoma susceptibility to NK cells

The melanoma killing signature only considers the relative protein abundance and its influence on the NK cell-mediated killing of melanoma cells. Furthermore, focusing on individual proteins neglect the synergistic effects of several proteins involved in pathways resulting in the same melanoma phenotype.

The PI3K-AKT-mTOR pathway is a highly regulated intracellular signalling pathway controlling cell cycle, cell survival/apoptosis as well as protein biosynthesis (Fingar and Blenis, 2004; Saxton and Sabatini, 2017). The RPPA analysis revealed that the PI3K-AKT-mTOR pathway might play an important role in the susceptibility of melanoma cells towards NK cell killing. Its central role in cell survival, proliferation and cell metabolism makes it an attractive target for cancer therapy (Porta et al., 2014). Therefore, many drugs were developed to target this pathway in cancer cells. In this study, several of these drug inhibitors were used to test the role of PI3K-AKT-mTOR signalling in the NKiToxMel.

Rapamycin is one of the first inhibitors known to inhibit mTORC1specifically (Benjamin et al., 2011). Rapamycin treatment of melanoma was shown to decrease melanoma cell proliferation (Bundscherer et al., 2008; Ciolczyk-Wierzbicka and Laidler, 2018) as well as invasive potential (Ciolczyk-Wierzbicka et al., 2020; Yang et al., 2010). However, the melanoma proliferation even at concentrations higher than 5 nM was only reduced by about 20 % (Lasithiotakis et al., 2008). This is in line with the observed reduction in WM3734 cell viability of maximum 23 % after treatment with 2.5-20 nM rapamycin (Figure 29). Nevertheless, rapamycin in the used concentrations were shown to diminish melanoma cell proliferation and metastatic potential (Molhoek et al., 2005; Rosenberg et al., 2015).

The treatment with rapamycin decreased susceptibility of WM3734 cells and 1205Lu cells to NK cells significantly after 24 h. That this effect was even more pronounced after a longer treatment period, might be caused by an additional inhibition of mTORC2 assembly, which was observed in other cancer cell lines (Sarbassov et al., 2006). According to the RPPA data, 1205Lu cells should have a higher PI3K-AKT-mTOR pathway activity than WM3734 cells. Therefore, it is reasonable that the effect of rapamycin treatment in 1205Lu is more dominant.

MK2206 is a known allosteric pan AKT inhibitor that inhibits AKT phosphorylation in a non-ATP competitive manner (Nitulescu et al., 2016). The usage of MK2206 showed promising clinical effects in combination with other cytotoxic and targeted therapies in advanced solid tumours, whereas monotherapy mainly failed (Molife et al., 2014; Xing et al., 2019). MK2206

inhibits AKT activity in multiple cancer cell lines, but the downstream effects differed a lot depending on the concentration and the targeted cell line. Effective inhibition of invasion and migration of glioblastoma cells was only observed at MK2206 concentrations higher than 5 μM, whereby 1 μM already reduced AKT activity (Narayan et al., 2017). In endometrial cancer cells, already 1 μM significantly decreased invasion (Winder et al., 2017). Also glycolytic metabolic effects by the decrease in glutamate and increase in glucose were more pronounced after MK2206 treatment with higher concentrations (3-5 μM) in human colorectal and prostate carcinoma (Al-Saffar et al., 2018). The reduced expression levels of glycolytic enzymes including hexokinase II (HK2) and lactate dehydrogenase alpha (LDHA) after MK2206 treatment explained the metabolic changes in these experimental settings. In addition, 5 μM MK2206 represses colorectal cancer-initiating stem cells (Malkomes et al., 2016). In melanoma, different cell lines were susceptible to concentrations above 300 nM after 24 h treatment (Rebecca et al., 2014). Nevertheless, cell growth and survival were rather not affected at concentrations lower than 1 μM. These findings are in line with the low toxicity in the investigated melanoma cell line (Figure 29). However, MK2206 significantly reduced the susceptibility of 1205Lu cells to NK cells (Figure 31G-L), which might be caused by the mutational status of this cell line. 1205Lu cell line has a deletion of PTEN. Given that PTEN is inhibiting the PI3K-AKT-mTOR pathway, PTEN loss would lead to the hyperactivation of this pathway (Carracedo and Pandolfi, 2008). Since other additional pathways feeding PI3K-AKT-mTOR signalling are less active, MK2206 and other drug inhibitors may have a stronger effect on 1205Lu cells. Interestingly, the susceptibility of WM3734 cells was not altered following MK2206 treatment. The PTEN status of WM3734 cell line is not known. Nevertheless, an active PTEN as well as other redundant signalling ways can lead to mTOR activation. WM3734 cells might rely less on AKT activity and can compensate the inhibition by MK2206 better. Accordingly, longer incubation of WM3734 cells with MK2206 even increased their susceptibility to NK cells after 2 h. AKT is a kinase with many substrates, thereby influencing distinct cellular mechanisms such as apoptosis. Activated AKT phosphorylates and inhibits the pro-apoptotic proteins such as BAD, thereby preventing the initiation of apoptosis (del Peso et al., 1997). MK2206 inhibits this anti-apoptotic function and can lower the apoptosis threshold of the melanoma cells. Since the two cell lines 1205Lu and WM3734 have distinct expression levels of proteins involved in apoptosis, this pro-apoptotic effect of the drug inhibitor influences the melanoma cell lines to a different extent.

PI3K inhibitors can be used for inhibiting the pathway upstream of AKT and mTOR. The pan PI3K inhibitor BKM120 exhibited strong cytotoxic effects on different tumour cell lines, including melanoma cells (Aasen et al., 2019; Hu et al., 2015; Koul et al., 2012; Niessner et al., 2016). Already 1 μM decreased cell viability of WM3734 cells after 48 h (Figure 31). Similar to

MK2206, also BKM120 decreased the susceptibility of melanoma cell lines to NK cells. However, the effects were stronger after 72 h of treatment, which might be caused by the high redundancy of neighboring pathways feeding the PI3K-AKT-mTOR signalling even after blocking of PI3K. Similar to MK2206 also BKM120 (1-2 μM) decreased the cell migration and invasion potential in glioblastoma cells and melanoma (Aasen et al., 2019; Speranza et al., 2016). Moreover, this drug also eliminated the stem cell subpopulation of breast cancer cells (Hu et al., 2015) and modulated the metabolic phenotype of AML cells to reduced basal glycolysis and glycolytic capacity (Allegretti et al., 2015).

The used inhibitors affect not only cancer cells but could also diminish NK cell cytotoxicity. Although residual drug concentration during the cytotoxicity experiments is negligibly low, possible negative side-effects on NK cells were experimentally excluded. The acute addition of 2.5 nM rapamycin in the assay did not decrease the susceptibility of the non-pretreated melanoma cell lines WM3734 and 1205Lu to NK cells (Figure 33 A+B). In addition, the killing of rapamycin pre-treated K562 was even slightly accelerated, which would contradict the assumption of an effective inhibition of NK cells by remaining or released drug inhibitor (Figure 32). These results are in agreement with the observations of Yang and colleagues showing that 4 h treatment with a relatively high concentration of 100 nM rapamycin did not impair NK cell cytotoxicity to sensitive target cells (Yang et al., 2018). On the contrary, rapamycin has shown to restore NK cell cytotoxicity in patients suffering from primary immunodeficiencies caused by PI3K110 delta mutations (Ruiz-Garcia et al., 2018). Since MK2206 pre-treatment enhanced NK cell cytotoxicity against WM3734 (Figure 31 D-F), inhibitory effects of MK2206 on NK cells during the killing can be excluded. This conclusion is further supported by the observation that only the NK cell-mediated killing of non-treated WM3734 was affected in the presence of 1 μM MK2206 (Figure 33 C+D). Nevertheless, MK2206 in concentrations of 1 μM and higher can affect cell proliferation of distinct immune cell populations (Abu-Eid et al., 2014; Ding et al., 2014). Further information about the effect of MK2206 on NK cell functionality are not available. BKM120 during the assay lowered the NK cell-mediated killing of non-treated and drug pre-treated WM3734 (Figure 33 E+F). Therefore, it seems to be likely that 1 μM BKM120 also inhibits NK cell function. It was shown that other PI3K inhibitors suppressed the movement of lytic granules to the immunological synapse and hence tumour lysis mediated by NK-92 (Jiang et al., 2000; Yea et al., 2014). However, the expected concentration during the killing assay should be dramatically lower. Furthermore, an impaired NK cell cytotoxicity alone would not explain the considerably reduced NK cell-mediated killing BKM120 pre-treated WM3734 cells in comparison to non-treated melanoma cells Figure 33 E+F).

In sum, targeting the PI3K-AKT-mTOR pathway with drug inhibitors reduced the susceptibility of melanoma cells towards NK cell killing. The usage of drugs inhibiting PI3K or mTOR was shown to alter the ligand expression profile on cancer cells. Rapamycin treatment decreased the surface expression of MICA in K562 (Boissel et al., 2006) and MICA/B as well as ULBPs in acute myeloid leukemia (Zhu et al., 2019). In addition, LY294002, another PI3K inhibitor, inhibited the expression of MICA/B in several breast cancer cell lines (Okita et al., 2012) as well as the expression of PD-L1 in prostate cancer cells (Xu et al., 2018a). Furthermore, the inhibition of mTOR also induced alterations in the MHC I immunopeptidome as 13 % of the MHC I-associated peptides were significantly overexpressed after rapamycin treatment (Fortier et al., 2007). Besides these direct effects on the ligand profile, the used drug inhibitors were shown to induce a cancer phenotype that was characterised by decreased migratory and invasive potential as well as lower glycolytic capacity. This is in line with the RPPA analysis, which revealed melanoma cells with more epithelial properties and lower glycolytic activity to be less susceptible to NK cells.

5.9 Melanoma-NK cell-co-cultures

Although natural killer cells have shown often promising success in many *in-vitro* studies, NK cell based immunotherapies are still not extensively used in clinical practice. One of the difficulties is the underestimation of reciprocal cell interactions and the development of therapy resistance. The establishment and further characterisation of melanoma co-cultures with primary NK cells and NK-92 allowed the investigation of NK cell -immune evasion of melanoma.

5.9.1 NK cell susceptibility of melanoma cells after co-culturing with NK cells

Melanoma cells co-cultured with primary NK cells or NK-92 cells were less susceptible to NK cells. This adaption correlated with increasing E:T ratio and the duration of the melanoma-NK cells-co-culture (Figure 36 and Figure 38). Similar results have been reported by (Balsamo et al., 2012), where the magnitude of NK cell resistance in melanoma increased with higher E:T ratio. Moreover, the authors observed an increase of classical (HLA A,B,C) and non-classical (HLA E,G) MHC class I molecules as well as the downregulation of MICA on melanoma cells co-cultured with NK cells for 2 days. These adaptions lowered the activation threshold of the NK cells as the effector cells receive enhanced inhibitory signals and decreased activating stimuli at the same time. The lower expression of MICA could be caused either by a complete downregulation or by shedding of these ligands. Notably, the authors showed that the ligand shedding promotes downregulation of the NKG2D receptor (Casado et al., 2009) and provided

an explanation why soluble MICA and ULBP2 are associated with poor prognosis and tumour progression (Paschen et al., 2014). The observed alterations in the ligand profile together with associated NK cell susceptibility of melanoma were completely reversible in absence of NK cells (Balsamo et al., 2012). Therefore, it can be assumed, that the acquired resistance during co-culture is most likely not caused by a selection process, but rather through an adaption of melanoma cells against NK cell cytotoxicity. However, longer co-culture periods reduced the susceptibility of the untreated WM3734 control as well. A high grade of genetic instability of cancer cells (Hanahan and Weinberg, 2011) could lead to mutation enrichment and hence an altered ligand profile of melanoma cells.

NK-92 cells, similarly as the primary NK cells, induced NK cell resistance in melanoma cells in a dose-dependent manner (Figure 38). In the absence of NK-92, the melanoma cell susceptibility recovered almost completely after 3 days. The reduced susceptibility was already detectable 24 h after co-culturing with NK-92 cells (Figure 39). Interestingly, melanoma co-cultured with NK-92 also induced a partial cross-resistance to primary NK cells (Figure 40). This finding indicated that co-culturing induces general molecular changes in melanoma cells that will affect the susceptibility to NK-92 as well as primary NK cells. In comparison to primary NK cells, NK-92 have a different receptor profile (less KIR receptors) as well as a lower cytotoxicity against melanoma. Therefore, the adaption to NK-92 might differ and hence may affect the melanoma killing mediated by primary NK cells to a lower level.

During the co-culture process, melanoma cells experienced an EMT-induced phenotype switch that mediates resistance to NK cells (Huergo-Zapico et al., 2018; Terry et al., 2017). This process was dependent on cell-to-cell interactions, receptor-ligand engagement as well as cytokine release. Key cytokine in this process is melanoma cell secreted cytokine TGF-β a known potent inducer of EMT (Xu et al., 2009). Although TGF-β induced EMT resulted in melanoma cells with mesenchymal properties (Huergo-Zapico et al., 2018), this TGF-β mediated melanoma phenotype did not correlate with a higher NK cell score. This can be explained by the inhibitory effect of TGF-β on NK cells. Melanoma secreted TGF-β caused a downregulation of NKG2D (Morgado et al., 2011) and inhibited the IL-2 induced upregulation of NKp30 and NKp44 (Pietra et al., 2012a) on NK cells. These phenotype changes have also been observed in melanoma progression in patients (da Silva et al., 2014). These exhausted NK cells were characterised by higher levels of inhibitory receptors (KIR3DL1 and KIR2DL3) and lower levels of activating receptors (NKG2D, NKp46, and DNAM-1) (da Silva et al., 2014). Without the inhibitory effects of TGF-β on NK cells, EMT-induced mesenchymal cells might enhance NK cell killing (Chockley and Keshamouni, 2016; Okita et al., 2018) and support the previous hypothesis that

melanoma cells with more mesenchymal properties (Figure 43) are more susceptible to NK cell killing.

Although the mode of killing is not further analysed in this thesis, several studies reported that melanoma cells, which failed to undergo complete apoptosis have a distinct phenotype. They gained invasiveness and migratory potential *in vitro* and *in vivo* (Berthenet et al., 2019). However, in the cited study apoptosis was induced by doxycycline and can probably not be comparable with cell-mediated apoptosis. Furthermore, it was shown that apoptosis reversal promoted cancer stem cell formation (Xu et al., 2018b).

Furthermore, it should be noted that soluble factors released by NK cells additionally affect the melanoma cell secretome and NK cell ligand profile. During the co-culture process, activated NK cells release IFN-γ that induces the secretion of IDO and PEG2 by melanoma cells and enhance the downregulation of activating receptors (Pietra et al., 2012a). In addition, IFN-γ showed a pro-tumour effect by increasing the expression of HLA-E in melanoma (Derre et al., 2006) and MHC class I and II molecules as well as PD-L1 in other cancers (Castro et al., 2018). These effects might contribute to the observed reduced melanoma susceptibility to NK cells after melanoma-NK cell co-culture.

5.9.2 RNA sequencing

RNA sequencing of melanoma cells co-cultured with primary NK cells or NK-92 cells revealed around 100 genes that were differentially expressed in both co-cultures compared to the control. However, only a small number of genes showed significantly different expression in both data sets. Interestingly, WM3734 cells co-cultured with NK-92 cells showed higher (~4 times) fold changes than WM3734 cells co-cultured with primary NK cells. The invariable cytotoxicity of the NK cell line in contrast to changing primary NK cell donors allows a more specific adaption to this cell line and might cause the higher fold-changes.

Most of the hits presented in Table 23 (marked in bold) are associated to the antigen-presenting machinery. After co-culturing, melanoma cells expressed more **beta-2-microglobulin,** which is a component of the MHC class I molecules (Wieczorek et al., 2017) and was shown to be associated with poor prognosis(Cursons et al., 2019). Moreover, **HLA-B** as a MHC class I molecule showed an increased gene expression, although the NK cell receptor KIR3DL1 responsible for HLA-B detection is only poorly expressed on NK-92 (Tao et al., 2014). The majority of melanoma cell lines (67 %) have alterations in the surface expression of HLA class I molecules. In particular HLA B is most frequently downregulated (35 %) in melanoma (Mendez

et al., 2009). These adaptions allow the evasion of T-cell recognition and hence ensure melanoma persistence. However, during the performed melanoma NK cell co-cultures, additional MHC class I molecules protect the melanoma cells against NK cell recognition, so that their upregulation increases the NK cell resistance. In addition to HLA-B, **HCP5**, a long non-coding RNA with retroviral origin and located centromeric of the HLA-B gene, was increased after co-culturing. Although HCP5 is not coding for a protein, it was shown to have regulatory functions that might render tumour malignancy (Kulski, 2019; Wei et al., 2019b). The upregulation of these three MHC class I related proteins might be a result of continuous IFN-γ exposure mediated by activated and killing NK cells (Castro et al., 2018; Mendez et al., 2009). In addition, genes involved in IFN-γ signalling and the antigen presentation machinery showed strongest suppression of NK cell killing (Freeman et al., 2019).

Even more dominant was the upregulation of **MHC class II molecules** in both co-cultures (Table 23). Less than 20 % of melanoma cells have constitutive expression of MHC class II molecules, which more than doubled (48.5 %) after IFN-γ treatment (Mendez et al., 2009). Although MHC class II molecules are shown to induce immune suppressive cytokines such as IL-10, the presence of MHC class II molecules in melanoma was associated with increased patient survival (Chen et al., 2019b; Johnson et al., 2016; Mendez et al., 2009). This is in line with the finding that some HLA-DP molecules are ligands for NKp44 and can activate NK cells (Niehrs and Altfeld, 2020). In contrast, **HLA-DR**-mediated signalling increased the migration and invasion of melanoma cells (Costantini and Barbieri, 2017). This is in agreement with the upregulation of the **complement component C1S** after co-culture (Table 23), which was also shown to be associated with the increased cell density and status of the mesenchymal marker ALCAM (activated leukocyte cell adhesion molecule) (van Kilsdonk et al., 2012). Also **TMEM158**, a transmembrane protein, was posivtively correlated to cell adhesion molecules and hence involved in invasivness of ovarian cancer cells (Cheng et al., 2015). Moreover, TMEM158 was found to be overexpressed in metastatic melanoma (Eriksson et al., 2016). In contrast, **absent in melanoma 2** (AIM2) is found predominatly in primary melanoma, whereas metastases often lack this protein (de Koning et al., 2014). Restoration of AIM2 was shown to promote an invasive phenotype of colorectal cancer (Patsos et al., 2010). In addition, AIM2-mediated IFN-γ dependent and independent MHC class II expression in this cancer type (Lee et al., 2012). The upregulation of AIM2 during the co-culture process might mediate the increase of MHC II molecules on the melanoma cell surface. This can be detected by NK cells and might raise their activation treshold. This assumption is in line with the observed lower susceptibility of HLA-DR1 transfected K562 to PBMCs and to a NK cell line (Jiang et al., 1996).

Together with the results from this study, the upregulation of MHC class II molecules seem to be involved in the immune escape process of melanoma and could be not only favourable for patient's survival.

5.10 Concluding remarks

Despite the recent advances in treating malignant melanoma, new and improved therapeutic approaches are needed in order to curb the disease. Natural killer cells are a promising tool for melanoma immunotherapy since melanoma cells with mesenchymal phenotype show high immunogenicity. This study not only provides a tool to predict the efficiency of NK cell-induced cytotoxicity of melanoma cells; it also reveals EMT and PI3K-AKT-mTOR signalling as important pathways involved in this immunogenic phenotype. Future therapeutic approaches with NK cells should not only target the maintenance of this phenotype by pharmacological manipulation but also the tumour microenvironment to prevent NK cell resistance and impaired NK cell cytotoxicity. Leading strategies might be the ACT of allogeneic or autologous pre-activated primary NK cells as well as NK cell lines or pluripotent stem cell-derived NK cells. Furthermore, combination therapy with CTLs and NK cells could mimic a functional immunosurveillance and lead to tumour clearance.

Appendix

Supplemental table 1. DGE analysis of WM3734 after co-culturing with primary NK cells. LogFC is the log fold-change that describes how strong a gene is over- (positive values) or under- (negative values) expressed after co-culturing with primary NK cells. The LogCPM are the log counts per million and is a measure for the gene expression level. Statistical significance is indicated by p-value and FDR (false discovery rate).

Gene	logFC	logCPM	p-value	FDR
POC1B-GALNT4	9.39	0.32	2.06E-18	2.85E-14
TBC1D3F	7.05	-1.30	8.67E-09	1.37E-05
DAPL1	7.02	-1.42	1.82E-05	9.37E-03
AC005280.1	6.15	2.36	9.54E-06	5.46E-03
AIM2	4.45	3.22	1.31E-52	7.27E-48
FAT3	3.53	1.23	4.49E-12	1.78E-08
TDRD6	3.25	-1.29	1.77E-05	9.19E-03
RP11-574K11.31	3.14	-0.32	5.94E-06	3.67E-03
PSKH1	3.00	-0.49	3.64E-10	9.47E-07
HLA-DQA1	2.98	4.76	1.36E-24	2.69E-20
ST8SIA5	2.57	2.96	2.14E-08	2.89E-05
HCP5	2.42	-0.47	9.75E-06	5.52E-03
PNLIPRP3	2.29	1.48	5.81E-09	1.04E-05
TMEM158	2.02	4.12	1.45E-24	2.69E-20
LPHN3	1.94	0.94	2.18E-06	1.51E-03
SEMA3A	1.71	3.29	2.17E-09	4.45E-06
LPAR3	1.70	2.15	9.15E-06	5.29E-03
ADAM19	1.64	3.04	3.76E-10	9.47E-07
MGLL	1.62	4.69	8.31E-07	6.88E-04
AIM1	1.59	2.94	2.46E-08	3.25E-05
SLC16A6	1.57	2.12	6.45E-08	7.61E-05
COL12A1	1.57	3.17	2.43E-12	1.04E-08
GLIPR1	1.56	1.66	1.27E-06	9.80E-04
TXNIP	1.55	1.41	6.15E-06	3.71E-03
KCNMA1	1.55	1.57	4.46E-07	4.19E-04
RP11-221J22.2	1.55	2.72	2.75E-09	5.26E-06
FLT1	1.52	2.55	2.11E-09	4.45E-06
FAM19A3	1.47	1.30	6.04E-06	3.68E-03
C1S	1.42	2.81	2.02E-06	1.42E-03
SPOCD1	1.33	2.77	1.43E-06	1.05E-03
CIITA	1.30	4.06	1.64E-09	3.65E-06
ITIH5	1.29	7.74	5.87E-07	5.17E-04
SPRR2D	1.24	3.82	1.29E-06	9.82E-04
AHNAK2	1.23	2.82	1.30E-05	7.08E-03
NR4A1	1.21	2.53	1.52E-06	1.11E-03
IGFBP5	1.12	6.41	4.19E-07	4.02E-04
MYOZ2	1.12	5.47	1.72E-10	5.60E-07

Gene	logFC	logCPM	p-value	FDR
HLA-DMB	1.11	5.41	7.15E-17	7.92E-13
COL8A1	1.09	3.65	1.18E-06	9.25E-04
HLA-DQB1	1.09	7.04	1.44E-15	1.14E-11
CXCL1	1.01	4.10	8.07E-09	1.32E-05
NRP1	1.01	6.21	1.15E-07	1.30E-04
KYNU	0.99	3.70	3.39E-07	3.42E-04
NLRP1	0.97	3.00	5.95E-06	3.67E-03
SCARA5	0.92	5.05	1.35E-11	4.68E-08
NOV	0.92	5.34	8.50E-06	4.96E-03
HLA-DPA1	0.91	9.32	9.13E-15	6.21E-11
HLA-DRA	0.90	10.37	1.01E-14	6.21E-11
PTN	0.90	6.03	8.46E-06	4.96E-03
HLA-DPB1	0.88	7.30	1.86E-13	1.03E-09
NRCAM	0.83	4.99	5.02E-08	6.07E-05
NPPC	0.82	3.45	6.61E-06	3.94E-03
HLA-DMA	0.80	7.43	6.44E-12	2.38E-08
ZNF689	0.78	5.08	5.05E-06	3.18E-03
HLA-B	0.77	8.47	9.69E-09	1.49E-05
LOXL2	0.77	6.07	1.75E-08	2.43E-05
SLC20A1	0.76	8.10	1.17E-05	6.47E-03
RP11-390P2.4	0.76	5.16	8.07E-09	1.32E-05
CD109	0.75	7.98	2.36E-09	4.68E-06
RNF128	0.75	5.56	1.47E-05	7.94E-03
HLA-DRB1	0.74	8.58	1.20E-08	1.74E-05
FAM133A	0.72	5.67	1.31E-06	9.82E-04
IVNS1ABP	0.72	6.31	6.55E-07	5.68E-04
PITPNC1	0.71	4.89	4.63E-06	2.99E-03
TNC	0.71	8.50	5.04E-08	6.07E-05
MTPN	0.70	8.25	7.82E-07	6.57E-04
ITGA1	0.68	5.27	3.96E-06	2.68E-03
LOXL3	0.66	6.55	4.97E-07	4.52E-04
B2M	0.65	10.71	4.61E-06	2.99E-03
ITGB8	0.65	7.24	7.21E-08	8.33E-05
CD74	0.62	10.74	2.72E-07	2.84E-04
FRMD4A	0.62	7.89	1.22E-05	6.71E-03
FAM216A	0.61	4.53	1.51E-05	8.04E-03
CTSA	-0.52	7.78	1.76E-05	9.19E-03
MGAT1	-0.69	6.13	2.96E-07	3.04E-04
OR2A9P	-0.69	5.18	7.02E-07	5.99E-04
DGCR6	-0.72	4.05	4.63E-06	2.99E-03
KRT18	-0.77	5.47	4.41E-06	2.95E-03
GYPC	-0.89	6.58	5.32E-07	4.75E-04
CERS4	-0.96	2.84	1.89E-05	9.63E-03
BMP7	-0.96	4.83	1.75E-07	1.90E-04
MGAT4A	-1.00	2.67	4.20E-07	4.02E-04

Gene	logFC	logCPM	p-value	FDR
RP11-14N7.2	-1.04	3.90	1.03E-08	1.54E-05
ATOH8	-1.10	3.84	2.28E-07	2.43E-04
CRTAC1	-1.10	3.54	1.56E-05	8.25E-03
PSCA	-1.12	6.72	1.03E-09	2.49E-06
PMEL	-1.16	8.48	3.97E-07	3.93E-04
PRSS33	-1.18	3.97	3.61E-10	9.47E-07
PIK3R2	-1.37	2.34	1.31E-09	3.03E-06
RAPGEF3	-1.39	1.86	4.79E-08	6.04E-05
SPP1	-1.40	6.58	1.01E-06	8.01E-04
EPHX2	-1.44	2.39	3.02E-10	9.31E-07
MAFB	-1.44	2.32	3.67E-10	9.47E-07
EPB41L4B	-1.47	1.44	4.68E-06	2.99E-03
MAGI1	-1.52	3.87	9.44E-07	7.64E-04
BCAN	-1.57	2.45	1.57E-07	1.74E-04
TESC	-1.96	1.64	8.21E-13	3.79E-09
EEF1A2	-2.22	2.72	1.40E-08	1.99E-05
CKMT1B	-2.37	0.93	1.15E-05	6.44E-03
NUP210	-2.42	1.83	3.86E-06	2.64E-03
CLU	-2.47	0.83	6.40E-09	1.11E-05
KCNG4	-2.69	-0.07	1.79E-06	1.27E-03
ZNF382	-2.69	-0.75	4.87E-07	4.50E-04
ILDR2	-3.39	-0.47	1.75E-06	1.26E-03
TMEM132D	-3.39	0.54	4.06E-08	5.23E-05
MYADM	-4.09	4.10	2.98E-09	5.52E-06
ADAMTS12	-4.65	-1.97	9.50E-07	7.64E-04
CTB-43P18.1	-8.12	-1.28	3.57E-13	1.80E-09
AC008964.1	-8.39	-0.99	3.68E-16	3.40E-12

Supplemental table 2. DGE analysis of WM3734 after co-culturing with NK-92 cells. LogFC is the log fold-change that describes how strong a gene is over- (positive values) or under- (negative values) expressed after co-culturing with NK-92 cells. The LogCPM are the log counts per million and is a measure for the gene expression level. Statistical significance is indicated by p-value and FDR (false discovery rate).

Gene	logFC	logCPM	PValue	FDR
TGIF2-C20orf24	12.58	3.24	1.47E-05	0.009114
AC000120.7	10.42	1.09	3.83E-07	0.000354
LGALS17A	9.94	-1.00	4.99E-08	6.24E-05
IER3IP1	9.71	0.64	6.43E-09	1.07E-05
AC004889.1	9.08	0.52	1.50E-09	2.91E-06
IDO1	9.07	3.82	1.96E-09	3.56E-06
CHRNE	9.04	-0.11	1.94E-07	0.000203
HCP5	8.19	1.76	9.79E-12	2.63E-08
HLA-DQA1	7.42	6.86	2.72E-19	1.39E-15
XAF1	7.29	3.39	4.68E-13	1.39E-09

Gene	logFC	logCPM	PValue	FDR
AIM2	6.88	5.02	4.65E-10	1.01E-06
APOL3	6.44	2.22	6.89E-10	1.38E-06
DPH1	6.38	3.60	8.93E-09	1.36E-05
SERPING1	6.00	0.70	9.01E-07	0.000769
GBP1P1	5.84	0.09	2.25E-06	0.001734
SLC15A3	5.57	-0.26	1.16E-06	0.000977
BST2	5.39	3.02	1.54E-06	0.001235
HLA-DOA	5.37	4.15	6.46E-09	1.07E-05
SPATA21	5.36	1.31	5.28E-06	0.003716
APOL1	5.34	5.64	2.03E-17	8.16E-14
IL15RA	4.89	0.63	5.14E-06	0.003662
IFI27	4.82	2.11	1.24E-05	0.007789
C1S	4.79	6.25	6.99E-09	1.12E-05
OAS2	4.73	3.31	1.03E-08	1.53E-05
A2M	4.51	7.20	1.76E-14	5.82E-11
HLA-B	3.97	10.19	4.71E-12	1.33E-08
BATF2	3.85	1.85	2.70E-08	3.53E-05
WARS	3.68	9.47	4.19E-15	1.48E-11
SNRPN	3.47	5.11	2.03E-09	3.58E-06
IRF1	3.46	4.58	7.36E-07	0.000638
ITIH6	3.39	3.00	4.07E-08	5.21E-05
HLA-DQB1	3.27	8.11	2.29E-10	5.15E-07
BOLA2	3.11	4.47	2.40E-07	0.000233
APOL6	3.11	6.52	9.03E-06	0.005917
HLA-F	3.06	4.96	1.85E-08	2.61E-05
RARRES3	3.05	2.47	3.17E-06	0.002351
KIAA1644	3.04	1.52	7.65E-06	0.005188
TAP1	2.94	6.68	7.84E-08	9.48E-05
STAT1	2.78	7.95	1.43E-06	0.001166
TMEM158	2.74	7.23	4.21E-07	0.000377
B2M	2.74	11.77	1.01E-05	0.006459
HLA-DPA1	2.63	9.93	1.35E-06	0.001118
PLA1A	2.62	7.18	7.92E-08	9.48E-05
HLA-DRA	2.49	10.89	2.07E-06	0.001618
HLA-DPB1	2.48	8.23	1.51E-07	0.000165
HLA-DMB	2.47	6.75	4.62E-06	0.003378
CD74	2.42	11.60	1.53E-07	0.000165
HLA-C	2.40	9.49	9.17E-08	0.000105
UBE2L6	2.08	7.40	6.13E-06	0.004258
SNURF	-2.07	6.52	2.91E-07	0.000278
ITFG2	-2.10	5.91	2.23E-07	0.00022
NOMO2	-2.13	3.52	2.62E-06	0.001966
RPLP0P6	-2.22	3.10	8.24E-06	0.005526
RP5-940J5.9	-2.31	8.83	2.12E-07	0.000213
RPS2P46	-2.42	4.01	8.88E-08	0.000104

Gene	logFC	logCPM	PValue	FDR
RPS2P5	-2.48	6.17	1.09E-08	1.57E-05
ACOT1	-2.52	2.87	2.02E-07	0.000206
CEMP1	-2.93	0.92	1.51E-05	0.009212
ABCB5	-3.11	2.77	3.56E-07	0.000334
ST8SIA2	-4.10	-0.70	6.68E-06	0.004589
SLAMF7	-4.20	3.08	3.78E-11	8.87E-08
AP000347.4	-4.26	0.57	2.09E-08	2.87E-05
PMFBP1	-4.94	0.79	2.97E-11	7.28E-08
CTD-2008A1.2	-6.01	2.33	3.05E-19	1.43E-15
WNK2	-6.61	-2.48	9.04E-06	0.005917
CT45A3	-6.99	-1.20	9.83E-06	0.006364
AP003419.16	-7.13	-1.00	4.96E-06	0.00358
RP11-211N8.3	-7.15	-2.43	1.05E-05	0.006618
AL358113.1	-7.33	-1.04	1.73E-06	0.001373
MRAP	-7.55	-1.63	1.55E-07	0.000165
RP11-264B17.5	-8.09	-0.83	9.37E-08	0.000105
AC092299.8	-8.14	-0.81	2.56E-06	0.001949
RP11-504P24.6	-8.23	-1.63	6.79E-07	0.000597
RP1-63M2.6	-8.27	-1.60	4.07E-07	0.00037
CYP4F59P	-8.33	-0.61	2.15E-08	2.88E-05
RP11-62J1.3	-8.61	0.07	4.84E-10	1.01E-06
PCDHGA8	-8.70	-0.19	7.65E-09	1.20E-05
COMMD3-BMI1	-8.88	0.57	1.09E-11	2.79E-08
RP11-498C9.3	-8.92	3.81	3.01E-29	2.83E-25
IDI2	-9.16	0.16	1.72E-09	3.22E-06
RP1-56K13.3	-9.24	0.68	2.25E-13	7.05E-10
RP11-589M4.1	-10.28	1.45	6.87E-16	2.58E-12
RP11-500M8.7	-10.40	1.59	5.55E-18	2.40E-14
RP11-2C24.6	-10.46	1.19	1.62E-19	9.12E-16
NICN1-AS1	-10.68	1.66	1.37E-21	8.58E-18
ATP6V1G2-DDX39B	-11.15	2.23	2.32E-26	1.63E-22
RP11-1100L3.8	-11.23	2.70	6.31E-28	5.08E-24
AC114546.1	-11.45	3.85	4.70E-32	6.62E-28
RP11-624G17.3	-11.85	2.92	1.98E-31	2.23E-27
RP11-1100L3.7	-12.44	3.37	6.05E-35	1.14E-30
AC005786.7	-14.39	5.21	5.27E-60	1.48E-55
RP11-161H23.5	-16.05	7.11	3.14E-79	1.77E-74

Supplemental table 3. DGE analysis of WM3734 after recovering of NK-92-co-culturing . LogFC is the log fold-change that describes how strong a gene is over- (positive values) or under- (negative values) expressed after recovering of co-culturing with NK-92 cells. The LogCPM are the log counts per million and is a measure for the gene expression level. Statistical significance is indicated by p-value and FDR (false discovery rate).

Gene	logFC	logCPM	p-value	FDR
RP11-161H23.5	15.93	7.11	1.08E-81	6.07E-77
AC005786.7	13.88	5.21	9.31E-59	2.62E-54
AC114546.1	13.06	3.85	1.26E-47	2.36E-43
RP11-1100L3.7	12.08	3.37	5.26E-35	7.40E-31
RP11-1100L3.8	11.65	2.70	3.44E-33	3.88E-29
RP11-624G17.3	11.71	2.92	7.25E-33	6.81E-29
RP11-498C9.3	8.29	3.81	7.12E-28	5.73E-24
ATP6V1G2-DDX39B	10.99	2.23	1.46E-27	1.03E-23
CTD-2008A1.2	6.23	2.33	9.44E-23	5.91E-19
NICN1-AS1	10.36	1.66	9.73E-22	5.48E-18
WARS	-3.23	9.47	2.79E-21	1.43E-17
PMFBP1	6.47	0.79	7.74E-20	3.63E-16
RP11-500M8.7	10.40	1.59	1.72E-19	7.43E-16
RP11-2C24.6	9.63	1.19	3.21E-17	1.29E-13
DPH1	-6.87	3.60	2.35E-16	8.82E-13
RP11-589M4.1	10.03	1.45	3.01E-16	1.06E-12
RP1-56K13.3	9.61	0.68	3.96E-16	1.31E-12
COMMD3-BMI1	9.63	0.57	1.34E-15	4.20E-12
APOL1	-3.28	5.64	3.06E-15	9.06E-12
RP4-545K15.3	-5.56	2.21	3.62E-14	1.02E-10
IDO1	-7.41	3.82	5.12E-13	1.37E-09
LGALS17A	-9.94	-1.00	2.17E-12	5.56E-09
RP11-62J1.3	8.90	0.07	6.33E-12	1.55E-08
SNRPN	-2.86	5.11	1.08E-11	2.52E-08
IRF1	-3.50	4.58	2.27E-11	5.11E-08
SPATA21	-7.21	1.31	5.53E-11	1.20E-07
IER3IP1	-9.71	0.64	6.81E-11	1.42E-07
RP11-651P23.4	5.52	0.96	1.41E-10	2.73E-07
NLRC5	-2.61	3.54	1.42E-10	2.73E-07
TAP1	-2.60	6.68	1.46E-10	2.73E-07
A2M	-2.44	7.20	6.25E-10	1.14E-06
BATF2	-3.09	1.85	7.87E-10	1.38E-06
RP11-862L9.3	2.74	3.48	1.92E-09	3.28E-06
IDI2	8.73	0.16	2.67E-09	4.43E-06
RP11-294J22.6	8.48	-0.85	4.30E-09	6.91E-06
RPS2P5	2.25	6.17	5.28E-09	8.26E-06
PCDHGA8	8.39	-0.19	6.93E-09	1.06E-05
CHRNE	-4.78	-0.11	1.34E-08	1.99E-05
AP003419.16	7.90	-1.00	2.13E-08	3.07E-05
AL358113.1	7.78	-1.04	3.63E-08	5.11E-05

Gene	logFC	logCPM	p-value	FDR
CYP4F59P	7.89	-0.61	4.66E-08	6.40E-05
SLC15A3	-4.56	-0.26	4.94E-08	6.62E-05
APOL4	-4.65	0.45	5.81E-08	7.60E-05
CT45A3	7.76	-1.20	6.38E-08	8.16E-05
RPL3P4	-2.49	6.77	7.12E-08	8.91E-05
UBA7	-2.31	2.53	7.76E-08	9.49E-05
MRAP	7.37	-1.63	8.61E-08	0.000103
RPS2P46	2.13	4.01	1.03E-07	0.000121
RARRES3	-2.58	2.47	1.06E-07	0.000122
RTN4RL2	-2.85	2.53	1.30E-07	0.000147
STAT1	-2.22	7.95	1.72E-07	0.00019
PSMB10	-2.00	5.05	1.78E-07	0.000192
RP11-264B17.5	7.66	-0.83	1.81E-07	0.000192
YBX1P10	7.95	-1.09	1.89E-07	0.000193
UBE2L6	-1.81	7.40	1.89E-07	0.000193
RP11-201K10.3	-8.86	0.14	2.59E-07	0.000261
RP11-538I12.2	8.05	-1.27	3.06E-07	0.000302
PSMB8	-1.72	6.51	3.98E-07	0.000387
AK4P1	7.56	-1.63	4.56E-07	0.000435
AP000347.4	3.56	0.57	4.72E-07	0.000443
HLA-B	-1.95	10.19	6.12E-07	0.000561
BGLAP	-4.00	-0.20	6.18E-07	0.000561
SNURF	1.76	6.52	6.34E-07	0.000567
APOL6	-2.51	6.52	9.65E-07	0.000849
APOL3	-3.12	2.22	1.09E-06	0.000946
IFITM1	-3.22	5.23	1.32E-06	0.001127
AC015987.2	14.69	5.25	1.54E-06	0.001293
NUDT4P1	7.26	-1.63	1.69E-06	0.001402
RAD51L3-RFFL	-7.60	-1.24	1.85E-06	0.001514
RP5-940J5.9	1.81	8.83	3.42E-06	0.002752
PIGY	7.25	-2.00	3.47E-06	0.002752
RAC2	5.13	-0.18	3.58E-06	0.002796
NOMO2	1.85	3.52	3.73E-06	0.00288
ACOT1	1.98	2.87	3.79E-06	0.002888
RP11-175K6.1	7.05	-2.06	4.03E-06	0.003022
PTGES3P3	7.16	-1.84	4.18E-06	0.003096
UBD	-7.46	1.46	4.25E-06	0.003109
GBP2	-1.85	4.95	4.56E-06	0.003294
TRIM64EP	-7.26	-1.64	4.85E-06	0.003458
AC000120.7	-4.58	1.09	5.43E-06	0.003819
C1S	-2.48	6.25	5.50E-06	0.003826
RP11-680F20.12	7.37	-1.80	6.11E-06	0.004194
TAPSAR1	-2.20	3.69	7.93E-06	0.005381
MT-ATP8	1.68	6.94	8.84E-06	0.005924
PCDHGB3	6.96	-1.69	9.23E-06	0.006114

Gene	logFC	logCPM	p-value	FDR
TYRP1	-1.62	5.79	9.66E-06	0.006327
MTND2P28	1.67	6.22	1.03E-05	0.006693
PSME2	-1.42	8.29	1.08E-05	0.006875
CTB-63M22.1	-1.96	3.08	1.09E-05	0.006875
HLA-E	-1.46	8.28	1.11E-05	0.006957
PIK3R2	8.50	-0.78	1.16E-05	0.007204
AC083899.3	2.31	1.27	1.21E-05	0.007435
ABCB5	2.38	2.77	1.25E-05	0.007572
IRF9	-1.63	4.65	1.31E-05	0.007755
SRP9P1	2.93	0.15	1.31E-05	0.007755
IL15RA	-3.15	0.63	1.32E-05	0.007764
ZNF770	-1.75	4.27	1.39E-05	0.008078
C1R	-1.65	5.26	1.44E-05	0.008291
AC092299.8	7.38	-0.81	1.46E-05	0.008313
HLA-C	-1.43	9.49	1.54E-05	0.008649
HLA-DQB1	-1.56	8.11	1.60E-05	0.008899
RP11-299G20.2	4.07	0.44	1.63E-05	0.009022

Supplemental table 4. DGE analysis of co-culture-recovered WM3734 compared to CTRL. LogFC is the log fold-change that describes how strong a gene is over- (positive values) or under- (negative values) expressed after recovering of co-culturing with NK-92 cells. The LogCPM are the log counts per million and is a measure for the gene expression level. Statistical significance is indicated by p-value and FDR (false discovery rate).

ID	logFC	logCPM	p-value	FDR
HLA-DQA1	6.56	6.86	1.39E-16	7.81E-12
NAA60	-4.86	0.87	2.34E-10	6.58E-06
AC004889.1	8.72	0.52	8.28E-09	0.000155
ITIH6	3.28	3.00	8.87E-08	0.001047
XAF1	4.91	3.39	9.30E-08	0.001047
HCP5	6.04	1.76	2.68E-07	0.002513
RP11-667K14.4	-8.46	-1.37	3.74E-07	0.003007
RP11-504P24.6	-8.23	-1.63	5.10E-07	0.003072
RP11-286N22.8	8.03	-1.13	5.27E-07	0.003072
RP1-63M2.6	-8.27	-1.60	5.46E-07	0.003072
RP11-201K10.3	-8.88	0.14	7.29E-07	0.00373
RP11-294J22.6	8.48	-0.85	1.81E-06	0.008473

Bibliography

Aasen, S.N., Parajuli, H., Hoang, T., Feng, Z., Stokke, K., Wang, J., Roy, K., Bjerkvig, R., Knappskog, S., and Thorsen, F. (2019). Effective Treatment of Metastatic Melanoma by Combining MAPK and PI3K Signaling Pathway Inhibitors. Int J Mol Sci *20*, 4235.

Abdul-Ghani, M., and Megeney, L.A. (2008). Rehabilitation of a contract killer: caspase-3 directs stem cell differentiation. Cell Stem Cell *2*, 515-516.

Abel, A.M., Yang, C., Thakar, M.S., and Malarkannan, S. (2018). Natural Killer Cells: Development, Maturation, and Clinical Utilization. Front Immunol *9*, 1869.

Abu-Eid, R., Samara, R.N., Ozbun, L., Abdalla, M.Y., Berzofsky, J.A., Friedman, K.M., Mkrtichyan, M., and Khleif, S.N. (2014). Selective inhibition of regulatory T cells by targeting the PI3K-Akt pathway. Cancer Immunol Res *2*, 1080-1089.

Akimov, S.S., Krylov, D., Fleischman, L.F., and Belkin, A.M. (2000). Tissue transglutaminase is an integrin-binding adhesion coreceptor for fibronectin. J Cell Biol *148*, 825-838.

Al-Saffar, N.M.S., Troy, H., Wong Te Fong, A.C., Paravati, R., Jackson, L.E., Gowan, S., Boult, J.K.R., Robinson, S.P., Eccles, S.A., Yap, T.A., *et al.* (2018). Metabolic biomarkers of response to the AKT inhibitor MK-2206 in pre-clinical models of human colorectal and prostate carcinoma. Br J Cancer *119*, 1118-1128.

Alavi, S., Stewart, A.J., Kefford, R.F., Lim, S.Y., Shklovskaya, E., and Rizos, H. (2018). Interferon Signaling Is Frequently Downregulated in Melanoma. Front Immunol *9*, 1414.

Aldrian, S., Trautinger, F., Frohlich, I., Berger, W., Micksche, M., and Kindas-Mugge, I. (2002). Overexpression of Hsp27 affects the metastatic phenotype of human melanoma cells in vitro. Cell Stress Chaperones *7*, 177-185.

Alexaki, V.I., Javelaud, D., and Mauviel, A. (2008). JNK supports survival in melanoma cells by controlling cell cycle arrest and apoptosis. Pigment Cell Melanoma Res *21*, 429-438.

Allegretti, M., Ricciardi, M.R., Licchetta, R., Mirabilii, S., Orecchioni, S., Reggiani, F., Talarico, G., Foa, R., Bertolini, F., Amadori, S., *et al.* (2015). The pan-class I phosphatidyl-inositol-3 kinase inhibitor NVP-BKM120 demonstrates anti-leukemic activity in acute myeloid leukemia. Sci Rep *5*, 18137.

Almeida, F.V., Douglass, S.M., Fane, M.E., and Weeraratna, A.T. (2019). Bad company: Microenvironmentally mediated resistance to targeted therapy in melanoma. Pigment Cell Melanoma Res *32*, 237-247.

Alonso, S.R., Tracey, L., Ortiz, P., Perez-Gomez, B., Palacios, J., Pollan, M., Linares, J., Serrano, S., Saez-Castillo, A.I., Sanchez, L., *et al.* (2007). A high-throughput study in melanoma identifies epithelial-mesenchymal transition as a major determinant of metastasis. Cancer Res *67*, 3450-3460.

American cancer society (2019). Melanoma skin cancer Key statitics. Available from https://www.cancer.org/cancer/melanoma-skin-cancer/about/key-statistics.html (04.04.2019).

American cancer society (2020). Treating melanoma skin cancer. Available from https://www.cancer.org/cancer/melanoma-skin-cancer/treating/by-stage.html (12.03.20).

Ames, E., Canter, R.J., Grossenbacher, S.K., Mac, S., Smith, R.C., Monjazeb, A.M., Chen, M., and Murphy, W.J. (2015). Enhanced targeting of stem-like solid tumor cells with radiation and natural killer cells. Oncoimmunology *4*, e1036212.

Andalib, A., Lawry, J., and Rees, R.c. (2000). Susceptibility of human WM melanoma cell lines to NK and LAK cytotoxicity and their relevance to the level of MHC class I and ICAM-I antigen expression Med J Islam Repub Iran *14*, 155-160.

Anderson, M., Marayati, R., Moffitt, R., and Yeh, J.J. (2017). Hexokinase 2 promotes tumor growth and metastasis by regulating lactate production in pancreatic cancer. Oncotarget *8*, 56081-56094.

Anft, M., Netter, P., Urlaub, D., Prager, I., Schaffner, S., and Watzl, C. (2020). NK cell detachment from target cells is regulated by successful cytotoxicity and influences cytokine production. Cell Mol Immunol *17*, 347-355.

Ansieau, S., Bastid, J., Doreau, A., Morel, A.P., Bouchet, B.P., Thomas, C., Fauvet, F., Puisieux, I., Doglioni, C., Piccinin, S., *et al.* (2008). Induction of EMT by twist proteins as a collateral effect of tumor-promoting inactivation of premature senescence. Cancer Cell *14*, 79-89.

Anvekar, R.A., Asciolla, J.J., Missert, D.J., and Chipuk, J.E. (2011). Born to be alive: a role for the BCL-2 family in melanoma tumor cell survival, apoptosis, and treatment. Front Oncol *1*.

Arai, S., Meagher, R., Swearingen, M., Myint, H., Rich, E., Martinson, J., and Klingemann, H. (2008). Infusion of the allogeneic cell line NK-92 in patients with advanced renal cell cancer or melanoma: a phase I trial. Cytotherapy *10*, 625-632.

Arbiser, J.L. (2018). Diablo: A Double-Edged Sword in Cancer? Mol Ther *26*, 678-679.

Arnon, T.I., Markel, G., and Mandelboim, O. (2006). Tumor and viral recognition by natural killer cells receptors. Semin Cancer Biol *16*, 348-358.

Arrigo, A.P., and Gibert, B. (2014). HspB1, HspB5 and HspB4 in Human Cancers: Potent Oncogenic Role of Some of Their Client Proteins. Cancers (Basel) *6*, 333-365.

Aruga, N., Kijima, H., Masuda, R., Onozawa, H., Yoshizawa, T., Tanaka, M., Inokuchi, S., and Iwazaki, M. (2018). Epithelial-mesenchymal Transition (EMT) is Correlated with Patient's Prognosis of Lung Squamous Cell Carcinoma. Tokai J Exp Clin Med *43*, 5-13.

Arvidsson, A.K., Rupp, E., Nanberg, E., Downward, J., Ronnstrand, L., Wennstrom, S., Schlessinger, J., Heldin, C.H., and Claesson-Welsh, L. (1994). Tyr-716 in the platelet-derived growth factor beta-receptor kinase insert is involved in GRB2 binding and Ras activation. Mol Cell Biol *14*, 6715-6726.

Aziz, S.A., Davies, M., Pick, E., Zito, C., Jilaveanu, L., Camp, R.L., Rimm, D.L., Kluger, Y., and Kluger, H.M. (2009). Phosphatidylinositol-3-kinase as a therapeutic target in melanoma. Clin Cancer Res *15*, 3029-3036.

Backes, C. (2016). Dissertation. Untersuchung zytotoxischer Mechanismen in humanen natürlichen Killerzellen. In Institut für Biophysik am Zentrum für integrative Physiologie und molekulare Medizin (Homburg: Universität des Saarlandes).

Backes, C.S., Friedmann, K.S., Mang, S., Knorck, A., Hoth, M., and Kummerow, C. (2018). Natural killer cells induce distinct modes of cancer cell death: Discrimination, quantification, and modulation of apoptosis, necrosis, and mixed forms. J Biol Chem *293*, 16348-16363.

Baker, N.E., and Yu, S.Y. (2001). The EGF receptor defines domains of cell cycle progression and survival to regulate cell number in the developing Drosophila eye. Cell *104*, 699-708.

Balch, C.M., Gershenwald, J.E., Soong, S.J., Thompson, J.F., Atkins, M.B., Byrd, D.R., Buzaid, A.C., Cochran, A.J., Coit, D.G., Ding, S.*, et al.* (2009). Final version of 2009 AJCC melanoma staging and classification. J Clin Oncol *27*, 6199-6206.

Balsamo, M., Manzini, C., Pietra, G., Raggi, F., Blengio, F., Mingari, M.C., Varesio, L., Moretta, L., Bosco, M.C., and Vitale, M. (2013). Hypoxia downregulates the expression of activating receptors involved in NK-cell-mediated target cell killing without affecting ADCC. Eur J Immunol *43*, 2756-2764.

Balsamo, M., Vermi, W., Parodi, M., Pietra, G., Manzini, C., Queirolo, P., Lonardi, S., Augugliaro, R., Moretta, A., Facchetti, F.*, et al.* (2012). Melanoma cells become resistant to NK-cell-mediated killing when exposed to NK-cell numbers compatible with NK-cell infiltration in the tumor. Eur J Immunol *42*, 1833-1842.

Barrow, A.D., Edeling, M.A., Trifonov, V., Luo, J., Goyal, P., Bohl, B., Bando, J.K., Kim, A.H., Walker, J., Andahazy, M.*, et al.* (2018). Natural Killer Cells Control Tumor Growth by Sensing a Growth Factor. Cell *172*, 534-548 e519.

Barrow, A.D., Martin, C.J., and Colonna, M. (2019). The Natural Cytotoxicity Receptors in Health and Disease. Front Immunol *10*, 909.

Barry, K.C., Hsu, J., Broz, M.L., Cueto, F.J., Binnewies, M., Combes, A.J., Nelson, A.E., Loo, K., Kumar, R., Rosenblum, M.D.*, et al.* (2018). A natural killer-dendritic cell axis defines checkpoint therapy-responsive tumor microenvironments. Nat Med *24*, 1178-1191.

Bauer, J., and Garbe, C. (2003). Acquired melanocytic nevi as risk factor for melanoma development. A comprehensive review of epidemiological data. Pigment Cell Res *16*, 297-306.

Benjamin, D., Colombi, M., Moroni, C., and Hall, M.N. (2011). Rapamycin passes the torch: a new generation of mTOR inhibitors. Nat Rev Drug Discov *10*, 868-880.

Berthenet, K., Castillo Ferrer, C., Popgeorgiev, N., Hernandez-Vargas, H., and Ichim, G. (2019). Failed apoptosis enhances melanoma cancer cells aggressiveness. bioRxiv, 755744.

Besser, M.J., Shoham, T., Harari-Steinberg, O., Zabari, N., Ortenberg, R., Yakirevitch, A., Nagler, A., Loewenthal, R., Schachter, J., and Markel, G. (2013). Development of allogeneic NK cell adoptive transfer therapy in metastatic melanoma patients: in vitro preclinical optimization studies. PLoS ONE *8*, e57922.

Besson, A., Dowdy, S.F., and Roberts, J.M. (2008). CDK inhibitors: cell cycle regulators and beyond. Dev Cell *14*, 159-169.

Bettum, I.J., Gorad, S.S., Barkovskaya, A., Pettersen, S., Moestue, S.A., Vasiliauskaite, K., Tenstad, E., Oyjord, T., Risa, O., Nygaard, V.*, et al.* (2015). Metabolic reprogramming supports the invasive phenotype in malignant melanoma. Cancer Lett *366*, 71-83.

Bhandaru, M., Martinka, M., Li, G., and Rotte, A. (2014). Loss of XRCC1 confers a metastatic phenotype to melanoma cells and is associated with poor survival in patients with melanoma. Pigment Cell Melanoma Res *27*, 366-375.

Binici, J., Hartmann, J., Herrmann, J., Schreiber, C., Beyer, S., Guler, G., Vogel, V., Tumulka, F., Abele, R., Mantele, W.*, et al.* (2013). A soluble fragment of the tumor antigen BCL2-associated athanogene 6 (BAG-6) is essential and sufficient for inhibition of NKp30 receptor-dependent cytotoxicity of natural killer cells. J Biol Chem *288*, 34295-34303.

Bjornsen, E.G., Thiruchelvam-Kyle, L., Hoelsbrekken, S.E., Henden, C., Saether, P.C., Boysen, P., Daws, M.R., and Dissen, E. (2019). B7H6 is a functional ligand for NKp30 in rat and cattle and determines NKp30 reactivity toward human cancer cell lines. Eur J Immunol *49*, 54-65.

Boissel, N., Rea, D., Tieng, V., Dulphy, N., Brun, M., Cayuela, J.M., Rousselot, P., Tamouza, R., Le Bouteiller, P., Mahon, F.X.*, et al.* (2006). BCR/ABL oncogene directly controls MHC class I chain-related molecule A expression in chronic myelogenous leukemia. J Immunol *176*, 5108-5116.

Bommhardt, U., Schraven, B., and Simeoni, L. (2019). Beyond TCR Signaling: Emerging Functions of Lck in Cancer and Immunotherapy. Int J Mol Sci *20*, 3500.

Bonneau, B., Prudent, J., Popgeorgiev, N., and Gillet, G. (2013). Non-apoptotic roles of Bcl-2 family: the calcium connection. Biochim Biophys Acta *1833*, 1755-1765.

Boone, B., Jacobs, K., Ferdinande, L., Taildeman, J., Lambert, J., Peeters, M., Bracke, M., Pauwels, P., and Brochez, L. (2011). EGFR in melanoma: clinical significance and potential therapeutic target. J Cutan Pathol *38*, 492-502.

Boopathy, G.T.K., and Hong, W. (2019). Role of Hippo Pathway-YAP/TAZ Signaling in Angiogenesis. Front Cell Dev Biol *7*, 49.

Botzler, C., Li, G., Issels, R.D., and Multhoff, G. (1998). Definition of extracellular localized epitopes of Hsp70 involved in an NK immune response. Cell Stress Chaperones *3*, 6-11.

Boulbes, D., Chen, C.H., Shaikenov, T., Agarwal, N.K., Peterson, T.R., Addona, T.A., Keshishian, H., Carr, S.A., Magnuson, M.A., Sabatini, D.M.*, et al.* (2010). Rictor phosphorylation on the Thr-1135 site does not require mammalian target of rapamycin complex 2. Mol Cancer Res *8*, 896-906.

Brandt, C.S., Baratin, M., Yi, E.C., Kennedy, J., Gao, Z., Fox, B., Haldeman, B., Ostrander, C.D., Kaifu, T., Chabannon, C.*, et al.* (2009). The B7 family member B7-H6 is a tumor cell ligand for the activating natural killer cell receptor NKp30 in humans. J Exp Med *206*, 1495-1503.

Brooks, A.G., Borrego, F., Posch, P.E., Patamawenu, A., Scorzelli, C.J., Ulbrecht, M., Weiss, E.H., and Coligan, J.E. (1999). Specific recognition of HLA-E, but not classical, HLA class I molecules by soluble CD94/NKG2A and NK cells. J Immunol *162*, 305-313.

Bryceson, Y.T., March, M.E., Ljunggren, H.G., and Long, E.O. (2006). Synergy among receptors on resting NK cells for the activation of natural cytotoxicity and cytokine secretion. Blood *107*, 159-166.

Budina-Kolomets, A., Webster, M.R., Leu, J.I., Jennis, M., Krepler, C., Guerrini, A., Kossenkov, A.V., Xu, W., Karakousis, G., Schuchter, L.*, et al.* (2016). HSP70 Inhibition Limits FAK-Dependent Invasion and Enhances the Response to Melanoma Treatment with BRAF Inhibitors. Cancer Res *76*, 2720-2730.

Bui, N.L., Pandey, V., Zhu, T., Ma, L., Basappa, and Lobie, P.E. (2018). Bad phosphorylation as a target of inhibition in oncology. Cancer Lett *415*, 177-186.

Bundscherer, A., Hafner, C., Maisch, T., Becker, B., Landthaler, M., and Vogt, T. (2008). Antiproliferative and proapoptotic effects of rapamycin and celecoxib in malignant melanoma cell lines. Oncol Rep *19*, 547-553.

Cancer Genome Atlas, N. (2015). Genomic Classification of Cutaneous Melanoma. Cell *161*, 1681-1696.

Cappello, S. (2015). Master thesis. NK cell mediated killing of melanoma. In Institut für BiophysikamZentrum für integrative Physiologie und molekulare Medizin (Homburg: Universität des Saarlandes).

Caramel, J., Papadogeorgakis, E., Hill, L., Browne, G.J., Richard, G., Wierinckx, A., Saldanha, G., Osborne, J., Hutchinson, P., Tse, G.*, et al.* (2013). A switch in the expression of embryonic EMT-inducers drives the development of malignant melanoma. Cancer Cell *24*, 466-480.

Carracedo, A., and Pandolfi, P.P. (2008). The PTEN-PI3K pathway: of feedbacks and cross-talks. Oncogene *27*, 5527-5541.

Carrega, P., Pezzino, G., Queirolo, P., Bonaccorsi, I., Falco, M., Vita, G., Pende, D., Misefari, A., Moretta, A., Mingari, M.C.*, et al.* (2009). Susceptibility of human melanoma cells to autologous natural killer (NK) cell killing: HLA-related effector mechanisms and role of unlicensed NK cells. PLoS ONE *4*, e8132.

Carretero, R., Romero, J.M., Ruiz-Cabello, F., Maleno, I., Rodriguez, F., Camacho, F.M., Real, L.M., Garrido, F., and Cabrera, T. (2008). Analysis of HLA class I expression in progressing and regressing metastatic melanoma lesions after immunotherapy. Immunogenetics *60*, 439-447.

Casado, J.G., Pawelec, G., Morgado, S., Sanchez-Correa, B., Delgado, E., Gayoso, I., Duran, E., Solana, R., and Tarazona, R. (2009). Expression of adhesion molecules and ligands for activating and costimulatory receptors involved in cell-mediated cytotoxicity in a large panel of human melanoma cell lines. Cancer Immunol Immunother *58*, 1517-1526.

Castro, F., Cardoso, A.P., Goncalves, R.M., Serre, K., and Oliveira, M.J. (2018). Interferon-Gamma at the Crossroads of Tumor Immune Surveillance or Evasion. Front Immunol *9*, 847.

Cerezo, M., Guemiri, R., Druillennec, S., Girault, I., Malka-Mahieu, H., Shen, S., Allard, D., Martineau, S., Welsch, C., Agoussi, S.*, et al.* (2018). Translational control of tumor immune escape via the eIF4F-STAT1-PD-L1 axis in melanoma. Nat Med *24*, 1877-1886.

Cerwenka, A., and Lanier, L.L. (2001). Natural killer cells, viruses and cancer. Nat Rev Immunol *1*, 41-49.

Chalhoub, N., and Baker, S.J. (2009). PTEN and the PI3-kinase pathway in cancer. Annu Rev Pathol *4*, 127-150.

Chan, C.J., Andrews, D.M., McLaughlin, N.M., Yagita, H., Gilfillan, S., Colonna, M., and Smyth, M.J. (2010). DNAM-1/CD155 interactions promote cytokine and NK cell-mediated suppression of poorly immunogenic melanoma metastases. J Immunol *184*, 902-911.

Chapman, P.B., Hauschild, A., Robert, C., Haanen, J.B., Ascierto, P., Larkin, J., Dummer, R., Garbe, C., Testori, A., Maio, M.*, et al.* (2011). Improved survival with vemurafenib in melanoma with BRAF V600E mutation. N Engl J Med *364*, 2507-2516.

Chen, C., and Zhang, X. (2017). IRE1alpha-XBP1 pathway promotes melanoma progression by regulating IL-6/STAT3 signaling. J Transl Med *15*, 42.

Chen, G., Cheng, Y., Zhang, Z., Martinka, M., and Li, G. (2011). Prognostic significance of cytoplasmic p27 expression in human melanoma. Cancer Epidemiol Biomarkers Prev *20*, 2212-2221.

Chen, J., Gao, F., and Liu, N. (2018). L1CAM promotes epithelial to mesenchymal transition and formation of cancer initiating cells in human endometrial cancer. Exp Ther Med *15*, 2792-2797.

Chen, Y.A., Lu, C.Y., Cheng, T.Y., Pan, S.H., Chen, H.F., and Chang, N.S. (2019a). WW Domain-Containing Proteins YAP and TAZ in the Hippo Pathway as Key Regulators in Stemness Maintenance, Tissue Homeostasis, and Tumorigenesis. Front Oncol *9*, 60.

Chen, Y.Y., Chang, W.A., Lin, E.S., Chen, Y.J., and Kuo, P.L. (2019b). Expressions of HLA Class II Genes in Cutaneous Melanoma Were Associated with Clinical Outcome: Bioinformatics Approaches and Systematic Analysis of Public Microarray and RNA-Seq Datasets. Diagnostics (Basel) *9*, 59.

Cheng, M., Sexl, V., Sherr, C.J., and Roussel, M.F. (1998). Assembly of cyclin D-dependent kinase and titration of p27Kip1 regulated by mitogen-activated protein kinase kinase (MEK1). Proc Natl Acad Sci USA *95*, 1091-1096.

Cheng, Z., Guo, J., Chen, L., Luo, N., Yang, W., and Qu, X. (2015). Overexpression of TMEM158 contributes to ovarian carcinogenesis. J Exp Clin Cancer Res *34*, 75.

Chester, C., Fritsch, K., and Kohrt, H.E. (2015). Natural Killer Cell Immunomodulation: Targeting Activating, Inhibitory, and Co-stimulatory Receptor Signaling for Cancer Immunotherapy. Front Immunol *6*, 601.

Cheung, L.W., and Mills, G.B. (2016). Targeting therapeutic liabilities engendered by PIK3R1 mutations for cancer treatment. Pharmacogenomics *17*, 297-307.

Chiossone, L., Dumas, P.Y., Vienne, M., and Vivier, E. (2018). Natural killer cells and other innate lymphoid cells in cancer. Nat Rev Immunol *18*, 671-688.

Chockley, P.J., Chen, J., Chen, G., Beer, D.G., Standiford, T.J., and Keshamouni, V.G. (2018). Epithelial-mesenchymal transition leads to NK cell-mediated metastasis-specific immunosurveillance in lung cancer. J Clin Invest *128*, 1384-1396.

Chockley, P.J., and Keshamouni, V.G. (2016). Immunological Consequences of Epithelial-Mesenchymal Transition in Tumor Progression. J Immunol *197*, 691-698.

Chomczynski, P., and Sacchi, N. (1987). Single-step method of RNA isolation by acid guanidinium thiocyanate-phenol-chloroform extraction. Anal Biochem *162*, 156-159.

Chon, H.S., Marchion, D.C., Xiong, Y., Chen, N., Bicaku, E., Stickles, X.B., Bou Zgheib, N., Judson, P.L., Hakam, A., Gonzalez-Bosquet, J.*, et al.* (2012). The BCL2 antagonist of cell death pathway influences endometrial cancer cell sensitivity to cisplatin. Gynecol Oncol *124*, 119-124.

Chouaib, S., Janji, B., Tittarelli, A., Eggermont, A., and Thiery, J.P. (2014). Tumor plasticity interferes with anti-tumor immunity. Crit Rev Immunol *34*, 91-102.

Ciolczyk-Wierzbicka, D., Gil, D., Zarzycka, M., and Laidler, P. (2020). mTOR inhibitor everolimus reduces invasiveness of melanoma cells. Hum Cell *33*, 88-97.

Ciolczyk-Wierzbicka, D., and Laidler, P. (2018). The inhibition of invasion of human melanoma cells through N-cadherin knock-down. Med Oncol *35*, 42.

Colell, A., Green, D.R., and Ricci, J.E. (2009). Novel roles for GAPDH in cell death and carcinogenesis. Cell Death Differ *16*, 1573-1581.

Conlon, K.C., Lugli, E., Welles, H.C., Rosenberg, S.A., Fojo, A.T., Morris, J.C., Fleisher, T.A., Dubois, S.P., Perera, L.P., Stewart, D.M.*, et al.* (2015). Redistribution, hyperproliferation, activation of natural killer cells and CD8 T cells, and cytokine production during first-in-human clinical trial of recombinant human interleukin-15 in patients with cancer. J Clin Oncol *33*, 74-82.

Cooley, S., Verneris, M.R., Curtsinger, J., McKenna, D., Weisdorf, D.J., Blazar, B.R., Waldmann, T.A., and Miller, J.S. (2012). Recombinant Human IL-15 Promotes in Vivo Expansion of Adoptively Transferred NK Cells in a First-in-Human Phase I Dose Escalation Study in Patients with AML. Blood *120*, 894-894.

Cooper, M.A., Fehniger, T.A., and Caligiuri, M.A. (2001). The biology of human natural killer-cell subsets. Trends Immunol *22*, 633-640.

Costantini, F., and Barbieri, G. (2017). The HLA-DR mediated signalling increases the migration and invasion of melanoma cells, the expression and lipid raft recruitment of adhesion receptors, PD-L1 and signal transduction proteins. Cell Signal *36*, 189-203.

Cullen, S.P., and Martin, S.J. (2008). Mechanisms of granule-dependent killing. Cell Death Differ *15*, 251-262.

Cursons, J., Souza-Fonseca-Guimaraes, F., Foroutan, M., Anderson, A., Hollande, F., Hediyeh-Zadeh, S., Behren, A., Huntington, N.D., and Davis, M.J. (2019). A Gene Signature Predicting Natural Killer Cell Infiltration and Improved Survival in Melanoma Patients. Cancer Immunol Res *7*, 1162-1174.

da Silva, I.P., Gallois, A., Jimenez-Baranda, S., Khan, S., Anderson, A.C., Kuchroo, V.K., Osman, I., and Bhardwaj, N. (2014). Reversal of NK-cell exhaustion in advanced melanoma by Tim-3 blockade. Cancer Immunol Res *2*, 410-422.

Dai, D.L., Martinka, M., and Li, G. (2005). Prognostic significance of activated Akt expression in melanoma: a clinicopathologic study of 292 cases. J Clin Oncol *23*, 1473-1482.

Danen, E.H., de Vries, T.J., Morandini, R., Ghanem, G.G., Ruiter, D.J., and van Muijen, G.N. (1996). E-cadherin expression in human melanoma. Melanoma Res *6*, 127-131.

Davies, H., Bignell, G.R., Cox, C., Stephens, P., Edkins, S., Clegg, S., Teague, J., Woffendin, H., Garnett, M.J., Bottomley, W.*, et al.* (2002). Mutations of the BRAF gene in human cancer. Nature *417*, 949-954.

Davies, M.A., Stemke-Hale, K., Tellez, C., Calderone, T.L., Deng, W., Prieto, V.G., Lazar, A.J., Gershenwald, J.E., and Mills, G.B. (2008). A novel AKT3 mutation in melanoma tumours and cell lines. Br J Cancer *99*, 1265-1268.

de Koning, H.D., van Vlijmen-Willems, I.M., Zeeuwen, P.L., Blokx, W.A., and Schalkwijk, J. (2014). Absent in Melanoma 2 is predominantly present in primary melanoma and primary squamous cell carcinoma, but largely absent in metastases of both tumors. J Am Acad Dermatol *71*, 1012-1015.

de Rham, C., Ferrari-Lacraz, S., Jendly, S., Schneiter, G., Dayer, J.M., and Villard, J. (2007). The proinflammatory cytokines IL-2, IL-15 and IL-21 modulate the repertoire of mature human natural killer cell receptors. Arthritis Res Ther *9*, R125.

DeBlaker-Hohe, D.F., Yamauchi, A., Yu, C.R., Horvath-Arcidiacono, J.A., and Bloom, E.T. (1995). IL-12 synergizes with IL-2 to induce lymphokine-activated cytotoxicity and perforin and granzyme gene expression in fresh human NK cells. Cell Immunol *165*, 33-43.

Debniak, T. (2004). Familial malignant melanoma - overview. Hered Cancer Clin Pract *2*, 123-129.

del Peso, L., Gonzalez-Garcia, M., Page, C., Herrera, R., and Nunez, G. (1997). Interleukin-3-induced phosphorylation of BAD through the protein kinase Akt. Science (80-) *278*, 687-689.

Demkova, L., and Kucerova, L. (2018). Role of the HGF/c-MET tyrosine kinase inhibitors in metastasic melanoma. Mol Cancer *17*, 26.

Denicourt, C., Saenz, C.C., Datnow, B., Cui, X.S., and Dowdy, S.F. (2007). Relocalized p27Kip1 tumor suppressor functions as a cytoplasmic metastatic oncogene in melanoma. Cancer Res *67*, 9238-9243.

Derre, L., Corvaisier, M., Charreau, B., Moreau, A., Godefroy, E., Moreau-Aubry, A., Jotereau, F., and Gervois, N. (2006). Expression and release of HLA-E by melanoma cells and melanocytes: potential impact on the response of cytotoxic effector cells. J Immunol *177*, 3100-3107.

Derynck, R., and Weinberg, R.A. (2019). EMT and Cancer: More Than Meets the Eye. Dev Cell *49*, 313-316.

Deutsche Krebsgesellschaft, Deutsche Krebshilfe, and AWMF (2019). Leitlinienprogramm Onkologie. Diagnostik, Therapie und Nachsorge des Melanoms, Kurzversion 3.2,2019, AWMF Registernummer: 032/024OL, Available from https://www.leitlinienprogramm-onkologie.de/leitlinien/melanom/ (29.02.2020).

Dibble, C.C., Asara, J.M., and Manning, B.D. (2009). Characterization of Rictor phosphorylation sites reveals direct regulation of mTOR complex 2 by S6K1. Mol Cell Biol *29*, 5657-5670.

Ding, W., Shanafelt, T.D., Lesnick, C.E., Erlichman, C., Leis, J.F., Secreto, C., Sassoon, T.R., Call, T.G., Bowen, D.A., Conte, M.*, et al.* (2014). Akt inhibitor MK2206 selectively targets CLL B-cell receptor induced cytokines, mobilizes lymphocytes and synergizes with bendamustine to induce CLL apoptosis. Br J Haematol *164*, 146-150.

Divito, K.A., Dolled-Filhart, M., Camp, R., Berger, A., Rimm, D., and Kluger, H. (2004). Evaluation of Bcl-2 expression in melanoma - A tissue microarray study. J Clin Oncol *22*, 7515-7515.

Dobin, A., Davis, C.A., Schlesinger, F., Drenkow, J., Zaleski, C., Jha, S., Batut, P., Chaisson, M., and Gingeras, T.R. (2013). STAR: ultrafast universal RNA-seq aligner. Bioinformatics *29*, 15-21.

Domingues, B., Lopes, J.M., Soares, P., and Populo, H. (2018). Melanoma treatment in review. Immunotargets Ther *7*, 35-49.

Dronca, R.S., Allred, J.B., Perez, D.G., Nevala, W.K., Lieser, E.A., Thompson, M., Maples, W.J., Creagan, E.T., Pockaj, B.A., Kaur, J.S.*, et al.* (2014). Phase II study of temozolomide (TMZ) and everolimus (RAD001) therapy for metastatic melanoma: a North Central Cancer Treatment Group study, N0675. Am J Clin Oncol *37*, 369-376.

Du, C., Fang, M., Li, Y., Li, L., and Wang, X. (2000). Smac, a Mitochondrial Protein that Promotes Cytochrome c–Dependent Caspase Activation by Eliminating IAP Inhibition. Cell *102*, 33-42.

Dumaz, N., Jouenne, F., Delyon, J., Mourah, S., Bensussan, A., and Lebbe, C. (2019). Atypical BRAF and NRAS Mutations in Mucosal Melanoma. Cancers (Basel) *11*, 1133.

Dunn, G.P., Old, L.J., and Schreiber, R.D. (2004). The three Es of cancer immunoediting. Annu Rev Immunol *22*, 329-360.

Dustin, M.L., and Long, E.O. (2010). Cytotoxic immunological synapses. Immunol Rev *235*, 24-34.

Eckert, R.L., Fisher, M.L., Grun, D., Adhikary, G., Xu, W., and Kerr, C. (2015). Transglutaminase is a tumor cell and cancer stem cell survival factor. Mol Carcinog *54*, 947-958.

Eissens, D.N., Van Der Meer, A., Van Cranenbroek, B., Preijers, F.W., and Joosten, I. (2010). Rapamycin and MPA, but not CsA, impair human NK cell cytotoxicity due to differential effects on NK cell phenotype. Am J Transplant *10*, 1981-1990.

Elmore, S. (2007). Apoptosis: a review of programmed cell death. Toxicol Pathol *35*, 495-516.

Elsner, L., Muppala, V., Gehrmann, M., Lozano, J., Malzahn, D., Bickeboller, H., Brunner, E., Zientkowska, M., Herrmann, T., Walter, L.*, et al.* (2007). The heat shock protein HSP70 promotes mouse NK cell activity against tumors that express inducible NKG2D ligands. J Immunol *179*, 5523-5533.

Eom, S., Kim, Y., Kim, M., Park, D., Lee, H., Lee, Y.S., Choe, J., Kim, Y.M., and Jeoung, D. (2014). Transglutaminase II/microRNA-218/-181a loop regulates positive feedback relationship between allergic inflammation and tumor metastasis. J Biol Chem *289*, 29483-29505.

Eriksson, J., Le Joncour, V., Nummela, P., Jahkola, T., Virolainen, S., Laakkonen, P., Saksela, O., and Hölttä, E. (2016). Gene expression analyses of primary melanomas reveal CTHRC1 as an important player in melanoma progression. Oncotarget *7*, 15065–15092.

Ernst, A.K., Putscher, A., Samatov, T.R., Suling, A., Galatenko, V.V., Shkurnikov, M.Y., Knyazev, E.N., Tonevitsky, A.G., Haalck, T., Lange, T.*, et al.* (2018). Knockdown of L1CAM significantly reduces metastasis in a xenograft model of human melanoma: L1CAM is a potential target for anti-melanoma therapy. PLoS ONE *13*, e0192525.

Fang, X., Cai, Y., Liu, J., Wang, Z., Wu, Q., Zhang, Z., Yang, C.J., Yuan, L., and Ouyang, G. (2011). Twist2 contributes to breast cancer progression by promoting an epithelial-mesenchymal transition and cancer stem-like cell self-renewal. Oncogene *30*, 4707-4720.

Farag, S.S., and Caligiuri, M.A. (2006). Human natural killer cell development and biology. Blood Rev *20*, 123-137.

Farkas, B., Hantschel, M., Magyarlaki, M., Becker, B., Scherer, K., Landthaler, M., Pfister, K., Gehrmann, M., Gross, C., Mackensen, A.*, et al.* (2003). Heat shock protein 70 membrane expression and melanoma-associated marker phenotype in primary and metastatic melanoma. Melanoma Res *13*, 147-152.

Felices, M., Chu, S., Kodal, B., Bendzick, L., Ryan, C., Lenvik, A.J., Boylan, K.L.M., Wong, H.C., Skubitz, A.P.N., Miller, J.S.*, et al.* (2017). IL-15 super-agonist (ALT-803) enhances natural killer (NK) cell function against ovarian cancer. Gynecol Oncol *145*, 453-461.

Felices, M., Lenvik, T.R., Davis, Z.B., Miller, J.S., and Vallera, D.A. (2016). Generation of BiKEs and TriKEs to Improve NK Cell-Mediated Targeting of Tumor Cells. In Natural Killer Cells: Methods and Protocols, S.S. Somanchi, ed. (New York, NY: Springer New York), pp. 333-346.

Feng, Q., Guo, P., Kang, S., and Zhao, F. (2018). High expression of TAZ/YAP promotes the progression of malignant melanoma and affects the postoperative survival of patients. Pharmazie *73*, 662-665.

Ferk, P., and Daris, B. (2018). The influence of dimethyl sulfoxide (DMSO) on metabolic activity and morphology of melanoma cell line WM-266-4. Cell Mol Biol (Noisy-le-grand) *64*, 41-43.

Ferrari de Andrade, L., Tay, R.E., Pan, D., Luoma, A.M., Ito, Y., Badrinath, S., Tsoucas, D., Franz, B., May, K.F., Jr., Harvey, C.J.*, et al.* (2018). Antibody-mediated inhibition of MICA and MICB shedding promotes NK cell-driven tumor immunity. Science (80-) *359*, 1537-1542.

Fingar, D.C., and Blenis, J. (2004). Target of rapamycin (TOR): an integrator of nutrient and growth factor signals and coordinator of cell growth and cell cycle progression. Oncogene *23*, 3151-3171.

Finlay-Schultz, J., Gillen, A.E., Brechbuhl, H.M., Ivie, J.J., Matthews, S.B., Jacobsen, B.M., Bentley, D.L., Kabos, P., and Sartorius, C.A. (2017). Breast Cancer Suppression by Progesterone Receptors Is Mediated by Their Modulation of Estrogen Receptors and RNA Polymerase III. Cancer Res *77*, 4934-4946.

Fok, J.Y., Ekmekcioglu, S., and Mehta, K. (2006). Implications of tissue transglutaminase expression in malignant melanoma. Mol Cancer Ther *5*, 1493-1503.

Fortes, C., Mastroeni, S., Mannooranparampil, T.J., Passarelli, F., Zappala, A., Annessi, G., Marino, C., Caggiati, A., Russo, N., and Michelozzi, P. (2015). Tumor-infiltrating lymphocytes predict cutaneous melanoma survival. Melanoma Res *25*, 306-311.

Fortier, M.-H.l.n., Caron, E., De Verteuil, D., Perreault, C., and Thibault, P. (2007). Influence of mTOR Signalling Pathway on the MHC I Immunopeptidome. Blood *110*, 3887-3887.

Frazao, A., Rethacker, L., Messaoudene, M., Avril, M.F., Toubert, A., Dulphy, N., and Caignard, A. (2019). NKG2D/NKG2-Ligand Pathway Offers New Opportunities in Cancer Treatment. Front Immunol *10*, 661.

Freeman, A.J., Vervoort, S.J., Ramsbottom, K.M., Kelly, M.J., Michie, J., Pijpers, L., Johnstone, R.W., Kearney, C.J., and Oliaro, J. (2019). Natural Killer Cells Suppress T Cell-Associated Tumor Immune Evasion. Cell Rep *28*, 2784-2794 e2785.

Freud, A.G., Mundy-Bosse, B.L., Yu, J., and Caligiuri, M.A. (2017). The Broad Spectrum of Human Natural Killer Cell Diversity. Immunity *47*, 820-833.

Fujino, S., Miyoshi, N., Ohue, M., Takahashi, Y., Yasui, M., Hata, T., Matsuda, C., Mizushima, T., Doki, Y., and Mori, M. (2018). Plateletderived growth factor receptorbeta gene expression relates to recurrence in colorectal cancer. Oncol Rep *39*, 2178-2184.

Fujiwara, Y., Nokihara, H., Yamada, Y., Yamamoto, N., Sunami, K., Utsumi, H., Asou, H., Takahash, I.O., Ogasawara, K., Gueorguieva, I.*, et al.* (2015). Phase 1 study of galunisertib, a TGF-beta receptor I kinase inhibitor, in Japanese patients with advanced solid tumors. Cancer Chemother Pharmacol *76*, 1143-1152.

Gandini, S., Sera, F., Cattaruzza, M.S., Pasquini, P., Abeni, D., Boyle, P., and Melchi, C.F. (2005a). Meta-analysis of risk factors for cutaneous melanoma: I. Common and atypical naevi. Eur J Cancer *41*, 28-44.

Gandini, S., Sera, F., Cattaruzza, M.S., Pasquini, P., Picconi, O., Boyle, P., and Melchi, C.F. (2005b). Meta-analysis of risk factors for cutaneous melanoma: II. Sun exposure. Eur J Cancer *41*, 45-60.

Garman, B., Anastopoulos, I.N., Krepler, C., Brafford, P., Sproesser, K., Jiang, Y., Wubbenhorst, B., Amaravadi, R., Bennett, J., Beqiri, M.*, et al.* (2017). Genetic and Genomic Characterization of 462 Melanoma Patient-Derived Xenografts, Tumor Biopsies, and Cell Lines. Cell Rep *21*, 1936-1952.

Garson, D., Dokhelar, M.C., Wakasugi, H., Mishal, Z., and Tursz, T. (1985). HLA class-I and class-II antigen expression by human leukemic K562 cells and by Burkitt-K562 hybrids: modulation by differentiation inducers and interferon. Exp Hematol *13*, 885-890.

Gasior, K., Hauck, M., Wilson, A., and Bhattacharya, S. (2017). A Theoretical Model of the Wnt Signaling Pathway in the Epithelial Mesenchymal Transition. Theor Biol Med Model *14*, 19.

Gherardi, E., Birchmeier, W., Birchmeier, C., and Vande Woude, G. (2012). Targeting MET in cancer: rationale and progress. Nat Rev Cancer *12*, 89-103.

Gibert, B., Eckel, B., Gonin, V., Goldschneider, D., Fombonne, J., Deux, B., Mehlen, P., Arrigo, A.P., Clezardin, P., and Diaz-Latoud, C. (2012). Targeting heat shock protein 27 (HspB1) interferes with bone metastasis and tumour formation in vivo. Br J Cancer *107*, 63-70.

Giehl, K., and Menke, A. (2008). Microenvironmental regulation of E-cadherin-mediated adherens junctions. Front Biosci *13*, 3975-3985.

Gimenez-Cassina, A., Garcia-Haro, L., Choi, C.S., Osundiji, M.A., Lane, E.A., Huang, H., Yildirim, M.A., Szlyk, B., Fisher, J.K., Polak, K.*, et al.* (2014). Regulation of hepatic energy metabolism and gluconeogenesis by BAD. Cell Metab *19*, 272-284.

Goodman, M.L., Trinca, G.M., Walter, K.R., Papachristou, E.K., D'Santos, C.S., Li, T., Liu, Q., Lai, Z., Chalise, P., Madan, R.*, et al.* (2019). Progesterone Receptor Attenuates STAT1-Mediated IFN Signaling in Breast Cancer. J Immunol *202*, 3076-3086.

Govindarajan, B., Bai, X., Cohen, C., Zhong, H., Kilroy, S., Louis, G., Moses, M., and Arbiser, J.L. (2003). Malignant transformation of melanocytes to melanoma by constitutive activation of mitogen-activated protein kinase kinase (MAPKK) signaling. J Biol Chem *278*, 9790-9795.

Grimm, E.A., Mazumder, A., Zhang, H.Z., and Rosenberg, S.A. (1982). Lymphokine-activated killer cell phenomenon. Lysis of natural killer-resistant fresh solid tumor cells by interleukin 2-activated autologous human peripheral blood lymphocytes. J Exp Med *155*, 1823-1841.

Grindstad, T., Richardsen, E., Andersen, S., Skjefstad, K., Rakaee Khanehkenari, M., Donnem, T., Ness, N., Nordby, Y., Bremnes, R.M., Al-Saad, S.*, et al.* (2018). Progesterone Receptors in Prostate Cancer: Progesterone receptor B is the isoform associated with disease progression. Sci Rep *8*, 11358.

Grob, J.J., and Bonerandi, J.J. (1998). The 'Ugly Duckling' Sign: Identification of the Common Characteristics of Nevi in an Individual as a Basis for Melanoma Screening. JAMA Dermatol *134*, 103-104.

Guldberg, P., thor Straten, P., Birck, A., Ahrenkiel, V., Kirkin, A.F., and Zeuthen, J. (1997). Disruption of the MMAC1/PTEN Gene by Deletion or Mutation Is a Frequent Event in Malignant Melanoma. Cancer Res *57*, 3660-3663.

Guo, C., Liu, S., Greenaway, F., and Sun, M.Z. (2013). Potential role of annexin A7 in cancers. Clin Chim Acta *423*, 83-89.

Hanahan, D., and Weinberg, R.A. (2011). Hallmarks of cancer: the next generation. Cell *144*, 646-674.

Hao, L., Ha, J.R., Kuzel, P., Garcia, E., and Persad, S. (2012). Cadherin switch from E- to N-cadherin in melanoma progression is regulated by the PI3K/PTEN pathway through Twist and Snail. Br J Dermatol *166*, 1184-1197.

Hao, L., Zhou, X., Liu, S., Sun, M., Song, Y., Du, S., Sun, B., Guo, C., Gong, L., Hu, J.*, et al.* (2015). Elevated GAPDH expression is associated with the proliferation and invasion of lung and esophageal squamous cell carcinomas. Proteomics *15*, 3087-3100.

Hatzivassiliou, G., Song, K., Yen, I., Brandhuber, B.J., Anderson, D.J., Alvarado, R., Ludlam, M.J., Stokoe, D., Gloor, S.L., Vigers, G.*, et al.* (2010). RAF inhibitors prime wild-type RAF to activate the MAPK pathway and enhance growth. Nature *464*, 431-435.

Henney, C.S., Kuribayashi, K., Kern, D.E., and Gillis, S. (1981). Interleukin-2 augments natural killer cell activity. Nature *291*, 335-338.

Herbst, R.S. (2004). Review of epidermal growth factor receptor biology. Int J Radiat Oncol Biol Phys *59*, 21-26.

Hoffman, M., Mittelman, A., Dworkin, B., Rosenthal, W., Beneck, D., Gafney, E., Arlin, Z., Levitt, D., and Podack, E. (1989). Severe intrahepatic cholestasis in patients treated with recombinant interleukin-2 and lymphokine-activated killer cells. J Cancer Res Clin Oncol *115*, 175-178.

Holly, E.A., Kelly, J.W., Shpall, S.N., and Chiu, S.H. (1987). Number of melanocytic nevi as a major risk factor for malignant melanoma. J Am Acad Dermatol *17*, 459-468.

Houben, R., Becker, J., Kappel, A., Terheyden, P., Brocker, E.-B., Goetz, R., and Rapp, U. (2004). Constitutive activation of the Ras-Raf signaling pathway in metastatic melanoma is associated with poor prognosis. J Carcinog *3*, 6.

Howlader, N., Noone, A.M., Krapcho, M., Miller, D., Brest, A., Yu, M., Ruhl, J., Tatalovich, Z., Mariotto, A., Lewis, D.R.*, et al.* (2018). SEER Cancer Statistics Review, 1975-2016, National Cancer Institute. Bethesda, MD, https://seer.cancer.gov/csr/1975_2016/, based on November 2018 SEER data submission, posted to the SEER web site, April 2019.

Hsu, J., Hodgins, J.J., Marathe, M., Nicolai, C.J., Bourgeois-Daigneault, M.C., Trevino, T.N., Azimi, C.S., Scheer, A.K., Randolph, H.E., Thompson, T.W.*, et al.* (2018). Contribution of NK cells to immunotherapy mediated by PD-1/PD-L1 blockade. J Clin Invest *128*, 4654-4668.

Hu, J., He, X., Baggerly, K.A., Coombes, K.R., Hennessy, B.T., and Mills, G.B. (2007). Non-parametric quantification of protein lysate arrays. Bioinformatics *23*, 1986-1994.

Hu, W., Wang, G., Huang, D., Sui, M., and Xu, Y. (2019). Cancer Immunotherapy Based on Natural Killer Cells: Current Progress and New Opportunities. Front Immunol *10*, 1205.

Hu, Y., Guo, R., Wei, J., Zhou, Y., Ji, W., Liu, J., Zhi, X., and Zhang, J. (2015). Effects of PI3K inhibitor NVP-BKM120 on overcoming drug resistance and eliminating cancer stem cells in human breast cancer cells. Cell Death Dis *6*, e2020.

Huberman, E., Heckman, C., and Langenbach, R. (1979). Stimulation of differentiated functions in human melanoma cells by tumor-promoting agents and dimethyl sulfoxide. Cancer Res *39*, 2618-2624.

Huenecke, S., Zimmermann, S.Y., Kloess, S., Esser, R., Brinkmann, A., Tramsen, L., Koenig, M., Erben, S., Seidl, C., Tonn, T.*, et al.* (2010). IL-2-driven regulation of NK cell receptors with regard to the distribution of CD16+ and CD16- subpopulations and in vivo influence after haploidentical NK cell infusion. J Immunother *33*, 200-210.

Huergo-Zapico, L., Parodi, M., Cantoni, C., Lavarello, C., Fernandez-Martinez, J.L., Petretto, A., DeAndres-Galiana, E.J., Balsamo, M., Lopez-Soto, A., Pietra, G.*, et al.* (2018). NK-cell Editing Mediates Epithelial-to-

Mesenchymal Transition via Phenotypic and Proteomic Changes in Melanoma Cell Lines. Cancer Res *78*, 3913-3925.

Imai, K., Matsuyama, S., Miyake, S., Suga, K., and Nakachi, K. (2000). Natural cytotoxic activity of peripheral-blood lymphocytes and cancer incidence: an 11-year follow-up study of a general population. Lancet *356*, 1795-1799.

Ito, M., Maruyama, T., Saito, N., Koganei, S., Yamamoto, K., and Matsumoto, N. (2006). Killer cell lectin-like receptor G1 binds three members of the classical cadherin family to inhibit NK cell cytotoxicity. J Exp Med *203*, 289-295.

Jaiswal, B.S., Janakiraman, V., Kljavin, N.M., Chaudhuri, S., Stern, H.M., Wang, W., Kan, Z., Dbouk, H.A., Peters, B.A., Waring, P.*, et al.* (2009). Somatic mutations in p85alpha promote tumorigenesis through class IA PI3K activation. Cancer Cell *16*, 463-474.

Jeong, K., Murphy, J.M., Rodriguez, Y.A.R., Kim, J.S., Ahn, E.E., and Lim, S.S. (2019). FAK inhibition reduces metastasis of alpha4 integrin-expressing melanoma to lymph nodes by targeting lymphatic VCAM-1 expression. Biochem Biophys Res Commun *509*, 1034-1040.

Jhappan, C., Noonan, F.P., and Merlino, G. (2003). Ultraviolet radiation and cutaneous malignant melanoma. Oncogene *22*, 3099-3112.

Jiang, K., Zhong, B., Gilvary, D.L., Corliss, B.C., Hong-Geller, E., Wei, S., and Djeu, J.Y. (2000). Pivotal role of phosphoinositide-3 kinase in regulation of cytotoxicity in natural killer cells. Nat Immunol *1*, 419-425.

Jiang, Y.Z., Couriel, D., Mavroudis, D.A., Lewalle, P., Malkovska, V., Hensel, N.F., Dermime, S., Molldrem, J., and Barrett, A.J. (1996). Interaction of natural killer cells with MHC class II: reversal of HLA-DR1-mediated protection of K562 transfectant from natural killer cell-mediated cytolysis by brefeldin-A. Immunology *87*, 481-486.

Johnson, D.B., Estrada, M.V., Salgado, R., Sanchez, V., Doxie, D.B., Opalenik, S.R., Vilgelm, A.E., Feld, E., Johnson, A.S., Greenplate, A.R.*, et al.* (2016). Melanoma-specific MHC-II expression represents a tumour-autonomous phenotype and predicts response to anti-PD-1/PD-L1 therapy. Nat Commun *7*, 10582.

Johnson, D.B., Lovly, C.M., Flavin, M., Panageas, K.S., Ayers, G.D., Zhao, Z., Iams, W.T., Colgan, M., DeNoble, S., Terry, C.R.*, et al.* (2015). Impact of NRAS mutations for patients with advanced melanoma treated with immune therapies. Cancer Immunol Res *3*, 288-295.

Jones, D.T., Trowbridge, I.S., and Harris, A.L. (2006). Effects of transferrin receptor blockade on cancer cell proliferation and hypoxia-inducible factor function and their differential regulation by ascorbate. Cancer Res *66*, 2749-2756.

Jorgensen, K., Davidson, B., and Florenes, V.A. (2006). Activation of c-jun N-terminal kinase is associated with cell proliferation and shorter relapse-free period in superficial spreading malignant melanoma. Mod Pathol *19*, 1446-1455.

Julien, L.A., Carriere, A., Moreau, J., and Roux, P.P. (2010). mTORC1-activated S6K1 phosphorylates Rictor on threonine 1135 and regulates mTORC2 signaling. Mol Cell Biol *30*, 908-921.

Kafka, A., Basic-Kinda, S., and Pecina-Slaus, N. (2014). The cellular story of dishevelleds. Croat Med J *55*, 459-467.

Kahana, O., Micksche, M., Witz, I.P., and Yron, I. (2002). The focal adhesion kinase (P125FAK) is constitutively active in human malignant melanoma. Oncogene *21*, 3969-3977.

Kang, H., Kim, H., Lee, S., Youn, H., and Youn, B. (2019). Role of Metabolic Reprogramming in Epithelial(-)Mesenchymal Transition (EMT). Int J Mol Sci *20*, 2042.

Kang, S., Oh, S.C., Min, B.W., and Lee, D.H. (2018). Transglutaminase 2 Regulates Self-renewal and Stem Cell Marker of Human Colorectal Cancer Stem Cells. Anticancer Res *38*, 787-794.

Kang, Y., and Massague, J. (2004). Epithelial-mesenchymal transitions: twist in development and metastasis. Cell *118*, 277-279.

Karre, K. (2002). NK cells, MHC class I molecules and the missing self. Scand J Immunol *55*, 221-228.

Kärre, K. (1985). Role of target histocompatibility antigens in regulation of natural killer activity: a reevaluation and a hypothesis. In: Callewaert D, Herberman RB, eds Mechanisms of Cytotoxicity by NK Cells San Diego: Academic Press, 81±91.

Kasioumi, P., Vrazeli, P., Vezyraki, P., Zerikiotis, S., Katsouras, C., Damalas, A., and Angelidis, C. (2019). Hsp70 (HSP70A1A) downregulation enhances the metastatic ability of cancer cells. Int J Oncol *54*, 821-832.

Kataoka, T.R., Ito, A., Asada, H., Watabe, K., Nishiyama, K., Nakamoto, K., Itami, S., Yoshikawa, K., Ito, M., Nojima, H.*, et al.* (2000). Annexin VII as a novel marker for invasive phenotype of malignant melanoma. Jpn J Cancer Res *91*, 75-83.

Kaufhold, S., and Bonavida, B. (2014). Central role of Snail1 in the regulation of EMT and resistance in cancer: a target for therapeutic intervention. J Exp Clin Cancer Res *33*, 62.

Keilholz, U., Mehnert, J.M., Bauer, S., Bourgeois, H., Patel, M.R., Gravenor, D., Nemunaitis, J.J., Taylor, M.H., Wyrwicz, L., Lee, K.W.*, et al.* (2019). Avelumab in patients with previously treated metastatic melanoma: phase 1b results from the JAVELIN Solid Tumor trial. J Immunother Cancer *7*, 12.

Khan, M., Arooj, S., and Wang, H. (2020). NK Cell-Based Immune Checkpoint Inhibition. Front Immunol *11*, 167.

Kiefel, H., Bondong, S., Pfeifer, M., Schirmer, U., Erbe-Hoffmann, N., Schafer, H., Sebens, S., and Altevogt, P. (2012). EMT-associated up-regulation of L1CAM provides insights into L1CAM-mediated integrin signalling and NF-kappaB activation. Carcinogenesis *33*, 1919-1929.

Kim, N.H., Cha, Y.H., Lee, J., Lee, S.H., Yang, J.H., Yun, J.S., Cho, E.S., Zhang, X., Nam, M., Kim, N.*, et al.* (2017). Snail reprograms glucose metabolism by repressing phosphofructokinase PFKP allowing cancer cell survival under metabolic stress. Nat Commun *8*, 14374.

Kirchberger, M.C., Ugurel, S., Mangana, J., Heppt, M.V., Eigentler, T.K., Berking, C., Schadendorf, D., Schuler, G., Dummer, R., and Heinzerling, L. (2018). MEK inhibition may increase survival of NRAS-mutated melanoma patients treated with checkpoint blockade: Results of a retrospective multicentre analysis of 364 patients. Eur J Cancer *98*, 10-16.

Kircher, D.A., Trombetti, K.A., Silvis, M.R., Parkman, G.L., Fischer, G.M., Angel, S.N., Stehn, C.M., Strain, S.C., Grossmann, A.H., Duffy, K.L.*, et al.* (2019). AKT1(E17K) Activates Focal Adhesion Kinase and Promotes Melanoma Brain Metastasis. Mol Cancer Res *17*, 1787-1800.

Kitano, S., Nakayama, T., and Yamashita, M. (2018). Biomarkers for Immune Checkpoint Inhibitors in Melanoma. Front Oncol *8*, 270.

Kleffel, S., Posch, C., Barthel, S.R., Mueller, H., Schlapbach, C., Guenova, E., Elco, C.P., Lee, N., Juneja, V.R., Zhan, Q.*, et al.* (2015). Melanoma Cell-Intrinsic PD-1 Receptor Functions Promote Tumor Growth. Cell *162*, 1242-1256.

Kleinschmidt, E.G., and Schlaepfer, D.D. (2017). Focal adhesion kinase signaling in unexpected places. Curr Opin Cell Biol *45*, 24-30.

Klingemann, H., Boissel, L., and Toneguzzo, F. (2016). Natural Killer Cells for Immunotherapy - Advantages of the NK-92 Cell Line over Blood NK Cells. Front Immunol *7*, 91.

Kloess, S., Kretschmer, A., Stahl, L., Fricke, S., and Koehl, U. (2019). CAR-Expressing Natural Killer Cells for Cancer Retargeting. Transfus Med Hemother *46*, 4-13.

Knorck, A., Marx, S., Friedmann, K.S., Zophel, S., Lieblang, L., Hassig, C., Muller, I., Pilch, J., Sester, U., Hoth, M.*, et al.* (2018). Quantity, quality, and functionality of peripheral blood cells derived from residual blood of different apheresis kits. Transfusion *58*, 1516-1526.

Koelblinger, P., Thuerigen, O., and Dummer, R. (2018). Development of encorafenib for BRAF-mutated advanced melanoma. Curr Opin Oncol *30*, 125-133.

Konjevic, G., Mirjacic Martinovic, K., Vuletic, A., Jovic, V., Jurisic, V., Babovic, N., and Spuzic, I. (2007). Low expression of CD161 and NKG2D activating NK receptor is associated with impaired NK cell cytotoxicity in metastatic melanoma patients. Clin Exp Metastasis *24*, 1-11.

Konjević, G., Vuletić, A., Martinović, K.M., and Džodić, R. (2017). The Role of Activating and Inhibitory NK Cell Receptors in Antitumor Immune Response. In Natural Killer Cells.

Kosnopfel, C., Sinnberg, T., Sauer, B., Busch, C., Niessner, H., Schmitt, A., Forchhammer, S., Grimmel, C., Mertens, P.R., Hailfinger, S.*, et al.* (2018). YB-1 Expression and Phosphorylation Regulate Tumorigenicity and Invasiveness in Melanoma by Influencing EMT. Mol Cancer Res *16*, 1149-1160.

Koul, D., Fu, J., Shen, R., LaFortune, T.A., Wang, S., Tiao, N., Kim, Y.W., Liu, J.L., Ramnarian, D., Yuan, Y., *et al.* (2012). Antitumor activity of NVP-BKM120--a selective pan class I PI3 kinase inhibitor showed differential forms of cell death based on p53 status of glioma cells. Clin Cancer Res *18*, 184-195.

Kozlowska, K., Cichorek, M., and Zurawska-Czupa, B. (1991). Heterogeneity of transplantable melanomas differing in the rate of growth and cellular differentiation in relation to their cell transglutaminase activity. Neoplasma *38*, 343-349.

Kruse, P.H., Matta, J., Ugolini, S., and Vivier, E. (2014). Natural cytotoxicity receptors and their ligands. Immunol Cell Biol *92*, 221-229.

Kudo-Saito, C., Shirako, H., Takeuchi, T., and Kawakami, Y. (2009). Cancer metastasis is accelerated through immunosuppression during Snail-induced EMT of cancer cells. Cancer Cell *15*, 195-206.

Kulichova, D., Danova, J., Kunte, C., Ruzicka, T., and Celko, A.M. (2014). Risk factors for malignant melanoma and preventive methods. Cutis *94*, 241-248.

Kulski, J.K. (2019). Long Noncoding RNA HCP5, a Hybrid HLA Class I Endogenous Retroviral Gene: Structure, Expression, and Disease Associations. Cells *8*, 480.

Kumar, R., Angelini, S., Czene, K., Sauroja, I., Hahka-Kemppinen, M., Pyrhonen, S., and Hemminki, K. (2003). BRAF mutations in metastatic melanoma: a possible association with clinical outcome. Clin Cancer Res *9*, 3362-3368.

Kumar, S. (2018). Natural killer cell cytotoxicity and its regulation by inhibitory receptors. Immunology *154*, 383-393.

Kummerow, C., Schwarz, E.C., Bufe, B., Zufall, F., Hoth, M., and Qu, B. (2014). A simple, economic, time-resolved killing assay. Eur J Immunol *44*, 1870-1872.

Kuphal, S., and Bosserhoff, A.K. (2006). Influence of the cytoplasmic domain of E-cadherin on endogenous N-cadherin expression in malignant melanoma. Oncogene *25*, 248-259.

Ladanyi, A. (2015). Prognostic and predictive significance of immune cells infiltrating cutaneous melanoma. Pigment Cell Melanoma Res *28*, 490-500.

Lade-Keller, J., Riber-Hansen, R., Guldberg, P., Schmidt, H., Hamilton-Dutoit, S.J., and Steiniche, T. (2013). E- to N-cadherin switch in melanoma is associated with decreased expression of phosphatase and tensin homolog and cancer progression. Br J Dermatol *169*, 618-628.

Lampugnani, M.G., Pedenovi, M., Niewiarowski, A., Casali, B., Donati, M.B., Corbascio, G.C., and Marchisio, P.C. (1987). Effects of dimethyl sulfoxide (DMSO) on microfilament organization, cellular adhesion, and growth of cultured mouse B16 melanoma cells. Exp Cell Res *172*, 385-396.

Lanier, L.L. (2005). NK cell recognition. Annu Rev Immunol *23*, 225-274.

Laplante, M., and Sabatini, D.M. (2012). mTOR signaling in growth control and disease. Cell *149*, 274-293.

Larkin, J., Chiarion-Sileni, V., Gonzalez, R., Grob, J.J., Cowey, C.L., Lao, C.D., Schadendorf, D., Dummer, R., Smylie, M., Rutkowski, P., *et al.* (2015). Combined Nivolumab and Ipilimumab or Monotherapy in Untreated Melanoma. N Engl J Med *373*, 23-34.

Larrea, M.D., Wander, S.A., and Slingerland, J.M. (2009). p27 as Jekyll and Hyde: regulation of cell cycle and cell motility. Cell Cycle *8*, 3455-3461.

Lasithiotakis, K.G., Sinnberg, T.W., Schittek, B., Flaherty, K.T., Kulms, D., Maczey, E., Garbe, C., and Meier, F.E. (2008). Combined inhibition of MAPK and mTOR signaling inhibits growth, induces cell death, and abrogates invasive growth of melanoma cells. J Invest Dermatol *128*, 2013-2023.

Lee, H.J., Li, C.F., Ruan, D., He, J., Montal, E.D., Lorenz, S., Girnun, G.D., and Chan, C.H. (2019). Non-proteolytic ubiquitination of Hexokinase 2 by HectH9 controls tumor metabolism and cancer stem cell expansion. Nat Commun *10*, 2625.

Lee, J., Li, L., Gretz, N., Gebert, J., and Dihlmann, S. (2012). Absent in Melanoma 2 (AIM2) is an important mediator of interferon-dependent and -independent HLA-DRA and HLA-DRB gene expression in colorectal cancers. Oncogene *31*, 1242-1253.

Lee, M.N., Ha, S.H., Kim, J., Koh, A., Lee, C.S., Kim, J.H., Jeon, H., Kim, D.H., Suh, P.G., and Ryu, S.H. (2009). Glycolytic flux signals to mTOR through glyceraldehyde-3-phosphate dehydrogenase-mediated regulation of Rheb. Mol Cell Biol *29*, 3991-4001.

Lee, N., Llano, M., Carretero, M., Ishitani, A., Navarro, F., Lopez-Botet, M., and Geraghty, D.E. (1998). HLA-E is a major ligand for the natural killer inhibitory receptor CD94/NKG2A. Proc Natl Acad Sci USA *95*, 5199-5204.

Lee, S.Y., Ju, M.K., Jeon, H.M., Lee, Y.J., Kim, C.H., Park, H.G., Han, S.I., and Kang, H.S. (2018). Oncogenic Metabolism Acts as a Prerequisite Step for Induction of Cancer Metastasis and Cancer Stem Cell Phenotype. Oxid Med Cell Longev *2018*, 1027453.

Lehmann, C., Zeis, M., and Uharek, L. (2001). Activation of natural killer cells with interleukin 2 (IL-2) and IL-12 increases perforin binding and subsequent lysis of tumour cells. Br J Haematol *114*, 660-665.

Leone, R.D., and Emens, L.A. (2018). Targeting adenosine for cancer immunotherapy. J Immunother Cancer *6*, 57.

Leu, J.I., Barnoud, T., Zhang, G., Tian, T., Wei, Z., Herlyn, M., Murphy, M.E., and George, D.L. (2017). Inhibition of stress-inducible HSP70 impairs mitochondrial proteostasis and function. Oncotarget *8*, 45656-45669.

Lever, J., Krzywinski, M., and Altman, N. (2017). Principal component analysis. Nat Methods *14*, 641-642.

Li, F.Z., Dhillon, A.S., Anderson, R.L., McArthur, G., and Ferrao, P.T. (2015a). Phenotype switching in melanoma: implications for progression and therapy. Front Oncol *5*, 31.

Li, G., Satyamoorthy, K., and Herlyn, M. (2001). N-cadherin-mediated intercellular interactions promote survival and migration of melanoma cells. Cancer Res *61*, 3819-3825.

Li, H., Chen, X., Gao, Y., Wu, J., Zeng, F., and Song, F. (2015b). XBP1 induces snail expression to promote epithelial- to-mesenchymal transition and invasion of breast cancer cells. Cell Signal *27*, 82-89.

Li, L., Yuan, H., Xie, W., Mao, J., Caruso, A.M., McMahon, A., Sussman, D.J., and Wu, D. (1999). Dishevelled proteins lead to two signaling pathways. Regulation of LEF-1 and c-Jun N-terminal kinase in mammalian cells. J Biol Chem *274*, 129-134.

Li, Y., Hofmann, M., Wang, Q., Teng, L., Chlewicki, L.K., Pircher, H., and Mariuzza, R.A. (2009). Structure of natural killer cell receptor KLRG1 bound to E-cadherin reveals basis for MHC-independent missing self recognition. Immunity *31*, 35-46.

Li, Y., and Sun, R. (2018). Tumor immunotherapy: New aspects of natural killer cells. Chin J Cancer Res *30*, 173-196.

Liang, X., Sun, R., Zhao, X., Zhang, Y., Gu, Q., Dong, X., Zhang, D., Sun, J., and Sun, B. (2017). Rictor regulates the vasculogenic mimicry of melanoma via the AKT-MMP-2/9 pathway. J Cell Mol Med *21*, 3579-3591.

Liao, Y., Smyth, G.K., and Shi, W. (2014). featureCounts: an efficient general purpose program for assigning sequence reads to genomic features. Bioinformatics *30*, 923-930.

Lim, E., Palmieri, C., and Tilley, W.D. (2016a). Renewed interest in the progesterone receptor in breast cancer. Br J Cancer *115*, 909-911.

Lim, S.O., Li, C.W., Xia, W., Lee, H.H., Chang, S.S., Shen, J., Hsu, J.L., Raftery, D., Djukovic, D., Gu, H.*, et al.* (2016b). EGFR Signaling Enhances Aerobic Glycolysis in Triple-Negative Breast Cancer Cells to Promote Tumor Growth and Immune Escape. Cancer Res *76*, 1284-1296.

Lin, C.Y., Tsai, P.H., Kandaswami, C.C., Chang, G.D., Cheng, C.H., Huang, C.J., Lee, P.P., Hwang, J.J., and Lee, M.T. (2011). Role of tissue transglutaminase 2 in the acquisition of a mesenchymal-like phenotype in highly invasive A431 tumor cells. Mol Cancer *10*, 87.

Liu, E., Marin, D., Banerjee, P., Macapinlac, H.A., Thompson, P., Basar, R., Nassif Kerbauy, L., Overman, B., Thall, P., Kaplan, M.*, et al.* (2020). Use of CAR-Transduced Natural Killer Cells in CD19-Positive Lymphoid Tumors. N Engl J Med *382*, 545-553.

Liu, G., Claret, F.X., Zhou, F., and Pan, Y. (2018). Jab1/COPS5 as a Novel Biomarker for Diagnosis, Prognosis, Therapy Prediction and Therapeutic Tools for Human Cancer. Front Pharmacol *9*, 135.

Liu, K., Tang, Z., Huang, A., Chen, P., Liu, P., Yang, J., Lu, W., Liao, J., Sun, Y., Wen, S.*, et al.* (2017a). Glyceraldehyde-3-phosphate dehydrogenase promotes cancer growth and metastasis through upregulation of SNAIL expression. Int J Oncol *50*, 252-262.

Liu, X., and Fan, D. (2015). The epithelial-mesenchymal transition and cancer stem cells: functional and mechanistic links. Curr Pharm Des *21*, 1279-1291.

Liu, X., Sun, Y., Ehrlich, M., Lu, T., Kloog, Y., Weinberg, R.A., Lodish, H.F., and Henis, Y.I. (2000). Disruption of TGF-beta growth inhibition by oncogenic ras is linked to p27Kip1 mislocalization. Oncogene *19*, 5926-5935.

Liu, Y., Cheng, Y., Xu, Y., Wang, Z., Du, X., Li, C., Peng, J., Gao, L., Liang, X., and Ma, C. (2017b). Increased expression of programmed cell death protein 1 on NK cells inhibits NK-cell-mediated anti-tumor function and indicates poor prognosis in digestive cancers. Oncogene *36*, 6143-6153.

Liu, Y.R., Sun, B., Zhao, X.L., Gu, Q., Liu, Z.Y., Dong, X.Y., Che, N., and Mo, J. (2013). Basal caspase-3 activity promotes migration, invasion, and vasculogenic mimicry formation of melanoma cells. Melanoma Res *23*, 243-253.

Lo, H.W., and Hung, M.C. (2006). Nuclear EGFR signalling network in cancers: linking EGFR pathway to cell cycle progression, nitric oxide pathway and patient survival. Br J Cancer *94*, 184-188.

Long, E.O., Kim, H.S., Liu, D., Peterson, M.E., and Rajagopalan, S. (2013). Controlling natural killer cell responses: integration of signals for activation and inhibition. Annu Rev Immunol *31*, 227-258.

Lopez-Bergami, P., Fitchman, B., and Ronai, Z. (2008). Understanding signaling cascades in melanoma. Photochem Photobiol *84*, 289-306.

Lopez-Soto, A., Huergo-Zapico, L., Galvan, J.A., Rodrigo, L., de Herreros, A.G., Astudillo, A., and Gonzalez, S. (2013). Epithelial-mesenchymal transition induces an antitumor immune response mediated by NKG2D receptor. J Immunol *190*, 4408-4419.

Lu, J., Tan, M., and Cai, Q. (2015). The Warburg effect in tumor progression: mitochondrial oxidative metabolism as an anti-metastasis mechanism. Cancer Lett *356*, 156-164.

Luna, J.I., Grossenbacher, S.K., Murphy, W.J., and Canter, R.J. (2017). Targeting Cancer Stem Cells with Natural Killer Cell Immunotherapy. Expert Opin Biol Ther *17*, 313-324.

Lunt, S.Y., and Vander Heiden, M.G. (2011). Aerobic glycolysis: meeting the metabolic requirements of cell proliferation. Annu Rev Cell Dev Biol *27*, 441-464.

Lv, D., Guo, L., Zhang, T., and Huang, L. (2017). PRAS40 signaling in tumor. Oncotarget *8*, 69076-69085.

Ma, X.H., Piao, S., Wang, D., McAfee, Q.W., Nathanson, K.L., Lum, J.J., Li, L.Z., and Amaravadi, R.K. (2011). Measurements of tumor cell autophagy predict invasiveness, resistance to chemotherapy, and survival in melanoma. Clin Cancer Res *17*, 3478-3489.

Ma, X.M., and Blenis, J. (2009). Molecular mechanisms of mTOR-mediated translational control. Nat Rev Mol Cell Biol *10*, 307-318.

Maccalli, C., Giannarelli, D., Chiarucci, C., Cutaia, O., Giacobini, G., Hendrickx, W., Amato, G., Annesi, D., Bedognetti, D., Altomonte, M*., et al.* (2017). Soluble NKG2D ligands are biomarkers associated with the clinical outcome to immune checkpoint blockade therapy of metastatic melanoma patients. Oncoimmunology *6*, e1323618.

Mace, P.D., Wallez, Y., Egger, M.F., Dobaczewska, M.K., Robinson, H., Pasquale, E.B., and Riedl, S.J. (2013). Structure of ERK2 bound to PEA-15 reveals a mechanism for rapid release of activated MAPK. Nat Commun *4*, 1681.

Madhunapantula, S.V., Sharma, A., and Robertson, G.P. (2007). PRAS40 deregulates apoptosis in malignant melanoma. Cancer Res *67*, 3626-3636.

Makinoshima, H., Takita, M., Matsumoto, S., Yagishita, A., Owada, S., Esumi, H., and Tsuchihara, K. (2014). Epidermal growth factor receptor (EGFR) signaling regulates global metabolic pathways in EGFR-mutated lung adenocarcinoma. J Biol Chem *289*, 20813-20823.

Malkomes, P., Lunger, I., Luetticke, A., Oppermann, E., Haetscher, N., Serve, H., Holzer, K., Bechstein, W.O., and Rieger, M.A. (2016). Selective AKT Inhibition by MK-2206 Represses Colorectal Cancer-Initiating Stem Cells. Ann Surg Oncol *23*, 2849-2857.

Mao, Y., Zhang, N., Xu, J., Ding, Z., Zong, R., and Liu, Z. (2012). Significance of heterogeneous Twist2 expression in human breast cancers. PLoS ONE *7*, e48178.

Marcais, A., Marotel, M., Degouve, S., Koenig, A., Fauteux-Daniel, S., Drouillard, A., Schlums, H., Viel, S., Besson, L., Allatif, O*., et al.* (2017). High mTOR activity is a hallmark of reactive natural killer cells and amplifies early signaling through activating receptors. Elife *6*.

Marcelina, E.J., Dorota, H.-Ł., and Malgorzata, P. (2016). Cadherins and their Role in Malignant Transformation: Implications for Skin Cancer Progression.

Marchion, D.C., Cottrill, H.M., Xiong, Y., Chen, N., Bicaku, E., Fulp, W.J., Bansal, N., Chon, H.S., Stickles, X.B., Kamath, S.G., *et al.* (2011). BAD phosphorylation determines ovarian cancer chemosensitivity and patient survival. Clin Cancer Res *17*, 6356-6366.

Martinez-Lostao, L., Anel, A., and Pardo, J. (2015). How Do Cytotoxic Lymphocytes Kill Cancer Cells? Clin Cancer Res *21*, 5047-5056.

Martinez-Ruiz, G., Maldonado, V., Ceballos-Cancino, G., Grajeda, J.P., and Melendez-Zajgla, J. (2008). Role of Smac/DIABLO in cancer progression. J Exp Clin Cancer Res *27*, 48.

Masui, K., Cavenee, W.K., and Mischel, P.S. (2014). mTORC2 in the center of cancer metabolic reprogramming. Trends Endocrinol Metab *25*, 364-373.

McGary, E.C., Onn, A., Mills, L., Heimberger, A., Eton, O., Thomas, G.W., Shtivelband, M., and Bar-Eli, M. (2004). Imatinib mesylate inhibits platelet-derived growth factor receptor phosphorylation of melanoma cells but does not affect tumorigenicity in vivo. J Invest Dermatol *122*, 400-405.

McNerney, M.E., Lee, K.M., and Kumar, V. (2005). 2B4 (CD244) is a non-MHC binding receptor with multiple functions on natural killer cells and CD8+ T cells. Mol Immunol *42*, 489-494.

MD Anderson (2019). Reverse Phase Protein Array (RPPA) Core Facility, Availabe from https://www.mdanderson.org/research/research-resources/core-facilities/functional-proteomics-rppa-core.html (13.11.2019).

Mehta, G.U., Malekzadeh, P., Shelton, T., White, D.E., Butman, J.A., Yang, J.C., Kammula, U.S., Goff, S.L., Rosenberg, S.A., and Sherry, R.M. (2018). Outcomes of Adoptive Cell Transfer With Tumor-infiltrating Lymphocytes for Metastatic Melanoma Patients With and Without Brain Metastases. J Immunother *41*, 241-247.

Melaiu, O., Catalano, C., De Santi, C., Cipollini, M., Figlioli, G., Pelle, L., Barone, E., Evangelista, M., Guazzelli, A., Boldrini, L., *et al.* (2017). Inhibition of the platelet-derived growth factor receptor beta (PDGFRB) using gene silencing, crenolanib besylate, or imatinib mesylate hampers the malignant phenotype of mesothelioma cell lines. Genes Cancer *8*, 438-452.

Melaiu, O., Lucarini, V., Cifaldi, L., and Fruci, D. (2019). Influence of the Tumor Microenvironment on NK Cell Function in Solid Tumors. Front Immunol *10*, 3038.

Mendez, R., Aptsiauri, N., Del Campo, A., Maleno, I., Cabrera, T., Ruiz-Cabello, F., Garrido, F., and Garcia-Lora, A. (2009). HLA and melanoma: multiple alterations in HLA class I and II expression in human melanoma cell lines from ESTDAB cell bank. Cancer Immunol Immunother *58*, 1507-1515.

Meng, Q., Wang, S., Tang, W., Wu, S., Gao, N., Zhang, C., Cao, X., Li, X., Zhang, Z., Aschner, M., *et al.* (2017). XRCC1 mediated the development of cervival cancer through a novel Sp1/Krox-20 swich. Oncotarget *8*, 86217-86226.

Menter, D.G., Patton, J.T., Updyke, T.V., Kerbel, R.S., Maamer, M., McIntire, L.V., and Nicolson, G.L. (1991). Transglutaminase stabilizes melanoma adhesion under laminar flow. Cell Biophys *18*, 123-143.

Menzies, A.M., and Long, G.V. (2014). Dabrafenib and trametinib, alone and in combination for BRAF-mutant metastatic melanoma. Clin Cancer Res *20*, 2035-2043.

Mergenthaler, P., Kahl, A., Kamitz, A., van Laak, V., Stohlmann, K., Thomsen, S., Klawitter, H., Przesdzing, I., Neeb, L., Freyer, D., *et al.* (2012). Mitochondrial hexokinase II (HKII) and phosphoprotein enriched in astrocytes (PEA15) form a molecular switch governing cellular fate depending on the metabolic state. Proc Natl Acad Sci USA *109*, 1518-1523.

Miller, A.J., and Mihm, M.C., Jr. (2006). Melanoma. N Engl J Med *355*, 51-65.

Miller, J.S., and Lanier, L.L. (2019). Natural Killer Cells in Cancer Immunotherapy. Annu Rev Cancer Biol *3*, 77-103.

Mitra, S.K., Hanson, D.A., and Schlaepfer, D.D. (2005). Focal adhesion kinase: in command and control of cell motility. Nat Rev Mol Cell Biol *6*, 56-68.

Molhoek, K.R., Brautigan, D.L., and Slingluff, C.L., Jr. (2005). Synergistic inhibition of human melanoma proliferation by combination treatment with B-Raf inhibitor BAY43-9006 and mTOR inhibitor Rapamycin. J Transl Med *3*, 39.

Molife, L.R., Yan, L., Vitfell-Rasmussen, J., Zernhelt, A.M., Sullivan, D.M., Cassier, P.A., Chen, E., Biondo, A., Tetteh, E., Siu, L.L.*, et al.* (2014). Phase 1 trial of the oral AKT inhibitor MK-2206 plus carboplatin/paclitaxel, docetaxel, or erlotinib in patients with advanced solid tumors. J Hematol Oncol *7*, 1.

Molina-Ortiz, I., Bartolome, R.A., Hernandez-Varas, P., Colo, G.P., and Teixido, J. (2009). Overexpression of E-cadherin on melanoma cells inhibits chemokine-promoted invasion involving p190RhoGAP/p120ctn-dependent inactivation of RhoA. J Biol Chem *284*, 15147-15157.

Morgado, S., Sanchez-Correa, B., Casado, J.G., Duran, E., Gayoso, I., Labella, F., Solana, R., and Tarazona, R. (2011). NK cell recognition and killing of melanoma cells is controlled by multiple activating receptor-ligand interactions. J Innate Immun *3*, 365-373.

Morris, J.C., Tan, A.R., Olencki, T.E., Shapiro, G.I., Dezube, B.J., Reiss, M., Hsu, F.J., Berzofsky, J.A., and Lawrence, D.P. (2014). Phase I study of GC1008 (fresolimumab): a human anti-transforming growth factor-beta (TGFbeta) monoclonal antibody in patients with advanced malignant melanoma or renal cell carcinoma. PLoS ONE *9*, e90353.

Munoz-Couselo, E., Adelantado, E.Z., Ortiz, C., Garcia, J.S., and Perez-Garcia, J. (2017). NRAS-mutant melanoma: current challenges and future prospect. Onco Targets Ther *10*, 3941-3947.

Murphy, K. (2012). Janeways Immunology. Garland Science, 8 edn, page 115 ff

Narayan, R.S., Fedrigo, C.A., Brands, E., Dik, R., Stalpers, L.J., Baumert, B.G., Slotman, B.J., Westerman, B.A., Peters, G.J., and Sminia, P. (2017). The allosteric AKT inhibitor MK2206 shows a synergistic interaction with chemotherapy and radiotherapy in glioblastoma spheroid cultures. BMC Cancer *17*, 204.

Narni-Mancinelli, E., Gauthier, L., Baratin, M., Guia, S., Fenis, A., Deghmane, A.E., Rossi, B., Fourquet, P., Escaliere, B., Kerdiles, Y.M.*, et al.* (2017). Complement factor P is a ligand for the natural killer cell-activating receptor NKp46. Sci Immunol *2*.

Nayyar, G., Chu, Y., and Cairo, M.S. (2019). Overcoming Resistance to Natural Killer Cell Based Immunotherapies for Solid Tumors. Front Oncol *9*, 51.

Ni, L., and Lu, J. (2018). Interferon gamma in cancer immunotherapy. Cancer Med *7*, 4509-4516.

Nianias, A., and Themeli, M. (2019). Induced Pluripotent Stem Cell (iPSC)-Derived Lymphocytes for Adoptive Cell Immunotherapy: Recent Advances and Challenges. Curr Hematol Malig Rep *14*, 261-268.

Nicholls, C., Li, H., and Liu, J.P. (2012). GAPDH: a common enzyme with uncommon functions. Clin Exp Pharmacol Physiol *39*, 674-679.

Nicholson, R.I., Gee, J.M., and Harper, M.E. (2001). EGFR and cancer prognosis. Eur J Cancer *37 Suppl 4*, S9-15.

Niehrs, A., and Altfeld, M. (2020). Regulation of NK-Cell Function by HLA Class II. Front Cell Infect Microbiol *10*, 55.

Niessner, H., Schmitz, J., Tabatabai, G., Schmid, A.M., Calaminus, C., Sinnberg, T., Weide, B., Eigentler, T.K., Garbe, C., Schittek, B.*, et al.* (2016). PI3K Pathway Inhibition Achieves Potent Antitumor Activity in Melanoma Brain Metastases In Vitro and In Vivo. Clin Cancer Res *22*, 5818-5828.

Nishimura, M., Mitsunaga, S., Akaza, T., Mitomi, Y., Tadokoro, K., and Juji, T. (1994). Protection against natural killer cells by interferon-gamma treatment of K562 cells cannot be explained by augmented major histocompatibility complex class I expression. Immunology *83*, 75-80.

Nitulescu, G.M., Margina, D., Juzenas, P., Peng, Q., Olaru, O.T., Saloustros, E., Fenga, C., Spandidos, D., Libra, M., and Tsatsakis, A.M. (2016). Akt inhibitors in cancer treatment: The long journey from drug discovery to clinical use (Review). Int J Oncol *48*, 869-885.

O'Donnell, J.S., Teng, M.W.L., and Smyth, M.J. (2019). Cancer immunoediting and resistance to T cell-based immunotherapy. Nat Rev Clin Oncol *16*, 151-167.

Okita, R., Mougiakakos, D., Ando, T., Mao, Y., Sarhan, D., Wennerberg, E., Seliger, B., Lundqvist, A., Mimura, K., and Kiessling, R. (2012). HER2/HER3 signaling regulates NK cell-mediated cytotoxicity via MHC class I chain-related molecule A and B expression in human breast cancer cell lines. J Immunol *188*, 2136-2145.

Okita, R., Shimizu, K., and Nakata, M. (2018). Epithelial-mesenchymal transition-induced metastasis could be a bait for natural killer cells. J Thorac Dis *10*, S3143-S3146.

Osborn, J.L., and Greer, S.F. (2015). Metastatic melanoma cells evade immune detection by silencing STAT1. Int J Mol Sci *16*, 4343-4361.

Paschen, A., Baingo, J., and Schadendorf, D. (2014). Expression of stress ligands of the immunoreceptor NKG2D in melanoma: regulation and clinical significance. Eur J Cell Biol *93*, 49-54.

Paschen, A., Sucker, A., Hill, B., Moll, I., Zapatka, M., Nguyen, X.D., Sim, G.C., Gutmann, I., Hassel, J., Becker, J.C*., et al.* (2009). Differential clinical significance of individual NKG2D ligands in melanoma: soluble ULBP2 as an indicator of poor prognosis superior to S100B. Clin Cancer Res *15*, 5208-5215.

Pastorino, J.G., and Hoek, J.B. (2003). Hexokinase II: the integration of energy metabolism and control of apoptosis. Curr Med Chem *10*, 1535-1551.

Patsos, G., Germann, A., Gebert, J., and Dihlmann, S. (2010). Restoration of absent in melanoma 2 (AIM2) induces G2/M cell cycle arrest and promotes invasion of colorectal cancer cells. Int J Cancer *126*, 1838-1849.

Paul, A., Krelin, Y., Arif, T., Jeger, R., and Shoshan-Barmatz, V. (2018). A New Role for the Mitochondrial Pro-apoptotic Protein SMAC/Diablo in Phospholipid Synthesis Associated with Tumorigenesis. Mol Ther *26*, 680-694.

Paul, S., Kulkarni, N., Shilpi, and Lal, G. (2016). Intratumoral natural killer cells show reduced effector and cytolytic properties and control the differentiation of effector Th1 cells. Oncoimmunology *5*, e1235106.

Paul, S., and Lal, G. (2017). The Molecular Mechanism of Natural Killer Cells Function and Its Importance in Cancer Immunotherapy. Front Immunol *8*, 1124.

Pena, J., Alonso, C., Solana, R., Serrano, R., Carracedo, J., and Ramirez, R. (1990). Natural killer susceptibility is independent of HLA class I antigen expression on cell lines obtained from human solid tumors. Eur J Immunol *20*, 2445-2448.

Pende, D., Rivera, P., Marcenaro, S., Chang, C.C., Biassoni, R., Conte, R., Kubin, M., Cosman, D., Ferrone, S., Moretta, L*., et al.* (2002). Major histocompatibility complex class I-related chain A and UL16-binding protein expression on tumor cell lines of different histotypes: analysis of tumor susceptibility to NKG2D-dependent natural killer cell cytotoxicity. Cancer Res *62*, 6178-6186.

Pesce, S., Greppi, M., Grossi, F., Del Zotto, G., Moretta, L., Sivori, S., Genova, C., and Marcenaro, E. (2019). PD/1-PD-Ls Checkpoint: Insight on the Potential Role of NK Cells. Front Immunol *10*, 1242.

Petrova, V., Arkhypov, I., Weber, R., Groth, C., Altevogt, P., Utikal, J., and Umansky, V. (2020). Modern Aspects of Immunotherapy with Checkpoint Inhibitors in Melanoma. Int J Mol Sci *21*, 2367.

Phan, G.Q., and Rosenberg, S.A. (2013). Adoptive cell transfer for patients with metastatic melanoma: the potential and promise of cancer immunotherapy. Cancer Control *20*, 289-297.

Phipps, L.E., Hino, S., and Muschel, R.J. (2011). Targeting cell spreading: a method of sensitizing metastatic tumor cells to TRAIL-induced apoptosis. Mol Cancer Res *9*, 249-258.

Pietra, G., Manzini, C., Rivara, S., Vitale, M., Cantoni, C., Petretto, A., Balsamo, M., Conte, R., Benelli, R., Minghelli, S*., et al.* (2012a). Melanoma cells inhibit natural killer cell function by modulating the expression of activating receptors and cytolytic activity. Cancer Res *72*, 1407-1415.

Pietra, G., Manzini, C., Vitale, M., Balsamo, M., Ognio, E., Boitano, M., Queirolo, P., Moretta, L., and Mingari, M.C. (2009). Natural killer cells kill human melanoma cells with characteristics of cancer stem cells. Int Immunol *21*, 793-801.

Pietra, G., Vitale, M., Moretta, L., and Mingari, M.C. (2012b). How melanoma cells inactivate NK cells. Oncoimmunology *1*, 974-975.

Pillet, A.H., Theze, J., and Rose, T. (2011). Interleukin (IL)-2 and IL-15 have different effects on human natural killer lymphocytes. Hum Immunol *72*, 1013-1017.

Placzek, W.J., Wei, J., Kitada, S., Zhai, D., Reed, J.C., and Pellecchia, M. (2010). A survey of the anti-apoptotic Bcl-2 subfamily expression in cancer types provides a platform to predict the efficacy of Bcl-2 antagonists in cancer therapy. Cell Death Dis *1*, e40.

Poli, A., Michel, T., Theresine, M., Andres, E., Hentges, F., and Zimmer, J. (2009). CD56bright natural killer (NK) cells: an important NK cell subset. Immunology *126*, 458-465.

Porta, C., Paglino, C., and Mosca, A. (2014). Targeting PI3K/Akt/mTOR Signaling in Cancer. Front Oncol *4*, 64.

Posch, C., Sanlorenzo, M., Vujic, I., Oses-Prieto, J.A., Cholewa, B.D., Kim, S.T., Ma, J., Lai, K., Zekhtser, M., Esteve-Puig, R., *et al.* (2016). Phosphoproteomic Analyses of NRAS(G12) and NRAS(Q61) Mutant Melanocytes Reveal Increased CK2alpha Kinase Levels in NRAS(Q61) Mutant Cells. J Invest Dermatol *136*, 2041-2048.

Poser, I., Dominguez, D., de Herreros, A.G., Varnai, A., Buettner, R., and Bosserhoff, A.K. (2001). Loss of E-cadherin expression in melanoma cells involves up-regulation of the transcriptional repressor Snail. J Biol Chem *276*, 24661-24666.

Postow, M.A., Callahan, M.K., and Wolchok, J.D. (2015). Immune Checkpoint Blockade in Cancer Therapy. J Clin Oncol *33*, 1974-1982.

Potrony, M., Badenas, C., Aguilera, P., Puig-Butille, J.A., Carrera, C., Malvehy, J., and Puig, S. (2015). Update in genetic susceptibility in melanoma. Ann Transl Med *3*, 210.

Poynter, J.N., Elder, J.T., Fullen, D.R., Nair, R.P., Soengas, M.S., Johnson, T.M., Redman, B., Thomas, N.E., and Gruber, S.B. (2006). BRAF and NRAS mutations in melanoma and melanocytic nevi. Melanoma Res *16*, 267-273.

Prickett, T.D., Agrawal, N.S., Wei, X., Yates, K.E., Lin, J.C., Wunderlich, J.R., Cronin, J.C., Cruz, P., Rosenberg, S.A., and Samuels, Y. (2009). Analysis of the tyrosine kinome in melanoma reveals recurrent mutations in ERBB4. Nat Genet *41*, 1127-1132.

Proud, C.G. (2011). mTOR Signalling in Health and Disease. Biochem Soc Trans *39*, 431-436.

Raisova, M., Hossini, A.M., Eberle, J., Riebeling, C., Wieder, T., Sturm, I., Daniel, P.T., Orfanos, C.E., and Geilen, C.C. (2001). The Bax/Bcl-2 ratio determines the susceptibility of human melanoma cells to CD95/Fas-mediated apoptosis. J Invest Dermatol *117*, 333-340.

Rajagopalan, S., and Long, E.O. (2013). Found: a cellular activating ligand for NKp44. Blood *122*, 2921-2922.

Ramaraj, P., and Cox, J.L. (2014). In vitro effect of progesterone on human melanoma (BLM) cell growth. Int J Clin Exp Med *7*, 3941-3953.

Ramos, D., Pellin-Carcelen, A., Agusti, J., Murgui, A., Jorda, E., Pellin, A., and Monteagudo, C. (2015). Deregulation of glyceraldehyde-3-phosphate dehydrogenase expression during tumor progression of human cutaneous melanoma. Anticancer Res *35*, 439-444.

Ran, C., Liu, H., Hitoshi, Y., and Israel, M.A. (2013). Proliferation-independent control of tumor glycolysis by PDGFR-mediated AKT activation. Cancer Res *73*, 1831-1843.

Rana, R., Vitale, M., Mazzotti, G., Manzoli, L., and Papa, S. (1990). Radiosensitivity of human natural killer cells: binding and cytotoxic activities of natural killer cell subsets. Radiat Res *124*, 96-102.

Raulet, D.H. (2003). Roles of the NKG2D immunoreceptor and its ligands. Nat Rev Immunol *3*, 781-790.

Rebecca, V.W., Massaro, R.R., Fedorenko, I.V., Sondak, V.K., Anderson, A.R., Kim, E., Amaravadi, R.K., Maria-Engler, S.S., Messina, J.L., Gibney, G.T., *et al.* (2014). Inhibition of autophagy enhances the effects of the AKT inhibitor MK-2206 when combined with paclitaxel and carboplatin in BRAF wild-type melanoma. Pigment Cell Melanoma Res *27*, 465-478.

Reiter, Z., Reiter, Y., Fishelson, Z., Shinitzky, M., Kessler, A., Loyter, A., Nussbaum, O., and Rubinstein, M. (1991). Resistance to NK Cell-Mediated Cytotoxicity (in K-562 Cells) does not Correlate with Class I MHC Antigen Levels. Immunobiology *183*, 23-39.

Ricaniadis, N., Kataki, A., Agnantis, N., Androulakis, G., and Karakousis, C.P. (2001). Long-term prognostic significance of HSP-70, c-myc and HLA-DR expression in patients with malignant melanoma. Eur J Surg Oncol *27*, 88-93.

Robert-Koch-Institut, and e.V., G.d.e.K.i.D. (2017). Krebs in Deutschland 2013-2014 (Berlin).

Robinson, T.O., and Schluns, K.S. (2017). The potential and promise of IL-15 in immuno-oncogenic therapies. Immunol Lett *190*, 159-168.

Rohaan, M.W., van den Berg, J.H., Kvistborg, P., and Haanen, J. (2018). Adoptive transfer of tumor-infiltrating lymphocytes in melanoma: a viable treatment option. J Immunother Cancer *6*, 102.

Rosenberg, S.A., Mule, J.J., Spiess, P.J., Reichert, C.M., and Schwarz, S.L. (1985). Regression of established pulmonary metastases and subcutaneous tumor mediated by the systemic administration of high-dose recombinant interleukin 2. J Exp Med *161*, 1169-1188.

Rosenberg, S.A., Niglio, S.A., Salehomoum, N., Chan, J.L., Jeong, B.S., Wen, Y., Li, J., Fukui, J., Chen, S., Shin, S.S., *et al.* (2015). Targeting Glutamatergic Signaling and the PI3 Kinase Pathway to Halt Melanoma Progression. Transl Oncol *8*, 1-9.

Rowshanravan, B., Halliday, N., and Sansom, D.M. (2018). CTLA-4: a moving target in immunotherapy. Blood *131*, 58-67.

Ruiz-Garcia, R., Vargas-Hernandez, A., Chinn, I.K., Angelo, L.S., Cao, T.N., Coban-Akdemir, Z., Jhangiani, S.N., Meng, Q., Forbes, L.R., Muzny, D.M., *et al.* (2018). Mutations in PI3K110delta cause impaired natural killer cell function partially rescued by rapamycin treatment. J Allergy Clin Immunol *142*, 605-617 e607.

Russell, J.H., and Ley, T.J. (2002). Lymphocyte-mediated cytotoxicity. Annu Rev Immunol *20*, 323-370.

Saenz-Santamaria, M.C., Reed, J.A., McNutt, N.S., and Shea, C.R. (1994). Immunohistochemical expression of BCL-2 in melanomas and intradermal nevi. J Cutan Pathol *21*, 393-397.

Saint-Jean, M., Knol, A.C., Volteau, C., Quereux, G., Peuvrel, L., Brocard, A., Pandolfino, M.C., Saiagh, S., Nguyen, J.M., Bedane, C., *et al.* (2018). Adoptive Cell Therapy with Tumor-Infiltrating Lymphocytes in Advanced Melanoma Patients. J Immunol Res *2018*, 3530148.

Salcedo, T.W., Azzoni, L., Wolf, S.F., and Perussia, B. (1993). Modulation of perforin and granzyme messenger RNA expression in human natural killer cells. J Immunol *151*, 2511-2520.

Salih, H.R., Rammensee, H.G., and Steinle, A. (2002). Cutting edge: down-regulation of MICA on human tumors by proteolytic shedding. J Immunol *169*, 4098-4102.

Samatar, A.A., and Poulikakos, P.I. (2014). Targeting RAS-ERK signalling in cancer: promises and challenges. Nat Rev Drug Discov *13*, 928-942.

Sanki, A., Li, W., Colman, M., Karim, R.Z., Thompson, J.F., and Scolyer, R.A. (2007). Reduced expression of p16 and p27 is correlated with tumour progression in cutaneous melanoma. Pathology *39*, 551-557.

Sanseviero, E., O'Brien, E.M., Karras, J.R., Shabaneh, T.B., Aksoy, B.A., Xu, W., Zheng, C., Yin, X., Xu, X., Karakousis, G.C., *et al.* (2019). Anti-CTLA-4 Activates Intratumoral NK Cells and Combined with IL15/IL15Ralpha Complexes Enhances Tumor Control. Cancer Immunol Res *7*, 1371-1380.

Sarbassov, D.D., Ali, S.M., Sengupta, S., Sheen, J.H., Hsu, P.P., Bagley, A.F., Markhard, A.L., and Sabatini, D.M. (2006). Prolonged rapamycin treatment inhibits mTORC2 assembly and Akt/PKB. Mol Cell *22*, 159-168.

Sarbassov, D.D., Guertin, D.A., Ali, S.M., and Sabatini, D.M. (2005). Phosphorylation and regulation of Akt/PKB by the rictor-mTOR complex. Science (80-) *307*, 1098-1101.

Sarin, A., Saxena, Q.B., Herberman, R.B., and Saxena, R.K. (1995). Enhanced MHC I antigen expression on tumour target cells is inversely correlated to lysis by allogenic but not by xenogenic NK cells. J Biosci *20*, 515-523.

Satyamoorthy, K., Li, G., Gerrero, M.R., Brose, M.S., Volpe, P., Weber, B.L., Van Belle, P., Elder, D.E., and Herlyn, M. (2003). Constitutive mitogen-activated protein kinase activation in melanoma is mediated by both BRAF mutations and autocrine growth factor stimulation. Cancer Res *63*, 756-759.

Saxton, R.A., and Sabatini, D.M. (2017). mTOR Signaling in Growth, Metabolism, and Disease. Cell *168*, 960-976.

Scherer, D., and Kumar, R. (2010). Genetics of pigmentation in skin cancer--a review. Mutat Res *705*, 141-153.

Schittek, B., Psenner, K., Sauer, B., Meier, F., Iftner, T., and Garbe, C. (2007). The increased expression of Y box-binding protein 1 in melanoma stimulates proliferation and tumor invasion, antagonizes apoptosis and enhances chemoresistance. Int J Cancer *120*, 2110-2118.

Schmidt, K.M., Dietrich, P., Hackl, C., Guenzle, J., Bronsert, P., Wagner, C., Fichtner-Feigl, S., Schlitt, H.J., Geissler, E.K., Hellerbrand, C., *et al.* (2018). Inhibition of mTORC2/RICTOR Impairs Melanoma Hepatic Metastasis. Neoplasia *20*, 1198-1208.

Schreiber, R.D., Old, L.J., and Smyth, M.J. (2011). Cancer immunoediting: integrating immunity's roles in cancer suppression and promotion. Science (80-) *331*, 1565-1570.

Seidel, J.A., Otsuka, A., and Kabashima, K. (2018). Anti-PD-1 and Anti-CTLA-4 Therapies in Cancer: Mechanisms of Action, Efficacy, and Limitations. Front Oncol *8*, 86.

Seki, H., Kanegane, H., Iwai, K., Konno, A., Ohta, K., Yachie, A., Taniguchi, N., and Miyawaki, T. (1994). Ionizing radiation induces apoptotic cell death in human TcR-gamma/delta+ T and natural killer cells without detectable p53 protein. Eur J Immunol *24*, 2914-2917.

Seliger, B., Maio, M., Cuaia, O., and Calabro, L. (2013). Expression and function of CTLA4 in melanoma. Journal of Clinical Oncology *31*, e20040-e20040.

Seshacharyulu, P., Ponnusamy, M.P., Haridas, D., Jain, M., Ganti, A.K., and Batra, S.K. (2012). Targeting the EGFR signaling pathway in cancer therapy. Expert Opin Ther Targets *16*, 15-31.

Shain, A.H., and Bastian, B.C. (2016). From melanocytes to melanomas. Nat Rev Cancer *16*, 345-358.

Shen, J., Pan, J., Du, C., Si, W., Yao, M., Xu, L., Zheng, H., Xu, M., Chen, D., Wang, S.*, et al.* (2017). Silencing NKG2D ligand-targeting miRNAs enhances natural killer cell-mediated cytotoxicity in breast cancer. Cell Death Dis *8*, e2740.

Shen, Y., Li, X., Dong, D., Zhang, B., Xue, Y., and Shang, P. (2018). Transferrin receptor 1 in cancer: a new sight for cancer therapy. Am J Cancer Res *8*, 916-931.

Sherman, M.Y., and Gabai, V.L. (2015). Hsp70 in cancer: back to the future. Oncogene *34*, 4153-4161.

Shi, H., Kong, X., Ribas, A., and Lo, R.S. (2011). Combinatorial treatments that overcome PDGFRbeta-driven resistance of melanoma cells to V600EB-RAF inhibition. Cancer Res *71*, 5067-5074.

Shi, W., Chen, Z., Li, L., Liu, H., Zhang, R., Cheng, Q., Xu, D., and Wu, L. (2019). Unravel the molecular mechanism of XBP1 in regulating the biology of cancer cells. J Cancer *10*, 2035-2046.

Shields, B.D., Koss, B., Mahmoud, F., Byrum, S.D., and Tackett, A.J. (2018). Abstract 2037: E-cadherin enhances immune control of metastatic melanoma. Cancer Res *78*, 2037-2037.

Shimasaki, N., Jain, A., and Campana, D. (2020). NK cells for cancer immunotherapy. Nat Rev Drug Discov *19*, 200-218.

Siegel, R.L., Miller, K.D., and Jemal, A. (2019). Cancer statistics, 2019. CA Cancer J Clin *69*, 7-34.

Simpson, L., and Parsons, R. (2001). PTEN: life as a tumor suppressor. Exp Cell Res *264*, 29-41.

Singh, A., and Settleman, J. (2010). EMT, cancer stem cells and drug resistance: an emerging axis of evil in the war on cancer. Oncogene *29*, 4741-4751.

Sinnberg, T., Sauer, B., Holm, P., Spangler, B., Kuphal, S., Bosserhoff, A., and Schittek, B. (2012). MAPK and PI3K/AKT mediated YB-1 activation promotes melanoma cell proliferation which is counteracted by an autoregulatory loop. Exp Dermatol *21*, 265-270.

Siu, M.K.Y., Jiang, Y.X., Wang, J.J., Leung, T.H.Y., Han, C.Y., Tsang, B.K., Cheung, A.N.Y., Ngan, H.Y.S., and Chan, K.K.L. (2019). Hexokinase 2 Regulates Ovarian Cancer Cell Migration, Invasion and Stemness via FAK/ERK1/2/MMP9/NANOG/SOX9 Signaling Cascades. Cancers (Basel) *11*, 813.

Sivori, S., Vacca, P., Del Zotto, G., Munari, E., Mingari, M.C., and Moretta, L. (2019). Human NK cells: surface receptors, inhibitory checkpoints, and translational applications. Cell Mol Immunol *16*, 430-441.

Smith-Garvin, J.E., Koretzky, G.A., and Jordan, M.S. (2009). T cell activation. Annu Rev Immunol *27*, 591-619.

Smolarz, B., Michalska, M.M., Samulak, D., Romanowicz, H., and Wojcik, L. (2019). Polymorphism of DNA repair genes in breast cancer. Oncotarget *10*, 527-535.

Sonder, S.L., Boye, T.L., Tolle, R., Dengjel, J., Maeda, K., Jaattela, M., Simonsen, A.C., Jaiswal, J.K., and Nylandsted, J. (2019). Annexin A7 is required for ESCRT III-mediated plasma membrane repair. Sci Rep *9*, 6726.

Souza-Fonseca-Guimaraes, F., Cursons, J., and Huntington, N.D. (2019). The Emergence of Natural Killer Cells as a Major Target in Cancer Immunotherapy. Trends Immunol *40*, 142-158.

Speranza, M.C., Nowicki, M.O., Behera, P., Cho, C.F., Chiocca, E.A., and Lawler, S.E. (2016). BKM-120 (Buparlisib): A Phosphatidyl-Inositol-3 Kinase Inhibitor with Anti-Invasive Properties in Glioblastoma. Sci Rep *6*, 20189.

Steelman, L.S., Bertrand, F.E., and McCubrey, J.A. (2004). The complexity of PTEN: mutation, marker and potential target for therapeutic intervention. Expert Opin Ther Targets *8*, 537-550.

Steller, E.J., Raats, D.A., Koster, J., Rutten, B., Govaert, K.M., Emmink, B.L., Snoeren, N., van Hooff, S.R., Holstege, F.C., Maas, C.*, et al.* (2013). PDGFRB promotes liver metastasis formation of mesenchymal-like colorectal tumor cells. Neoplasia *15*, 204-217.

Stickles, X.B., Marchion, D.C., Bicaku, E., Al Sawah, E., Abbasi, F., Xiong, Y., Bou Zgheib, N., Boac, B.M., Orr, B.C., Judson, P.L.*, et al.* (2015). BAD-mediated apoptotic pathway is associated with human cancer development. Int J Mol Med *35*, 1081-1087.

Stojanovic, A., Correia, M.P., and Cerwenka, A. (2013). Shaping of NK cell responses by the tumor microenvironment. Cancer Microenviron *6*, 135-146.

Stratford, A.L., Habibi, G., Astanehe, A., Jiang, H., Hu, K., Park, E., Shadeo, A., Buys, T.P., Lam, W., Pugh, T.*, et al.* (2007). Epidermal growth factor receptor (EGFR) is transcriptionally induced by the Y-box binding protein-1 (YB-1) and can be inhibited with Iressa in basal-like breast cancer, providing a potential target for therapy. Breast Cancer Res *9*, R61.

Straume, O., Shimamura, T., Lampa, M.J., Carretero, J., Oyan, A.M., Jia, D., Borgman, C.L., Soucheray, M., Downing, S.R., Short, S.M.*, et al.* (2012). Suppression of heat shock protein 27 induces long-term dormancy in human breast cancer. Proc Natl Acad Sci USA *109*, 8699-8704.

Strojan, P. (2010). Role of radiotherapy in melanoma management. Radiol Oncol *44*, 1-12.

Suck, G., Odendahl, M., Nowakowska, P., Seidl, C., Wels, W.S., Klingemann, H.G., and Tonn, T. (2016). NK-92: an 'off-the-shelf therapeutic' for adoptive natural killer cell-based cancer immunotherapy. Cancer Immunol Immunother *65*, 485-492.

Sullivan, R.J., Hamid, O., Gonzalez, R., Infante, J.R., Patel, M.R., Hodi, F.S., Lewis, K.D., Tawbi, H.A., Hernandez, G., Wongchenko, M.J.*, et al.* (2019). Atezolizumab plus cobimetinib and vemurafenib in BRAF-mutated melanoma patients. Nat Med *25*, 929-935.

Sultan, M., Coyle, K.M., Vidovic, D., Thomas, M.L., Gujar, S., and Marcato, P. (2017). Hide-and-seek: the interplay between cancer stem cells and the immune system. Carcinogenesis *38*, 107-118.

Sulzmaier, F., Opoku-Ansah, J., and Ramos, J.W. (2012). Phosphorylation is the switch that turns PEA-15 from tumor suppressor to tumor promoter. Small GTPases *3*, 173-177.

Sun, T., Zhao, N., Zhao, X.L., Gu, Q., Zhang, S.W., Che, N., Wang, X.H., Du, J., Liu, Y.X., and Sun, B.C. (2010). Expression and functional significance of Twist1 in hepatocellular carcinoma: its role in vasculogenic mimicry. Hepatology *51*, 545-556.

Sun, X., Ou, Z., Xie, M., Kang, R., Fan, Y., Niu, X., Wang, H., Cao, L., and Tang, D. (2015). HSPB1 as a novel regulator of ferroptotic cancer cell death. Oncogene *34*, 5617-5625.

Tait, S.W., Parsons, M.J., Llambi, F., Bouchier-Hayes, L., Connell, S., Munoz-Pinedo, C., and Green, D.R. (2010). Resistance to caspase-independent cell death requires persistence of intact mitochondria. Dev Cell *18*, 802-813.

Tanaka, J., and Miller, J.S. (2020). Recent progress in and challenges in cellular therapy using NK cells for hematological malignancies. Blood Rev, 100678.

Tang, Z., Yuan, S., Hu, Y., Zhang, H., Wu, W., Zeng, Z., Yang, J., Yun, J., Xu, R., and Huang, P. (2012). Over-expression of GAPDH in human colorectal carcinoma as a preferred target of 3-bromopyruvate propyl ester. J Bioenerg Biomembr *44*, 117-125.

Tao, S., He, Y., Ying, Y., He, J., Zhu, F., and Lv, H. (2014). P061. Hum Immunol *75*, 94.

Tarze, A., Deniaud, A., Le Bras, M., Maillier, E., Molle, D., Larochette, N., Zamzami, N., Jan, G., Kroemer, G., and Brenner, C. (2007). GAPDH, a novel regulator of the pro-apoptotic mitochondrial membrane permeabilization. Oncogene *26*, 2606-2620.

Terren, I., Orrantia, A., Vitalle, J., Zenarruzabeitia, O., and Borrego, F. (2019). NK Cell Metabolism and Tumor Microenvironment. Front Immunol *10*, 2278.

Terry, S., Savagner, P., Ortiz-Cuaran, S., Mahjoubi, L., Saintigny, P., Thiery, J.P., and Chouaib, S. (2017). New insights into the role of EMT in tumor immune escape. Mol Oncol *11*, 824-846.

The Skin Cancer Foundation (2020). Melanoma treatment. Availbe from https://www.skincancer.org/skin-cancer-information/melanoma/melanoma-treatments/ (29.02.2020).

Thomas, N.E., Busam, K.J., From, L., Kricker, A., Armstrong, B.K., Anton-Culver, H., Gruber, S.B., Gallagher, R.P., Zanetti, R., Rosso, S., *et al.* (2013). Tumor-infiltrating lymphocyte grade in primary melanomas is independently associated with melanoma-specific survival in the population-based genes, environment and melanoma study. J Clin Oncol *31*, 4252-4259.

Tibes, R., Qiu, Y., Lu, Y., Hennessy, B., Andreeff, M., Mills, G.B., and Kornblau, S.M. (2006). Reverse phase protein array: validation of a novel proteomic technology and utility for analysis of primary leukemia specimens and hematopoietic stem cells. Mol Cancer Ther *5*, 2512-2521.

Tóth, J., and Kubeš, M. (1993). Masking of HLA class I molecules expressed on K-562 target cells can restore their susceptibility to NK cell cytolysis. Immunobiology *188*, 134-144.

Tremblay-McLean, A., Coenraads, S., Kiani, Z., Dupuy, F.P., and Bernard, N.F. (2019). Expression of ligands for activating natural killer cell receptors on cell lines commonly used to assess natural killer cell function. BMC Immunol *20*, 8.

Trowbridge, I.S., and Omary, M.B. (1981). Human cell surface glycoprotein related to cell proliferation is the receptor for transferrin. Proc Natl Acad Sci USA *78*, 3039-3043.

Ueno, T., Elmberger, G., Weaver, T.E., Toi, M., and Linder, S. (2008). The aspartic protease napsin A suppresses tumor growth independent of its catalytic activity. Lab Invest *88*, 256-263.

Ueno, T., Linder, S., and Elmberger, G. (2003). Aspartic proteinase napsin is a useful marker for diagnosis of primary lung adenocarcinoma. Br J Cancer *88*, 1229-1233.

Urick, M.E., Rudd, M.L., Godwin, A.K., Sgroi, D., Merino, M., and Bell, D.W. (2011). PIK3R1 (p85alpha) is somatically mutated at high frequency in primary endometrial cancer. Cancer Res *71*, 4061-4067.

Vahedi, S., Chueh, F.Y., Chandran, B., and Yu, C.L. (2015). Lymphocyte-specific protein tyrosine kinase (Lck) interacts with CR6-interacting factor 1 (CRIF1) in mitochondria to repress oxidative phosphorylation. BMC Cancer *15*, 551.

Vallejo-Diaz, J., Chagoyen, M., Olazabal-Moran, M., Gonzalez-Garcia, A., and Carrera, A.C. (2019). The Opposing Roles of PIK3R1/p85alpha and PIK3R2/p85beta in Cancer. Trends Cancer *5*, 233-244.

van den Oord, J.J., Vandeghinste, N., De Ley, M., and De Wolf-Peeters, C. (1994). Bcl-2 expression in human melanocytes and melanocytic tumors. Am J Pathol *145*, 294-300.

van Groningen, J.J., Klink, S.L., Bloemers, H.P., and Swart, G.W. (1995). Expression of tissue-type transglutaminase correlates positively with metastatic properties of human melanoma cell lines. Int J Cancer *60*, 383-387.

van Kilsdonk, J.W., Takahashi, N., Weidle, U., Burtscher, H., Jarry, J., Daha, M.R., Swart, G.W., and van Kempen, L.C. (2012). Modulation of activated leukocyte cell adhesion molecule-mediated invasion triggers an innate immune gene response in melanoma. J Invest Dermatol *132*, 1462-1470.

Verhagen, A.M., Ekert, P.G., Pakusch, M., Silke, J., Connolly, L.M., Reid, G.E., Moritz, R.L., Simpson, R.J., and Vaux, D.L. (2000). Identification of DIABLO, a Mammalian Protein that Promotes Apoptosis by Binding to and Antagonizing IAP Proteins. Cell *102*, 43-53.

Verma, A., and Mehta, K. (2007). Tissue transglutaminase-mediated chemoresistance in cancer cells. Drug Resist Updat *10*, 144-151.

Vetter, C.S., Groh, V., thor Straten, P., Spies, T., Brocker, E.B., and Becker, J.C. (2002). Expression of stress-induced MHC class I related chain molecules on human melanoma. J Invest Dermatol *118*, 600-605.

Viel, S., Marcais, A., Guimaraes, F.S., Loftus, R., Rabilloud, J., Grau, M., Degouve, S., Djebali, S., Sanlaville, A., Charrier, E., *et al.* (2016). TGF-beta inhibits the activation and functions of NK cells by repressing the mTOR pathway. Sci Signal *9*, ra19.

Viglietto, G., Motti, M.L., Bruni, P., Melillo, R.M., D'Alessio, A., Califano, D., Vinci, F., Chiappetta, G., Tsichlis, P., Bellacosa, A., *et al.* (2002). Cytoplasmic relocalization and inhibition of the cyclin-dependent kinase inhibitor p27(Kip1) by PKB/Akt-mediated phosphorylation in breast cancer. Nat Med *8*, 1136-1144.

Vivier, E., Ugolini, S., Blaise, D., Chabannon, C., and Brossay, L. (2012). Targeting natural killer cells and natural killer T cells in cancer. Nat Rev Immunol *12*, 239-252.

Vlaykova, T., Talve, L., Hahka-Kemppinen, M., Hernberg, M., Muhonen, T., Collan, Y., and Pyrhonen, S. (2002). Immunohistochemically detectable bcl-2 expression in metastatic melanoma: association with survival and treatment response. Oncology *62*, 259-268.

Vyas, M., Reinartz, S., Hoffmann, N., Reiners, K.S., Lieber, S., Jansen, J.M., Wagner, U., Muller, R., and von Strandmann, E.P. (2017). Soluble NKG2D ligands in the ovarian cancer microenvironment are associated with an adverse clinical outcome and decreased memory effector T cells independent of NKG2D downregulation. Oncoimmunology *6*, e1339854.

Wander, S.A., Zhao, D., and Slingerland, J.M. (2011). p27: a barometer of signaling deregulation and potential predictor of response to targeted therapies. Clin Cancer Res *17*, 12-18.

Wang, K., Han, Y., Cho, W.C., and Zhu, H. (2019). The rise of human stem cell-derived natural killer cells for cancer immunotherapy. Expert Opin Biol Ther *19*, 141-148.

Wang, L., Schumann, U., Liu, Y., Prokopchuk, O., and Steinacker, J.M. (2012). Heat shock protein 70 (Hsp70) inhibits oxidative phosphorylation and compensates ATP balance through enhanced glycolytic activity. J Appl Physiol *113*, 1669-1676.

Wang, Y., Shi, J., Chai, K., Ying, X., and Zhou, B.P. (2013). The Role of Snail in EMT and Tumorigenesis. Curr Cancer Drug Targets *13*, 963-972.

Wee, P., and Wang, Z. (2017). Epidermal Growth Factor Receptor Cell Proliferation Signaling Pathways. Cancers (Basel) *9*, 52.

Wei, J., Wang, L., Zhu, J., Sun, A., Yu, G., Chen, M., Huang, P., Liu, H., Shao, G., Yang, W.*, et al.* (2019a). The Hippo signaling effector WWTR1 is a metastatic biomarker of gastric cardia adenocarcinoma. Cancer Cell Int *19*, 74.

Wei, S.C., Duffy, C.R., and Allison, J.P. (2018). Fundamental Mechanisms of Immune Checkpoint Blockade Therapy. Cancer Discov *8*, 1069-1086.

Wei, X., Gu, X., Ma, M., and Lou, C. (2019b). Long noncoding RNA HCP5 suppresses skin cutaneous melanoma development by regulating RARRES3 gene expression via sponging miR-12. Onco Targets Ther *12*, 6323-6335.

Weinberg, F., Ramnath, N., and Nagrath, D. (2019). Reactive Oxygen Species in the Tumor Microenvironment: An Overview. Cancers (Basel) *11*.

Whiteman, D.C., Whiteman, C.A., and Green, A.C. (2001). Childhood sun exposure as a risk factor for melanoma: a systematic review of epidemiologic studies. Cancer Causes and Control *12*, 69–82.

Wieczorek, M., Abualrous, E.T., Sticht, J., Alvaro-Benito, M., Stolzenberg, S., Noe, F., and Freund, C. (2017). Major Histocompatibility Complex (MHC) Class I and MHC Class II Proteins: Conformational Plasticity in Antigen Presentation. Front Immunol *8*, 292.

Williams, B.A., Wang, X.H., Leyton, J.V., Maghera, S., Deif, B., Reilly, R.M., Minden, M.D., and Keating, A. (2018). CD16(+)NK-92 and anti-CD123 monoclonal antibody prolongs survival in primary human acute myeloid leukemia xenografted mice. Haematologica *103*, 1720-1729.

Wilson, M.A., and Schuchter, L.M. (2016). Chemotherapy for Melanoma. Cancer Treat Res *167*, 209-229.

Winder, A., Unno, K., Yu, Y., Lurain, J., and Kim, J.J. (2017). The allosteric AKT inhibitor, MK2206, decreases tumor growth and invasion in patient derived xenografts of endometrial cancer. Cancer Biol Ther *18*, 958-964.

World Health organization (2020). FAQ, Available from https://www.who.int/uv/faq/skincancer/en/index1.html (06.03.2020).

Wu, F.Y., Wang, S.E., Sanders, M.E., Shin, I., Rojo, F., Baselga, J., and Arteaga, C.L. (2006). Reduction of cytosolic p27(Kip1) inhibits cancer cell motility, survival, and tumorigenicity. Cancer Res *66*, 2162-2172.

Wu, H., Goel, V., and Haluska, F.G. (2003). PTEN signaling pathways in melanoma. Oncogene *22*, 3113-3122.

Wu, Y., Tian, Z., and Wei, H. (2017). Developmental and Functional Control of Natural Killer Cells by Cytokines. Front Immunol *8*, 930.

Xing, Y., Lin, N.U., Maurer, M.A., Chen, H., Mahvash, A., Sahin, A., Akcakanat, A., Li, Y., Abramson, V., Litton, J.*, et al.* (2019). Phase II trial of AKT inhibitor MK-2206 in patients with advanced breast cancer who have tumors with PIK3CA or AKT mutations, and/or PTEN loss/PTEN mutation. Breast Cancer Res *21*, 78.

Xu, J., Lamouille, S., and Derynck, R. (2009). TGF-beta-induced epithelial to mesenchymal transition. Cell Res *19*, 156-172.

Xu, L., Begum, S., Hearn, J.D., and Hynes, R.O. (2006). GPR56, an atypical G protein-coupled receptor, binds tissue transglutaminase, TG2, and inhibits melanoma tumor growth and metastasis. Proc Natl Acad Sci USA *103*, 9023-9028.

Xu, L.J., Ma, Q., Zhu, J., Li, J., Xue, B.X., Gao, J., Sun, C.Y., Zang, Y.C., Zhou, Y.B., Yang, D.R.*, et al.* (2018a). Combined inhibition of JAK1,2/Stat3PDL1 signaling pathway suppresses the immune escape of castrationresistant prostate cancer to NK cells in hypoxia. Mol Med Rep *17*, 8111-8120.

Xu, Y., So, C., Lam, H.M., Fung, M.C., and Tsang, S.Y. (2018b). Apoptosis Reversal Promotes Cancer Stem Cell-Like Cell Formation. Neoplasia *20*, 295-303.

Yan, S., Holderness, B.M., Li, Z., Seidel, G.D., Gui, J., Fisher, J.L., and Ernstoff, M.S. (2016). Epithelial-Mesenchymal Expression Phenotype of Primary Melanoma and Matched Metastases and Relationship with Overall Survival. Anticancer Res *36*, 6449-6456.

Yang, C., Tsaih, S.W., Lemke, A., Flister, M.J., Thakar, M.S., and Malarkannan, S. (2018). mTORC1 and mTORC2 differentially promote natural killer cell development. Elife *7*.

Yang, J., Cheng, D., Zhou, S., Zhu, B., Hu, T., and Yang, Q. (2015). Overexpression of X-Box Binding Protein 1 (XBP1) Correlates to Poor Prognosis and Up-Regulation of PI3K/mTOR in Human Osteosarcoma. Int J Mol Sci *16*, 28635-28646.

Yang, J., Nie, J., Ma, X., Wei, Y., Peng, Y., and Wei, X. (2019). Targeting PI3K in cancer: mechanisms and advances in clinical trials. Mol Cancer *18*, 26.

Yang, Z., Lei, Z., Li, B., Zhou, Y., Zhang, G.M., Feng, Z.H., Zhang, B., Shen, G.X., and Huang, B. (2010). Rapamycin inhibits lung metastasis of B16 melanoma cells through down-regulating alphav integrin expression and up-regulating apoptosis signaling. Cancer Sci *101*, 494-500.

Yea, S.S., So, L., Mallya, S., Lee, J., Rajasekaran, K., Malarkannan, S., and Fruman, D.A. (2014). Effects of novel isoform-selective phosphoinositide 3-kinase inhibitors on natural killer cell function. PLoS ONE *9*, e99486.

Yeung, C., Hilton, J., Clemons, M., Mazzarello, S., Hutton, B., Haggar, F., Addison, C.L., Kuchuk, I., Zhu, X., Gelmon, K.*, et al.* (2016). Estrogen, progesterone, and HER2/neu receptor discordance between primary and metastatic breast tumours-a review. Cancer Metastasis Rev *35*, 427-437.

Yeung, K.T., and Yang, J. (2017). Epithelial-mesenchymal transition in tumor metastasis. Mol Oncol *11*, 28-39.

Yi, Y.S., Baek, K.S., and Cho, J.Y. (2014). L1 cell adhesion molecule induces melanoma cell motility by activation of mitogen-activated protein kinase pathways. Pharmazie *69*, 461-467.

Yin, J., Vogel, U., Ma, Y., Qi, R., Sun, Z., and Wang, H. (2007). The DNA repair gene XRCC1 and genetic susceptibility of lung cancer in a northeastern Chinese population. Lung Cancer *56*, 153-160.

Yingling, J.M., McMillen, W.T., Yan, L., Huang, H., Sawyer, J.S., Graff, J., Clawson, D.K., Britt, K.S., Anderson, B.D., Beight, D.W.*, et al.* (2018). Preclinical assessment of galunisertib (LY2157299 monohydrate), a first-in-class transforming growth factor-beta receptor type I inhibitor. Oncotarget *9*, 6659-6677.

Yokoyama, W.M. (2005). Natural killer cell immune responses. Immunol Res *32*, 317-325.

Yu, J., Li, J., Chen, Y., Cao, W., Lu, Y., Yang, J., and Xing, E. (2017). Snail Enhances Glycolysis in the Epithelial-Mesenchymal Transition Process by Targeting FBP1 in Gastric Cancer. Cell Physiol Biochem *43*, 31-38.

Yu, J.S., and Cui, W. (2016). Proliferation, survival and metabolism: the role of PI3K/AKT/mTOR signalling in pluripotency and cell fate determination. Development *143*, 3050-3060.

Zhang, B., Zhang, J., and Tian, Z. (2008). Comparison in the effects of IL-2, IL-12, IL-15 and IFNalpha on gene regulation of granzymes of human NK cell line NK-92. Int Immunopharmacol *8*, 989-996.

Zhang, C., Hu, Y., and Shi, C. (2020). Targeting Natural Killer Cells for Tumor Immunotherapy. Front Immunol *11*, 60.

Zhang, J.Y., Zhang, F., Hong, C.Q., Giuliano, A.E., Cui, X.J., Zhou, G.J., Zhang, G.J., and Cui, Y.K. (2015). Critical protein GAPDH and its regulatory mechanisms in cancer cells. Cancer Biol Med *12*, 10-22.

Zhang, X.D., Borrow, J.M., Zhang, X.Y., Nguyen, T., and Hersey, P. (2003). Activation of ERK1/2 protects melanoma cells from TRAIL-induced apoptosis by inhibiting Smac/DIABLO release from mitochondria. Oncogene *22*, 2869-2881.

Zhang, Y., Xia, M., Jin, K., Wang, S., Wei, H., Fan, C., Wu, Y., Li, X., Li, X., Li, G.*, et al.* (2018). Function of the c-Met receptor tyrosine kinase in carcinogenesis and associated therapeutic opportunities. Mol Cancer *17*, 45.

Zhao, B., Li, L., and Guan, K.L. (2010a). Hippo signaling at a glance. J Cell Sci *123*, 4001-4006.

Zhao, C., Zhang, W., Zhu, X., Xu, Y., Yang, K., Wei, D., Liang, S., Zhao, F., Zhang, Y., Chen, X.*, et al.* (2019). TWIST2: A new candidate tumor suppressor in prostate cancer. Prostate *79*, 1647-1657.

Zhao, Y., Yang, Z.Q., Wang, Y., Miao, Y., Liu, Y., Dai, S.D., Han, Y., and Wang, E.H. (2010b). Dishevelled-1 and dishevelled-3 affect cell invasion mainly through canonical and noncanonical Wnt pathway, respectively, and associate with poor prognosis in nonsmall cell lung cancer. Mol Carcinog *49*, 760-770.

Zhou, B.P., Deng, J., Xia, W., Xu, J., Li, Y.M., Gunduz, M., and Hung, M.C. (2004). Dual regulation of Snail by GSK-3beta-mediated phosphorylation in control of epithelial-mesenchymal transition. Nat Cell Biol *6*, 931-940.

Zhou, J., Yi, Q., and Tang, L. (2019a). The roles of nuclear focal adhesion kinase (FAK) on Cancer: a focused review. J Exp Clin Cancer Res *38*, 250.

Zhou, L., Lv, X., Yang, J., Zhu, Y., Wang, Z., and Xu, T. (2018a). Overexpression of Napsin A resensitizes drug-resistant lung cancer A549 cells to gefitinib by inhibiting EMT. Oncol Lett *16*, 2533-2538.

Zhou, M., Liu, X., Li, Z., Huang, Q., Li, F., and Li, C.Y. (2018b). Caspase-3 regulates the migration, invasion and metastasis of colon cancer cells. Int J Cancer *143*, 921-930.

Zhou, X.-P., Gimm, O., Hampel, H., Niemann, T., Walker, M.J., and Eng, C. (2000). Epigenetic PTEN Silencing in Malignant Melanomas without PTEN Mutation. Am J Pathol *157*, 1123-1128.

Zhou, Y., Song, K.Y., and Giubellino, A. (2019b). The Role of MET in Melanoma and Melanocytic Lesions. Am J Pathol *189*, 2138-2148.

Zhu, H., Lai, Y.S., Li, Y., Blum, R.H., and Kaufman, D.S. (2018). Concise Review: Human Pluripotent Stem Cells to Produce Cell-Based Cancer Immunotherapy. Stem Cells *36*, 134-145.

Zhu, Z., Bai, Y., Lu, X., Ding, J., and Qi, C. (2019). Rapamycin downregulates NKG2D ligands in acute myeloid leukemia cells via an activation of the STAT3 pathway: a potential mechanism for rapamycin-induced immune escape in leukemia. Transl Cancer Res *8*, 473-482.

Zhuang, L., Lee, C.S., Scolyer, R.A., McCarthy, S.W., Zhang, X.D., Thompson, J.F., Screaton, G., and Hersey, P. (2006). Progression in melanoma is associated with decreased expression of death receptors for tumor necrosis factor-related apoptosis-inducing ligand. Hum Pathol *37*, 1286-1294.

Zitvogel, L., Tesniere, A., and Kroemer, G. (2006). Cancer despite immunosurveillance: immunoselection and immunosubversion. Nat Rev Immunol *6*, 715-727.

Acknowledgements

First and foremost, I would like to thank Prof. Dr. Ivan Bogeski and Prof. Dr Markus Hoth for their support and the opportunity to work in their labs on an exciting biomedical project.

I would like to express my gratitude to my supervisors Prof. Dr Ivan Bogeski and Carsten Kummerow for initiating this project and allowing me to develop together with this project during the last years. I always appreciated the regular exchange of ideas and the discussion of my results. The different perspective of you, helped me to critically analyse problems and examine it from different angles. I am grateful that you always gave me the trust and freedom to work independently and allowed the development of own hypothesis and ideas. Furthermore, I would like to offer my special thanks to PhD Adina Monica Vultur for sharing her scientific expertise and providing constructive comments and suggestions that promoted not only this project but also my scientific confidence.

Furthermore, I am thankful for the valuable scientific advice and support of my thesis committee members, Prof. Dr. Alexander Flügel and Prof. Dr. Michael P. Schön, which helped to advance my doctoral project. Moreover, many thanks to Prof. Dr. Lutz Walter, Prof. Dr. Ralf Dressel and Prof. Dr. Thomas Meyer, who kindly agreed to be members of my examination committee.

I would also like to express my acknowledgement to all assistance and support I received during the time in the Department of Biophysics in Homburg. I want to thank Cora Hoxha and Carmen Hässig for excellent technical support in isolating PBMCs and primary NK cells. Furthermore, I am grateful to Gertrud Schwär, who performed and supported RNA-isolation for the RNA sequencing of the melanoma-NK cell-co-culture. Special thanks to Sandra Janku for her helping hand and warm encouragements. Moreover, I would like to thank all the members of the 'Killing Club' for weekly scientific exchange and illuminating discussions. Finally, I want to thank all former PhD students of the AG Hoth in Homburg for scientific exchange and help as well as enjoyable lunch breaks and running tours.

I wish to extend my special thanks to Prof. Dr. Ivan Bogeski who gave me the possibility to continue my doctorate in Göttingen. The move to Göttingen and the involved experience to build-up a lab was a challenge that contributed to my scientific but also personal development. In this regard, I would like to thank Andrea Paluschkiwitz and Dr. Christine Gibhardt as well as all the members of the Institute of Cardiovascular Physiology for the inviting and enjoyable working environment that allowed me to settle into the lab in Göttingen.

I am grateful for the assistance given by Andrea Paluschkiwitz who supported this work with RNA-isolation, cDNA synthesis, qRT-PCR experiments and the determination of melanoma cell proliferation. Furthermore, I would like to thank all my fellow lab colleagues of the AG Bogeski for their support in the last years, in particular to Dr. Christine Gibhardt for all her scientific advice and support, to Ioana Todoran for her help and advice in performing immunoblots, to Magdalena Shumanska for her support in isolating PBMCs and primary NK cells and last but not least to Dr. Hsu-Min Sung for establishing the heatmaps in R.

Acknowledgements to D.V.M., D.Sc Meenhard Herlyn and Patricia Brafford of The Wistar Institute, Philadelphia, U.S.A, for providing the melanoma cell lines, RPPA data and advice in its analysis. Furthermore, I want to thank Prof. Dr. Tobias Legler and the Institute of Transfusion Medicine at UMG as well as Prof. Hermann Eichler and the Institute of Clinical Hemostaseology and Transfusion Medicine at Saarland University Medical Center for providing human blood samples.

Acknowledgements to the epigenetics group of Prof. Dr. Jörn Walter of Saarland University in Saarbrücken for RNA sequencing. In this regard, special thanks to Dr. Giles Gasperoni and Dr. Karl Nordström for performing and analysing the RNA sequencing. Additional thanks to Kathrin Kattler for advice and support in PCA analysis. Furthermore, I want to thank Dr. Verena Lorenz of the Department of Dermatology, Venereology and Allergology for providing excellent *SNAI1* primers. Acknowledgements to Prof. Dr. Blanche Schwappach to allow access to the FACS Canto II and Odyssey® CLx imaging system.

Moreover, I want to thank my friends and colleagues for proof-reading the thesis and formatting advice.

Finally, I want to thank my family and friends who supported me my whole life and always believed in me. There are no words to express my gratitude to you.